THE UNIVERSITY OF HULL

Investigate WSB-1 as a novel BRCAness biomarker in breast cancer

Being a Thesis submitted for the Degree of Doctor of Philosophy in the University of Hull

By

Chun Li

B.M, M.S

Feb 2023

Abstract

Background

Radiotherapy currently has become one of the major therapeutic approaches in the treatments for cancers. However, hypoxia presents a significant challenge to the effectiveness of radiotherapy and is associated with radio-resistance. Previous studies have shown that hypoxia can lead the alteration of DNA damage response pathways and genomic instability, which correlates with increased therapeutic resistance. Metastatic breast cancer is one of the most aggressive types of breast cancer and, unfortunately, with limited options regarding therapeutic strategies and reliable predictive biomarkers. Recent studies shown that DNA repair-deficient cancers, including BRCA1/2-deficient breast cancers, are sensitive to PARP inhibitors (PARPi), a phenotype described as BRCAness. We have previously found that the hypoxia-inducible factor WSB-1 is associated with increased breast cancer metastasis. However, its role in the DDR remains unclear. In this study, we evaluated the role of WSB-1 in DDR regulation in hypoxia in breast cancer.

Methodology

RNA-Sequencing analysis was performed after WSB-1 depletion on the MDA-MB-231 cell line to evaluate its impact on DDR pathways. Interesting hits were validated *in vitro* at mRNA and protein level using WSB-1 siRNA or overexpression. Moreover, the impact of WSB-1 on DNA damage response was evaluated by DNA damage biomarkers γH2AX and 53BP1 foci, cell cycle progression, as well as chromosome instability. In addition, *in silico* analyses of patient gene expression datasets were also performed for *WSB1* vs DNA repair. Finally, sensitivity of DDR inhibitors (DDRis) such as PARP inhibitors (PARP1i), ATM inhibitors (ATMi), and ATR inhibitors (ATRi), were investigated using viability assays alongside WSB-1 expression modulation, either as single agents or in combination with radiotherapy.

Results

Transcriptome-wide RNA-Seq analysis showed that WSB-1 depletion was associated with upregulation of various DDR pathways. These were validated at mRNA and protein level *in vitro* after WSB-1 depletion, and reciprocally, WSB-1 overexpression downregulated these DDR factors. Further, γH2AX and 53BP1 foci were increased when overexpressed WSB-1 and decreased after WSB-1 depletion after IR under normoxia and hypoxia. cell cycle arrest and potentially chromosome instability were also observed when overexpressed WSB-1. Moreover, *WSB1* expression correlation analysis in breast cancer patient gene expression datasets also been showed inversely correlated with DNA repair gene signature. Finally, it was observed that WSB-1 overexpression increased Olaparib (PARPi), KU-55933 (ATMi), and VE-822 (ATRi) sensitivity *in vitro*.

Conclusions

Our results show that WSB-1 expression in hypoxic breast cancer is associated with modulation of DDR factor expression. Furthermore, WSB-1 overexpression led to increased PARPi, ATMi, ATRi sensitivity alone or combined with radiation sensitivity *in vitro*. Therefore, we propose that elevated WSB-1 expression could be a potential BRCAness biomarker in metastatic breast cancer and could promote increased sensitivity to DDR targeted therapies.

Acknowledgements

First and foremost, I would like to express my sincere appreciation to my supervisor, Dr. Isabel Pires, for providing me with the opportunity to work in her lab and for her unwavering support throughout this project. I am truly grateful for her consistent encouragement and patience.

I also extend my gratitude to Prof. Michael J Lind and Dr. Rajarshi Roy for dedicating their valuable time and offering invaluable insights, particularly from the clinical perspective. Their professional guidance has been instrumental to this project.

I am deeply thankful for the time and effort invested by all my supervisors, especially during our regular weekly meetings in the midst of the pandemic lockdown. These interactions greatly aided in maintaining my motivation and preventing any sense of isolation.

Furthermore, I would like to acknowledge the supervisors and fellow students in our adaptive radiotherapy cluster, along with the invaluable assistance of our lab members Ellie, Emily, Lucy, Olivia, Sapphire, and Islam.

A special thanks goes out to my dear friends Larissa, Laden, Beverly, Darren, and Michelle, who not only made my PhD journey enjoyable but also filled it with unforgettable memories. And, of course, my heartfelt thanks to my family for their unwavering support.

Lastly, I am grateful to the University of Hull for awarding me a full scholarship, which has made this academic journey possible.

Publications

1. **Chun Li**, Lucy Wiseman, Ene Okoh, Michael Lind, Rajarshi Roy, Andrew W. Beavis, Isabel M. Pires. (2022). **Exploring hypoxic biology to improve radiotherapy outcomes.** Expert Reviews in Molecular Medicine 24, e21, 1–18. doi: 10.1017/erm.2022.14

2. Sarah D Edge, Isaline Renard, Emily Pyne, **Chun Li**, Hannah Moody, Rajarshi Roy, Andrew W Beavis, Stephen J Archibald, Christopher J Cawthorne, Stephen G Maher, Isabel M Pires. **PI3K inhibition as a novel therapeutic strategy for neoadjuvant chemoradiotherapy resistant oesophageal adenocarcinoma.** British Journal of Radiology, 2021 Mar 1;94(1119):20201191. doi: 10.1259/bjr.20201191.

Table of Contents

List of Figures

List of Tables

Abbreviations

ATM: Ataxia-telangiectasia mutated

ATR: Ataxia telangiectasia and Rad3-related

BC: Breast Cancer

BRCA1: Breast cancer gene 1

BRCA2: Breast cancer gene 2

BER: base excision repair

°C: Degree Celsius

cm: Centimetre

CO_2: carbon dioxide

CDKs: cyclin-dependent kinases

CKIs: cyclin-dependent kinase inhibitors

CDK1: Cyclin-dependent kinases 1

CDK2: Cyclin-dependent kinases 2

CDK4/6: Cyclin-dependent kinases 4/6

CtIP: C-terminal binding protein-interacting protein

DDRs: DNA damage responses

DSBs: double-strand breaks

DNA-PK: DNA-dependent protein kinase

DMSO: Dimethylsulfoxide

EDTA: Ethylenediaminetetra acetic acid

ERs: oestrogen receptors

FIH: factor inhibiting HIF

g: Gram

h: hour

HR: Homologous recombination repair

HIFs: hypoxia-inducible factors

HREs: hypoxia response elements

HER-2: human epidermal growth factor receptor 2

IR: Ionizing radiation

ICL: Inter-strand crosslinks

L: Litre

MSI: microsatellite instability

MS: microsatellite sequence

MMR: mismatch repair

MRN: MRE11/RAD50/NBS1 complex

NER: nuclear excision repair

NHEJ: non-homologousend-joining repair

O_2: Oxygen

ODD: oxygen-dependent degradation domain

PBS: phosphate buffered saline

PRs: progesterone receptors

PARP: Poly (ADP-ribose) polymerase

PI3K: Phosphoinositide 3-kinase

PHDs: prolyl hydroxylases

RT: Radiation therapy

pCR: pathologic complete response

RB1: retinoblastoma 1

RPA: replication protein A

ROS: reactive oxygen species

SSBs: single-strand breaks

SOCS: suppressor of cytokine signalling

SFM: serum-free medium

TNBC: Triple-Negative Breast Cancers

μg: Microgram

VHL: von Hippel-Lindau

WSB-1: WD repeat and SOCS box containing-1

Chapter 1

Introduction

1.1 Breast cancer

1.1.1 Overview

Breast cancer is the most common cancer in women worldwide, accounting for 12.5% of all new cancer cases (Loibl et al., 2021). The incidence rates of breast cancer have risen the past four decades, including increasing by 0.5% annually in the United States (Giaquinto et al., 2022). A study predicted that, by 2040, breast cancer will be increased to over 3 million new cases and 1 million deaths worldwide every year (Rabionet Diaz, 2021, Arnold et al., 2022). In the UK and according to Breast Cancer Now, 80% of women aged 50 and over are diagnosed breast cancer, and just over 10,000 women under the age of 50 cases per year are diagnosed with breast cancer (BreastCancerNow, 2022). Breast cancer is also the second leading cause of cancer death in women worldwide (Loibl et al., 2021). Statistics from the United States predicted approximately 43,250 women out of 287,850 new cases will die from breast cancer in 2022 (Giaquinto et al., 2022). In the UK, breast cancer is the 4th most common cause of cancer death, accounting for 7% of all cancer deaths (CancerResearchUK, 2022).

1.1.2 Subtypes

The Cancer Genome Atlas Project (TCGA) has distinguished invasive breast cancer into four main subtypes, including Luminal A, Luminal B, HER2-enriched, and basal-like breast cancer, based on mRNA gene expression levels (Brigham et al., 2012).

Luminal breast cancers are oestrogen-receptor (ER) positive tumours that are divided into two subgroups with different clinical outcomes: Luminal A and Luminal B subtypes. Luminal A breast cancer constitutes about 50-60% of all breast cancers and Luminal B breast cancer comprises 15-20% of all breast cancer (Johnson et al., 2020). Luminal A subtype breast cancer are characterised by ER positive and/or progesterone-receptor (PR) positive, and human epidermal growth factor receptor 2 (HER-2) negative with low grade and tend to have the better prognosis compared to Luminal B.

Luminal B subtype breast cancer are ER positive, PR negative, and/or Her-2 positive with higher grade and worse prognosis than Luminal A. This subtype breast cancer also has high proliferation expression such as Ki67 and low expression of PR.

Her-2 amplified breast cancer is characterised by the high expression of the Her-2 and negative for ER and PR, with high proliferation related protein Ki67. Her-2 amplified breast cancers usually have worse prognosis than Luminal A and Luminal B breast cancer. Clinically, Her-2 amplified breast cancer are classified as based on immunohistochemistry (IHC) and/or fluorescence in situ hybridization (FISH) methods (Yoshimura et al.).

The Triple-Negative Breast Cancers (TNBC) are characterised as ER-negative, PR-negative, and HER2-negative subtype of breast cancer. They comprise about 20% of all breast cancer subtypes and often are more biologically aggressive and have worse clinical outcome than other subtypes breast cancer (Yin et al., 2020). Approximately 10% of all TNBC have BRCA germline mutations (Hartman et al., 2012).

The details of the characteristics of these subtypes are summarised in Table 1.1

Table 1. 1 The details of the characteristics of different subtypes of breast cancer

	Luminal A	Luminal B	Her-2 amplified	Based-like
ER	+	+	-	-
PR	≥20%+	<20%+	-	-
Her-2	- (can be positive)	- (can be positive)	+	-
Ki67	<14%+	≥14%+	Any	Any

1.1.3 Diagnosis

Breast cancer is typically diagnosed by combination methods including physical examinations, imaging techniques and pathological diagnosis (He et al., 2020). Physical examination is proceeded by a healthcare provider to examine for any lumps or abnormalities in the breast tissue. If a lump or abnormality is detected, further examination will be processed.

It has been showed that various imaging techniques could be used for diagnosis and monitoring patients with breast cancer in various stages (Jafari et al., 2018). Positron emission tomography/computed tomography (PET/CT) was found can improve the diagnostic accuracy of breast cancer recurrence (Zangheri et al., 2004). The pathological diagnosis of breast cancer includes IHC analysis of paraffin sections to detect the ER, PR, and Her-2 status, and in situ hybridization can detect *Her-2* gene amplification as a confirmatory test for IHC (Leong and Zhuang, 2011).

1.1.4 Treatment

The treatment strategies for breast cancer currently includes conventional therapies such as local treatments surgery and radiotherapy, and systemic treatments like chemotherapy, targeted therapy and immunotherapy (Costa et al., 2020).

1.1.4.1 Chemotherapy

Chemotherapy is a conventional cancer treatment which can be used for most types of breast cancer. It has also been shown to significantly improve long term outcomes of early stages triple negative breast cancer (Chaudhary, 2020). Chemotherapy agents such as anthracycline and taxane (Song and Hu, 2021) are widely used for the treatments of early stage and metastatic breast cancer (Andreopoulou and Sparano, 2013). In addition, chemotherapy agents such as platinum agents has been used in *BRCA1/2*-mutated TNBC on some early metastatic studies with response rates up to 50-60% (Chaudhary, 2020). In another study, a high pathological complete response (pCR) rate (83.3%) to single agent cisplatin in *BRCA1*

mutation carriers was reported (Byrski et al., 2010). Moreover, among recent clinical trials, the combination of platinum agents including cisplatin or carboplatin with novel targeted therapeutics such as EGFR inhibitor Cetuximab(Sabatier et al., 2019) or PARP inhibitor (Rodler et al., 2023) for patients with TNBCs or metastatic breast cancer are under clinical trials evaluation. A phase III trials showed the combination of Trastuzumab, Paclitaxel, and Carboplatin were effective in Her-2 positive metastatic breast cancer (Robert et al., 2006). Carboplatin combined with Sacituzumab Govitecan-hziy (NCT05382299) and pembrolizumab (NCT05382286) to treat metastatic TNBCs have entered phase III (Ali et al., 2022).

1.1.4.2 Radiation therapy

Radiation therapy (RT) can be used to treat breast cancer at almost every stage. After breast-conserving surgery, the risk of local recurrence can be reduced by IR (ionising radiation) up to 50-60% in stage 0 ductal carcinoma *in situ* breast cancer (Polgár et al., 2022). In stage I-II invasive breast cancer, radiation still used as a standard treatment following breast-conserving surgery, except patients with stage I and age ≥70 years would consider hormonal therapy without RT (Polgár et al., 2022). In metastatic breast cancer, RT can offer effective palliation of symptomatic lesions (Jutzy et al., 2018). Moreover, metastatic breast cancer patients treated with stereotactic body radiotherapy have shown promising results regard to long-term survival outcomes (Milano et al., 2012). Studies also found that regional lymph node irradiation and partial breast irradiation have consistent benefits in overall survival in patients (Haussmann et al., 2020).

1.1.4.3 Hormonal therapy

Hormonal therapy, also known as endocrine therapy, is another effective strategy for breast cancer treatments that are based on targeting oestrogen and progesterone. Oestrogen and progesterone are the primary regulators of breast tissue growth and differentiation by activating their receptors, the oestrogen receptors (ERs) and progesterone receptors (PRs). Therefore, hormonal therapy is used to treat luminal breast cancers that are positive for either

ER or PR, which including selective oestrogen receptor modulators (SERMs), such as tamoxifen and fulvestrant, and aromatase inhibitors (AIs), such as anastrozole and letrozole (Dalmau et al., 2014).

1.1.4.4 Targeted therapy

Targeted therapy are strategies that targets key molecules which are crucial in cancer cell growth and survival.

Cyclin-dependent kinase (CDK) 4/6 plays a vital role in CyclinD1-CDK4/6–RB1 pathway, regulates cell cycle and mediates cellular proliferation. Further details in Section 1.2.2. CDK4/6 inhibitors are commonly used for hormone receptor-positive (HR+) and HER2-negative metastatic breast cancer which represents a milestone in cancer therapeutics (Spring et al., 2020).

Poly (ADP-ribose) polymerase (PARP) inhibitors which specifically inhibits DNA damage repair pathway by inhibiting PARP, are approved by the Food and Drug Administration (FDA) for the treatments in ER or PR negative and BRCA mutated breast cancers, and also now is under investigation for the treatment of earlier stages of BC, as well as in patients without BRCA mutations (Cortesi et al., 2021). These types of therapy will be discussed further in Section 1.6.

Another example of targeted therapy for breast cancer is phosphatidylinositol 3-kinase (PI3K) inhibitors. PI3K inhibitors alpelisib have been approved to treat HR+/HER2–*PIK3CA*-mutated advanced/metastatic breast cancer patients (Narayan et al., 2021). Recently, immunotherapy has also used as a strategy for breast cancer treatments by stimulating the immune response against cancer cells which has been proven to improving the survival of patients (Williams et al., 2017). For example, immune checkpoint inhibitors that target programmed death 1 (PD-1) or programmed death ligand 1 (PD-L1) in combination with neoadjuvant chemotherapy, which includes surgery, chemotherapy, radiotherapy and hormonal therapy that use to shrink tumour before main treatments, have

shown significantly improved pathological complete response (pCR) rates in patients with early TNBC (Mittendorf et al., 2020, Nanda et al., 2020).

Furthermore, other emerging targeted therapies are under investigation to improve breast cancer treatments, for example, histone deacetylase enzyme inhibitors (such as tucidinostat) could interfere with tumour-promoting signals and suppress tumour growth. Summary of the current treatments for breast cancers is depicted in Figure 1.1.

1.1.5 Breast Cancer Biomarkers

Biomarkers are biological or physiological characteristic that can be used as a measurement of either normal or pathological biological processes or the responses to treatments and play a critical role in improving the drug development process (Pritzker, 2015). Therefore, it is essential to identify and validate biomarkers of breast cancer that could allow an early detection of the tumour or give predictive information about the response to a therapy and finally improve the therapeutic outcomes and help guide therapy.

Breast cancer biomarkers are crucial for the accurate and fast diagnosis, prognosis, and the prediction of treatment response, which can control the developments of the disease, monitor the response throughout cancer treatments. Moreover, because the heterogeneity of tumours and the differences among individual patient, personalised or unique treatments are in high demand and the development of novel biomarkers for diagnosis, prognosis, as well as the prediction of personalised treatments are also in urgently needed. From the perspective of predictive biomarkers of breast cancer, the hormonal receptor ER and PR are the most common used and well-established predictive marker for the response of endocrine therapy treatments in breast cancer(Mosly et al., 2018). For ER+, endocrine therapy treatments including selective oestrogen receptor modulators (SERMs), and aromatase inhibitors (AIs), etc would be used and have been shown to improve outcome. HER-2 which was also a predictive biomarker and used in predicting response to trastuzumab (Herceptin™) (Payne et al., 2008). Inherited mutations in *BRCA1* and *BRCA2* genes are not only associated with high

risks of breast cancer (Kuchenbaecker et al., 2017), but also can be used as predictive biomarkers for treatments such as platinum-based chemotherapy and PARP inhibitors.

Although there are several treatment strategies for breast cancer (see Section 1.1.4), therapeutic resistance is a major challenge. For example, some HR+ breast cancers cannot benefit from hormone therapy due to hormone resistance (Augereau et al., 2017). For hard-to-treat metastatic breast cancers, such as HR+ metastatic breast cancers can ultimately develop resistance which also called acquired resistance to hormonal therapies (Dalmau et al., 2014). Recently, studies found that the combination of therapies can achieve a better outcome. Hormone therapy have been combined with CDK4/6 inhibitors (palbociclib, ribociclib, abemaciclib) as the first- or second-line drug in most countries and shown to improve the outcome of patients with HR+ advanced breast cancer remarkably (Shah et al., 2018). Unfortunately, some patients could eventually develop acquired drug resistance to CDK4/6 inhibitors (Scheidemann and Shajahan-Haq, 2021). Many preclinical studies have suggested that combination strategies with other signal pathway inhibitors to extend the use of CDK4/6 inhibitors (Xu et al., 2021, Rampioni Vinciguerra et al., 2022). More importantly, discovering reliable biomarkers that could predict and monitor the respond to the combination of different therapeutic treatments are crucial.

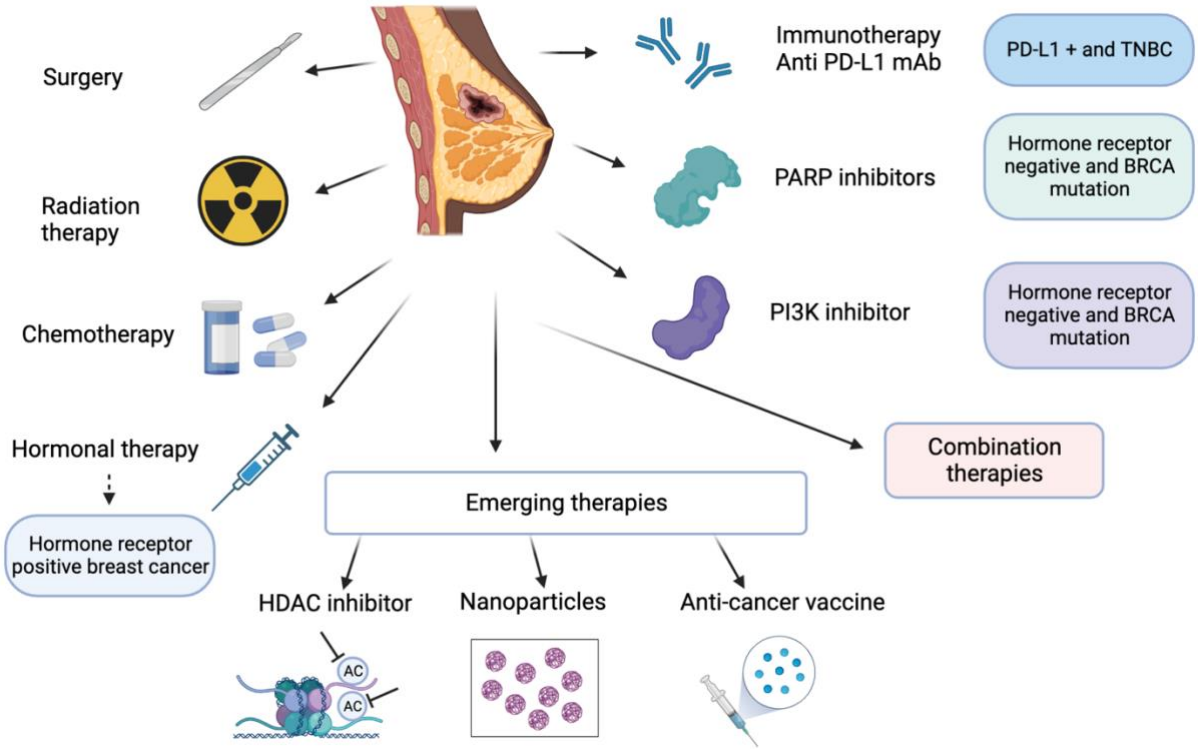

Figure 1. 1 Current strategies for breast cancer treatments

Breast cancer treatments currently includes conventional therapies such as surgery and radiotherapy, and systemic treatments like chemotherapy, targeted therapy, and immunotherapy. Further novel therapies are emerging, which including HDAC inhibitors, Nanoparticles, and anti-cancer vaccines.

PD-L1: programmed cell death-ligand 1; TNBC: triple negative breast cancer; PARP: poly (ADP-ribose) polymerase; BRCA: Breast Cancer gene; PI3K: phosphatidylinositol 3-kinase; HDAC: Histone deacetylase. (Created using Biorender.com)

1.2 The DNA Damage Response

The DNA damage response (DDR) is a complex network of numerous genes and proteins involves, responsible for sensing different types of DNA damage, mediating DNA repair, regulating cell cycle regulation, and respond to replication stress, etc (Pilié et al., 2019).

1.2.1 Different types of DNA Damage and their repair pathways

DNA damage occur thousands of times a day, as cells are continuously exposed to different sources of damage, endogenous and exogenous. Exogenous damage sources include radiation and chemical agents, and endogenous sources include for example replication errors, DNA base mismatches, topoisomerase-DNA complexes, and reactive oxygen species (ROS) from cellular metabolism (Chatterjee and Walker, 2017). Many different types of DNA damage can occur, including mismatches in DNA bases and other base damage, DNA crosslinking damage, single-strand breaks (SSBs), and double-strand breaks (DSBs).
DNA bases damage can be caused by Reactive Oxygen Species (ROS) (Jaruga and Dizdaroglu, 1996, Halliwell and Gutteridge, 1990), DNA alkylation (Tsuzuki et al., 1998, Fu et al., 2012), base loss caused by the hydrolysis of bases, bulky adduct formation, DNA crosslinking, and DNA strand breaks, including single and double stranded breaks (Bauer et al., 2015).

DNA base mismatches can lead to the damage of DNA and increase the risks of a wide variety of cancers (Win et al., 2012). For example, Microsatellite Instability (MSI) is a phenomenon in which microsatellite sequences (MS), short and repetitive DNA sequences (generally double base CA/GA repeats or single base A/T repeats), change due to insertion or deletion mutations during DNA replication. MSI was first discovered in colorectal cancer in 1993, where was found highly associated with the occurrence of cancer (Ionov et al., 1993).

SSBs are the most common lesions, which are discontinuities in strands caused by the loss or mismatch of a single nucleotide at the sites of 5′- and/or 3′-termini (Caldecott, 2008).

Unrepaired SSBs compromise DNA replication and transcription programs, leading to genome instability and diseases (Balakrishnan and Stewart, 2019).

DBSs are one of the most deleterious and complex types of DNA damage, and most DSBs that can be attributed to endogenous processes are produced during DNA replication (Cannan and Pederson, 2016). Improper SSB repair may result in DSBs occurring in actively replicating DNA(Morgan and Lawrence, 2015). During DNA replication, a replicative polymerase that encounters a SSB in the template strand may stall, leading to a collapse of the replicative fork and subsequently the formation of DSB (Pfeiffer et al., 2000). DNA damage caused by exogenous sources, such as IR during RT, often generates a cluster of oxidative lesions in DNA. Near-simultaneous BER repair of closely opposed lesions in such cluster lesions can produce SSBs in both DNA strands, which may convert to a DSB (Cannan and Pederson, 2016).

In response to different types of DNA damage, there are several essential DNA repair pathways involved in maintaining the genome stability in human cells(Lord and Ashworth, 2012). These include mismatch repair (MMR) pathway, base excision repair (BER) pathway, nucleotide excision repair (NER) pathway, homologous recombination repair (HR) pathway, non-homologous end-joining (NHEJ) pathway. Various types of DNA damage caused by different resources including key protein involved in respective DNA damage repair pathways are summarized in Figure 1.2.

1.2.1.1 BER (Base excision repair)

BER is the predominant DNA repair pathway responsible for the repair of small base lesions which typically results from deamination, oxidation, or methylation, as well as SSBs, contributing to the protection of genome integrity (Li et al., 2013). This type or repair includes short-patch BER (responsible for repairing single nucleotide alterations) and long-patch BER (which can at least generate two nucleotides to correct multiple bases) (Lindahl, 2001a, Fortini and Dogliotti, 2007, Robertson et al., 2009). BER consists of five key steps

(Figure 1.3). First step is the recognition and excision of the inappropriate base damage by DNA glycosylases, including as OGG1, NTH1, NEIL, UDG, and MPG (Lindahl, 2001b, Krokan and Bjørås, 2013). For example, OGG1 (8-oxoguanine glycosylase) targets oxoguanine (Dianov et al., 1998). Once OGG1 recognizes an 8-Oxo-2'-deoxyguanosine lesion within DNA, it efficiently removes 8-oxo-dG from the damage site through its glycosylase activity (Bruner et al., 2000). Second step is the incision of the DNA backbone adjacent the abasic site (Hill et al., 2001). APE1 (Apurinic apyrimidinic endonuclease-1) is required for the incision of the DNA adjacent to the apurinic (AP) site, which generate 3'-phospho-α,β-unsaturated aldehyde (3'dRP) and 5'-phosphate termini (Doetsch and Cunningham, 1990). For short-patch BER, a single nucleotide gap is generated and subsequently Polβ fills the single nucleotide gap with the correct nucleotide and the nick is sealed by a complex of DNA ligase IIIa and scaffold protein X-ray cross complementing protein-1 (XRCC1). Long-patch BER is utilised when a 5' blocking lesion is produced through the oxidation or reduction of the AP site that is resistant to the Polβ dRP lyase activity. In this instance, Polβ inserts the correct single complementary nucleotide, but then there is a switch to the replicative polymerases d or e. Pol d or e then proceed to synthesise 2-12 nucleotides from the 3' end of the repair site, displacing a 5'-flap in a process called strand displacement (Krokan and Bjørås, 2013). The flap structure is then subject to removal by flap endonuclease-1 (FEN-1) in association with proliferating cell nuclear antigen (PCNA), and the nick is sealed through DNA ligase I activity.

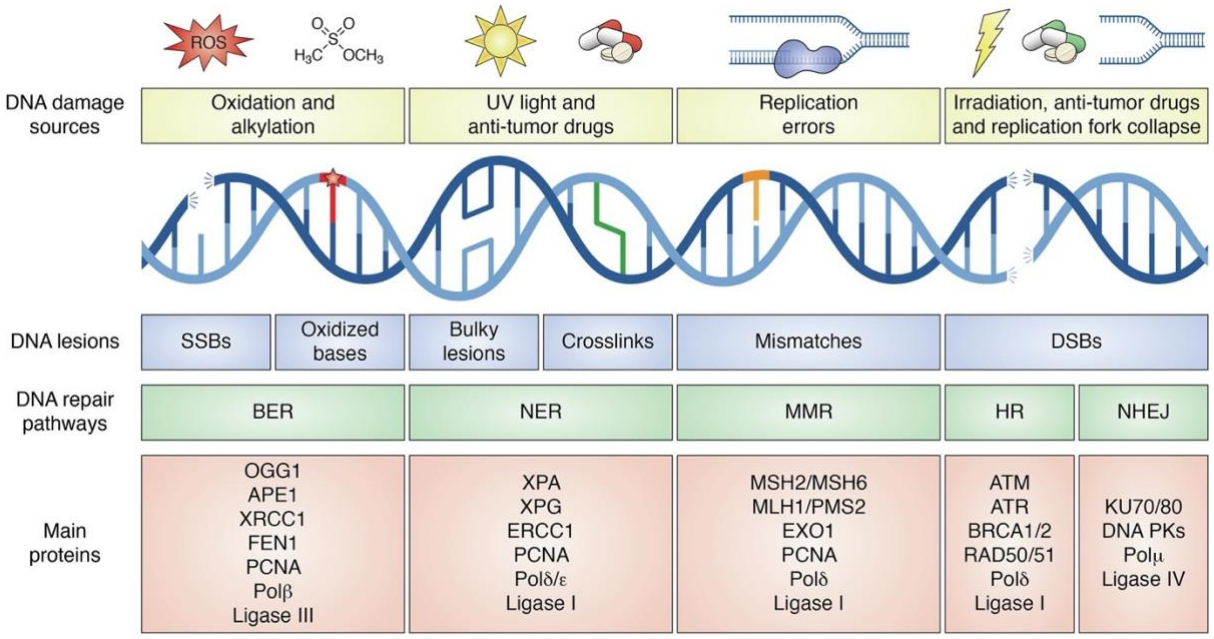

Figure 1. 2 Overview of DNA Damage Response

Different DNA lesions caused by different damage sources and of respective DNA repair pathways are shown in the Figure. The major proteins involved in the DNA repair pathways are also shown.

BER, base excision repair; DSBs, double-strand breaks; HR, homologous recombination; MMR, mismatch repair; NER, nucleotide excision repair; NHEJ, non-homologous end joining; SSBs, single-strand breaks.

(From Giuseppe Dall'Agnese, et al. 2023)

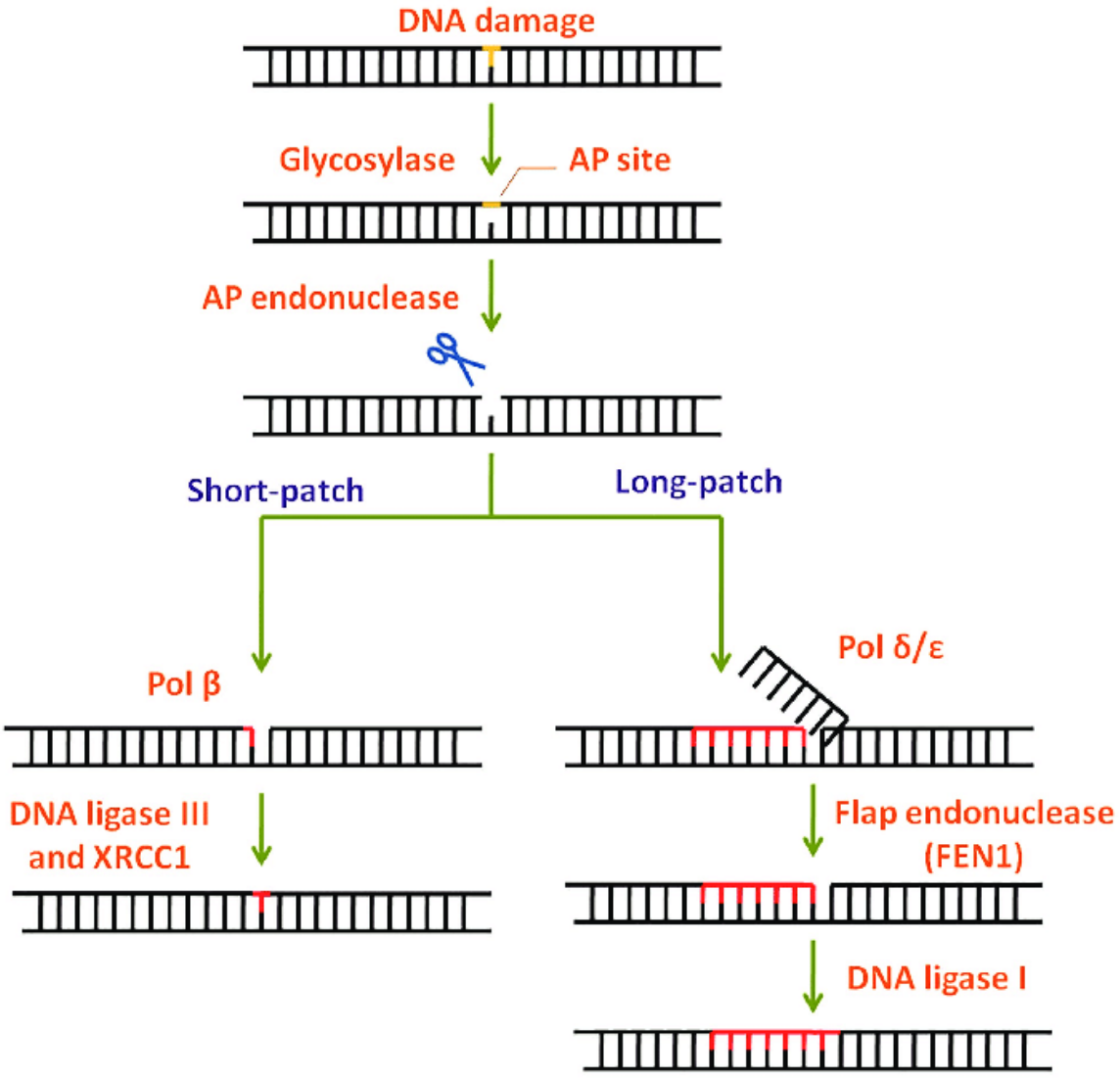

Figure 1. 3 The base excision repair (BER) pathways

In BER, the damaged base is recognised and removed by a base specific glycosylase generating an abasic site. Apurinic/apyrimidinic (AP) endonuclease then cleaves the phosphodiester backbone at the AP site. Depending on the number of damaged bases, short-patch or long-patch BER is initiated by DNA polymerase and completed by DNA ligase. AP: Apurinic/apyrimidinic; XRCC1: X-ray cross complementing protein-1; FEN-1: flap endonuclease-1. (From Apurva Barve et, al. 2021)

1.2.1.2 NER (Nucleotide excision repair)

NER is the most flexible DNA repair pathway, coping with a large number of small base lesions and bulky adducts produced by radiation or some cancer chemotherapeutic agents (Buschta-Hedayat et al., 1999). As mentioned before, AP site lesions are mainly repaired by BER pathways. However, some AP site lesions cannot be repaired by BER pathways, can be repaired by NER pathways (Kitsera et al., 2019, Swanson et al., 1999). NER includes two differentially regulated sub-pathways transcription coupled repair (TC-NER), where the actively transcribed strands of genes are given preference for repair, and global genome repair (GG-NER), where both the non-transcribed strands of a transcribed gene, as well as non-transcribed regions of the genome are repaired (Lindahl and Wood, 1999)(Figure 1.4). In GG-NER, the XPC–hHR23B protein complex recognises the damage over the entire genome (Sugasawa et al., 1998). TC-NER is initiated by the recognition of damage by the stalling of RNA polymerase II at a lesion on the transcribed DNA strands(Lainé and Egly, 2006). The basic mechanism of NER contains several steps: the recognition of damaged sites, a dual incision on both sides of the lesion, the removal of the damaged oligonucleotide, resynthesis to fill the gap and ligation (Wood, 1997).

In global genome nucleotide excision repair (GG-NER), the damage sensor XPC, in complex with UV excision repair protein RAD23 homologue B (RAD23B) recognizes the DNA lesion(Sugasawa et al., 1998). While in the transcription-coupled NER (TC-NER), damage is indirectly recognized during transcript elongation by the stalling of RNA polymerase II at a lesion(Lainé and Egly, 2006). After damage recognition, the TFIIH (transcription initiation factor IIH) complex is recruited to the lesion in both GG-NER and TC-NER(Volker et al., 2001). During the DNA helix unwinding step, the XPF–ERCC1 heterodimer binds to the damaged strand and create an incision 5′ to the lesion, while XPG create an incision 3’ to the lesion(Volker et al., 2001). DNA polymerases POLD/E is recruited and finally the NER reaction is completed through sealing the final nick by DNA ligase 1(Barnes et al., 1992) or DNA ligase 3(Paul-Konietzko et al., 2015).

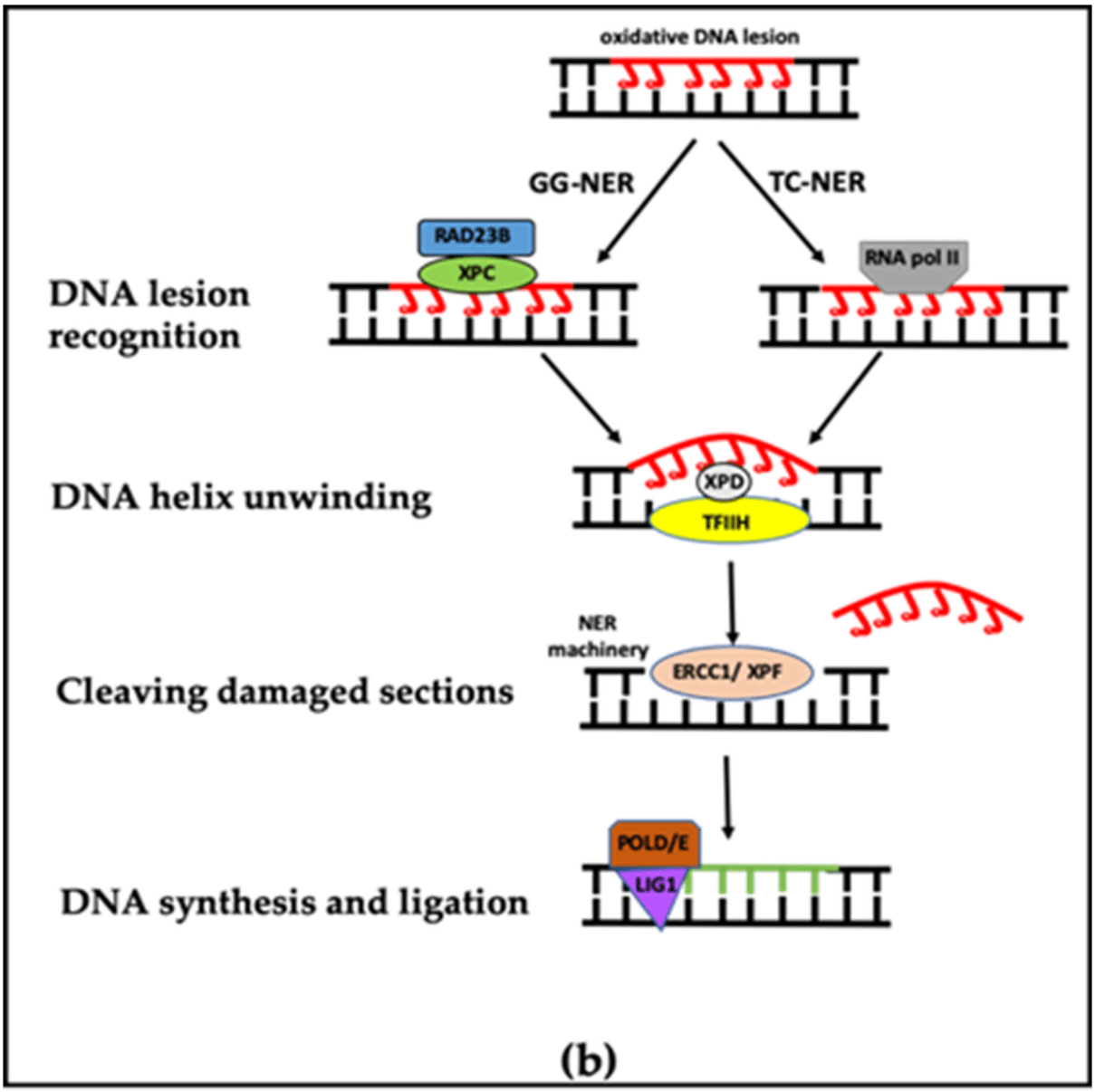

Figure 1. 4 NER pathways

The pathway is divided in two sub-pathways: global genome nucleotide excision repair (GG-NER) recognizes lesions anywhere in the genome, whereas transcription-coupled repair (TCR) recognizes only lesions in actively transcribed genes. The reaction consists of: (1) DNA damage recognition; (2) DNA unwinding through the activity of the XPD and TFIIH; (3) dual incision at the two sites of the mismatch, performed by the heterodimer endonucleases ERCC1/XPF; (4) DNA synthesis by a DNA polymerase POLD/E; (5) DNA ligation carried out by DNA ligase 1 during the S phase of the cell cycle or Ligase 3/XRCC1 complex throughout the cell cycle. (From Richard D. Wood, 2021)

1.2.1.3 MMR (Mismatch Repair) pathway

MMR is primarily responsible for repairing the mismatches and insertion/deletion mispairs in DNA base generated during DNA replication and recombination, and therefore, prevent mutations(Modrich and Lahue, 1996). Human MMR proteins include hMLH1, hMSH2, hMSH6 and hPMS2 which are the most common and frequently studied (Vasan et al., 2019). During MMR (Figure 1.5), MutSα (a heterodimer of MSH2-MSH6) or MutSβ (a heterodimer of MSH2 and MSH3) start DNA repair by recognising a DNA mismatch error and subsequently allow the recruitment of MutL (a heterodimer of MLH1-PMS2) protein complexes as well as proliferating cell nuclear antigen (PCNA) and replication factor C (RFC)(Pećina-Šlaus et al., 2020). This assembly will initiate endonuclease activity of PMS2 which makes single strand breaks near the mismatch. Exonuclease 1 (EXO1) removes the error from the daughter strand; DNA polymerases contributes to DNA synthesis; and finally, DNA ligase 1 (LIG1) joins up the gaps in the DNA sequence(van Oers et al., 2010).

1.2.1.4 DSB repair: HR (Homologous recombination) and NHEJ (non-homologous end joining)

There are two main pathways responsible for the repair of DSBs: HR (Homologous Recombination) and NHEJ (Non-Homologous End Joining) (Kozlov, 2017). And NHEJ pathways can be further divided into classical-NHEJ (c-NHEJ) and alternative-NHEJ (a-NHEJ)(Frit et al., 2014) (Figure 1.6).

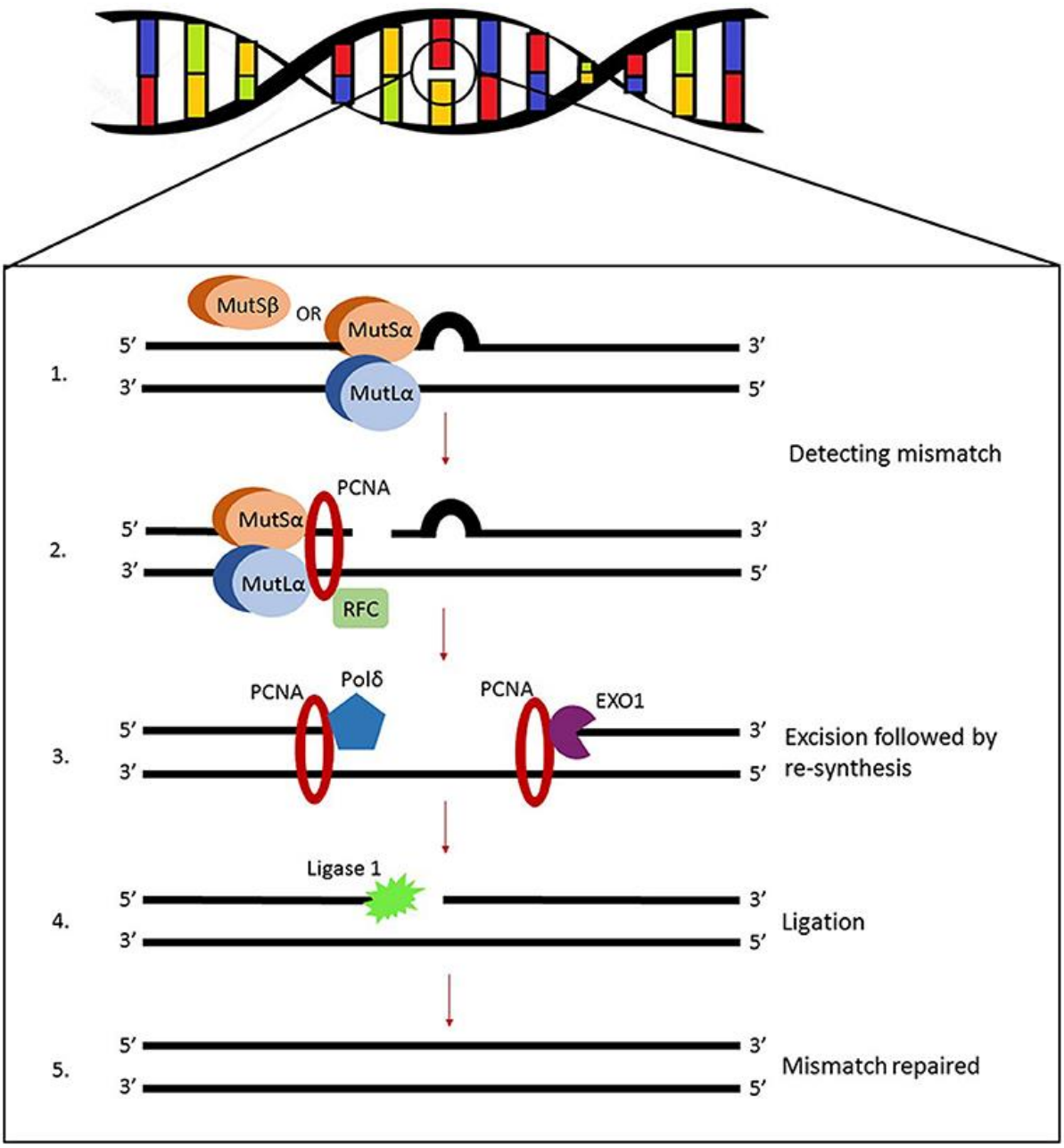

Figure 1. 5 Mismatch repair (MMR) pathway

MutSα or MutSβ recognizes a DNA replication error and subsequently allows the recruitment of MutLα as well as PCNA and RFC. The assembly will initiate endonuclease activity of PMS2 which makes single strand breaks near the mismatch. EXO1 removes the error from the daughter strand; DNA polymerases contributes to DNA synthesis; and finally, DNA ligase 1 joins up the gaps in the DNA sequence.

PCNA: proliferating cell nuclear antigen; RFC: replication factor C; EXO1: Exonuclease 1. (From Nives Pećina-Šlaus, et al, 2020)

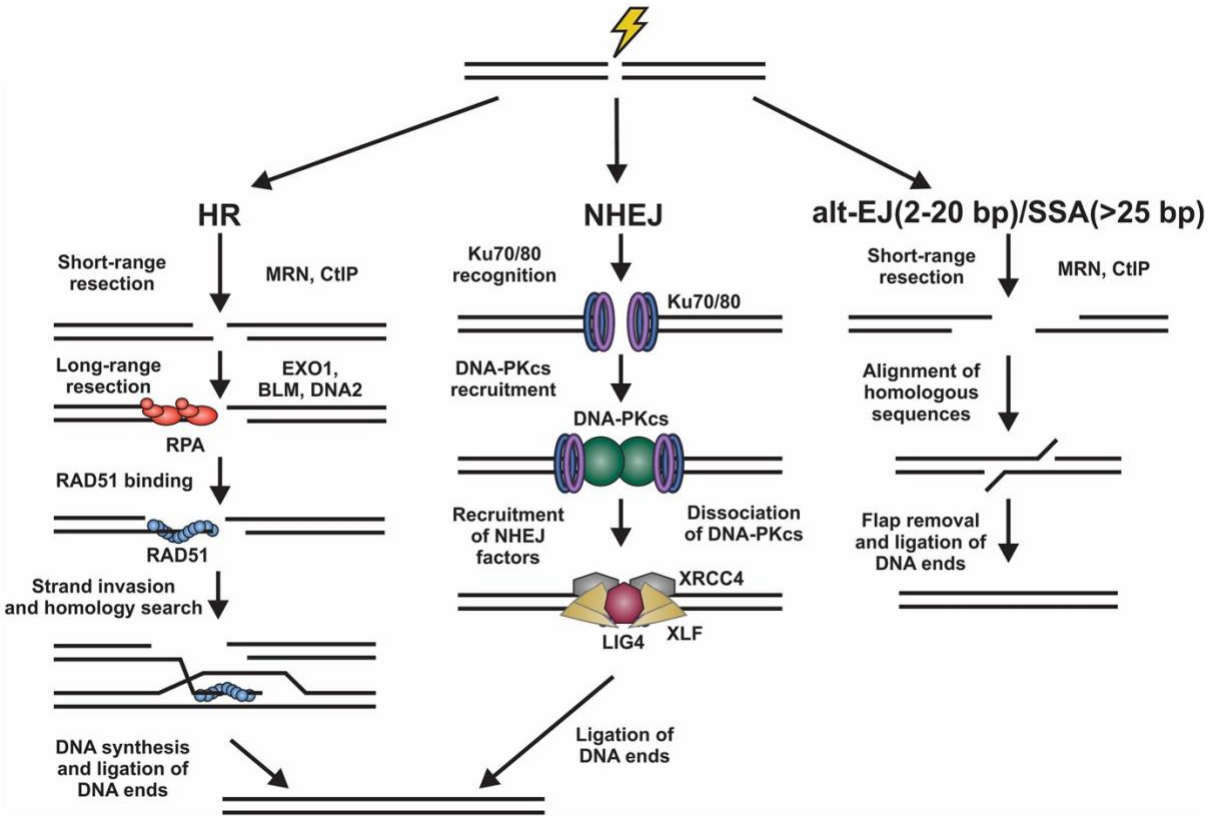

Figure 1. 6 The repair of DSBs by HR and NHEJ pathways

In HR pathways, the MRN-CtIP-complex starts resection on the breaks to generate ssDNA. The ssDNA is first coated by RPA, which is subsequently replaced by Rad51 with the help of BRCA2. These Rad51 nucleoprotein filaments mediate strand invasion on the homologous template. In NHEJ pathways, the Ku70/80 heterodimer recognizes the DNA ends, which recruits DNA-PKcs. If the ends are incompatible, nucleases such as Artemis can trim the ends. Further, the XRCC4-DNA Ligase IV-XLF ligation complex seals the break.

DSBs: Double strand breaks; HR: NHEJ MRN: Mre11/Rad50/Nbs1; XRCC4: X-ray cross complementing protein; ssDNA: single strand DNA; RPA: Replication protein A. (From Stephanie M. Ackerson, et al. 2021)

The first step in HR is to clean up the ends of the DSB by nucleolytic resection in the 5' to 3' direction by the Mre11/Rad50/Nbs1 (MRN) complex (Dudás and Chovanec, 2004). The MRN recognises DNA damage, and alongside with C-terminal binding protein interacting protein (CtIP), promotes the resection of 5′ strands to generate 3′ single-stranded generate a 3' single strand DNA (ssDNA) tail (Dudás and Chovanec, 2004, Chen et al., 2008). Each component of MRN has different function. For example, Mre11 has inherent endonuclease activity and 3' to 5' exonuclease activity, RAD50 promote the unwinding of DNA through its ATPase action and Nbs1 is crucial for signalling from damage sensors to the MRN complex (Paull and Gellert, 1999). The MRN: BRCA1: CtIP complex is important for initiation of DSB repair by HR (Chen et al., 2008). BRCA1 binds CtIP via its BRCT domains located at the C terminus of the protein, which also promotes the binding of BRCA1 to MRN, whilst CtIP also binds Nbs1 directly (Chen et al., 2008). Thus, the MRN: BRCA1: CtIP complex promotes the resection of 5′ strands to generate 3′ single-stranded generate a 3' single strand DNA (ssDNA) tail. This newly generated ssDNA is further elongated by multiple nucleases and DNA helicases, such as EXO1, DNA2, and BLM to extend the 3′-ssDNA for HR-mediated repair (Huertas and Jackson, 2009). ssDNA is highly unstable and is quickly bound by RAD52 (Parsons et al., 2000) and Replication Protein A (RPA) (Kim et al., 1994). RAD51 as a recombinase, replaces RPA in a BRCA1 or BRCA2 dependent process (Moynahan et al., 2001), ultimately performs the recombinase reaction using a homologous DNA sequence template (Tavares et al., 2019, Krajewska et al., 2015). BRCA1 directly interacts with PALB2 and recruits BRCA2/RAD51 to DSB sites to form RAD51-ssDNA filaments for strand invasion (Sy et al., 2009, Zhang et al., 2009). BRCA1 functions in two distinct steps: (1) 5′ to 3′ resection of DSBs to generate 3′ ssDNA overhangs, and (2) loading of the RAD51 recombinase onto the ssDNA.

NHEJ repairs DSBs without using a homologous DNA sequence template. In NHEJ, when DSBs are generated, abundant Ku70 and Ku80 form into a heterodimer and recognise the DSBs with high affinity, then the heterodimer Ku70/80, damaged DNA and DNA-PKcs forms a DNA-PK complex (Spagnolo et al., 2006). If necessary, the ends can be trimmed by

nucleases (such as Artemis) or filled in by DNA polymerases Pol λ and Pol μ to create compatible ends. The DNA ligase IV complex, consisting of the catalytic subunit DNA ligase IV (Lig4), its cofactor XRCC4, and XRCC44 like factor (XLF), perform the ligation step of repair (Chang et al., 2017). NHEJ can participate in the process of DSBs repair when HR is absent, for example, in cell cycle phase G2/M NHEJ is elevated, while HR is absent(Mao et al., 2008). However, there is evidence which showed that HR and NHEJ can not only compete for the repair of the same DNA lesion but also collaborate in the repair of distinct lesions(Orii et al., 2006).

The regulation of pathway choice during DSB repair depends on multiple variables, and one of the main determinants is the cell cycle phase (Shrivastav et al., 2008). For example, during S-phase or G2, the DSB formation triggers a DNA damage checkpoint that prevents cells from progressing through mitosis which activates HR, whereas NHEJ predominates in G1 when homologous template is unavailable (Karanam et al., 2012). Other studies also suggested that in G2 phase, NHEJ is the preferred pathway when DSB repair proceeds rapidly if rapid rejoining does not ensue, then resection occurs promoting repair by HR (Shibata et al., 2011).

1.2.2 Cell cycle

The cell cycle is a series of tightly integrated events includes different stages, G1, S, G2, and M that allow the cell to grow and proliferate (Otto and Sicinski, 2017). G1, also known as the first phase, is the phase in which the cell grows physically larger, in preparation for DNA replication, copies organelles, and synthesizes mRNA and protein that are required for DNA synthesis in next step (Darzynkiewicz et al., 1980). When mitosis begins, cells transit into S phase where DNA replication occurs in this phase (Reddy, 1994). During the G2 phase, the cells grow more, proteins and organelles are synthesized, and prepare for mitosis (Bender and Prescott, 1962). And chromosome segregation occurs in the M phase (Jackman and Pines, 1997). After the M phase, cell division occurs, and the cell cycle can begin again.

1.2.2.1 Cyclin-Dependent Kinases (CDKs) and cyclin-dependent kinase inhibitors (CKIs)

This four-phase process is controlled by the regulated activity of numerous Cyclin-Dependent Kinases (CDKs) and their cyclin partners (Lundberg and Weinberg, 1998, Tsutsui et al., 1999, Pagano et al., 1993), which positively regulate or accelerate cell cycle progression; whereas, cyclin-dependent kinase inhibitors (CKIs) are acting to repress cell cycle progression in response to regulatory signals (Besson et al., 2008). Cyclin D–CDK4/CDK6 is associated with the G1 transition, cyclin E–CDK2 is associated the G1/S transition, Cyclin A–CDK2 is with S phase, and Cyclin B–CDK1 is with the G2/M transition (Moiseeva et al., 2019). Different CKIs inhibit different CDKs respectively. The Ink4 family including p16 ^{Ink4a}, p15 ^{Ink4b}, p18 ^{Ink4c}, and p19 ^{Ink4} can interrupt the association with cyclin D by binding to CDK4/6 and therefore, inhibit the activities of CDK4/6 (Cánepa et al., 2007). The Kip family includes p21 ^{Waf1}, p27 ^{Kip1} and p57 ^{Kip2} can block the activities of CDKs by binding to cyclin and CDK subunits (Besson et al., 2008). Moreover, CDK1 and CDK2 are also negatively regulated by Wee1 and CDC25A. (Figure 1.7).

1.2.2.2 Cell cycle checkpoints in response to DNA damage

In the G1/S phase, DNA damage leading primarily to DSBs is sensed by the MRN which activates ATM. p53 is released and stabilized from the inhibition of MDM2 (Li and Kurokawa, 2015), then p53 is phosphorylated by the Ataxia-telangiectasia mutated (ATM) kinase (Banin et al., 1998, Saito et al., 2002). The activation of p53 in turn induce a large variety of transcriptional targets, such as p21 (Harper et al., 1995). Accumulated p21 inhibits cyclin–CDK complexes including cyclinE-CDK2 and cyclinA-CDK4/6. Studies found CDK4/6 is responsible for the induction of the phosphorylation of RB, which disrupt the interaction of RB/E2F, while CDK2 activation can trigger the hyperphosphorylation of Rb (Lundberg and Weinberg, 1998), therefore, ultimately inhibits the release of E2F and block cell cycle progression.

The activation of ATM also phosphorylates the CHK2 kinase, which in turn phosphorylates the CDC25A protein(Falck et al., 2001), ultimately results in cyclin A/CDK2 inactivation and

arrest in G1/S phase. During S phase, in responds to DNA damage, ATM is activated, and ATM also results in cyclin A/CDK2 inactivation via ATM/CHK2/CDC25A pathways(Falck et al., 2001). The G2/M checkpoint prevents cells with an incomplete or damaged genome to enter mitosis. In response to DNA damage induced during S phase, the G2/M checkpoint is activated via the phosphorylation of CHK1 by Ataxia telangiectasia and Rad3 related (ATR) and CHK2 by ATM respectively. G2/M is dependent upon the action of ATR for activation, whereas ATM is dispensable, apart from when the checkpoint is triggered by damage that occurs during the G2 phase itself. (Figure 1.8)

1.2.3 DNA Replication stress response

DNA replication stress corresponds to the slowing down or stalling of the replication fork progression and/or DNA synthesis (Zeman and Cimprich, 2014). Both exogenous and endogenous sources can cause the stalling of replication forks, and in respond to the replication stress, different signalling pathways are activated. Sources of replication stress include depletion of nucleotide pools, oncogene-induced stress (such as that mediated by Myc), RNA:DNA hybrids, and R-loops (three-stranded nucleic acid structure containing an RNA:DNA hybrid and a displaced ssDNA strand may interfere with replication and cause DNA damage)(Zeman and Cimprich, 2014). Conflicts between replication and transcription complexes are also one of the sources of replication stress (Bermejo et al., 2012). In addition, DNA crosslinks which could be repaired by Fanconi Anemia (FA) pathway, G-quadruplexes, secondary structures which form in GC-rich DNA, and considered as hard to replicate regions, and the misincorporation of ribonucleotides into replicating DNA (Ubhi and Brown, 2019) all can cause DNA replication stress (Figure 1.9 A).

DNA replication stress results in aberrant replication fork, which generate a variety of responses, including an increase in ssDNA (Feng et al., 2011, Byun et al., 2005). The replication protein A (RPA) binds to ssDNA, which recruit a number of replication stress response proteins (Maréchal and Zou, 2015). RPA acts as a platform for the recruitment of sensor proteins, such as ataxia telangiectasia and Rad3-related (ATR)-interacting protein

(ATRIP), topoisomerase II binding protein 1 (TOPBP1), and Ewing tumour-associated antigen 1 (ETAA1). This promotes the recruitment and activation of the central replication-stress-response kinase ATR, and activates its downstream effectors to either restart replication or lead to fork collapse (Berti and Vindigni, 2016) (Figure 1.9 B). Fork restart is thought to be driven by the meiotic recombination 11 (MRE11) and DNA2 (Costanzo et al., 2001, Thangavel et al., 2015). Studies suggest that PARP1 and the histone methyltransferase complex PTIP/mixed-lineage leukaemia protein 3 et 4 (MLL3/4) promote the recruitment of MRE11 to stalled forks (Bryant et al., 2009). It has also been shown that BRCA2 plays as a protector in the processing of replication forks (Fradet-Turcotte et al., 2016). Moreover, the stalled fork protection does not depend on the ability of BRCA2 to interact with DNA, and is to load and stabilise polymerized RAD51 instead (Schlacher et al., 2011). Otherwise, collapse of the fork into double-stranded DNA breaks, in the presence of underlying deficiencies of double-stranded DNA breaks repair, may drive the cell towards apoptosis or senescence (Cannan and Pederson, 2016).

DNA replication stress primarily occurs during S phase, results in consequences during mitosis. Therefore, ATR is activated during S or G2 phase normally, which also activate ATR downstream CHK1. The key G1/S transition regulator p53 is often deficient in tumour cells, therefore, the G2/M checkpoint is crucial to prevent tumour from entering mitoses.

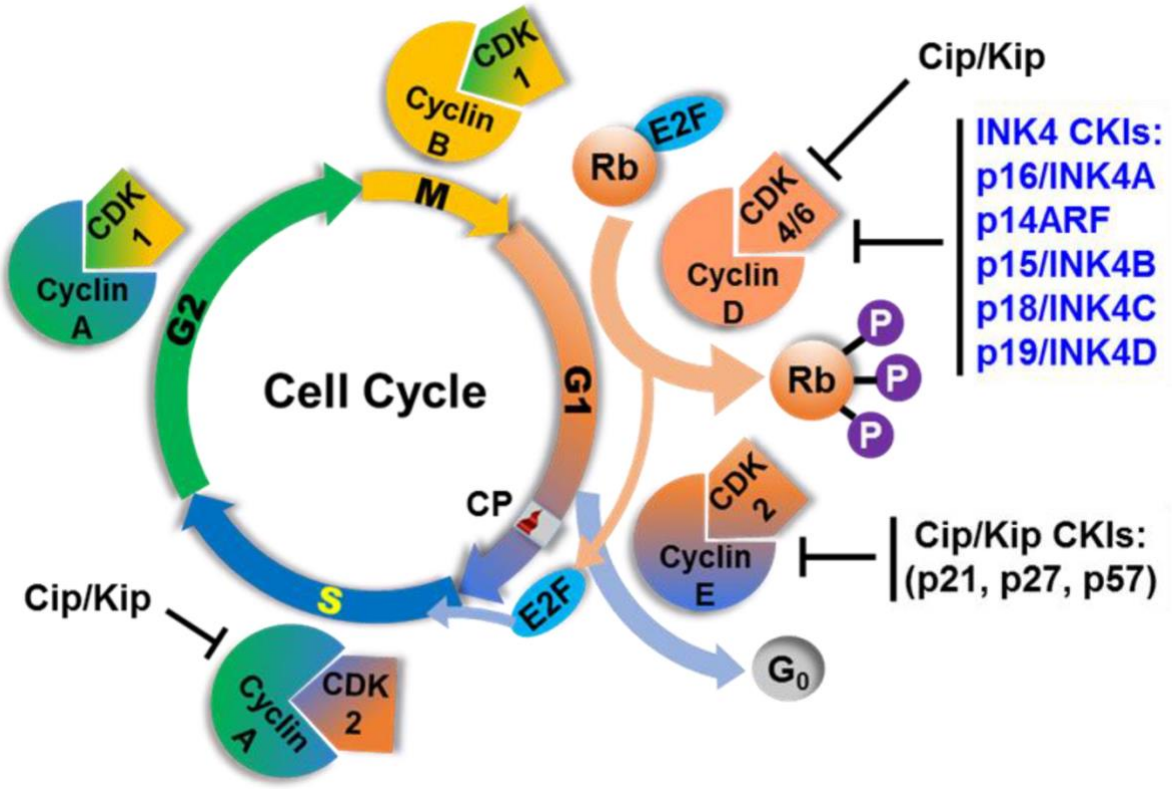

Figure 1. 7 The cell cycle, Cyclin-CDKs and CKIs

The cell cycle includes four distinct phases, G1, S G2, and M. Each colour represents a distinct phase or CDKs and CKIs involved in a specific phase. Cyclin D–CDK4/CDK6 is associated with the G1 transition, cyclin E–CDK2 is associated the G1/S transition, Cyclin A–CDK2 is with S phase, and Cyclin B–CDK1 responsible for the G2, G2/M transition, and M phase.

CDKs: Cyclin-Dependent Kinases; CKIs: Cyclin-dependent kinase inhibitors. (From Farruk Lutful Kabir, et al. 2016)

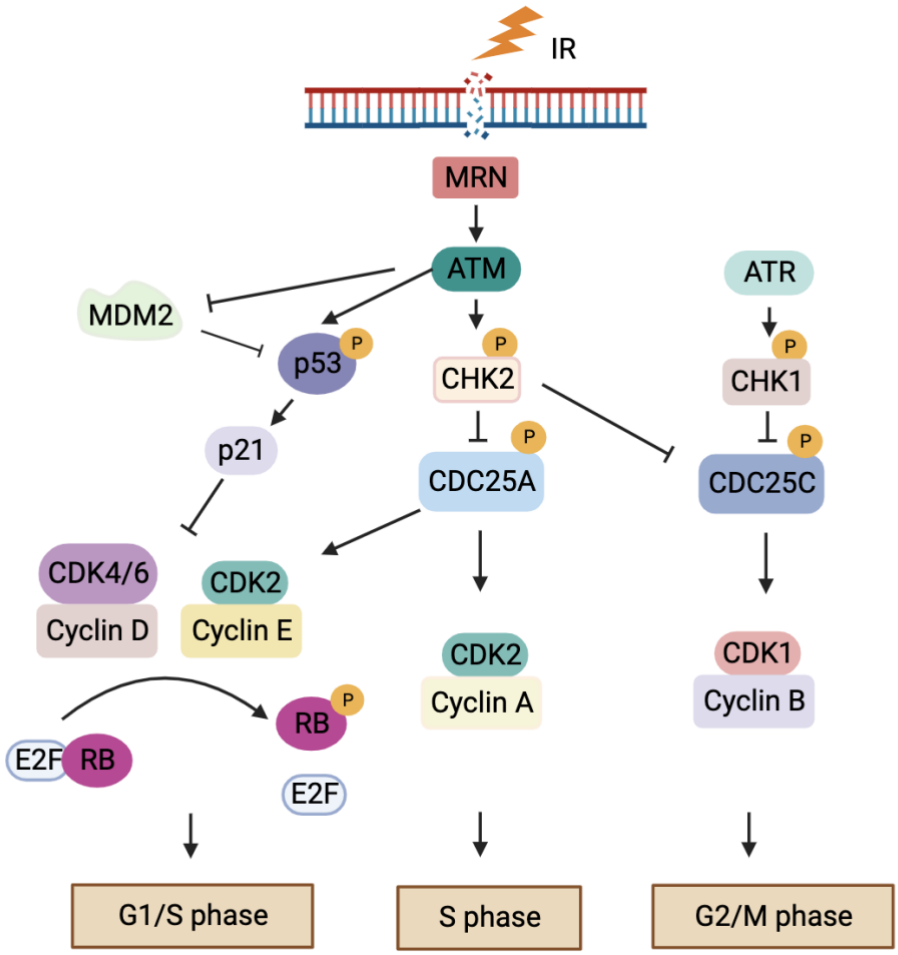

Figure 1. 8 The cell cycle checkpoint response to DNA damage

In response to DNA damage such as IR induced DNA damage, the cell activates ATM. ATM phosphorylates p53, CHK2, therefore further activate their downstream targets and lead the cell cycle arrest. ATR is also activated respond to DNA damage in G2/M phase. MRN: Mre11, Rad50 and Nbs1 complex; MDM2: Mouse double minute 2 homolog. (Created from Biorender.com)

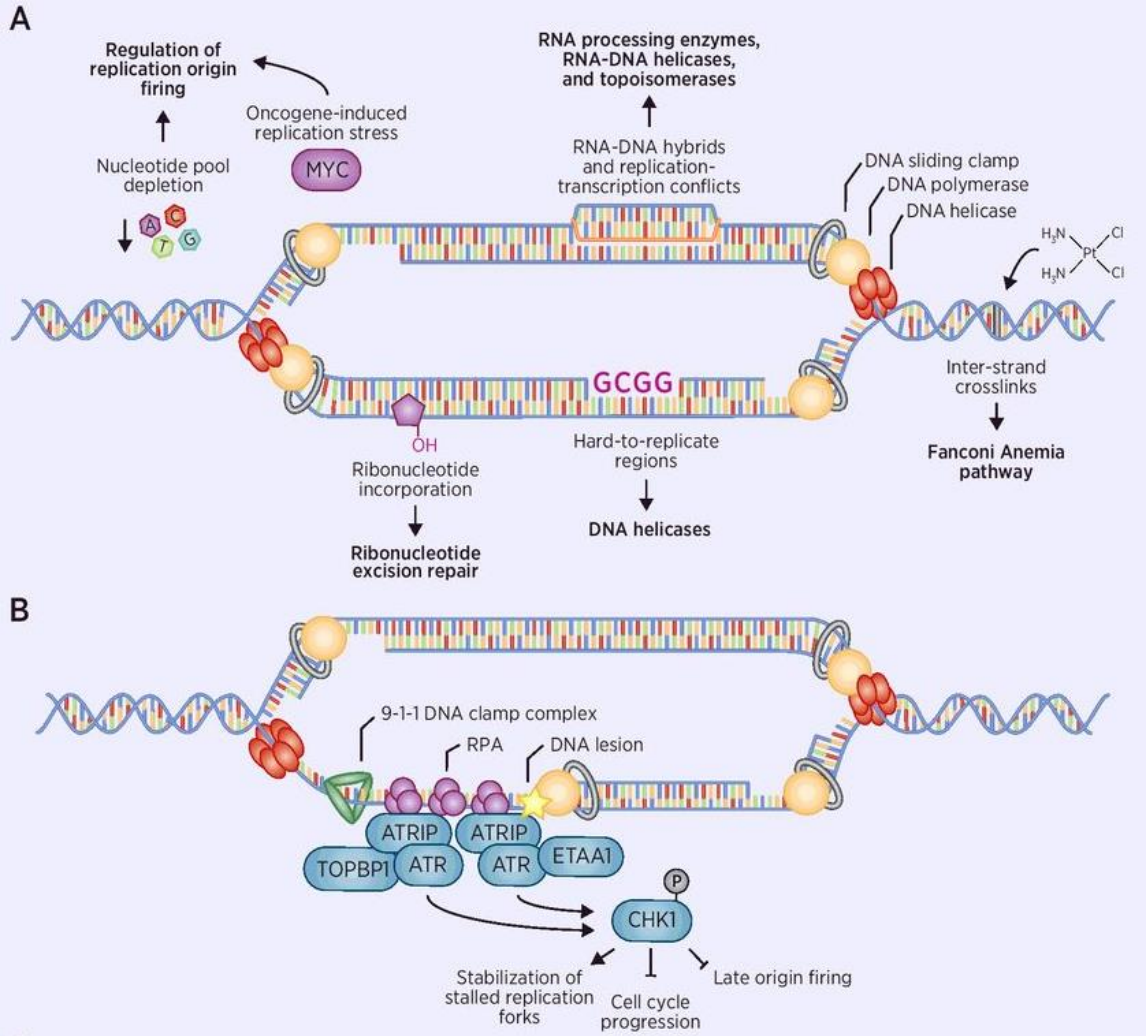

Figure 1. 9 DNA replication stress

A. Sources of replication stress; B. Replication stress activates signalling response. (From Tajinder Ubhi, et al. 2019)

1.3 Radiotherapy and key principles of radiobiology

In the past decade, RT has become one of the major therapeutic approaches in cancer treatment, with 40% of patients have radiotherapy as part of their treatment (Dilalla et al., 2020). For example, radiotherapy is used in all stages of lung cancer treatment and is required at least once in over half of patients (Brown et al., 2019). It can also be used in combination with surgery or chemotherapy, which has become a highly effective treatment. As outlined in Section 1.1.4, RT is also used as a therapeutic approach in breast cancer. Moreover, a study estimated the number of 5-year cancer survivors treated with radiation between 2000 and 2030, showed that a large increase will be seen in the number of cancer survivors treated with radiation (Bryant et al., 2017).

1.3.1 Radiation causes DNA damage

Ionising radiation (IR) is a type of high-energy radiation that releases electrons from atoms and molecules generating ions which can break covalent bonds.

DNA is the primary target of radiation in the cell during radiotherapy (Coleman and Turrisi, 1990). Radiotherapy causes extensive amounts of DNA damage, which the cancer cells are unable to effectively repair, leading to cell death (Coleman and Turrisi, 1990, Dunne-Daly, 1999). Specifically, radiation can destroy cancer cells by either a direct effect or indirect effect (Baskar et al., 2014) (Figure 1.10). In the direct effect, the ionised electrons are absorbed by cancer cells and damage DNA via direct energy deposition. In the indirect effect, the ionised electrons interact with water molecules, leading to water radiolysis, which produce highly reactive free radicals, which can then cause damage to DNA(Baskar et al., 2014). Oxygen is required to chemically modify DNA (Oxygen fixation hypothesis) (Howard-Flanders and Moore, 1958, Ewing, 1998). The extensive DNA damage is not repairable repaired leads to cell death (Baskar et al., 2014). A variety of DNA lesions can be induced by IR, which include base damage, Single strand break (SSB), double strand break (DSB), and cross-linkage with protein or DNA (Figure 1.10).

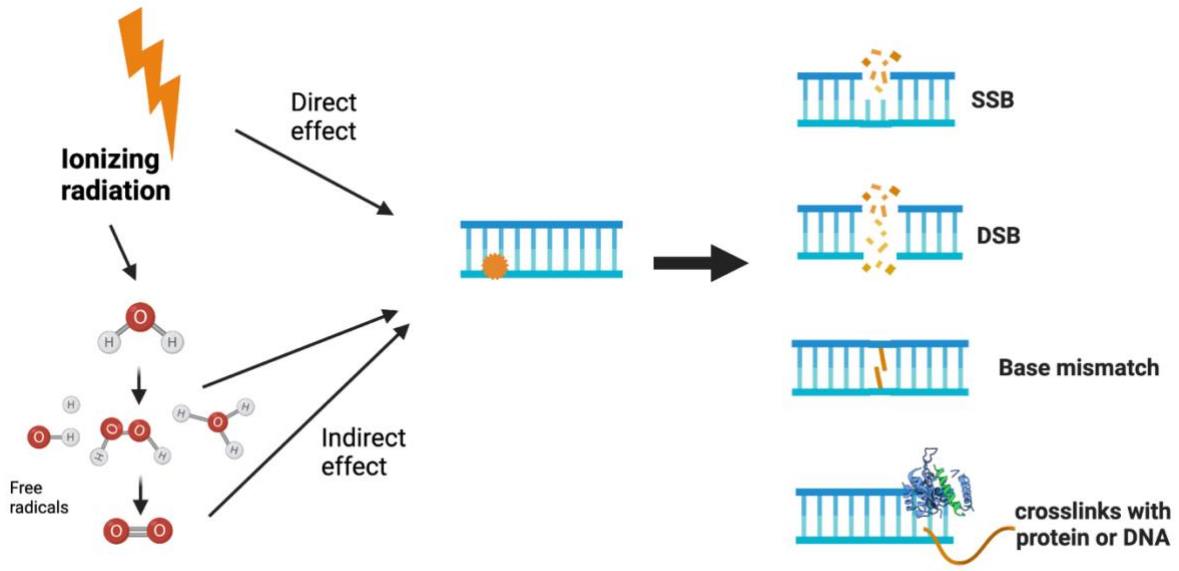

Figure 1. 10 Radiation causes DNA damage directly and indirectly

Ionizing Radiation (IR) damages DNA by direct effect and indirect effect. In direct effect, radiation is absorbed by cancer cells and lead to DNA damage directly. In indirect effect, high-energy radiation can affect the water molecules, which can produce highly reactive free radicals, and damage DNA indirectly, therefore lead to cancer cells death. SSB: Single strand break; DSB: Double strand break. (Generated from Biorender.com)

1.3.2 DNA damage repair pathways respond to DNA damage induced by IR

Most DNA damage induced by IR consists of DNA base damage and SSBs, which are normally repaired through the BER pathway (Hegde et al., 2008). Details of BER repair pathway see Session 1.2.1.1. DSBs is also a major type of DNA damage caused by IR and is primarily responsible for IR-induced cell death (Vignard et al., 2013). As mentioned in Session 1.2.1.4 and Session 1.2.2.2, DSBs are repaired either by NHEJ pathways which including c-NHEJ and a-NHEJ throughout the cell cycle or by HR during the S phase and G2 phase (Pannunzio et al., 2018, Archange et al., 2008). DNA damage repair pathways respond to DNA damage induced by IR are summarized in Figure 1.11.

1.3.3 The 4Rs of Radiotherapy

The 4Rs of radiotherapy describe the radiobiological rationale for fractionated radiotherapy and include Repair, Reassortment, Repopulation, and Reoxygenation (Withers, 1975). Later, Radiosensitivity was added as the 5th R of radiobiology (Steel et al., 1989). Balancing these biological effects by either increasing radiation damage in the tumour cells or decreasing the damage to the normal tissues has become one of the strategies to maximise the therapeutic outcome to RT.

Repair refers the capacity to repair radiation-induced DNA damage or normal vs tumour tissue and it influences the biological effects of dose rate and time between fractions (Steel et al., 1989, Sachs et al., 1997). There are three types of damages to cells, including lethal damage, which leads to the death of the cell; sublethal damage, which can be repaired if given some time to do so; and potentially lethal damage when cells can recover under certain circumstances such as time(Bedford, 1991). For normal tissue cells, it is beneficial for the treatment if the damage can be repaired. On the other hand, for tumour cells, post-radiation survival allows them to proliferate.

Reassortment (or Redistribution) refers to the different cellular radiosensitivity at different stages of the cell cycle. G2/M has been found to be the most sensitive stage to radiotherapy, while the late S phase is considered the most resistant (Sinclair, 1968).

Another factor influencing the adaptation of fractionation in radiotherapy is *Reoxygenation*. Low oxygen (hypoxic) tumour tissue is relatively resistant to radiation (Crabtree et al., 1933). During radiotherapy, oxygen is necessary to chemically modify free radicals to target DNA. Under normoxia, oxygen quickly interacts with the free radicals, causing strand breaks that lead to permanent DNA damage. In hypoxic conditions, the DNA radicals are reduced by compounds containing sulfhydryl groups (SH groups), which restore the DNA to its original form. Oxygen can 'fix' the radiation-induced damage into a permanently irreparable state, a concept known as the oxygen fixation hypothesis, as depicted in Figure 1.12. The surviving hypoxic cells after a fraction of radiotherapy are likely to become reoxygenated, and this increase in oxygenation makes the hypoxic cells more radiosensitive. The oxygen effect is often quantified by the oxygen enhancement ratio (OER), which describes the ratio of doses with oxygenation and hypoxia generating the same biological effect (Hall and Giaccia, 2006, Wenzl and Wilkens, 2011).

Repopulation refers to the surviving tumour cells after radiation proliferate rapidly and fractionation allows normal tissues to repopulate or regenerate. Effective suppression of tumour cell repopulation is one of the key factors for the success of radiotherapy.

Radiosensitivity is considered the 5th R, which refers to the fact that the response to radiation varies based on tumour intrinsic and individual radiosensitivity, as well as tissue-specific characteristics. Sensitiser-enhancement ratio (SER) is the ratio of the radiation dosage required to decrease the survival fraction to 50% in the absence of sensitizer to the dose required to achieve the same survival fraction with sensitizer.

Lately, a 6th R of radiobiology has been under consideration, namely the *reactivation of the anti-tumour immune response* (Boustani et al., 2019). RT has the ability to modify the tumour microenvironment and activate an anti-tumour immune response, providing a new strategy for combining radiotherapy and immunotherapy.

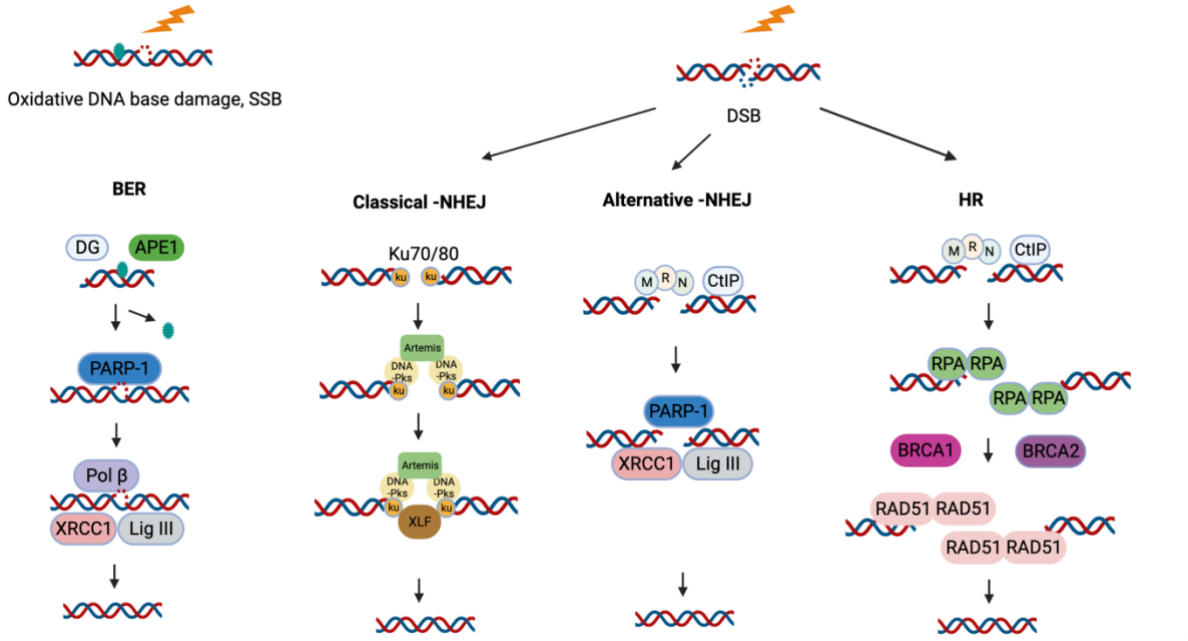

Figure 1. 11 DNA damage repair pathways respond to DNA damage induced by Ionizing Radiation

DSBs: DNA double-strand breaks; DNA-PK: DNA-dependent protein kinase; NHEJ: non-homologous end joining; ATM: Ataxia-telangiectasia mutated; HR: Homologous recombination; BRCA1/2: BReast CAncer gene 1/2; RAD51: DNA repair protein RAD51 homolog 1; SSBs: DNA single-strand breaks; BER: Base excision repair; ssDNA: single strand DNA; RPA: replication protein A; ATR: Ataxia telangiectasia and Rad3-related; CHK1: Checkpoint kinase 1; CHK2: Checkpoint kinase 2. (Created from Biorender.com)

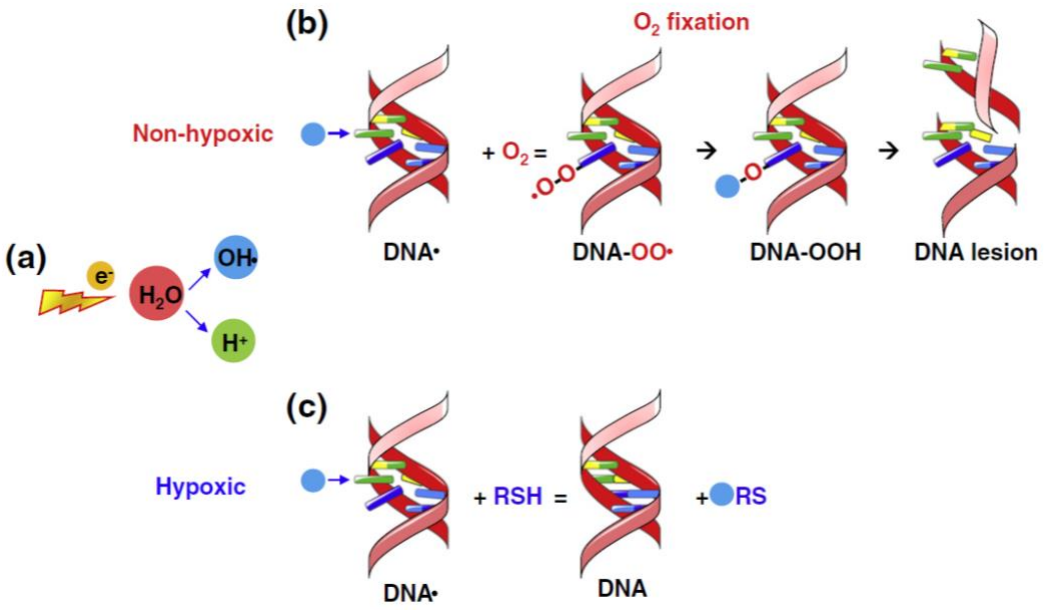

Figure 1. 12 The oxygen fixation hypothesis

(a) Ionizing radiation interacts with water molecules and produce ROS, (b) Under normoxic conditions, oxygen is required and assists the stabilization of ROS- mediated DNA damage, which results in double-strand breaks. (c) Under hypoxic conditions, the lack of oxygen enables reduction of ROS by cellular thiol groups that impedes the generation of double strand breaks. OH•, hydroxyl radical; O•, oxygen atom bearing an unpaired electron; SH, thiol groups. (From Sergio Rey et al., 2017)

1.3.4 The linear-quadratic (L-Q) model

The linear-quadratic (LQ) model is a most commonly used tool for quantitative predictions of dose or fractionation dependencies in radiotherapy (Fowler, 1989). It has been shown that the LQ model reasonably predicts normal tissue dose–response relations in the dose per fraction range of 1.8 to 20 Gy both *in vitro* and *in vivo* (Brown et al., 2014). The L-Q model also provides standard method for modelling the relationship between cell survival and radiation delivered dose with the formula: SF = e-(αD+ βD2) (Fowler, 1989). Here, SF represents the surviving fraction of cells, D is the single-fraction dose, and α and β are the linear and quadratic coefficients. α is proportional to the dose (linear), assuming that at low doses, a single electron causes a Double Strand Break (DSB). β is proportional to the square of the dose (quadratic), assuming that DSBs may occur due to 2 independent electrons. This relationship can be plotted into a quadratic response curve, with survival typically represented on a logarithmic scale, as shown in Figure 1.13. The α/β value corresponds to the dose at which the linear α and quadratic β contributions are equal defining the degree of curvature of the survival curve (McMahon, 2018). A low α/β value indicates a pronounced fractionation effect, meaning a significant increase in tolerance or effectiveness with a reduction in dose per fraction, while a high α/β value, in contrast, suggests a minor fractionation effect. As shown in Figure 1.13, with increasing dose, high α/β cell lines (solid line) exhibit nearly constant rates of cell killing, while low α/β lines (dashed line) display a pronounced curvature, resulting in greater cell killing per unit dose at higher doses (3 Gy onwards). At low doses, the response is primarily driven by one-hit events, whereas at higher doses, multi-hit killing becomes more important. These effects are balanced when the dose matches the α/β ratio of the cell line (5 Gy in the example below) (McMahon, 2018). Radiosensitizing agents that selectively sensitize tumour cells without affecting normal tissue cells would provide therapeutic benefits (Franken et al., 2013).

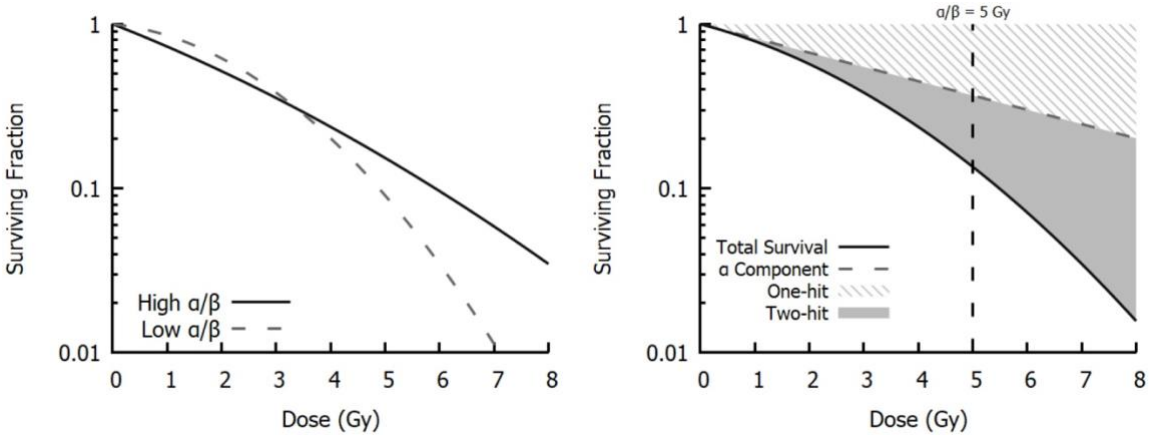

Figure 1. 13 Illustration of LQ curves.

Left: Responses for cell lines with high and low α/β ratios.

Right: Separation into one- and two-hit kinetics. (From Stephen Joseph McMahon, 2018)

1.4 DDR signalling pathways as targets for radiotherapy sensitisation in cancer

In the past decades, efforts have been made to increase the effectiveness of therapies by combination radiotherapy and/or chemotherapy with other targeted therapies (Nguyen et al., 2002, Jagodinsky et al., 2020). As outlined in section 1.3.4, radiation can trigger a DNA damage response, therefore, targeting DDR signalling pathways has become one of the most effective strategies for overcoming resistance to radiotherapy, and in recent years, some important and breakthroughs have already been achieved (Huang and Zhou, 2020). Recent studies and current clinical trials of chemical inhibitors targeting key DDR proteins, including PARP inhibitors (Sim et al., 2021, Loap et al., 2021), DNA-PK inhibitors (Triest et al., 2018, Romesser et al., 2021), ATM/ATR inhibitors (Reddy et al., 2019, Waqar et al., 2022), CDK inhibitors (DeWire et al., 2018), CHK1/2 inhibitors (Zeng et al., 2017), and WEE1 inhibitors (Kong et al., 2020), especially the combination with radiation. Details see Table 1.2. Clinically relevant DDR targets are summarised in Figure 1.14. Details of how these inhibitors work and the combination with radiation will be further discussed below, with a summary of clinical trials evaluating the combination of targeting DDR pathways and radiation in various cancer showed in Table 1.2. Moreover, a concept called 'Synthetic lethality' has been the focus of recent research(Farmer et al., 2005, Bryant et al., 2005, Bryant and Shall, 2015). This refers to a phenomenon that when two or more genes inactivated together can result in cell death, while a cell with a mutation/inactivation in either gene alone means a cell can survive. The most common example of 'Synthetic lethality' providing therapeutic solutions is the use of PARP inhibitors, which is the first clinically approved drugs to target oncogenic mutations of genes BRCA1/2 tumours (Lord and Ashworth, 2017). Recently, several more studies of synthetic lethality in various DNA repair pathways expanded DDR and DNA repair-targeting clinical strategies, with various DDR inhibitors in preclinical and clinical development (Pilié et al., 2019).

Table 1. 2 Clinical trials evaluating the combination of targeting DDR pathways and Radiation in various cancer

Drug Name	Cancer types	ClinicalTrials.gov Identifier	Clinical trial (recruiting/active/ completed)	Combination with RT	References
PARP-1 inhibitors					
Olaparib	Inflammatory Breast cancer	NCT03598257	Phase II	Radiation	(Michmerhuizen et al., 2019)
Olaparib	TNBC	NCT03109080	Phase I	Radiation	(Kirova et al., 2020)
Olaparib	GBM	NCT03212742	Phase I/IIa	IMRT, TMZ	(Lesueur et al., 2019)
Olaparib	GBM	N/A	Two parallel phase I	Radiation	(Fulton et al., 2018)
Olaparib	NSCLC, BC, HNSCC	NCT01562210 NCT02227082 NCT02229656	Three Parallel Phase I Trials	Radiation, Cisplatin	(de Haan et al., 2019)
Olaparib	NSCLC	NCT04380636	Phase III	Radiation, Cisplatin, Carboplatin, etc.	/
Olaparib	Head and Neck Cancer	NCT02308072	Phase I	IMRT, Cisplatin	(Forster et al., 2016)
Olaparib	Prostate Cancer	NCT03317392	Phase I/II	Radium Ra 223 Dichloride	/
Olaparib	SCLC	NCT04728230	Phase I/II	Radiation, Carboplatin,Durvalumab,Etoposide	/
Olaparib	Pancreatic Cancer	NCT05411094	Phase I	Radiation	/
Olaparib	BRCA Mutant Non-HER2-positive Breast Cancer	NCT02849496	phase II	Atezolizumab, X ray	/
Olaparib	Advanced Solid Tumors	NCT03842228	Phase I	X ray, Copanlisib, MEDI4736 (Durvalumab)	/
Veliparib	Peritoneal carcinomatosis	NCT01264432	Phase I	low dose fractionated whole abdominal radiation	(Reiss et al., 2017)
Veliparib	Brain metastases from NSCLC	NCT01657799	Phase II	WBRT, Placebo	(Chabot et al., 2017)

Veliparib	NSCLC	NCT02412371	Phase I	Radiation, Carboplatin, Paclitaxel	(Kozono et al., 2019)
Veliparib	Rectal cancer	NCT01589419	Phase I	Radiation, Capecitabine	(Czito et al., 2017)
Veliparib	Head and Neck Cancer	NCT01711541	Phase I/II	Radiation, Cisplatin, Carboplatin, etc.	(Jelinek et al., 2018)
Veliparib	Cancer patients with Brain metastases	NCT00649207	Phase I	WBRT	(Mehta et al., 2015)
Veliparib	Pancreatic Cancer	NCT01908478	Phase I	Radiation, Gemcitabine	(Tuli et al., 2019)
Veliparib	Breast Cancer	NCT01477489	Phase I	Radiation	(Jagsi et al., 2018)
Veliparib	Gliosarcoma	NCT01514201	Phase I/II	3D CRT, TMZ	(Baxter et al., 2020)
Veliparib	Gliosarcoma	NCT03581292	Phase II	Radiation, TMZ	/
Veliparib	Lung Adenocarcinoma	NCT01386385	Phase I/II	3D CRT, Carboplatin, Paclitaxel	(Argiris et al., 2019)
Veliparib					
Iniparib	Gliosarcoma	/	Phase I	Radiation, TMZ	(Blakeley et al., 2015)
Iniparib	Glioblastoma	NCT00687765	Phase I/II	Radiation, TMZ	/
Niraparib	Prostate Cancer	NCT04194554	Phase I/II	SBRT, Leuprolide, Abiraterone Acetate	/
Niraparib	NIVIX	NCT03644342	Phase I/II	Radiation	/
Niraparib	TNBC	NCT04837209	Phase II	Radiation, Dostarlimab	/
Niraparib	TNBC	NCT03945721	Phase I	Radiation	/
Niraparib	HPV-negative HNSCC	NCT04681469	Phase II	Radiation, Dostarlimab	/
Niraparib					
Talazoparib	Gynecologic cancers	/	Phase I	Radiation	(Lakomy et al., 2020)
Talazoparib	Recurrent High-grade Glioma	NCT04740190	Phase II	low dose whole brain radiation	/
DNA PK inhibitors					
M3814	Advanced Solid Tumours	NCT02516813	Phase I	Radiation, Cisplatin	(Triest et al., 2018)
M3814	Rectal Cancer	NCT03770689	Phase I/II	Radiation, Capecitabine, Placebo	(Romesser et al., 2020)

M3814	Solid Tumours	NCT03724890	Phase I	Radiation, Avelumab	(Bendell et al., 2019)
M3814	Gliosarcoma	NCT04555577	Phase I	Radiation, Temozolomide	/
M3814	Prostate Cancer	NCT04071236	Phase I/II	Radiation, Avelumab	/
M3814	Advanced/Metastatic Solid Tumours and Hepatobiliary Malignancies	NCT04068194	Phase I/II	Radiation, Avelumab	/
M3814	Localized Pancreatic Cancer	NCT04172532	Phase I/II	Radiation	/
ATM inhibitors					
AZD1390	Brain cancer	NCT03423628	Phase I	Radiation	(Reddy et al., 2019)
AZD6738	Solid tumours	NCT02223923	Phase I	Radiation	(Dillon et al., 2018)
M3541	Solid Tumours	NCT03225105	Phase I	Radiation	(Waqar et al., 2022)
XRD-0394	Advanced Cancer Patients	NCT05002140	Phase I	Palliative radiotherapy	/
ATR inhibitors					
BAY 1895344	Recurrent Head and Neck Cancer	NCT04576091	Phase I	Radiation, Elimusertib	/
AZD673	Leukaemia	NCT01955668	Phase I	Radiation	/
VX-970	HNSCC	NCT02567422	Phase I	Radiation, Cisplatin	/
VX-970	NSCLC brain metastases	NCT02589522	Phase I	WBRT	/
VX-970	Oesophageal Adenocarcinoma Squamous Cell Carcinoma	NCT03641547	Phase I	Radiation, Cisplatin, Capecitabine	(van Werkhoven et al., 2020)
RP-3500	Solid Tumours	NCT05566574	Phase I/II	EBRT	/
Pan-CDK inhibitors					
Alvocidib	Pancreatic Cancer	NCT00047307	Phase I	3D-CRT, Gemcitabine	/
CDK4/6 inhibitors					
Ribociclib	High Grade Gliomas (HGG)	NCT02607124	Phase I/II	Radiation	(DeWire et al., 2018)

Palbociclib	Head and Neck Cancer	NCT03024489	Phase I/II	IMRT, Cetuximab	Annals of Oncology (2019) 30 (suppl_5): v449-v474. 10.1093/annonc/mdz252
Palbociclib	HR+ Breast Cancer Brain Metastases	N/A	Clinical Study	Radiation	(Figura et al., 2019)
Palbociclib Abemaciclib	Breast Cancer Stage IV	NCT03870919	N/A	Radiation	/
CHK inhibitors					
Prexasertib	HNSCC	NCT02555644	Phase I	Radiation, Cisplatin, Cetuximab	(Zeng et al., 2017)
WEE1 inhibitors					
AZD1775	Pancreas Adenocarcinoma	NCT02037230	Phase I/II	Radiation, Gemcitabine	(Cuneo et al., 2019)
AZD1775	Glioblastoma	NCT01849146 NCT01922076	Phase I	Radiation, TMZ	(Alexander et al., 2017)
AZD1775	Cervical cancer	NCT01958658	Phase I	Radiation, Cisplatin	/
AZD1775	HNSCC	ISRCTN76291951 NCT03028766	Phase I	Radiation, Cisplatin	(Kong et al., 2020)
AZD1775	Cervical, Upper Vaginal and Uterine Cancers	NCT03345784	Phase I	Radiation, Cisplatin	/
AZD1775	HNSCC	NCT02585973	Phase I	Radiation, Cisplatin	/

TNBC: Triple negative breast cancer; GBM: Glioblastoma; IMRT: Intensity modulated radiotherapy, TMZ: Temozolomide; Non-small cell lung cancer (NSCLC); BC: Breast cancer; HNSCC: head and neck squamous cell carcinoma; NSCLC: Non-Small Cell Lung Cancer; SCLC: Small Cell Lung Cancer; WBRT: whole brain radiation therapy; SBRT: Stereotactic body radiotherapy; 3D CRT: 3-Dimensional Conformal Radiation Therapy; EBRT: External Beam Radiotherapy; NIVIX: Metastatic Invasive Carcinoma of the Cervix

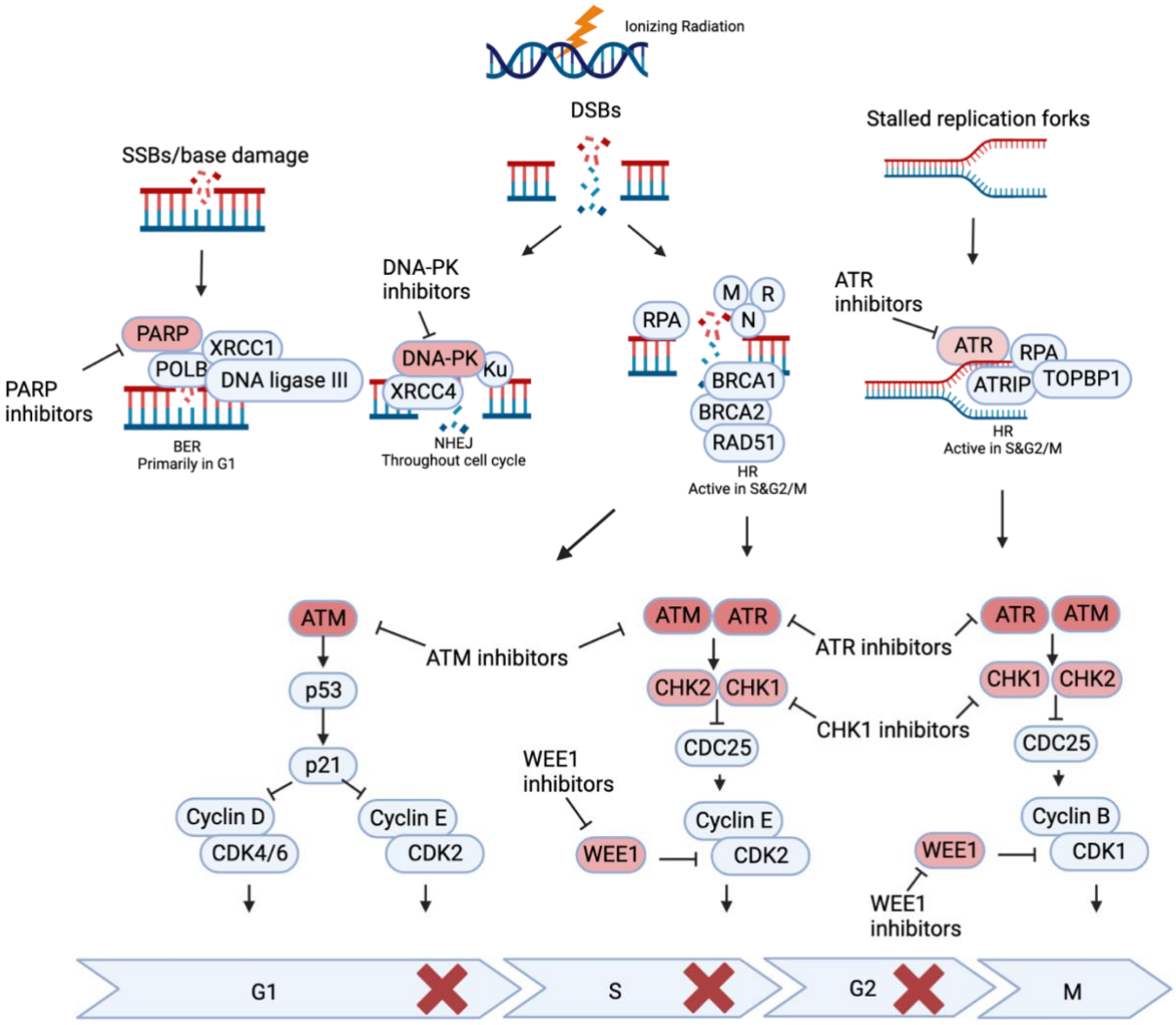

Figure 1. 14 Radiation induced DNA damage respond and clinically relevant DDR targets

Radiation induces SSB, DSB and stalled replication forks and triggers BER, NHEJ, and HR pathways, which activate ATM/ATR and their downstream and cause cell cycle arrest.
SSBs: single-strand DNA breaks; DSBs: double-strand DNA breaks; PARP: Poly (ADP-ribose) polymerase; MRN: MRE11, RAD50 and NBS1 complex; BER: base-excision repair; NHEJ: non-homologous end joining; HR: homologous recombination; ATRIP: ATR-interacting protein; POLB: DNA polymerase-β; RPA: replication protein A; TOPBP1: DNA topoisomerase 2-binding protein. (Created using Biorender.com)

1.4.1 PARP inhibitor (PARPi)

PARPi are the first clinically approved drugs and successful example based on the theory of synthetic lethality. PARP inhibition prevents the repair of damaged DNA by blocking PARP enzyme activity and PARylation reactions(Pommier et al., 2016). It is well known that BRCA1/2 are important components of the HR pathway for DSBs repair (see Section 1.2.1.4). Deficiency in *BRCA1/2* genes leads to high susceptibility for development of breast and ovarian cancer (Li et al., 2022). PARPi-mediated inhibition of PARP-1 can lead increased cell death in a BRCA mutation-induced HRR deficient cancer cell, through synthetic lethality(Bryant et al., 2005, Bryant and Shall, 2015) (Lord and Ashworth, 2017). The mechanism underpinning this is as follows: In normal cells, both BER pathway and HR pathways are functionally active for DNA damage repair. In cells that have lost BRCA1/2 functionality, HR pathways is dysfunctional, and BER and other DNA-repair processes can compensate for the loss of HR pathways. When PARP1 is inhibited, cells have lost BER function, but, if BRCA1/2 remains functional, HR repairs the relevant DNA damage. In the cancer cells with BRCA1/2 deficiency, when PARP1 is inhibited DNA damage repair by either HR or BER is not possible, which leads to cell death. More recently, it has been proposed that alteration/inactivation of other DNA repair genes such as ATM, RAD51 and CHEK2 etc.(Byrum et al., 2019) can lead to a phenotype which can mimic defects in BRCA1/2 genes, thus lead to DNA repair deficiency, which has been defined as 'BRCAness' (Lord and Ashworth, 2016). Cells with BRCAness, such as that caused by the deficiency in DNA repair and DDR factors such as RAD51, ATR, ATM, CHK1, CHK2 etc. can therefore also be sensitive to PARP inhibition (McCabe et al., 2006). The mechanism of synthetic lethality linked with BRCAness is shown in Figure 1.15.

An increasing number of clinical trials (See Table 1.2) have been carried out that clarify the benefits of PARPi in management of various BRCA mutated solid tumours (Kamel et al., 2018). In addition, PARPi also improves the therapeutic efficacy including ionizing radiation (Ramakrishnan Geethakumari et al., 2017). PARPi was proved to be a radiosensitizer in preclinical and clinical studies due to the synergic effects in DNA damage caused by ionizing

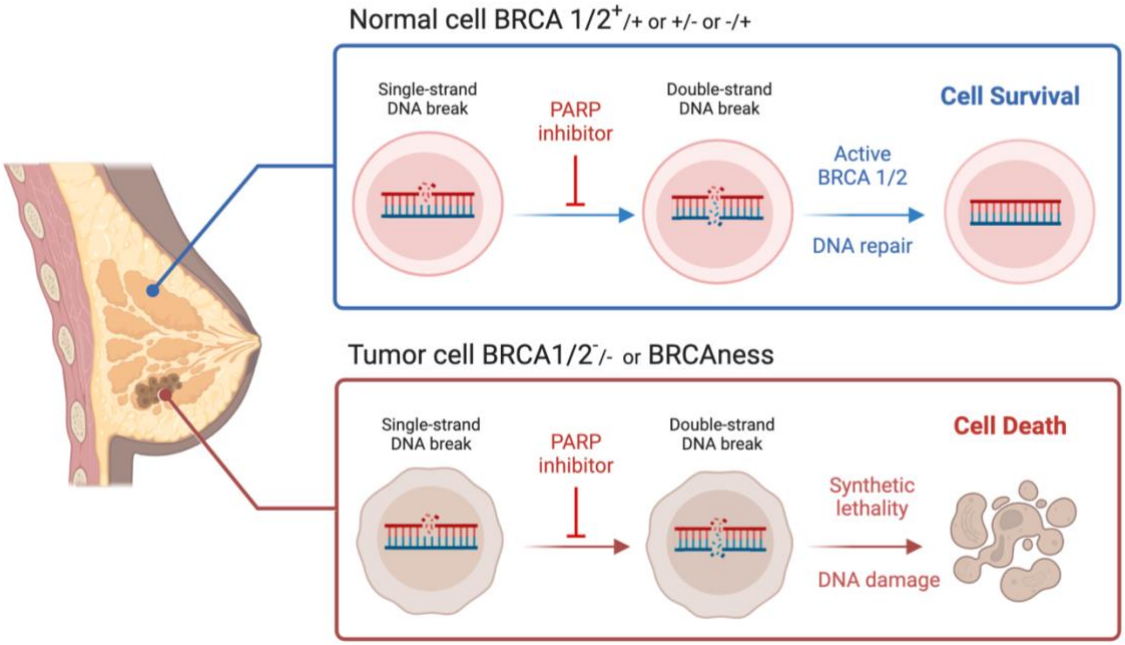

Figure 1. 15 Synthetic lethality-PARP inhibition

The inhibition of PARP-1 and BRCA mutation or BRCAness induced HRR deficiency in cancer cell becomes synthetic lethal. In normal cell with BRCA1/2, BRCA1/2 can participate in DNA repair in tumour cell with loss of BRCA1/2 or BRCAness, PARP inhibition can induce synthetic and lead to cancer cell death. BRCA1/2: BReast CAncer gene1/2. (Created from Biorender.com)

radiation (Lesueur et al., 2017, Barcellini et al., 2021). These exciting and promising preclinical studies of synthetic lethality to HR-defective tumours, as well as the radio-potentiation have led to a significant number of clinical trials of the combination with PARP1i and radiation to improve the response to radiotherapy. The active and completed clinical trials of PARPi combined with RT are summarised in Table 1.2.

1.4.2 DNA-PK inhibitors

NHEJ is a primary determinant of resistance to X-rays, γ-rays, and protons throughout the cell cycle (Nickoloff et al., 2017). DNA-PKcs plays a vital role in NHEJ pathways (see Section X), therefore, blocking NHEJ by inhibiting DNA-PKcs has long been considered as a radiosensitisation strategy. A study showed that the inhibition of DNA-PK led to increased sensitivity in Gastric cancer cells to IR (Geng et al., 2019). Moreover, another study found that the highly selective DNA-PK inhibitor (AZD7648), is an efficient sensitizer of radiation, as well as doxorubicin and Olaparib activity (Fok et al., 2019)**.** Another DNA-PK inhibitor peposertib (M3814) could enhance the efficacy of IR in xenograft models of cervical cancer (Gordhandas et al., 2022). To our knowledge, M3814 is the only DNA-PK inhibitor currently in clinical development (see Table 1.2).

1.4.3 ATM/ATR inhibitors

As mentioned in Section 1.2, ATM and ATR are both central kinases in response to DNA damage (Maréchal and Zou, 2013). Therefore, ATM and ATR inhibition has been explored clinically as a therapeutic target (Sarkaria et al., 1999, Taylor et al., 2015). Previously, there was a study have indicated that ATM inhibition is synthetic lethal with loss of genes in the Fanconi anaemia pathway/BRCA pathway (Cai et al., 2020). Moreover, ATM inhibition using inhibitor sc-23921 increases the radiosensitivity of uveal melanoma cells to both photon and proton RT (Hussain et al., 2020). The combination of ATM inhibitor (M3541) and radiotherapy in advanced solid tumours has entered phrase I clinical trial (Waqar et al., 2022). For ATR inhibition, BAY 1895344 also currently studied in clinical trials in combination with radiotherapy for head and neck squamous cell carcinoma (Mowery et al.,

2022). ATR inhibitor VE-821 in recently preclinical study has shown to increases sensitivity of radiation in chondrosarcoma cells (Lohberger et al., 2023). Current clinical trials of ATM and ATR inhibitors are summarised in Table 1.2.

1.4.4 CHK inhibitors

CHK2 and CHK1 play important roles in the regulation of cell cycle but also DNA repair(Stracker et al., 2009). Moreover, CHK1 is also a key player during DNA replication in S-phase by stabilisation of the replication forks (Chen et al., 2012). Therefore, CHK1 and CHK2 represent attractive targets as well as the combination with established cancer therapies, including radiotherapy (Zeng et al., 2017, Do et al., 2021). Studies showed that MK-8776, a novel CHK1 inhibitor enhances radiation-induced cell death (Suzuki et al., 2017). AZD7762, a dual CHK1 and CHK2 inhibitor was shown to increase IR-induced apoptosis in cancer cells (Morgan et al., 2010). Despite the preclinical results of the combination of CHK1 inhibitors with radiation is promising, clinical trials have not been as impressive as other cell cycle checkpoint inhibitors and only one CHK1/2 inhibitors Prexasertib has entered clinical trial (Qiu et al., 2018) (Table 1.2).

1.4.5 Pan-CDK inhibitor

As discussed in Section 1.2.2, cell cycle is mainly controlled by a complex composed of cyclin and cyclin dependent kinases (CDKs), and different cell cycle checkpoints have different regulatory functions in response to DNA damage. Therefore, targeting cell cycle checkpoints that block cell division has been a therapeutic approach for cancer treatment, which includes targeting several CDKs such as CDK1, CDK1, CDK2, CDK4/6, and CDK7. Flavopiridol, which was the first CDK modulator tested in clinical trials, is a semisynthetic flavone that directly competes with the ATP substrate and reversibly inhibits kinase activity of multiple classes of CDKs, including CDK1, CDK2, CDK4/6 and CDK7 with a clear block in cell cycle progression at the G1/S and G2/M boundaries (Senderowicz, 1999). A small molecular CDK inhibitor SNS-032 which can selectively inhibit CDK1, 2, 7, and 9 has shown sensitises radioresistant tumour cells to radiation hypoxic non-small cell lung cancer

cells; however, it is now discontinued due to a high toxicity (Kodym et al., 2009). To our knowledge, only Flavopiridol (Alvocidib) is studied combined with RT in clinical trial in pancreatic cancer (NCT00047307) (Schwartz, 2003).

1.4.6 CDK4/6 inhibitors

CDK4/6 inhibitors can prevent the phosphorylation of the RB which leads to cancer cell cycle arrest in G1 phrase and thus inhibit the proliferation of Rb-positive tumour cells (Pernas et al., 2018). Studies have also found that besides blocking cell cycle, CDK4/6 inhibitors also can suppress tumour growth by induce pathways in quiescence, senescence, metabolism, and immune systems (Klein et al., 2018). CDK4/6 inhibitors have been used in clinic, and three CDK4/6 inhibitors have already been approved for use together with hormonal therapy to treat advanced, ER-positive breast cancer patients including Palbociclib (Finn et al., 2020), ribociclib and abemaciclib (Byers, 2021). are demonstrated substantial improvements in progression-free survival. pre-clinical studies have found CDK4/6i have a synergistic radio-sensitizing effect (Bosacki et al., 2021). For example, CDK6 inhibitor Palbociclib (PD0332991) was showed to suppresses cell proliferation and enhances radiation sensitivity in medulloblastoma cells (Whiteway et al., 2013). Study also showed that CDK4/6 inhibitors can enhance radiosensitivity in HPV negative head and neck squamous cell carcinomas (Göttgens et al., 2019). Preclinical studies have been showed the safety and tolerance of the combination of radiation with CDK4/6i such as Palbociclib (Chowdhary et al., 2019) and ribociclib (Ippolito et al., 2019) in metastatic breast cancer patients. There are also several ongoing clinical trials testing the safety and efficiency of CDK4/6i combined with radiotherapy (summarized in Table 1.2).

1.4.7 CDK1/2 inhibitors

CDK1 and CDK2 play crucial roles in regulating cell cycle progression from G1 to S, through S, and G2 to M phase(Warren et al., 2019). The inhibition of CDK1/2 can orchestrate cancer cell growth. Moreover, CDK1/2 inhibitors also can be combined with IR, which increase the sensitivities to radiation. For example, AZD5438, a dual CDK1 and CDK2

inhibitor has been shown to enhance the radio-sensitivity of non-small cell lung cancer by impairing HR repair of DSBs (Raghavan et al., 2012). However, there are no CDK1/2 inhibitors approved by FDA.

1.4.8 WEE1 Kinase Inhibitor

WEE1 kinase is a key regulator of the G2/M phase transition that allows DNA repair before mitotic entry. AZD1775 in combination with DNA-damaging therapies in various cancer types has advanced to clinical trials (Matheson et al., 2016). And recently, a study of the combination of AZD1775 and IR has shown significantly increased apoptosis in cervical cancer cells (Lee et al., 2019). Moreover, preclinical research showed PD0166285 effectively abrogates the IR-induced G2 arrest in osteosarcoma cells (PosthumaDeBoer et al., 2011). More clinical studies have summarized in Table 1.2.

1.5 Tumour Hypoxia and radiotherapy resistance

1.5.1 An overview of tumour hypoxia

Oxygen is essential for cell metabolism. In normal tissues, the oxygen supply matches the metabolic requirements of the cells. However, in tumour tissues, oxygen consumption increases significantly and exceeds the supply, resulting in a drop of normal oxygen levels (8%/60 mmHg oxygen) to hypoxic levels (1%/7.5 mmHg oxygen) (Vaupel et al., 1989). Regions with low oxygen levels are generally termed as hypoxic regions, and those cancer cells at hypoxic regions is more likely to develop into a more aggressive phenotype and become resistant to therapy including radiotherapy (Al Tameemi et al., 2019). In conditions of radiobiological hypoxia, hypoxia-driven genomic instability is attributed to cells resistance to radiation-induced DNA damage. Hypoxia affects the DDR, including the repression of the DNA repair pathways, and cell cycle arrest.

The adaptation to decreased oxygen availability in cancer cells is by increasing the activity of the hypoxia-inducible factors (HIFs), which are heterodimeric transcription factors consisting of an oxygen-sensitive α subunit (HIF-α) and a constitutively expressed β subunit (HIF-β).

There are three HIF-α subunits includes HIF-1α, HIF-2α and HIF-3α that have been identified, which are all regulated by an oxygen-dependent mechanism. The expression of HIFs is also tightly regulated by ubiquitin-proteasome systems. For example, in normoxia, HIF-1α and HIF-2α can be hydroxylated by prolyl hydroxylases (PHDs) and factor inhibiting HIF (FIH) proteins with the coactivators p300 and CBP (CREB binding protein) within its oxygen-dependent degradation domain (ODD) of PHDs, which rescues the von Hippel-Lindau (VHL) protein and results in their poly-ubiquitination and subsequent proteasome degradation (Kubaichuk and Kietzmann, 2019). Under normoxia condition, HIF-1α can be hydroxylated by PHD which recruit an E3 ubiquitin ligase VHL protein target HIF-1α for degradation. Under hypoxic conditions, the prolyl and hydroxylation are inhibited, and the HIF-1α protein are stabilized, which increased interaction with its co-activators(Liu et al., 2015). The accumulation of HIF-1α heterodimerizes with HIF-1β, and bind to the hypoxia response elements (HREs) located in the promoters of HIF-1α target genes, thus activates their transcription.

1.5.2 Hypoxia causes radioresistance

The efficacy of radiotherapy is severely influenced by the hypoxic tumour microenvironment, being especially sensitive to the oxygen status of the cells, as hypoxic tumour cells are resistant to the damage from IR (Crabtree et al., 1933). There are mainly two hypotheses that explain the mechanisms why hypoxia causes radio-resistance.

One is called the oxygen fixation hypothesis, which explains that cancer cells are killed directly or indirectly by free radicals under radiation as mentioned in Section 1.2. During indirect effect of radiation, the DNA radicals are reduced under hypoxic condition by compounds containing sulfhydryl groups (SH groups), which repair the DNA to its original form, see Section 1.3.

Another hypothesis involved in radioresistance of tumour cells is via a HIF-1 signalling mediated biological mechanism. HIF-1α plays a pivotal role in the response to hypoxia which can activate the transcription of its downstream target genes, and these target genes involved in cell proliferation, glucose metabolism, apoptosis, invasion, metastasis, and DNA repair,

etc, and ultimately cause radioresistance (Liu et al., 2015). Studies have found high HIF-1α expression is highly associated with poor prognostic outcomes and low survival rates in cancer patients (Lin et al., 2017, Potharaju et al., 2019). Therefore, targeting the HIF pathway has become one of the attractive strategies for the treatments of hypoxic tumours. HIF-1 actives its target genes and multiple pathways, affects glucose metabolism, the cancer microenvironment, epithelial-mesenchymal transition (EMT), cell cycle regulation, and autophagy, etc. therefore, inducing radio-resistance (Vaupel et al., 1989), see Figure 1.16.

1.6 WSB-1

1.6.1 WSB-1 structure

WD repeat and SOCS box containing-1 (WSB-1), which is located in the locus 17p11.1, was identified as one of the members of the WD40-repeat containing proteins with the suppressor of cytokine signalling (SOCS) box (Hilton et al., 1998). WD40 repeat proteins are well-known to function as scaffolds for protein-protein interactions, and the SOCS box-containing proteins can promote the linkage of substrates to the ElonginB/C-Cullin2 complex (Linossi and Nicholson, 2012). There are two core interaction sites namely the BC-box and the Cul-box in the SOCS box are responsible for mediating ubiquitination. And it has been shown that the SOCS box is crucial for a E3 ligase to recognize specific substrates and mediate the polyubiquitination or degradation. WSB-1 role as an E3 ubiquitin ligase is to be the substrate recognition subunit of an ECS (Elongin BC-Cul5-Rbx1) ubiquitin ligase complex (Dentice et al., 2005).

There are HREs on the promoter of *WSB1* (Tong et al., 2013), located on 354-358bp, 553-557bp, 860-864bp, and 1982-1986bp. WSB-1 generates three distinct protein isoforms (Archange et al., 2008). WSB-1 isoform 1 is composed of three domains including an N-terminal domain(Archange et al., 2008), eight WD-40 repeats, and a SOCS box. WSB-1 isoform 2 has one WD-40 repeat but lack of almost the entire N-terminal domain. WSB-1 isoform 3 consists of two WD-40 repeats and lack of SOCS box (Figure 1.17)

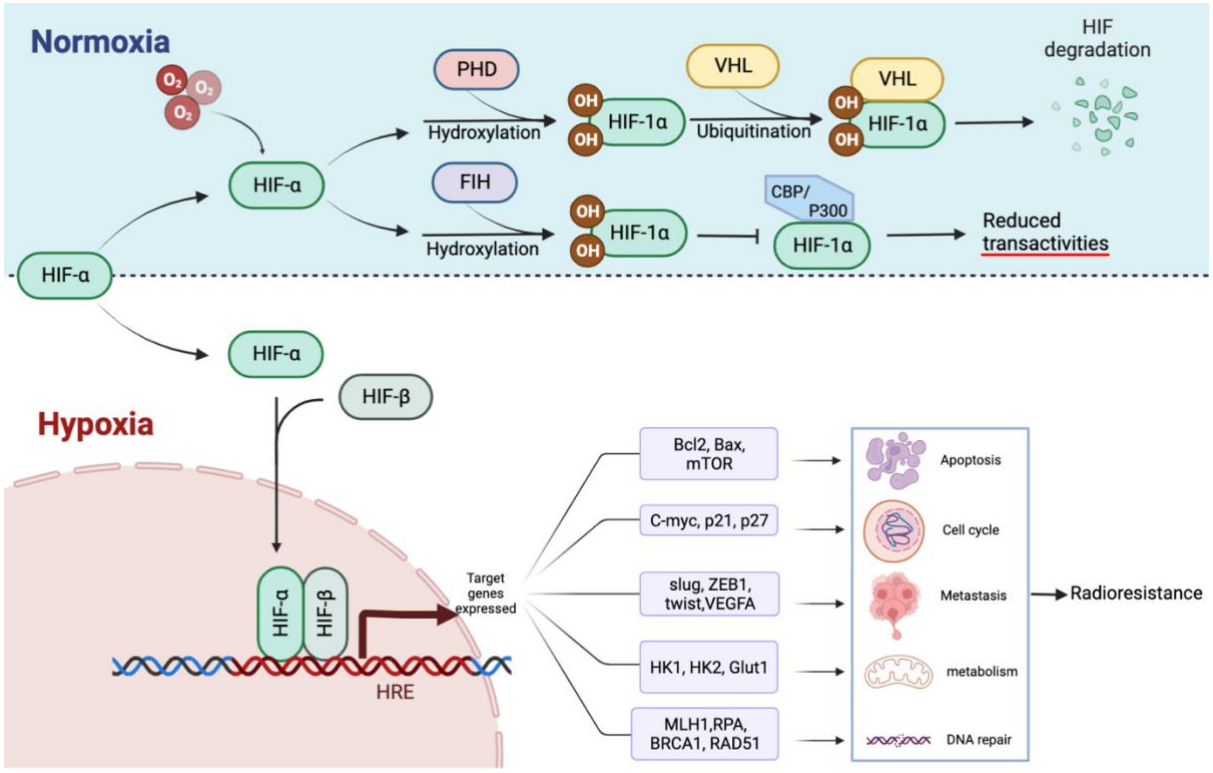

Figure 1. 16 Mechanisms for HIF-α-mediated radiotherapy resistance

This schematic illustrates the key mechanisms for HIF stabilisation in hypoxic conditions, and high- lights key pathways up-regulated by HIF that contribute to hypoxia-mediated radiotherapy resistance. HIF, hypoxia-inducible factor; PHD, prolyl hydroxylases; FIH, factor-inhibiting HIF; VHL, von Hippel–Lindau; OH, hydroxyl groups; CBP, CREB binding protein; HRE, hypoxia response elements. (Created form Biorender.com)

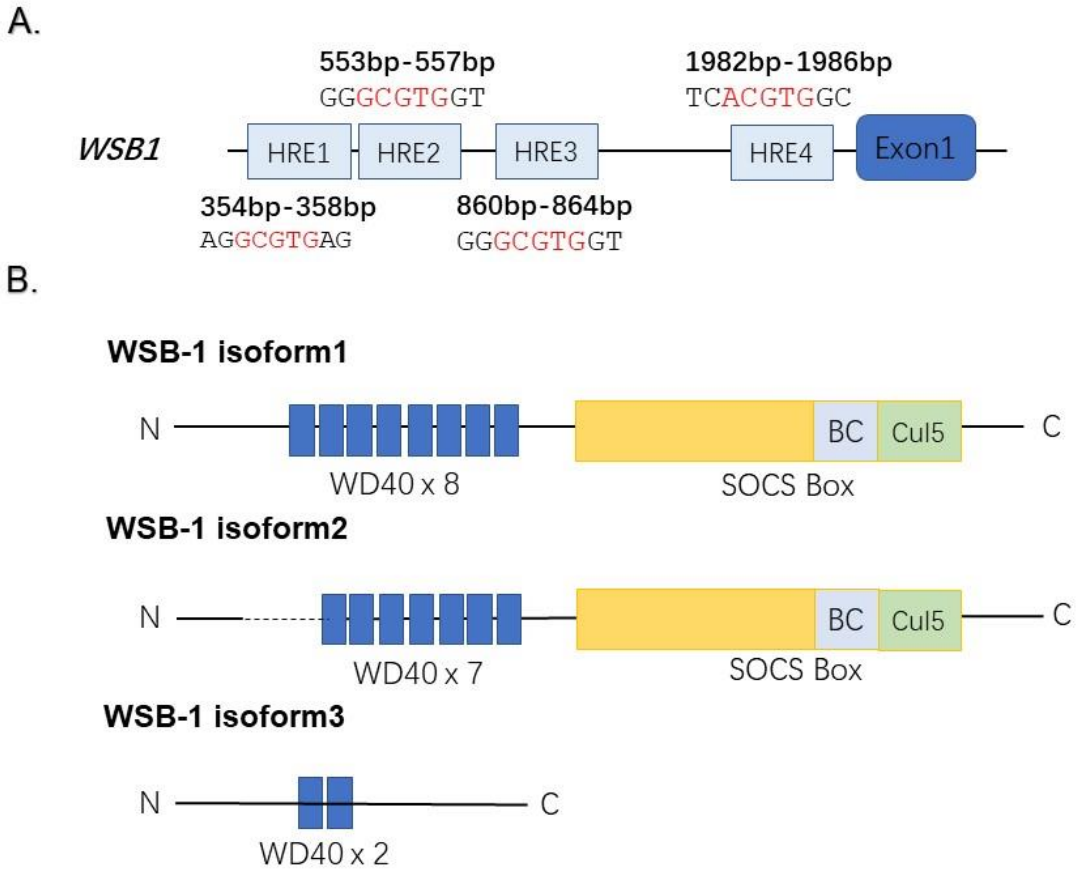

Figure 1. 17 The structure of WSB-1
A: There are HREs on the promoter of WSB1, located on 354-358bp, 553-557bp, 860-864bp, and 1982-1986bp B: there are three distinct WSB-1 protein isoforms. WSB-1 isoform 1 is composed of three domains including an N-terminal domain, eight WD-40 repeats, and a SOCS box. WSB-1 isoform 2 has one WD-40 repeat but lack of almost the entire N-terminal domain. WSB-1 isoform 3 consists of two WD-40 repeats and lack of SOCS box. WSB-1: WD repeat and SOCS box containing-1, HRE: Hypoxic respond element; BC: BC-box; Cul5: Cul5-box; N: N-terminal; C: C-terminal. (Original figure)

The three distinct protein isoforms of WSB-1 have different functions (Archange et al., 2008). WSB-1 isoforms 1 and 2 seems to increase cell proliferation, whereas the function of WSB-1 isoform 3 is being debated according to different studies(Archange et al., 2008). Archange et al. reported that WSB-1 isoforms 1 and 2 increase cell proliferation and enhanced sensitivity to gemcitabine- and doxorubicin-induced apoptosis in pancreatic cancer cells, while WSB-1 isoform 3 has opposite effect on cell proliferation and enhanced resistance to apoptosis (Archange et al., 2008). Another study also showed that silenced all WSB-1 isoform (isoforms 1, 2, and 3) in neuroblastoma cells reduced cell growth and survival and sensitized chemotherapeutic agents, whereas silenced WSB-1 isoforms 1 and 2 alone had no effect, which highlighted the important role of WSB-1 isoform 3 in tumour cell growth and potential target in neuroblastoma therapy (Shichrur et al., 2014).

1.6.2 Regulatory functions of WSB-1

Given that WSB-1 is an E3 ubiquitin ligase, the first function we notice is its ubiquitination. Normally, the ubiquitination process includes recognition, conjugation, and ligation three steps, which involves three different ubiquitin enzymes: ubiquitin-activating enzyme (E1), ubiquitin-conjugating enzyme (E2) and ubiquitin ligases E3 (Mercier, 2022). The E3 ligases play a central role in mediating the transfer of ubiquitin to the substrates involved in cancer development and have the potential application of cancer targets and biomarkers. WSB-1 can act as a substrate-recognising subunit of the ECS ubiquitin ligase complex and participate in the modification and degradation of multiple proteins (Dentice et al., 2005).

LRRK2, also known as dardarin, are associated with an increased risk of Parkinson's disease and Crohn's disease, can be ubiquitinated by WSB-1(Nucifora et al., 2016). Hypothyroidism is the result of underactive thyroid with inadequate production of thyroid hormone(Almandoz and Gharib, 2012). Ubiquitination is an essential step in the control of D2 activity in hypothyroidism, and TEB4 and WSB-1 can mediate the loss of D2 activity by ubiquitination degradation (Egri and Gereben, 2014, Werneck de Castro et al., 2015). As described in section 1.5, VHL is the substrate recognition component of an E3 ubiquitin ligase and functions as a master regulator of HIF activity by targeting the hydroxylated HIF-alpha subunit for ubiquitylation and proteasomal degradation under normoxia. Several studies identified that WSB-1 negatively regulates pVHL protein by stimulating the ubiquitination of pVHL, which leads to the stabilization of HIF-1α protein and thereby promoting tumour metastasis (Chen et al., 2017, Kim et al., 2015). Hypoxia-driven WSB-1 can promote the proteasomal degradation

of Rho GDP dissociation inhibitor 2 (RhoGDI2), enhance the activity of Rho proteins and promotes migration(Cao et al., 2015).

Studies also showed that WSB-1 increases the expression of VEGF and metalloproteinase (MMP) activity and promotes metastasis in hormone receptor-negative breast cancer under hypoxia (Poujade et al., 2018). Recent study found that WSB1 is a direct target gene of c-Myc, WSB1 also regulates c-Myc expression through WNT/β-catenin pathway, which forms a positive feedback loop, leading to cancer initiation and development (Gao et al., 2022).

WSB-1 has been shown to play a role in immune regulation by participating in the maturation degradation of the interleukin-21 receptor (IL-21R) (Nara et al., 2011a). Interleukin-21 (IL-21) has been proven to play an important role in the immune system and the biological functions of IL-21 are mediated by binding to its corresponding receptor, IL-21R. Moreover, the IL-21/IL-21R signalling axis can regulate the cytokine production of T cell subsets by enhancing the expression of T-bet and STAT4 in human T cells, resulting in an augmented production of IFN-γ (Solaymani-Mohammadi et al., 2019), ultimately regulating the immune and inflammatory responses. G-CSF-R is the major cytokine receptor involved in neutrophil development. Studies also showed that in myeloid leukaemia, WSB proteins play a role in G-CSF-R membrane expression, WSB induces ubiquitylation of the G-CSF-R and affects its expression (Erkeland et al., 2007).

Further, studies showed WSB-1 was regulated by several miRNA, for instance, it has been reported that WSB-1 may be a target of miRNA-191 (Guerau-de-Arellano et al., 2015). WSB-1 also is the target of miRNA-23 that promotes invasiveness and metastasis in mouse and human angiosarcoma (Hanna et al., 2017). miR-592 directly binds to the 3'-UTR of the WSB-1 gene, thus disrupting HIF-1α protein stabilization (Jia et al., 2016). Furthermore, WSB-1 is regulated by KSHV miRNA, kshv-miR-K12-6-3p and kshv-miR-K12-8-5p (Quan et al., 2015).

1.6.3 WSB-1 and hypoxia

As Section 1.6.1 discussed, there are HREs -GCGTG-, which are located on 354-358bp, 553-557bp, 860-864bp, and 1982-1986bp, on the promoter of *WSB1*. The published evidence also strongly suggests that WSB-1 is markedly increased in response to hypoxia and is a direct target gene of HIF-1 (Tong et al., 2013, Poujade et al., 2018). In addition, it has been shown that WSB-1 expression is induced in a HIF1α-dependent but HIF2α-independent manner under hypoxic condition in breast cancer (Poujade et al., 2018). Moreover, as discussed in Section

1.6.2, WSB-1 as a E3 ligase, stabilizes HIF-1α by promoting the ubiquitination of pVHL under nornoxia and hypoxia (Chen et al., 2017, Kim et al., 2015). Therefore, WSB-1 and HIF-1 forms a positive feedback loop. The relationship between WSB-1 and HIF-1 is summarised in Figure 1.18.

1.6.4 WSB-1 and DDR

WSB-1's role in DDR have also been explored. Studies have shown that WSB-1 is involved in several key processes related to DNA damage response(Choi et al., 2008, Wang et al., 2015, Kim et al., 2017b). For example, HIPK2, which can control DNA damage-induced cell fate and cytokinesis, can be ubiquitinated and degraded by WSB-1 (Choi et al., 2008). ATM, a major upstream kinase of the DDR pathway, has also been shown to be ubiquitinated by WSB-1, resulting in ATM degradation during tumour initiation (Kim et al., 2017b). Interestingly, it was also found that some key DNA repair factors such as *TP53* and *BRCA1* appear with WSB-1 in the same chromosome 17 (Wang et al., 2015). Overall, the research on WSB-1 suggests that it is an important protein involved in the response to DNA damage. Further studies are needed to fully understand the mechanisms by which WSB-1 functions and its potential therapeutic applications in the treatment of DNA damage and cancer.

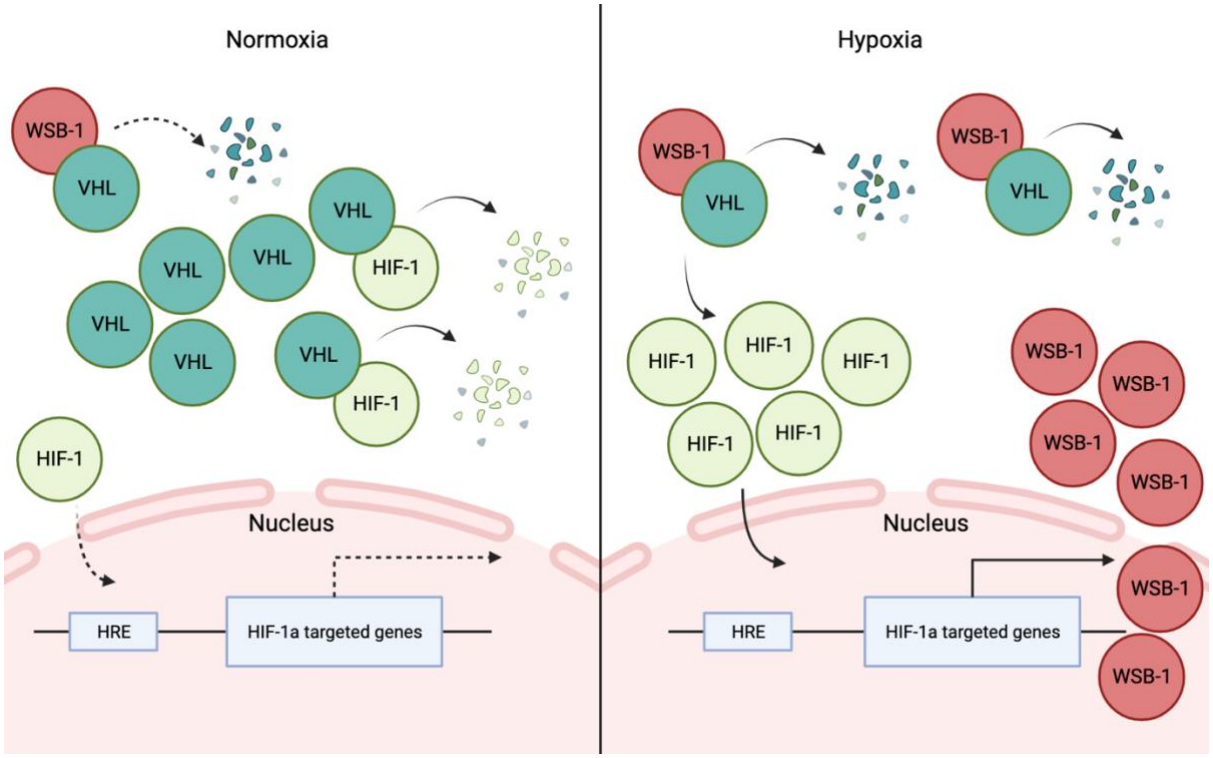

Figure 1. 18 WSB-1 and HIF-1a forms positive feedback loop
WSB-1 promotes ubiquitination and degradation of VHL protein, which stabilizes HIF-1a under normoxia and hypoxia. There're also HREs on the promoter of WSB1, which means WSB1 is one of the targeted genes of HIF-1a.
WSB-1: WD repeat and SOCS box containing-1, HIF-1: hypoxia-inducible factors -1; VHL: Von Hippel–Lindau tumor suppressor; HRE: Hypoxia respond elements. (Created form Biorender.com)

1.7 Objectives and aims of this thesis

Breast cancer is the most common cancer in the world, in the UK, 1 in 7 women are diagnosed with breast cancer in their lifetime (CancerResearchUK, 2022). The treatments for breast cancer includes surgery, chemotherapy, radiotherapy, hormonal therapy, and targeted therapy etc. Recent studies have found that combination therapies can achieve a better outcome.

Radiotherapy has become one of the major therapeutic approaches in the treatments for cancers. Moreover, the combination radiotherapy with chemotherapy, targeted therapy has become a highly effective treatment.

However, the resistance to radiotherapy is still a most challenge for cancer treatments. Hypoxia is one of the causes of radioresistance. As described above, WSB-1 is a downstream target gene of HIF-1α, which target HIPK2 and ATM for degradation, thus affecting the DDR. However, the role of WSB-1 in DDR under hypoxic conditions in breast cancer, especially its roles in the resistance to radiotherapy and in the DDR, remains unclear. Consequently, this thesis aims at investigating the role of WSB-1 in breast cancer and explore its role in response to RT and the DDR.

Therefore, specific objectives of different chapters in this thesis are as follows:

- in Chapter 3, the novel roles for WSB-1 in gene expression and signalling pathways in breast cancer will be investigated.

- in Chapter 4, the impact of WSB-1 modulation on the DDR in breast cancer will be evaluated.

- Chapter 5 will be focus on the evaluation of WSB-1-regulated DDR signalling as a therapeutic target in breast cancer, both as single agents and in combination with radiotherapy

Chapter 2

Material and Methods

2.1 Cell culture

2.1.1 Cell lines

Four different human breast cancer cell lines were used in this study, including Luminal A breast cancer cell line MCF7, Luminal B breast cancer cell line BT474, triple negative basal-B mammary carcinoma breast cancer cell lines MDA-MB-231 and triple negative basal-A mammary carcinoma breast cancer cell lines MDA-MB-468. Cell lines were originally purchased from the American Type Culture Collection (ATCC) and mycoplasma-free test were regularly conducted. Each cell line's characteristics are summarised in Table 2.1.

2.1.2 Cell line sub-culture

Cells were maintained in a humidified atmosphere in a CO_2 incubator (RS Biotech, UK) with 5% CO_2, at 37^{o}C. All reagents including Dulbecco's Modified Eagle Medium (DMEM) High Glucose Media (PAA/GE Healthcare Life Science, UK) or Roswell Park Memorial Institute (RPMI) 1640 medium (Thermo Fisher Scientific, US) supplemented with 10% heat inactivated FBS (FoetusBovine Serum, Gibco/Life Technologies, UK), 1X phosphate buffered saline (PBS) (BioWest, Switzerland) and 1X trypsin-Ethylenediaminetetraacetic acid (EDTA) (BioWest, Switzerland) were pre-warmed at 37^{o}C in a bead bath (Clifton Bath Armor, Scientific laboratory supplies, UK). For regular subculture, used media was discarded and cells were gently washed with 1X PBS. 1X trypsin-EDTA were used and incubated at 37^{o}C less than 5 minutes to detached cells Then the trypsin was inactivated by fresh media and cells were resuspended, then either counted or an aliquot was then placed into fresh media in a fresh flask, at the appropriate dilution range from 1:2 to 1:16, which were depending on the cell lines or experiments schedule.

Table 2. 1 The details of cell lines used in this study (from atcc.org)

Cell line	MCF-7	BT474	MDA-MB-231	MDA-MB-468
Tissue of origin	derived from pleural effusion of a metastatic breast cancer	mammary gland; breast/duct	derived from pleural effusion of a metastatic breast cancer	derived from pleural effusion of a metastatic breast cancer
Morphology	epithelial	epithelial	epithelial	epithelial
Culture	adherent	adherent, patchy	adherent	adherent
Disease	adenocarcinoma	ductal carcinoma	adenocarcinoma	adenocarcinoma
Age	69 years adult	60 years adult	51 years adult	51 years adult
Gender	female	female	female	female
Ethnicity	Caucasian	Caucasian	Caucasian	Black
Culture Medium	Dulbecco's Modified Eagle Medium (DMEM)	Roswell Park Memorial Institute medium (RPMI)	Dulbecco's Modified Eagle Medium (DMEM)	Dulbecco's Modified Eagle Medium (DMEM)
ER status	+	+	-	-
PR status	+	+	-	-
Her-2 status	-	+	-	-
P53 status	WT	Mutated	Mutated	Mutated
Classification	Luminal A	Luminal B	Basal like	Basal like
***BRCA1* Mutation**	WT	WT	WT	WT

2.1.3 Cell counting

Cells were counted before experimental setup. In order to do this, cell suspension was gently pipetted in a single cell suspension several times. The cell suspension was then diluted 1:2 in a 0.4% trypan blue solution (Gibco, Thermo Fisher Scientific, UK). And cells were counted in a four-quadrant of a Neubauer haemocytometer (Marienfeld Superior, Germany). The haemocytometer is a specimen slide which is used to determine the concentration of cells in a liquid sample. A grid is etched into the glass of the haemocytometer. Each square of the grid represents a total volume of 0.1 mm^3 or 10^{-4} cm^3. Since 1 cm^3 is equivalent to 1 ml, the total number of cells will be determined by multiplying the number of counted cells per square by the haemocytometer factor 10^4. When counting cells, the L rule was followed which means cells that stay on the top and right lines of a square were not be counted, cells on the bottom and left side were counted. The number of cells were calculated by the following formula:
Number of cells in one large square (4x4 small squares) = n x 10^4 cells/ml
For a total number of the cells the resulting value of cells/mL must be multiplied with the volume in mL in which the cells were originally resuspended in.

2.1.4 Storing cells

Once cells reach 70-85% confluency, cells were trypsinized, resuspended in media, harvested in a 12ml tubes, and centrifuged, then the surface of the cell were washed carefully by 1X PBS then PBS was discarded. Then cells were resuspended in FBS (Gibco, Life Technologies, UK) which contained 10% DMSO (dimethyl sulfoxide). Finally, cells were aliquoted into a 1.5 ml cryovials (Nunc, Thermo Scientific, UK) and were placed in a freezing container (Nalgene, Thermo Scientific, UK) in a -80°C freezer for 48h, then the cryovials were transferred into liquid nitrogen for long term storage.

2.1.5 Thawing and recovering cells

To recover cells from freezing, cryovial was brought up quickly from the liquid nitrogen to room temperature and thawed in 37 °C water beam. The cell was then transferred into a 12 ml tube contains with prewarmed media, centrifuged, and supernatant was discarded to remove the DMSO that was used when freezing cells to reduce toxicity. The cells were resuspended in fresh media and transferred into a T25 flask, and then passaged as described in Section 2.1.2.

2.2. Transfection

2.2.1 siRNA (silencing RNA) transfection

siWSB-1 (WSB-1 siRNA) and siNT (non-targeting siRNA) oligos were purchased from siGENOME (Dharmacon/Thermo Scientific), see Table 2.2 for details.

Transfection was conducted by using Dharmafect (Thermo-Fisher, US). In brief, cells were seeded at $2x10^5$ cells per well of a 6-well plate or 35mm in the appropriate completed growth medium (supplemented with serum). Cells were then incubated at 37°C with 5% CO_2 overnight. For each transient transfection, 25 nM siRNA was used. Diluted siRNA solution and diluted Dharmafect were combined, gently mixed, and incubated at room temperature for 20-30 min as per manufacturer's instructions. Spent media was removed from the wells and the transfection solution overlayed over the cells. These were then exposed to either normoxic (20% O_2) and/or hypoxic (2% O_2) conditions as per experimental design.

2.2.2 Plasmid DNA transfection

The pFLAG-CMV2-WSB1 plasmid, where WSB1 sequence was inserted in the pFLAG-CMV2 plasmid, was used for transfection in this study. This WSB-1 plasmid was a kind gift from Prof. Hironobu Asao, Yamagata University, Japan (Nara et al., 2011b). Map of the pFLAG-CMV2 plasmid is showed in Figure 2.1

DH5a chemical competent cells (stored at -80°C) were thawed in ice for 10 minutes. Around 1 µL (10pg-100ng) plasmid DNA was added to DH5a competent cells, and the vial was kept in ice for 15 mins. The vial of DH5a and plasmid DNA were heat shocked for 45 sec at 42°C in a water bath (Grant, UK), and 950 µL LB media was added to the vial, incubated in the shaker (Infors HT, UK) at 37°C 200 rpm for 1 hour. 50 µL of the resulted LB media with DH5a was added to the centre of the pre-warm LB plate with the ampicillin (100 µg/mL). Spreader was sterilised in a flame and was cooled down before spreading the DH5a cell solution. Plates then were kept upside down in the 37°C bacteria incubator for 16~18 hours. Next day, a medium sized colony was picked using a pipette tip, which was ejected into a prewarmed 50 mL LB medium with ampicillin (100 µg/mL), and then incubated in the shaker at 37°C 200 rpm for 8 hours. When the LB medium turned cloudy, 5 mL of the cultured medium was added into a 250 mL LB medium with the ampicillin (100 µg/mL) and incubated in shaker at 37°C 200 rpm for a further 12~16 hours.

Table 2. 2 The sequences of non-targeting siRNA and siWSB-1

Target	Company	Catalogue number	Concentration	Target sequence
Non-targeting	siGENOME (Dharmacon/Thermo Scientific)	D-001210-02-20	25nM	Non-targeting siRNA #2 UAAGGCUAUGAAGAGAUAC
WSB-1	siGENOME SMARTpool (Dharmacon/Thermo Scientific)	M-013015-01-0020	25nM	Targets WSB-1 isoforms 1, 2 and 3 UAUGGGACCUGAAAGAUGA GGAAACAUGAUGAAAGUAU GAAGUGGUCAGAGAUUUAA GAAAACUCCUCCUUAACUU

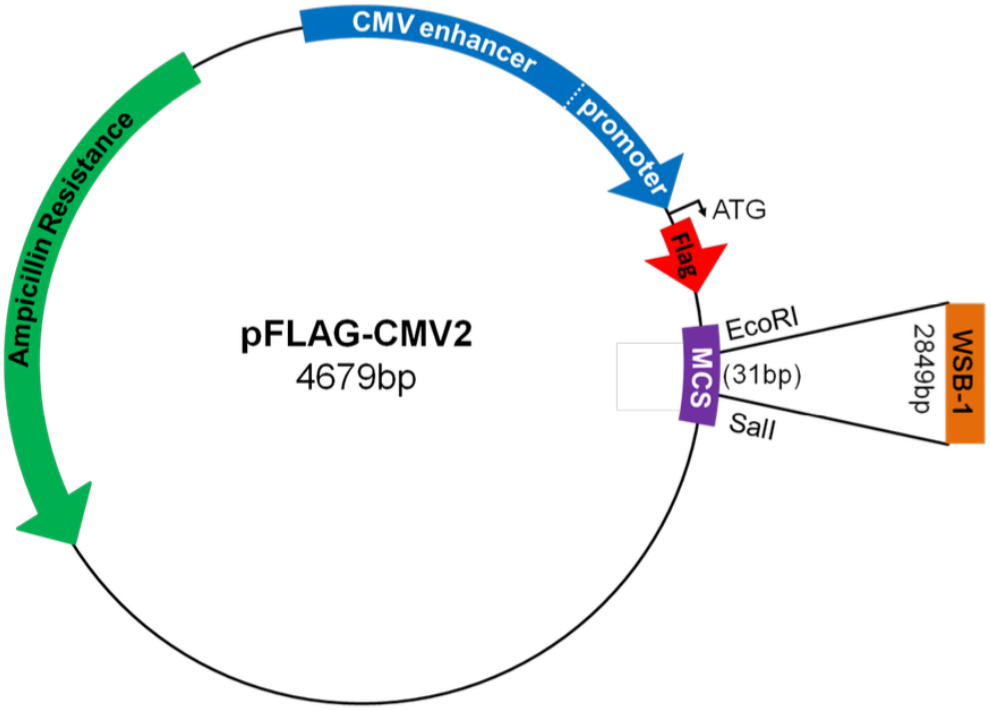

Figure 2.1 Structure of the pFLAG-CMV2-WSB1 plasmid (From Flore-Anne's thesis, 2016)

WSB1 sequence was inserted in the pFLAG-CMV2 plasmid. MCS: multiple cloning site.

Plasmid purification was performed using E.Z.N.A.@ Endo-Free Plasmid DNA kit (Omega bio-Tek, UK). In brief, 250 mL of the culture was collected in a 50 ml centrifuge bottle and centrifuge at 4000 x g for 10 mins at room temperature, with supernatant discarded. Then resuspension buffer containing RNase A were added to the bacterial pellet and vortexed to mix. Lysis buffer was added to the centrifuge tube and the tube gently inverted 10 times to mix. Then cold N3 buffer was added, and tubes were rotated gently. The lysate was transferred into the barrel Lysate clearance filter syringe and expel the cleared lysate into 50 centrifuge tubes. 1 volume ETR buffer was added, and the cleared supernatant was transferred into the HiBind DNA Maxi Column and centrifuge at 4000 x g for 3 mins. Plasmid DNA was bound to the HiBind DNA Maxi Column through centrifuging. Then the column was washed by ETR wash buffer, EHBC buffer and DNA wash buffer. Finally, Endo-Free Eluntion buffer was added, sat at room temperature for 5 mins and centrifuged at 4000 x g for 5 mins. Plasmid DNA stock was measured by Nanodrop Light (Thermo Fisher Scientific) and plasmid DNA was stored at -20°C.

Transfection was performed using TurboFect Transfection Reagent (Thermo Scientific, UK) as per manufacturer's instructions. In brief, cells were seeded 2 $x10^5$ cells per well in 6-well plates or 35mm dishes in 2 ml of the appropriate complete growth medium. Cells were then incubated at 37°C with 5 % CO_2 overnight. For each transient transfection, pFLAG-CMV2-WSB1 plasmid DNA was diluted 1:1 with serum-free medium (SFM), and TurboFect Transfection reagent was also diluted in SFM (diluted volume was followed by the recommendations of the manufacturer). The two solutions were combined and incubated at room temperature for 20-30 min and aliquoted into each well. After 24 hours the plates were transferred into normoxic (20% O_2) or hypoxic (1% O_2) conditions, according to experimental design.

2.3 Hypoxia exposure

Hypoxic conditions were maintained in a H35 Hypoxystation hypoxia chamber (Don Whitley Scientific, UK). The standard condition in the chamber was set as temperature (37°C), humidity (75%), and CO_2 (5%), and oxygen concentrations (1%) were also set prior to the experiment start. For RNA and protein extraction, samples in hypoxic condition were lysed in the chamber to prevent reoxygenation at the end of the experiment. For clonogenic assays, cells were placed in the carry box and sealed securely in the chamber before bringing out

from the chamber. In parallel, control samples in normoxic condition were incubated in a CO_2 incubator with 5% CO_2, 20% concentrations oxygen, a humid atmosphere at 37°C.

2.4 Drug treatments

The three small molecule inhibitors used in this study: PARP inhibitor Olaparib/AZD2281 (#S1060) (Stratech, UK), ATM inhibitor KU-55933 (#S1092) (Stratech, UK), and ATR inhibitor VE-822 (#S7102-SEL) (Stratech, UK). Olaparib, KU-55933, and VE-822 stocks were prepared by dissolving in DMSO at 50 mM, aliquoted, and stored at -20°C.

2.5 RNA Isolation

Total RNA was extracted by the Aurum total RNA mini kit (BioRad, UK), and following the manufacturer's spin protocol for mammalian cells. Briefly, media was removed from cells, and cells were washed with 1X PBS. Cells were lysed directly by using the kit lysis buffer, collected into a 2 ml microcentrifuge tube, and mixed with equal volume of 70% ethanol thoroughly. Then the lysate solution was transferred into the RNA binding columns, which was washed several times by low stringency high low stringency wash solutions as per manufacturer’s instructions. DNase I was added during the purification to effectively remove genomic DNA contamination. Total RNA was eluted in 1:100 ratio by the elution solution. RNA yield and integrity were assessed using a Nanodrop Light (Thermo Fisher Scientific, UK) and stored at -80°C until used.

2.6 Reverse Transcription (cDNA Synthesis)

RevertAid H Minus First Strand cDNA Synthesis Kit (Thermo Scientific, UK) was used to reverse transcribed the mRNA from total RNA extraction into cDNA. According to manufacturer’s instructions, 1 µg total mRNA was diluted and mixed with oligo dT, dNTP Mix, RNAse Inhibitor, Reaction Buffer, and reverse transcriptase, and the solution incubated at the following conditions: 42 °C for 60 min, 70°C for 5 min. Samples were then stored at -20°C.

2.7 Quantitative real time PCR (qPCR)

2.7.1 qPCR analyses

qPCR analyses were performed on Biosystems StepOnePlus™ Real-Time PCR System by using SYBR Green (Quanti Nova) with ROX (Reference Dye) and Quanti TECT primer assays (Qiagen, NL), as per manufacturers' instructions. The details of primers used in this study were summarized in Table 2.3. *B2M* expression was used as an internal housekeeping gene control for normalization.

Table 2. 3 List of primers used for qPCR (final concentration of 0.1µM)

Gene	Product name	CATALOG No.
B2M	Hs_B2M_1_SG QuantiTect Primer Assay	QT00088935
WSB1	Hs_WSB1_1_SG QuantiTect Primer Assay	QT00064127
BRCA1	Hs_BRCA1_1_SG QuantiTect Primer Assay	QT00039305
BRCA2	Hs_BRCA2_1_SG QuantiTect Primer Assay	QT00008449
RAD51	Hs_RAD51AP1_1_SG QuantiTect Primer Assay	QT00079758
CDK6	Hs_CDK6_1_SG QuantiTect Primer Assay	QT00019985
E2F1	Hs_E2F1_1_SG QuantiTect Primer Assay	QT00016163
RB1	Hs_CRB1_1_SG QuantiTect Primer Assay	QT00021343

2.7.2 Fold change calculation

The 2-ΔΔCT method was used to analyse the relative changes in gene expression(Livak and Schmittgen, 2001). B2M was used as the housekeeping gene. All qRT-PCR analyses were performed in biological triplicates for each sample and a 2-Way ANOVA comparison siNT (control sample) vs siWSB-1 was used to determine statistical significance by Prism 9 (GraphPad Software Inc, USA).

2.8 Protein analysis

2.8.1 Protein extraction

Cells were seeded in different densities, treated, and incubated in different conditions according to different experimental requirements. At the schedule time points, cells were taken out from the incubator into room temperature, cells surfaces were gently washed with 1X PBS and discarded, then small amount of fresh 1X PBS were added into the dishes and cells were scrapped from the dishes, collected in a microcentrifuge tubes, centrifuged at

20,000 g for a few seconds, then pellet remained, and supernatant was removed. The pellet was resuspended in UTB lysis buffer (9 M Urea; 75 mM Tris-HCl pH 7.5; 0.15 M β-mercaptoethanol). The whole cell lysate samples were sonicated using a Bioruptor (Diagenode, Belgium) on high setting for 15 min by 30 sec intervals. Samples were then centrifuged at 20,000 g for 15mins, and supernatants were transferred in clean microcentrifuge tubes and stored at -20°C.

2.8.2 Protein quantification

NanoDrop™ Lite Spectrophotometer (Thermo Scientific, UK) was used in this study to quantify the concentration of whole protein extracted from cells. In brief, fresh UTB lysis buffer was used to blank the machine twice, then 2 µL per sample was added and the concentrations of the protein were measured by the machine.

2.8.3 Sample preparation

Then Protein samples were prepared in UTB lysis buffer to 30ug-50ug per well, and sample buffer (3.3% SDS; 6 M Urea; 17 mM Tris-HCl pH 7.5; 0.01% bromophenol blue; 0.07 M β-mercaptoethanol) was then added to each sample to a final volume of 15-20ul. Finally, the mixture was heated at 100°C for 5 min in a heat block (Techne Dri-Block DB-3D, Sigma Aldrich, UK). Afterwards, samples can either straight to loading or stored at -20°C.

2.8.4 SDS-PAGE

Protein samples were firstly run through SDS-PAGE (sodium dodecylsulfate polyacrylamide gel electrophoresis) then analysed by Western blotting. Firstly, a concentrating stacking gel was set up, follow the recipe (1.5 M Tris-HCl pH 6.8, 30% acrylamide/0.8% bis-acrylamide, 10% SDS, 10% TEMED and 10% APS in the appropriate volumes, see Table 2.4) and different percentage (subject to protein molecular weights) acrylamide separating gel was also set up following the recipe (1.5 M Tris-HCl pH 8.8, 30% acrylamide/0.8% bis-acrylamide, 10% SDS, 10% TEMED and 10% APS in the appropriate volumes, see Table 2.4). 30-50 ug of protein samples were loaded per well. A molecular weight ladder (Geneflow, UK) was loaded alongside the samples. Electrophoresis was performed in a tank filled with 1X running buffer (see Table 2.5) and ran at 100-120V for approximately 1.5 hours.

2.8.5 Western blot

Electrophoresis was stopped when the molecular weight ladder was separated in a desirable range. Proteins were then transferred onto a PVDF membrane (polyvinylidene difluoride; GE Healthcare) after being activated in methanol for 15 sec. The transfer was performed in 1X blotting buffer containing (see Table 2.4) for 2 hours at 80V. After the transfer, the PVDF membrane was blocked in blocking solution of 5% skimmed powdered milk in 1xTBS-T for 1 hour. 1xTBS-T was diluted from the premade 10% 10X TBS (Tris-Buffered Saline) added 0.1% Tween 20. 1L 10% 10X TBS contained 88g NaCl; 24g Tris base; pH 7.4 in a final volume of 1L MilliQ water. The membrane was then incubated with the primary antibody (information on primary antibodies used in this study were summarised in Table 2.5). diluted in a solution of 1% milk-TBS-T overnight in the cold room at 4°C. Next day, the membrane was washed in TBS-T 10min for 3 times at room temperature. Then the membrane was incubated with the HRP-conjugated polyclonal secondary antibody (Dako, Denmark) diluted to 1:2000 in 1% milk-TBS-T for 1h at room temperature. Then the membrane was washed in TBS-T 10min for 3 times after secondary antibody. Finally, the membrane was incubated with Clarity Western ECL solution (BioRad, UK) for 1min and imaged using the ChemiDoc XRS+ System (BioRad, UK) and the images were analysed by Image Lab software (BioRad, UK).

Table 2. 4 Composition for 6%/10%/12%/15%SDS-PAGE (for two 1mm-thick gels)

	Separating gel	**Stacking gel**
H_2O	8.13ml	6.1ml
Tris HCl	3.75ml (1.5M)	2.5ml (0.5M)
Acrylamide	2.92ml (6% Gel) 4.95ml (10% Gel) 5.8ml (12% Gel) 7.25ml (15% Gel)	1.3ml
10% SDS	150ul	100ul
10% APS	75ul	100ul
TEMED	18ul	20ul

Table 2. 5 Recipes of running buffer and transfer buffer

	10X running buffer	**10X transfer buffer**
Tris (free base)	15.2 g	15.2 g
Glycine	72.1 g	72.1 g
SDS	5 g	/
MilliQ water	to 500 ml	to 500 ml

Table 2. 6 List of the antibodies used for Western Blotting

Antibody	Manufacturer	Reference	Dilution	Origin	Size (kDa)
β-Actin	Santa Cruz	sc-69879	1:10000	Mouse	42
GAPDH	Ambion	AM4300	1:5000	Mouse	36
Flag	Sigma	F3165	1:2000	Mouse	N/A
HIF-1α	BD Biosciences	610958	1:500	Mouse	120
WSB-1	Genetex	GTX115792	1:1000	Rabbit	21
E2F1	Cell Signalling	3742	1:1000	Rabbit	70
RAD51	Santa Cruz	sc-398587	1:1000	Rat	37
BRCA1	Novus	NB100-598SS	1:500	Mouse	220
Phospho-BRCA1 (Ser1524)	Cell Signalling	9009	1:1000	Rabbit	220
RB1	Cell Signalling	9309	1:2000	Mouse	110
Phospho-Rb (Ser807/811)	Cell Signalling	8516	1:1000	Rabbit	110
Phospho-CHK1 (Ser345)	Cell Signalling	2348	1:1000	Rabbit	56
Phospho-P53 (Ser15)	Cell Signalling	9286	1:1000	Mouse	53
γH2AX	Cell Signalling	9718	1:1000	Rabbit	15
P53(DO-1)	Santa Cruz	SC-126	1:1000	Mouse	53
Goat anti-Mouse IgG (H+L) Secondary Antibody, HRP	Invitrogen	A16066	1:2000	/	/
Goat anti-Rabbit IgG (H+L) Secondary Antibody	Invitrogen	31460	1:2000	/	/

2.9 Immunofluorescence (IF)

2.9.1 IF staining

Cells were seeded in a sterile glass coverslip at the required cell density and left adhere overnight, and transfected/treated as per experimental design. At the end of the experiment cells were washed with 1x PBS and fixed using 4% formaldehyde (Fisher Scientific, UK) diluted in 1x PBS for 15 minutes at room temperature.

After fixation, cells were washed once with 1x PBS and permeabilized with ice-cold Lysis buffer (0.5% Triton X-100 in 1x PBS) for 10 minutes at room temperature. Next, cells were incubated with IF blocking buffer (2% BSA Tween diluted in 1x PBS) for at least 1 hour at room temperature. Cells were then washed with ice-cold PBS-Tween 0.25% and incubated overnight with the corresponding primary antibodies (see table 2.7) at 4°C. The following morning, cells were first washed with 1x PBS, and then incubated with the corresponding secondary antibodies 1:250 diluted with 2% BSA in PBS-Tween 0.1% of Alexa A488 (IgG (H+L) Cross-Adsorbed Goat anti-Rabbit, Alexa Fluor™ 488, Invitrogen™, USA) and/or Alexa A568 (IgG (H+L) Cross-Adsorbed Goat anti-Rabbit, Alexa Fluor™ 568, Invitrogen™, USA), for single or double labelling for 1 hour in a humidified chamber at 37°C. Next the slides were washed twice in ice-cold PBS-Tween 0.25% and finally washed in 1x PBS. Then cover slips were mounted with Invitrogen™ ProLong™ Gold Antifade Mount DAPI (Invitrogen™ P36941, USA) according to the manufacturer's instructions. Finally, the corners of the cover slides were sealed with clear nail polish and slides were stored at 4°C in the dark until imaging. Images were acquired with the Fluorescence microscope (Zeiss, Germany) and processed with AxioVision AxioVS40 V4.8.1.0 (Zeiss, Germany).

Table 2. 7 List of the antibodies used for Immunofluorescence

Antibody	Manufacturer	Reference	Dilution	Origin	Size (kDa)
γH2AX	Merckmillipore	JBW301	1:500	Mouse	/
53BP1	Novus	NB100-904	1:1000	Rabbit	/
Alexa Fluor™ 488	Invitrogen™	10328172	1:250	/	/
Alexa Fluor™ 568	Invitrogen™	10463022	1:250	/	/

2.9.2 Foci scoring

2200 high through-put imaging system at 100x magnification were taken the Fluorescence microscope (Zeiss, Germany) then scored manually by Fujii (NIH-Bethesda, USA). Scoring criteria was as follow: at least 100 cells per condition were counted, where cells with more than 5 foci were considered positive.

2.10 MTS Assay

The impact of drug treatments on short term cell viability, which does not measure proliferation and viability, were evaluated by using the MTS assay (The CellTiter 96® AQueous One Solution Cell Proliferation Assay, Promega, USA). MTS assay was performed as per manufacturer details. In brief, cells were seeded in a 96-well plate (1x 10^3 cells per well per condition) with transfection reagents and treated with the various experimental conditions noted in the respective Results section. At the end of the relevant timepoint, media were removed, and MTT reagent was added, and the cells were incubated at 37 °C for 4 hours. Colorimetric changes were quantitated spectrophotometrically at 490 nm and the average values were determined from triplicate reading wells. The corresponding DMSO vehicle control for each timepoint was normalised to 100% viability and the cell viability for each treatment group calculated. Dose response curves were calculated using nonlinear repression (curve fit): log (inhibitors concentration) vs response -variable slope by GraphPad Prism 9.

2.11 Clonogenic Survival Assay

2.11.1 Clonogenic survival assay

Cells were seeded and left adhere overnight, then cells were transfected with mock or overexpressed WSB-1 plasmid followed as described in Section 2.4.2. After 24h, cells were harvested and suspended into a single cell and re seeded into 6 well plates. Seeding densities and DDR inhibitors concentration were optimised (Details shown in result Section Chapter 5). After 4h of drugs treatments, cells were exposed to 2 Gy, 4 Gy, 6 Gy irradiation dose respectively. X-ray irradiation was carried out at a dose rate of 1.87 Gy/min by the RS-2000 irradiator (Rad Source Technologies, USA). The plates were remained in the incubator undisturbed until staining. For staining, in brief, media was gently removed and gently rinsed by 1X PBS, then PBS was removed and crystal violet staining solution (0.1% w/v crystal

violet, 70% v/v methanol, 30% v/v dH2O) were applied to each well. Plates were incubated at room temperature for 30 min. Crystal violet solution was then removed from the wells and inactivated in sodium hydroxide (NaOH) solution. Plates were gently and carefully immersed in a container filled with cold tap water to remove excess crystal violet and set aside to air dried at room temperature. Colonies were analysed and counted using a Gel Count system (Oxford Optronics, UK).

2.11.2 Data analysis and calculation

To generate the radiation dose–response curves, surviving fractions from colony survival data were first calculated as followed: number of colonies formed after treatment/number of cells seeded 3x plating efficiency x100). And the data were fitted to the linear quadratic (LQ) model according to the formulae from Anbalagan's paper (Anbalagan et al., 2015) . LQ, the sensitiser enhancement ratios (SER), and Statistical significance (2-Way ANOVA multiple comparison test) were calculated was calculated using by Prism 9 (GraphPad Software Inc, USA).

2.12 Flow cytometry

2.12.1 Cells harvest

$1x10^5$ MCF-7 and MDA-MB-231 cells were seeded in 6-well plate and left adhered overnight, transfected with flag-WSB-1 plasmid for 24hours. After 24hours, media from dishes were collected in a 12ml tube, cells were washed by PBS which also collected into the 12ml tubes. Then cells were trypsinised, pipetted into single cells, stopped the trypsin by the medium collected from the tube, tubes were transferred at the ice, then centrifuged for 5min (2000 rpm) after centrifuged, cells were resuspended with 1ml ice cold PBS, centrifuged for another 5 min (2000 rpm), resuspended cells and 5 ml -20^{o}C 70% ethanol were dropwise while vortexing. Cells were kept in -20^{o}C until staining.

2.12.2 Propidium iodide (PI) staining

For DNA content analysis, fixed cells were centrifuged, and washed once with PBS, to increase membrane permeability, cells were resuspended in 0.5 mL of blocking solution (1X PBS, 2% BSA, 0.1% Tween-20, 0.1% Triton X100) for 1 hour before staining. The plasma membrane of the cells was permeabilised by using Triton-X and the cells were treated with RNase A to remove RNAs from the cells Finally, the cells were treated with RNase A to

remove RNAs from the cells and a fluorescent dye propidium iodide (PI) was also used to quantitatively staining the DNA.

2.12.3 Flow cytometry analysis

After staining, cells were transferred to FACS tubes, then samples were run on the BD Biosciences LSRFortessa^{TM} flow cytometer. The cells and their PI-stained nucleus intercept the Yellow Green Laser (561 nm) beam causing lights, which were detected and electronically recorded. Recorded results then exported as FlowJo-compatible CSV files and analysed using FlowJo® V10 software (FlowJo LLC, Ashland, OR, USA).

2.14 *In silico* analyses

2.14.1 Pathways enrichment analysis

The RNA-seq results were produced previously by our lab (Poujade and Pires, unpublished), in which MDA-MB-231 cells were either transfected with siNT or siWSB1 (see section 2.3) and exposed to hypoxic (2% O_2) or normoxic (20% O_2) conditions respectively for 24 hours (See section 2.4). RNA was extracted as noted in Section 2.4, and RNA Sequencing (RNA-Seq) was performed by LC Sciences (Houston, USA).
The upregulated genes by WSB1 depleted under hypoxia condition were used to do the enrichment analysis. An online analysis website (https://www.networkanalyst.ca/) was used to perform the heatmap and bubble figure (Zhou et al., 2019a). Another online analysis website, Gene Annotation & Analysis Resource (https://metascape.org/) was used to perform biology functions and pathways enrichments from different ontology sources (Zhou et al., 2019c).

2.14.2 Online database patient gene expression analysis

RNA-sequencing datasets (RNA Seq V2 RSEM) for breast invasive carcinoma tumours were downloaded from the patients datasets accessed through cBioportal (http://www.cbioportal.org) (Cerami et al., 2012), using datasets Breast Cancer- METABRIC dataset (n = 2509). In order to examine the relationship between *WSB1* expression and DNA repair signatures or DNA repair pathways including HR pathways, MMR pathways, BER pathways and NHEJ pathways. Gene sets of DNA repair signatures or DNA repair pathways were downloaded from GSEA (https://www.gsea-msigdb.org/). The median expression of *WSB1* were determined. Expression values for DNA repair genes were also calculated by

quantifying the median expression of different gene sets from GSEA respectively. Log10 transformed values of the median DNA repair genes expression values were plotted against Log10 conversion of the median expression of *WSB1* genes by R studio (R studio, USA). Spearman's and Pearson's correlation coefficient was calculated with p-value <0.05 considered significant.

2.15 Statistical analysis

Every experiment was repeated at least three times independently unless otherwise stated. Mean and SE values were compared by using unpaired t tests when one variable was tested. For multiple comparisons (more than two groups) 2-way ANOVA multiple comparison tests were used. $P < 0.05$ was considered statistically significant. $p < 0.05$ was considered statistically significant. The software Prism 9 (GraphPad Software Inc, USA) was used for all statistical analyses, except pathways enrichment analysis which was analysed by the platform itself.

Chapter 3

Investigating novel roles for WSB-1 in gene expression and signalling pathways in breast cancer

3.1 Introduction

Hypoxia has a significant impact on the effectiveness of radiotherapy, with HIF-1α contributing to radioresistance by activating its target genes involved in cell growth, glucose metabolism, angiogenesis, DNA damage repair, invasion, and metastasis (Li et al., 2022). Studies have found high HIF-1α expression is highly associated with poor prognostic outcomes and low survival rates in cancer patients (Lin et al., 2017, Potharaju et al., 2019). As noted in Chapter 1, ionising radiation triggers DNA damage response, and ATM, ATR and DNA PK, these three phosphoinositide 3-kinase-related kinases, play vital roles in DNA damage repair respond to radiation. Hypoxia can activate these three kinases which can increase the repair of damaged DNA caused by radiation. For example, ATM is phosphorylated and active under hypoxic condition even autophosphorylated in the absence of DNA damage during hypoxia (Bencokova et al., 2009). Hypoxia-induced replication arrest by activating ATR-dependent signalling (Hammond et al., 2002, Pires et al., 2010). Hypoxia can also activate DNA-PK and studies found that DNA-PK is an oxygen-dependent regulator of HIF-1α stability (Bouquet et al., 2011). HIF-1 can also downregulate cyclin kinase such as CDK2 and control the function of cyclin kinase inhibitor (CKI), such as p27, p21, (Goda et al., 2003) which normally act to halt cell division in response to DNA damage. This can allow cancer cells to continue to divide, even in the presence of radiation-induced DNA damage. Therefore, HIF-1 modulates signalling pathways including DDR pathways and cause radio resistance.

As noted in chapter 1, WSB-1 is one of the members of the WD40-repeat containing proteins with the SOCS box (Hilton et al., 1998). WSB-1 as an E3 ubiquitin ligase, acts as the substrate recognition subunit of the ECS (Elongin BC-Cul5-Rbx1) ubiquitin ligase complexes, function as modulating ubiquitination in cells (Dentice et al., 2005). Studies have found that WSB-1 reduces the pVHL protein by degrading pVHL as a substrate-recognising subunit of the ECS ubiquitin ligase complex, which stabilizes HIF-1α (Chen et al., 2017, Kim et al., 2015). Moreover, WSB-1 is one of the downstream target genes of HIF-1 and increased in response to hypoxia (Tong et al., 2013, Poujade et al., 2018). Therefore, WSB-1 regulates HIF-1 and affects its activity, meanwhile HIF mediates *WSB1* transcriptional expression, which forms a positive feedback loop.

Studies have found that increased WSB-1 expression was correlated with good prognosis in neuroblastoma (Chen et al., 2006) and high WSB-1 expression was also associated with

progression and metastasis in osteosarcoma (Cao et al., 2015). WSB-1 increased the expression of VEGF and metalloproteinase (MMP) activity and promotes metastasis in oestrogen or progesterone receptors negative breast cancer under hypoxia (Poujade et al., 2018). WSB-1 has been shown to play a role in immune regulation by participating in the maturation degradation of the interleukin-21 receptor (IL-21R) (Nara et al., 2011a). And WSB-1 induces ubiquitylation of the G-CSF-R which affects neutrophil development in myeloid leukaemia (Erkeland et al., 2007).

Interestingly, WSB-1 also plays an important role in DDR. Previous works showed that HIPK2 which is the important factor in cell proliferation and apoptosis can be degraded by WSB-1 (Choi et al., 2008). ATM as a major upstream kinase of the DDR pathway has also been shown to be ubiquitinated by WSB-1, resulting in ATM degradation during tumour initiation (Kim et al., 2017b). However, the role of WSB-1 in DNA damage response in breast cancer especially under hypoxia still unclear.

3.1.1 Hypothesis, aims, and objectives of this chapter

Recently our lab has identified WSB-1 is an important factor in regulating metastasis in hormonal receptor negative breast cancer under hypoxia. However, its role in the DDR has not been investigated. Studies found that WSB-1 also can degrade HIPK2 or ATM and therefore affect DNA repair. In a previous publication from our lab, it was found that WSB-1 depleted led to changes in gene expressions in metastasis-related factors(Poujade et al., 2018) . Furthermore, unpublished RNA-seq analysis from our lab identified that WSB-1 depletion led to dramatic changes in gene expression for a variety of cellular pathways, including the DDR (Poujade and Pires, unpublished).

Therefore, our hypothesis is that WSB-1 plays an important role in mediating the regulation of the expression of DDR signalling factors in hypoxic breast cancer. The aims and objectives of this chapter are therefore to investigate the novel role of WSB-1 in breast cancer, especially its role in DDR signalling under hypoxia.

The specific aims of this chapter are to:
1: Investigate novel pathways regulated by WSB-1 in hypoxic breast cancer by analysing WSB-1 regulated transcriptomic changes
2. Analysis of the transcriptional factor enrichment after WSB-1 depletion under hypoxia.

3. Validate the impact of WSB-1 modulation in regulation of expression of DDR signalling factors under hypoxia in breast cancer *in vitro.*

3.2 Experimental design

3.2.1 Investigating the impact of WSB-1 depletion on the transcriptional changes in MDA-MB- 231 cells by RNA sequencing

In order to investigate the roles in genomic stability of WSB-1 in breast cancer under hypoxia, RNA sequencing (RNA-Seq) data was initially generated by Dr. Flore-Anne Poujade, a previous student in the lab (Poujade, 2016). In her study, MDA-MB-231 cells were transfected either non targeting siRNA (siNT) control or WSB-1 siRNA (siWSB-1) and exposure to either normoxic (20%O_2) or hypoxic (2% O_2) conditions. Then total RNA was extracted and sequenced. Biological functions enrichment and the IPA analysis showed a dramatic gene expression change to several pathways, which are further explored and analysed in this chapter, specifically the hypoxic branch of the experiment.

The differential expressed genes (DEGs) ($p<0.05$ and Fold change over 1.5) between this two groups (siNT vs siWSB-1) were used to generate a heatmap, as well as and pathway enrichment analysis using two different online platforms: ExpressAnalyst (https://www.expressanalyst.ca/) (Zhou et al., 2019b) and Metascape (https://metascape.org/) (Zhou et al., 2019c). The pathways enrichment on NetworkAnalyst used KEGG pathways enrichment. Pathway and process enrichment analysis on Metascape were carried out with different ontology sources including KEGG Pathway, Canonical Pathways, WikiPathways, Reactome pathways, PANTHER Pathway, CORUM, and GO Biological Processes. These ontology sources are all widely used methods in current enrichment analysis platforms which consist of the systematic analysis of gene functions, linking genomic information with higher order functional information to classify and identify the function of gene sets.

3.2.2 *In silico* evaluation of Transcription Factor enrichment downstream of WSB-1

In order to elucidate regulatory factors downstream of WSB1, another transcription factor enrichment analysis ChEA3 (ChIP-X Enrichment Analysis 3) database was used to evaluate the potential transcriptional factors (TF) enrichment which is the downstream of WSB-1 could have caused the changes of the upregulated gene-sets WSB-1 depletion under hypoxia. ChEA3 (https://amp.pharm.mssm.edu/ChEA3) is a transcription factor enrichment analysis tool that ranks TFs associated with user-submitted gene sets (Keenan et al., 2019).

3.2.3 Validation of the impact of WSB-1 depletion and hypoxia exposure on DDR pathways

To validate the RNA-seq data results, two Luminal breast cancer cell lines, MCF-7 and BT474, and two triple negative basal like breast cancer cells, MDA-MB-231 and MDA-MB-468, were transfected with WSB-1 (siWSB-1) or non-targeting siRNA (siNT) and exposed 24 h to 20% O_2 (normoxia) or 1% O_2 (hypoxia). RNA and protein were extracted and analysed by qPCR (Section 2.7) and/or western blotting (Section 2.7) for validation of expression levels of WSB-1 and various DDR pathways genes proteins and changes in their expression in response to was detected by Western blot. WSB-1 overexpression was also used to analyse the impact of WSB-1 modulation in this process. For this, a WSB-1-Flag expressing plasmid were transfected in these four breast cancer cell lines (with mock transfection used as a control), and RNA or protein were extracted and analysed by qPCR or Western blot as before.

3.3 Results

3.3.1 Bioinformatic analysis of RNA-sequencing dataset (siNT vs si-WSB-1)

In order to evaluate the role of WSB-1 in breast cancer under hypoxia, specifically its impact on gene expression changes, RNA-Seq data which was initially generated by Dr. Flore-Anne Poujade, a previous student in the lab (Poujade, 2016) was analysed using various pathway enrichment tools, as noted in section 3.2. Briefly, RNA seq data was generated using MDA-MB-231 cells transfected with either non-targeting siRNA (siNT) or WSB-1 siRNA, (siWSB-1) exposed to either normoxic (20% O_2) or hypoxic (2% O_2) conditions for 24 hours.

Figure 3.1 shows the DEG gene list in hypoxia expression heatmap, generated using online platform ExpressAnalyst (Zhou et al., 2019b). Here, genes that were upregulated are presented in red and downregulated in blue. The heatmap clearly shows the distinct patterns of gene expression changes induced by WSB-1 depletion.

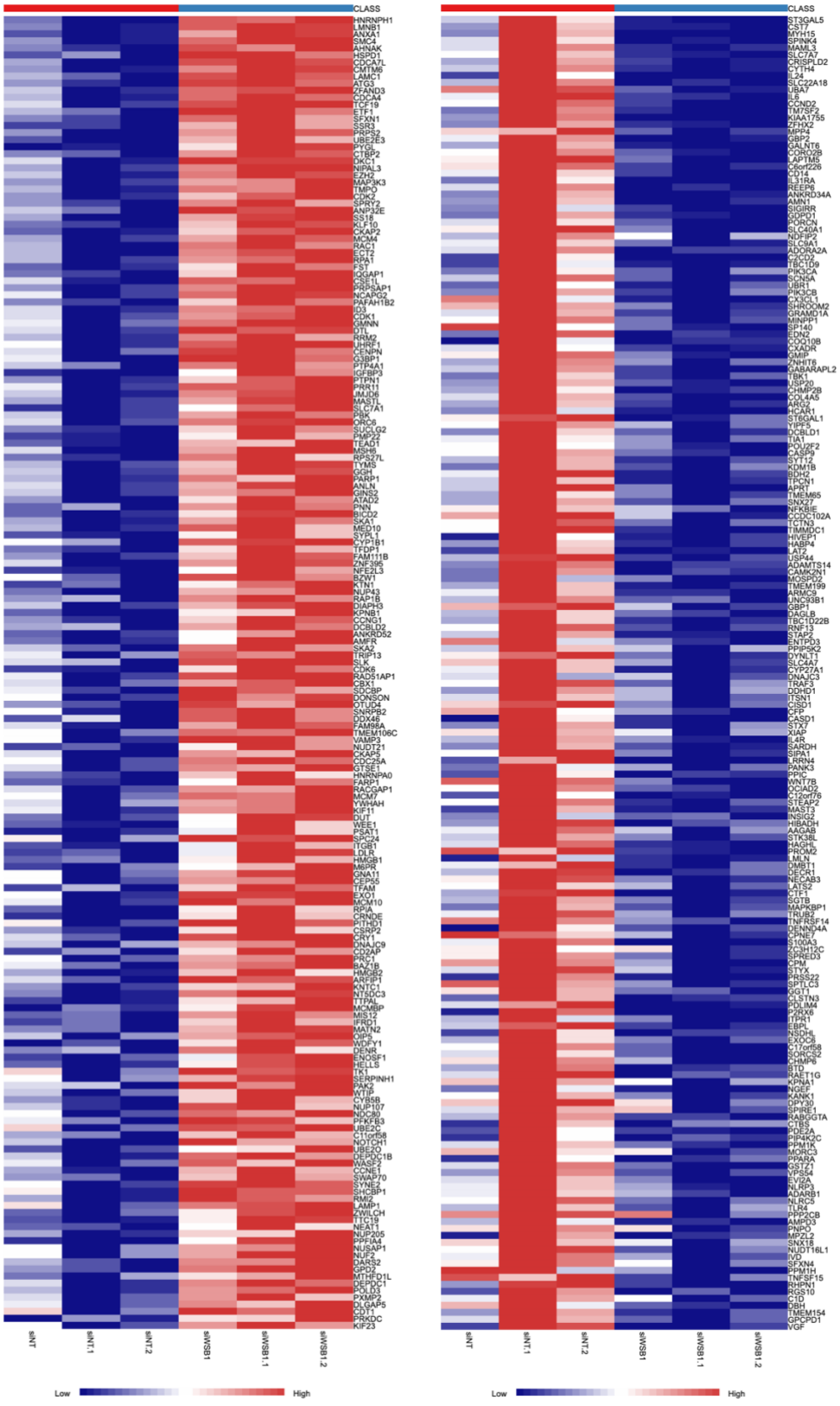

Figure 3. 1 Heatmap for the downregulated genes between siNT and siWSB-1 in 2%O_2
MDA-MB-231 cells were treated with either non-targeting siRNA (siNT) or WSB-1 siRNA(siWSB-1), exposed to hypoxic (2% O_2) conditions for 24 hours. RNA samples were prepared and analysed by RNA-seq (n=3). Heatmap was generated by ExpressAnalyst (https://www.expressanalyst.ca/) shows the significantly upregulated (Left) and downregulated (down) DEG (differentially expressed genes) following WSB-1 depletion ($p<0.05$), Expression changes are represented in blue (low) to red (high).

3.3.2 WSB-1 depletion changed transcriptional expression in DDR pathway

DEGs between siNT vs siWSB-1 in 2% O_2, including both upregulated genes and downregulated genes, were used to perform KEGG pathways enrichment analysis from ExpressAnalyst showed in Figure 3.2, with top 30 pathways enriched shown in Table 3.1. Depletion of WSB-1 under hypoxia led to gene expression changes of factors involved in DDR-relevant pathways including: cell cycle, which has 53 hits out of 124 genes (p=5.16E-19); DNA replication, which has 26 hits out of 36 genes (p=2.17E-17); p53 signalling pathways, which has 25 hits out of 72 genes (p=1.73E-07); BER, which has 15 hits out of 33 genes (p=1.00E-06); MMR, which has 12 hits out of 23 genes (p=1.99E-06); Fanconi anemia pathway, which has 18 hits out of 54 genes (p=1.76E-05); and HR, which has 15 hits out of 41 genes (p=2.52E-05).

As these were predominantly clustered in the upregulated genes group, upregulated DEGs only were used to perform further KEGG pathways enrichments when WSB-1 depletion under hypoxia using the online platform ExpressAnalyst. As Figure 3.3 showed, upregulated genes enriched in Top 5 DDR-relevant pathways including, including cell cycle pathway, which has 29 hits out of 124 genes (p= 1.31E-23); DNA replication pathway, which has 14 hits out of 36 genes (2.41E-15); Fanconi anemia pathway, which has 11 hits out of 54 genes (p= 6.67E-09); p53 signalling pathways, which has 12 hits out of 72 genes (p= 1.49E-08); and HR pathways, which has 9 hits out of 41 genes (p=2.52E-05). These results indicate that depletion of WSB-1 let to upregulation of genes expression for factors relevant to the DDR.

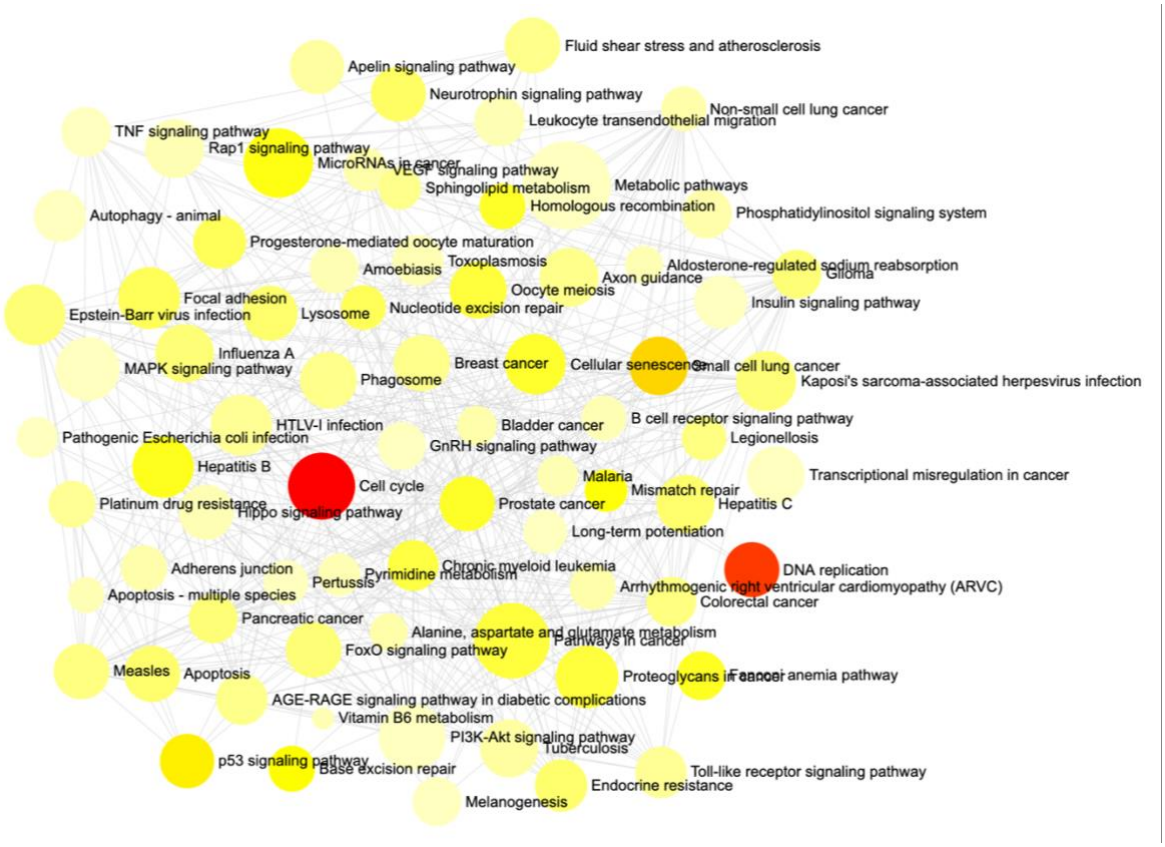

Figure 3.2 WSB-1 depletion associated with transcriptional changes of DNA Damage Response
KEGG pathway enrichments of the upregulated genes following WSB-1 depletion under hypoxia generated from ExpressAnalyst (https://www.expressanalyst.ca/) (Welch's t-test, $p<0.05$). Every yellow bubble represents one pathway, whilst red bubbles represent the top two highest enrichments, and orange bubble is the third highest enrichment.

Table 3. 1 Top 30 enriches KEGG pathways after WSB-1 depletion under hypoxia

Pathway	Total	Expected	Hits	P.Value	FDR
Cell cycle	124	14.2	53	5.16E-19	1.64E-16
DNA replication	36	4.14	26	2.17E-17	3.45E-15
Small cell lung cancer	93	10.7	32	4.24E-09	4.50E-07
p53 signalling pathway	72	8.27	25	1.73E-07	1.38E-05
Base excision repair	33	3.79	15	1.00E-06	6.38E-05
Mismatch repair	23	2.64	12	1.99E-06	0.000106
MicroRNAs in cancer	299	34.4	61	4.01E-06	0.000182
Hepatitis B	163	18.7	38	1.25E-05	0.000498
Fanconi anemia pathway	54	6.2	18	1.76E-05	0.000623
Prostate cancer	97	11.1	26	2.34E-05	0.000729
Homologous recombination	41	4.71	15	2.52E-05	0.000729
Cellular senescence	160	18.4	36	4.76E-05	0.00126
Oocyte meiosis	125	14.4	29	0.000144	0.00351
Proteoglycans in cancer	201	23.1	41	0.000155	0.00351
Pathways in cancer	530	60.9	88	0.00017	0.0036
Chronic myeloid leukemia	76	8.73	20	0.000263	0.00522
Focal adhesion	199	22.9	39	0.000519	0.00971
Nucleotide excision repair	47	5.4	14	0.000563	0.00994
Progesterone-mediated oocyte maturation	99	11.4	23	0.000668	0.0112
Neurotrophin signalling pathway	119	13.7	26	0.000833	0.0132
Hepatitis C	155	17.8	31	0.00133	0.0188
Lysosome	123	14.1	26	0.00139	0.0188
Endocrine resistance	98	11.3	22	0.0014	0.0188
Apoptosis	136	15.6	28	0.00142	0.0188
Pancreatic cancer	75	8.62	18	0.00168	0.0206
Glioma	75	8.62	18	0.00168	0.0206
FoxO signalling pathway	132	15.2	27	0.00189	0.0223
Kaposi's sarcoma-associated herpesvirus infection	186	21.4	35	0.00206	0.0234
Epstein-Barr virus infection	201	23.1	37	0.00232	0.0247

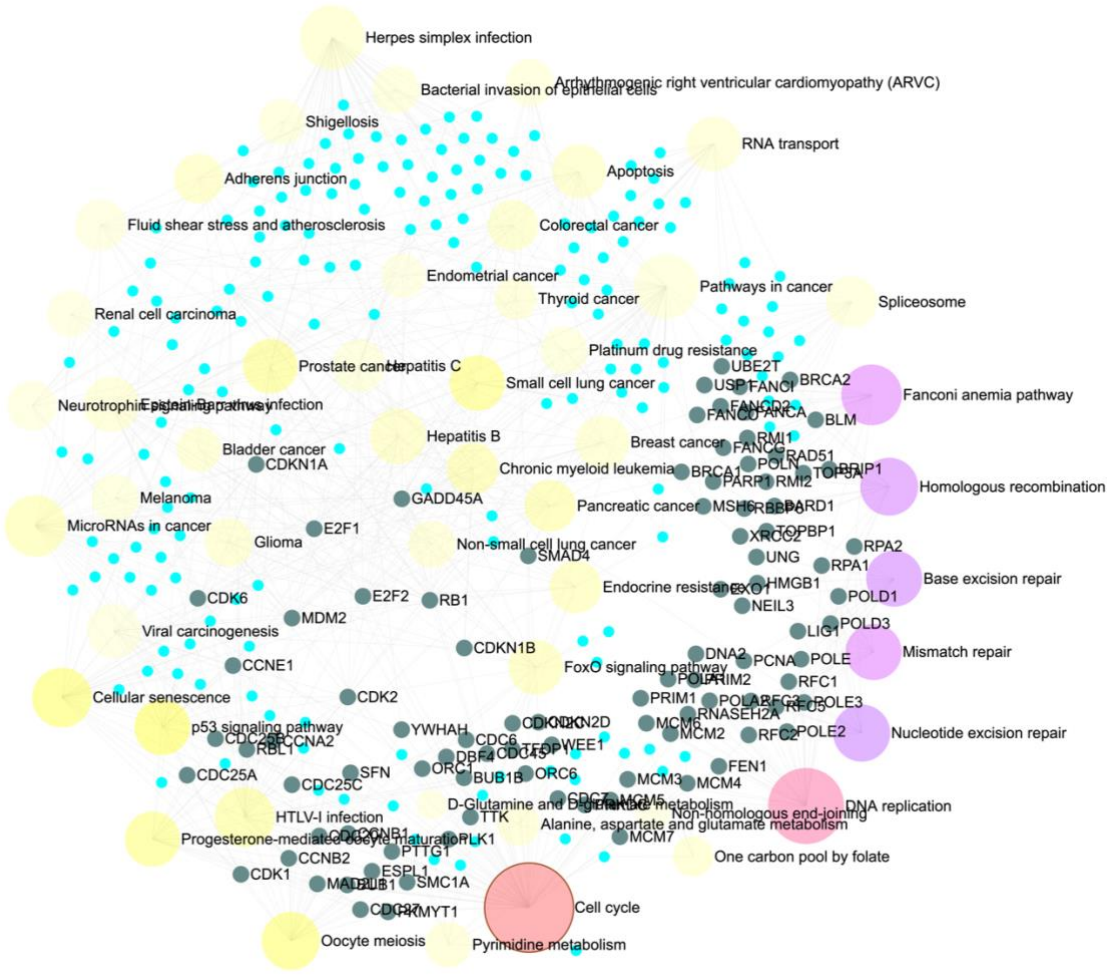

Figure 3. 3 WSB-1 depletion associated with transcriptional changes of DNA Damage Response
KEGG pathway enrichments of the upregulated genes following WSB-1 depletion under hypoxia generated from ExpressAnalyst (https://www.expressanalyst.ca/) (Welch's t-test, $p<0.05$) Every yellow bubble represents one pathway while red bubble represents the top two highest enrichments. Larger bubbles indicate higher number of genes enriched and blue bubble represent one gene and genes names.

3.3.3 WSB-1 depletion is associated with gene changes in DDR pathway from various pathways enrichment analyses

Metascape, another online platform that includes various pathways enrichment analyses, was used to perform the different gene expression pathways enrichments between siNT vs siWSB1 under hypoxia, as shown in Figure 3.4. Top 20 clusters with their representative enriched terms are summarised in Table 3.2. For upregulated and downregulated different gene expression between siNT vs siWSB1, pathway and process enrichment analysis has been carried out with KEGG (KEGG Pathway), Canonical Pathways, Wiki (WikiPathways), Reactome (Reactome pathways), PANTHER Pathway, CORUM, and GO (GO Biological Processes). Amongst these different gene changes respond to WSB-1 depletion under hypoxia compared to siNT group, 215 genes were enriched in cell cycle (Reactome Gene Sets), 201 genes were enriched in mitotic cell cycle (GO Biological Processes), and 182 genes were enriched in regulation of cell cycle process (GO Biological Processes). Interestingly, there were 39 genes enriched in DNA IR-damage and cellular response via ATR, and 41 genes enriched in miRNA regulation of DNA damage response. These results further indicated that WSB-1 depleted under hypoxia drove modulation of expression of DDR factors.

3.3.4 *In silico* analysis of TF enrichment after WSB-1 depletion in hypoxia

In order to elucidate regulatory factors downstream of WSB-1, a transcription factor (TF) enrichment analysis tool ChEA3 (ChIP-X Enrichment Analysis 3) database was used using the RNA-seq dataset to determine potential TFs downstream of WSB-1 that could drive the gene expression changes observed. Top 25 TF are shown in Figure 3.5 and details of these TF are noted in Table 3.3. TFs enriched in this analysis included E2F family members including E2F8, E2F7, E2F2, E2F1, and E2F4. p53, an important factor in cell cycle control and DNA damage repair, was also shown as enriched. These results showed WSB-1 depletion under hypoxia is associated with DNA damage respond and could affect cell cycle regulation and DNA damage repair by regulating E2F family and p53.

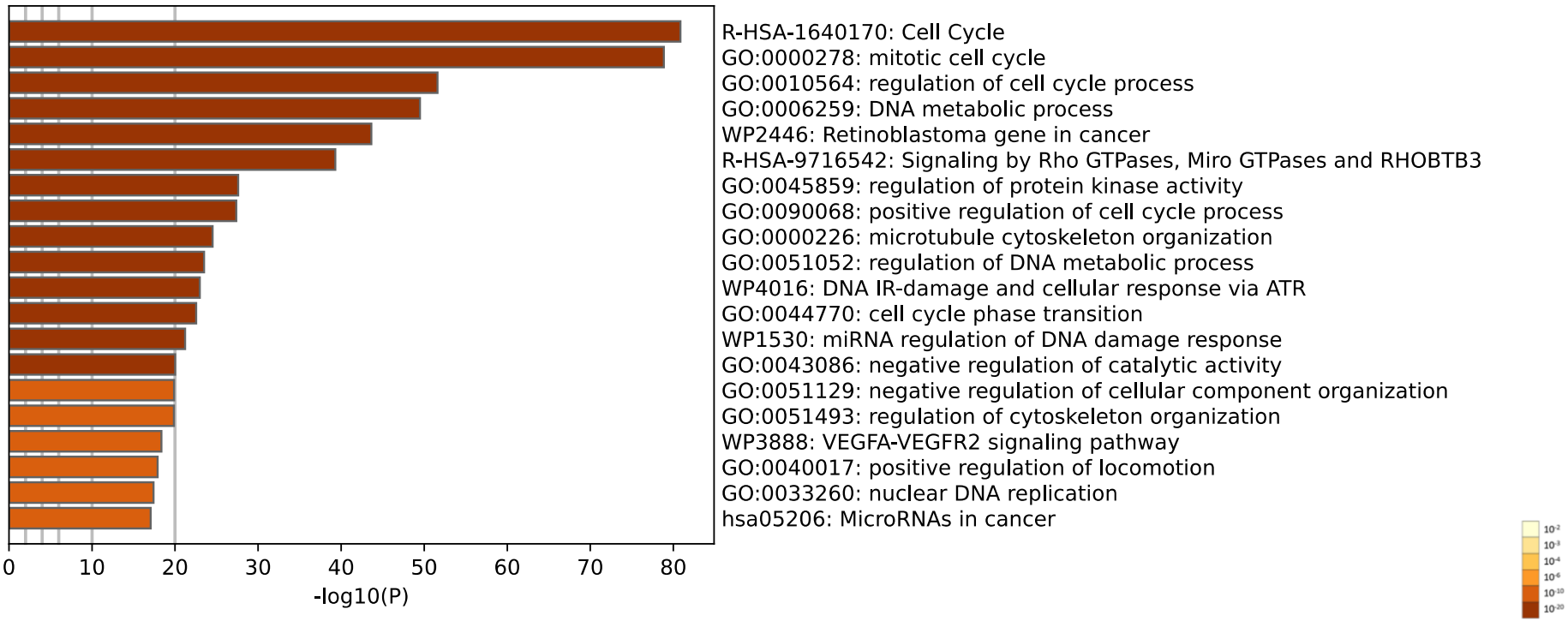

Figure 3. 4 WSB-1 depletion is associated with gene changes in DDR pathway from various pathways enrichment analyses
Bar graph of enriched terms across different gene expression between siNT vs siWSB-1, colour by p-values, terms with a p-value < 0.01, a minimum count of 3, Log10(P) is the p-value in log base 10.

Table 3. 2 Top 20 enriched clusters after WSB-1 depletion under hypoxia

GO	Category	Description	Count	%	Log10 (p)	Log10 (q)
R-HSA-1640170	Reactome	Cell Cycle	215	10.07	-80.86	-76.51
GO:0000278	GO	mitotic cell cycle	201	9.42	-78.86	-74.82
GO:0010564	GO	regulation of cell cycle process	182	8.53	-51.60	-48.10
GO:0006259	GO	DNA metabolic process	185	8.67	-49.48	-46.04
WP2446	Wiki	Retinoblastoma gene in cancer	58	2.72	-43.63	-40.28
R-HSA-9716542	Reactome	Signaling by Rho GTPases, Miro GTPases and RHOBTB3	161	7.54	-39.29	-36.12
GO:0045859	GO	regulation of protein kinase activity	134	6.28	-27.59	-24.76
GO:0090068	GO	positive regulation of cell cycle process	77	3.61	-27.36	-24.55
GO:0000226	GO	microtubule cytoskeleton organization	112	5.25	-24.52	-21.78
GO:0051052	GO	regulation of DNA metabolic process	110	5.15	-23.49	-20.84
WP4016	Wiki	DNA IR-damage and cellular response via ATR	39	1.83	-22.98	-20.37
GO:0044770	GO	cell cycle phase transition	58	2.72	-22.55	-19.99
WP1530	Wiki	miRNA regulation of DNA damage response	41	1.92	-21.22	-18.73
GO:0043086	GO	negative regulation of catalytic activity	133	6.23	-20.01	-17.57
GO:0051129	GO	negative regulation of cellular component organization	122	5.72	-19.87	-17.43
GO:0051493	GO	regulation of cytoskeleton organization	103	4.83	-19.86	-17.42
WP3888	Wiki	VEGFA-VEGFR2 signaling pathway	87	4.08	-18.35	-15.97
GO:0040017	GO	positive regulation of locomotion	107	5.01	-17.90	-15.53
GO:0033260	GO	nuclear DNA replication	19	0.89	-17.41	-15.07
hsa05206	KEGG	MicroRNAs in cancer	69	3.23	-17.06	-14.72

Top 20 clusters with their representative enriched terms (one per cluster). "Count" is the number of genes in the upregulated and downregulated genes upon WSB-1 depletion in hypoxia with membership in the given ontology term. "%" is the percentage of all the upregulated and downregulated genes upon WSB-1 depletion in hypoxia that are found in the given ontology term. "Log10(P)" is the p-value in log base 10. "Log10(q)" is the multi-test adjusted p-value in log base 10.

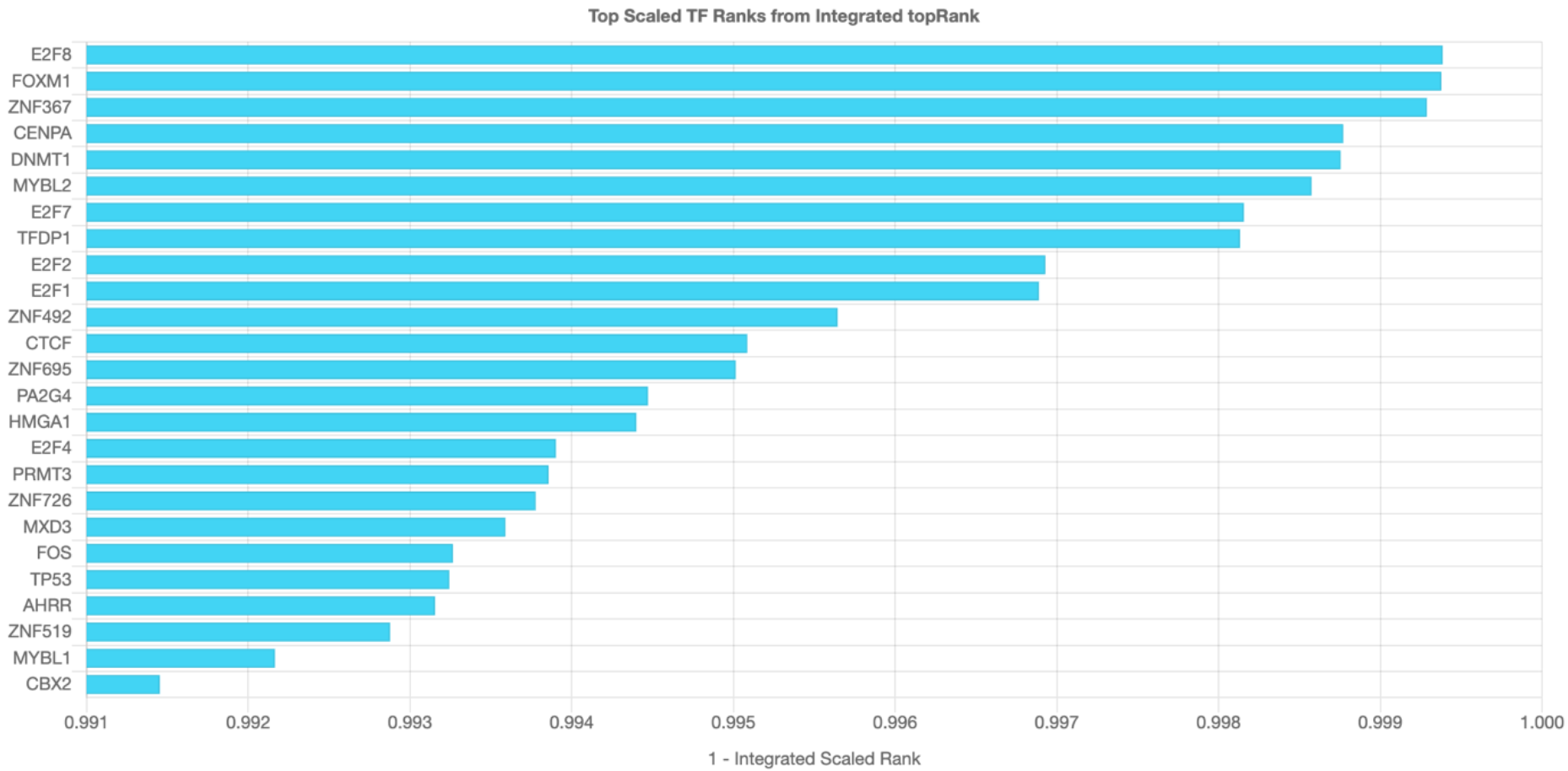

Figure 3. 5 Top 25 transcriptional factors enriched upon WSB-1 depletion
Bar graph of Top 25 enriched transcriptional factors upon WSB-1 depletion under hypoxia generated from ChEA3 (https://amp.pharm.mssm.edu/ChEA3),
The transcriptional factor gene names are shown at the base of histograms while the number in the histograms is their place in the rank.

Table 3. 3 Top 25 transcriptional factors upon WSB-1 depletion

Rank	TF	P value	Library
1	*E2F8*	6.14E-04	ARCHS4 Coexpression
2	*FOXM1*	6.22E-04	GTEx Coexpression
3	*ZNF367*	7.12E-04	Enrichr Queries
4	*CENPA*	0.001229	ARCHS4 Coexpression
5	*DNMT1*	0.001245	GTEx Coexpression
6	*E2F7*	0.001843	ARCHS4 Coexpression
7	*MYBL2*	0.002137	Enrichr Queries
8	*TFDP1*	0.002489	GTEx Coexpression
9	*E2F2*	0.003071	ARCHS4 Coexpression
10	*E2F1*	0.003111	GTEx Coexpression
11	*ZNF492*	0.004356	GTEx Coexpression
12	*CTCF*	0.004914	ARCHS4 Coexpression
13	*HMGA1*	0.004978	GTEx Coexpression
14	*ZNF695*	0.004986	Enrichr Queries
15	*PA2G4*	0.005528	ARCHS4 Coexpression
16	*MXD3*	0.005698	Enrichr Queries
17	*E2F4*	0.006098	Literature ChIP-seq
18	*PRMT3*	0.006143	ARCHS4 Coexpression
19	*ZNF726*	0.006223	GTEx Coexpression
20	*E2F5*	0.006734	ReMap ChIP-seq
21	*TP53*	0.006757	ARCHS4 Coexpression
22	*AHRR*	0.006845	GTEx Coexpression
23	*ZNF519*	0.007123	Enrichr Queries
24	*ZNF530*	0.007835	Enrichr Queries
25	*CBX2*	0.008547	Enrichr Queries

3.3.5 WSB-1 depletion increased gene expression of key DNA repair and cell cycle regulation factors (RNA level)

The details of the fold changes and p value of the top 30 upregulated genes that responded to WSB-1 depletion under hypoxia which are involved in DDR pathways (including cell cycle, DNA replication, and DNA repair) are shown in Table 3.1. Amongst these upregulated genes, cell cycle regulation factors such as E2F family such as *E2F1*, *E2F2* and cell cycle kinases including *CDK6*, *CDK2*, *CDK1*, *WEE1*, were significantly upregulated respond to WSB-1 depletion under hypoxia. Key DNA repair factors in HR pathway such as *BLM, RAD51, XRCC2, BRCA1,* and *BRCA2* were also significantly upregulated by WSB-1 depletion. These results indicate that WSB-1 depletion upregulated key DNA repair factors and cell cycle regulators that involved in DDR pathways under hypoxia in MDA-MB-231.
To independently validate the impact of WSB-1 depletion on DNA repair and cell cycle regulation, a panel of cell lines, including two Luminal breast cancers cell lines (MCF-7, BT474) and two TNBC cells (MDA-MB-231, MDA-MB-468) were transfected with WSB-1 siRNA (siWSB-1) or non-targeting control (siNT) and exposed to normoxic (20% O_2) or hypoxic (1% O_2) conditions.

As the Figure 3.6 shows, *WSB1* was significantly depleted under normoxia and hypoxia conditions in all cell lines, to different degrees, from approximately 50% for MCF7 ($p<0.0001$), 70% for BT474 ($p<0.0001$), 90% for MDA-MB-231 ($p<0.0001$), and 50% for MDA-MB-468 ($p<0.05$). WSB-1 was also upregulated in hypoxic conditions for all cell lines, as previously reported (Poujade et al., 2018).

Regarding the DNA repair factors *BRCA1*, *BRCA2*, and *RAD51*, a trend was observed for all cell lines regarding the impact of WSB-1 depletion, in which these factors were upregulated to various degrees.

As shown in Figure 3.7, in MCF-7, after WSB-1 depletion *BRCA1* expression increased by 2.5-fold change under normoxia ($p<0.0001$). Under hypoxia after WSB-1 depletion, *BRCA1* increased 1.0-fold change ($p<0.0001$) compared to siNT control. *BRCA1* decreased by 0.8-fold change under hypoxia alone but this change was not statistic significant. When WSB-1 was depleted, *BRCA2* increased by 1.9-fold change under normoxia ($p<0.01$), and under hypoxia after WSB-1 depletion, *BRCA2* increased 1.8-fold change ($p=0.0001$) compared to siNT control. Under hypoxia alone, *BRCA2* decreased by 0.7-fold change, which was not statistic significant. When WSB-1 was depleted, *RAD51* increased by 2.6-fold change under

normoxia ($p<0.01$). Under hypoxia after WSB-1 depletion, *RAD51* increased 3.3-fold change ($p<0.0001$) compared to siNT control. Under hypoxia alone, *RAD51* decreased by 0.5-fold change, which is not statistic significant.

In BT474 cells (Figure 3.7), when WSB-1 was depleted, *BRCA1* increased by 1.5-fold change under normoxia ($p<0.01$). Under hypoxia after WSB-1 depletion, *BRCA1* increased 0.0695-fold change compared to siNT control, and this change is not statistic significant. And under hypoxia, *BRCA1* decreased by 0.6 -fold change ($p<0.05$). When WSB-1 was depleted, *BRCA2* increased by 2.6-fold change under normoxia ($p<0.001$). Under hypoxia, WSB-1 depletion let to an increase of *BRCA2* expression by 0.9-fold when compared to siNT control ($p<0.01$). Although *BRCA2* decreased by 0.4-fold change under hypoxia, this change is not statistic significant. Compared to siNT control, when WSB-1 was depleted, *RAD51* increased by 1.6 -fold change under normoxia and increased 0.7 -fold change under hypoxia alone. However, these changes are not statistic significant. *RAD51* decreased by 0.9 -fold change under hypoxia, which is also not statistic significant.

In MCF-7, WSB-1 depletion led to increased *E2F1* expression by 2.7-fold change under normoxia, however this change is not statistically significant. Under hypoxia alone, *E2F1* decreased by 0.5-fold change but the decreased is also not statistically significant. Under hypoxia after WSB-1 depletion, *E2F1* was increased by 3.0-fold change compared to siNT control ($p<0.01$). When WSB-1 was depleted, *RB1* increased by 1.2-fold change under normoxia ($p<0.05$). Under hypoxia, WSB-1 depletion let to *RB1* expression increase of 0.6-fold change ($p<0.0001$) compared to siNT control. And under hypoxia alone, *RB1* decreased by 0.7-fold change ($p<0.01$). *CDK6* expression increased by 2.5-fold change under normoxic ($p<0.01$) and hypoxic ($p<0.0001$) conditions after WSB-1 depletion. Under hypoxia alone, *CDK6* decreased by 0.8-fold change, but this change is not statistic significant (Figure 3.9).

And in BT474 cells, when WSB-1 was depleted, *E2F1* expression increased by 2.4-fold change under normoxia ($p<0.05$) and decreased 0.06-fold change when compared to siNT. Under hypoxia alone, *E2F1* decreased by 0.7-fold change, *RB1* expression increased by 1.1-fold and 0.05-fold change respectively under normoxia and hypoxic conditions, albeit not significantly. Under hypoxia alone, *RB1* decreased by 0.9 -fold change which is also not statistic significant. Compared to siNT control, WSB-1 depletion led to *CDK6* expression increase by 2.5 -fold change under normoxia ($p<0.0001$) and 0.9-fold change under hypoxia

($p<0.0001$) when compared to siNT. Under hypoxia alone, *CDK6* decreased by 0.7 -fold change ($p<0.05$). (Figure 3.9)

Taken together, a trend of an upregulation of cell cycle regulation genes *E2F1, RB1* and *CDK6* was observed when WSB-1 was depleted *in* luminal A breast cancer cell line MCF7 and luminal B breast cancer cell line BT474 under normoxia and hypoxia.

Regarding the triple negative cell lines, as shown in Figure 3.8 showed, in MDA-MB-231, under hypoxia after WSB-1 depletion, *BRCA1* increased 1.4 -fold change ($p<0.0001$) compared to siNT. Under hypoxia alone, *BRCA1* decreased by 0.7-fold change which is not statistic significant. When WSB-1 was depleted, *BRCA2* increased 3 -fold change under normoxia ($p<0.0001$). And under hypoxia alone, *BRCA2* decreased by 0.7-fold change which is not statistic significant. Under hypoxia, WSB-1 depletion led to *BRCA2* expression to increased 1.4-fold change compared to siNT ($p<0.001$). After WSB-1 depletion, *RAD51* increased by 3.6-fold change under normoxia ($p<0.0001$). Under hypoxia, WSB-1 depletion led to *RAD51* expression increase by 1.3-fold change ($p<0.0001$) compared to siNT control. Under hypoxia alone, *RAD51* decreased by 0.6-fold change ($p<0.05$).

For MDA-MB-468 (Figure 3.8), WSB-1 depletion *BRCA1* increased by 1.8-fold change under normoxia ($p<0.001$). Under with depleted WSB-1, *BRCA1* decreased by 0.05-fold change compared to siNT and this change is not statistic significant. Under hypoxia alone, *BRCA1* decreased by 0.38-fold change ($p<0.01$). WSB-1 depletion led to an increase of *BRCA2* expression by 1.2-fold change under normoxia ($p<0.05$). Under hypoxia, WSB-1 depletion led to increased *BRCA2* 0.4-fold change compared to siNT ($p<0.01$). Under hypoxia alone, *BRCA2* decreased by 0.5-fold change($p<0.001$). When depleted WSB-1, *RAD51* increased by 1.7-fold change under normoxia ($p<0.05$). Under hypoxia alone, *RAD51* decreased by 0.5-fold change which is not statistic significant, and under hypoxia after WSB-1 depletion, *RAD51* increased 0.8 -fold change compared to siNT control ($p<0.01$).

Table 3. 4 The top 30 upregulated genes involved in DDR pathways when depleted was WSB-1 under hypoxia

Gene ID	Gene full name	Fold change	p value	Enrich KEGG pathway
E2F2	E2F Transcription Factor 2	5.0	5.00E-05	Cell cycle
CDK6	Cyclin Dependent Kinase 6	4.5	5.00E-05	Cell cycle
CDK2	Cyclin Dependent Kinase 2	4.3	5.00E-05	Cell cycle
WEE1	WEE1 G2 Checkpoint Kinase	4.1	5.00E-05	Cell cycle
FANCD2	FA Complementation Group D2	3.8	5.00E-05	Fanconi anemia pathway
ORC6	Origin Recognition Complex Subunit 6	3.4	5.00E-05	Cell cycle
BLM	BLM RecQ Like Helicase			Fanconi anemia pathway
		3.4	5.00E-05	HRR
RAD51	RAD51 Recombinase	3.3	5.00E-05	Fanconi anemia pathway
				HRR
EXO1	Exonuclease 1	3.3	5.00E-05	MMR
PLK1	Polo Like Kinase 1	3.2	5.00E-05	Cell cycle
RMI2	RecQ Mediated Genome Instability 2	3.0	5.00E-05	Fanconi anemia pathway
BRCA1	BRCA1 DNA Repair Associated	2.9	5.00E-05	Fanconi anemia pathway
XRCC2	X-Ray Repair Cross Complementing 2	2.9	5.00E-05	HRR
CDK1	Cyclin Dependent Kinase 1	2.8	5.00E-05	Cell cycle
NEIL3	Nei Like DNA Glycosylase 3	2.7	5.00E-05	BER
E2F1	E2F Transcription Factor 1	2.7	5.00E-05	Cell cycle
FANCI	FA Complementation Group I	2.6	5.70E-03	Fanconi anemia pathway
MCM7	Minichromosome Maintenance Complex Component 7	2.6	5.00E-05	Cell cycle DNA replication
CDC45	Cell Division Cycle 45	2.6	5.00E-05	Cell cycle
POLE	DNA Polymerase Epsilon, Catalytic Subunit	2.6	5.00E-05	DNA replication BER NER
RFC3	Replication Factor C Subunit 3	2.6	5.00E-05	DNA replication MMR NER

CCNA2	Cyclin A2	2.5	3.00E-04	Cell cycle
BRCA2	BRCA2 DNA Repair Associated	2.5	5.00E-05	Fanconi anemia pathway HRR
MCM2	Minichromosome Maintenance Complex Component 2	2.5	2.00E-04	Cell cycle DNA replication
PKMYT1	Protein Kinase, Membrane Associated Tyrosine/Threonine 1	2.5	1.10E-03	Cell cycle
BRIP1	BRCA1 Interacting Protein C-Terminal Helicase 1	2.4	5.00E-05	Fanconi anemia pathway
TTK	TTK Protein Kinase	2.5	5.00E-05	Cell cycle
CDC6	Cell Division Cycle 6	2.3	5.00E-05	Cell cycle
FANCG	FA Complementation Group G	2.3	5.00E-05	Fanconi anemia pathway
FANCA	FA Complementation Group A	1.2	3.35E-03	Fanconi anemia pathway

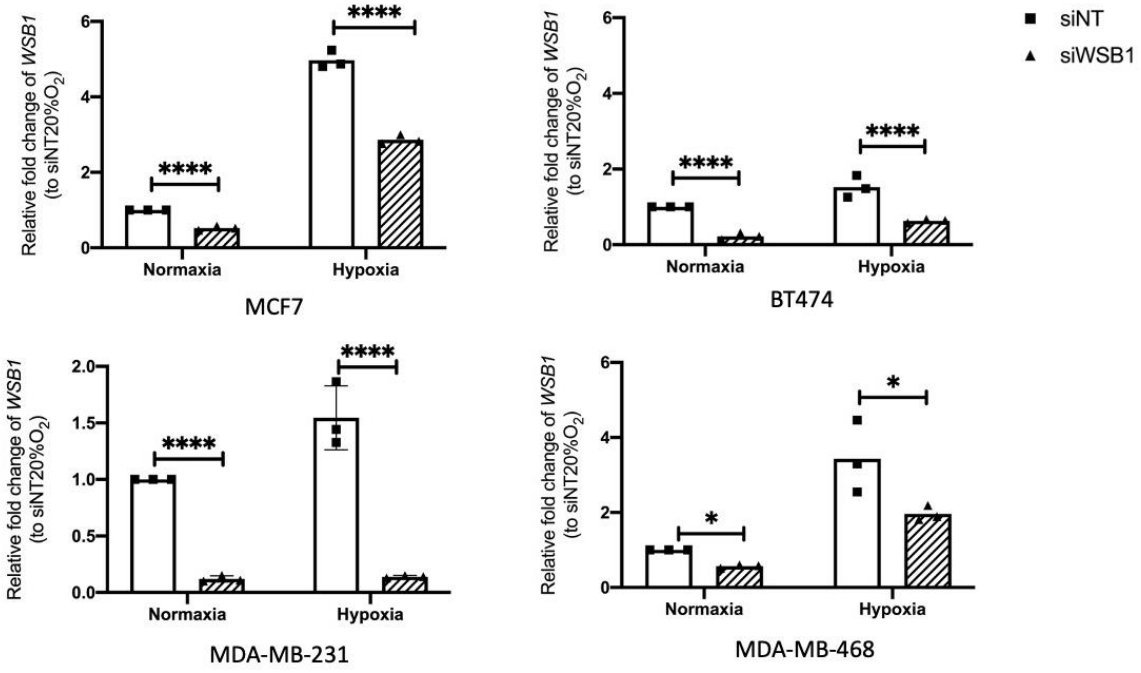

Figure 3.6 Validation of WSB-1 depletion in MCF7, BT474, MDA-MB-231, and MDA-MB-468
MCF-7, BT474, MDA-MB-231, and MDA-MB-468 cells were transfected with WSB-1 (siWSB-1) or non-targeting siRNA (siNT) and exposed 24 h to 20% (normoxia) or 1% O_2 (hypoxia). mRNA samples were extracted, reversed into cDNA and analysed by qPCR for validation of expression levels of *WSB1* expression. *B2M* was used as a housekeeping gene, and control sample was siNT 20% O_2. Histograms represent the average of n=3 independent biological repeats Error bars represent mean ± SEM. Statistical significance was determined using 2-Way ANOVA with multiple comparisons. * $p<0.05$; ** $p<0.01$; *** $p<0.001$; **** $p<0.0001$

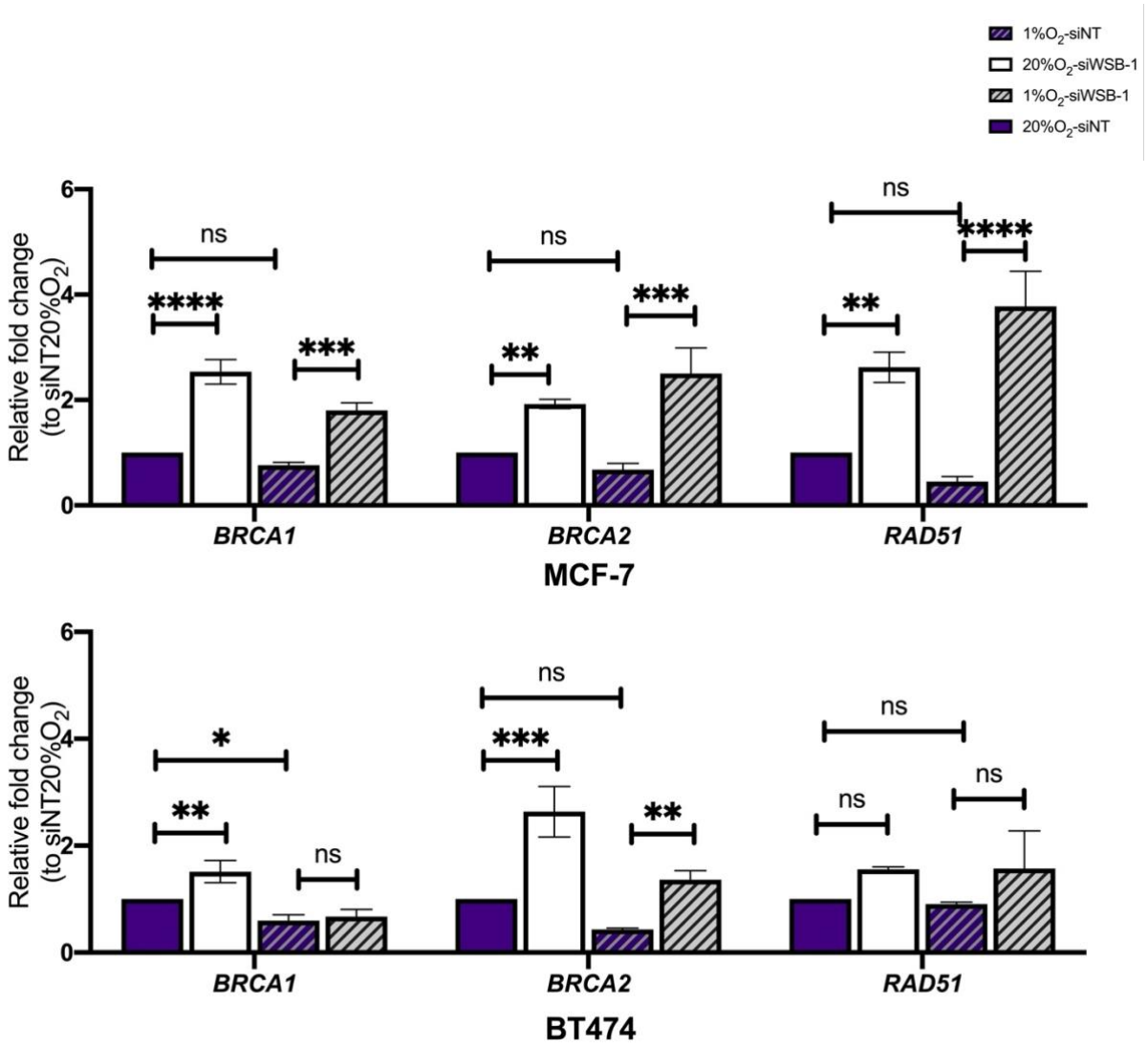

Figure 3. 7 WSB-1 depletion upregulated DNA repair factors in MCF7 and BT474
MCF-7, BT474 were transfected with WSB-1 (siWSB-1) or non-targeting siRNA (siNT) and exposed 24 h to 20% (normoxia) or 1% O_2 (hypoxia). mRNA samples were extracted, reversed into cDNA and analysed by qPCR for validation of expression levels of DNA repair factors *BRCA1, BRCA2, RAD51*. n=3 independent biological repeats. * $p<0.05$; ** $p<0.01$; *** $p<0.001$; **** $p<0.0001$, ns: not significant, 2-Way ANOVA multiple comparison siNT vs siWSB-1, Error bars represent mean ± SEM.

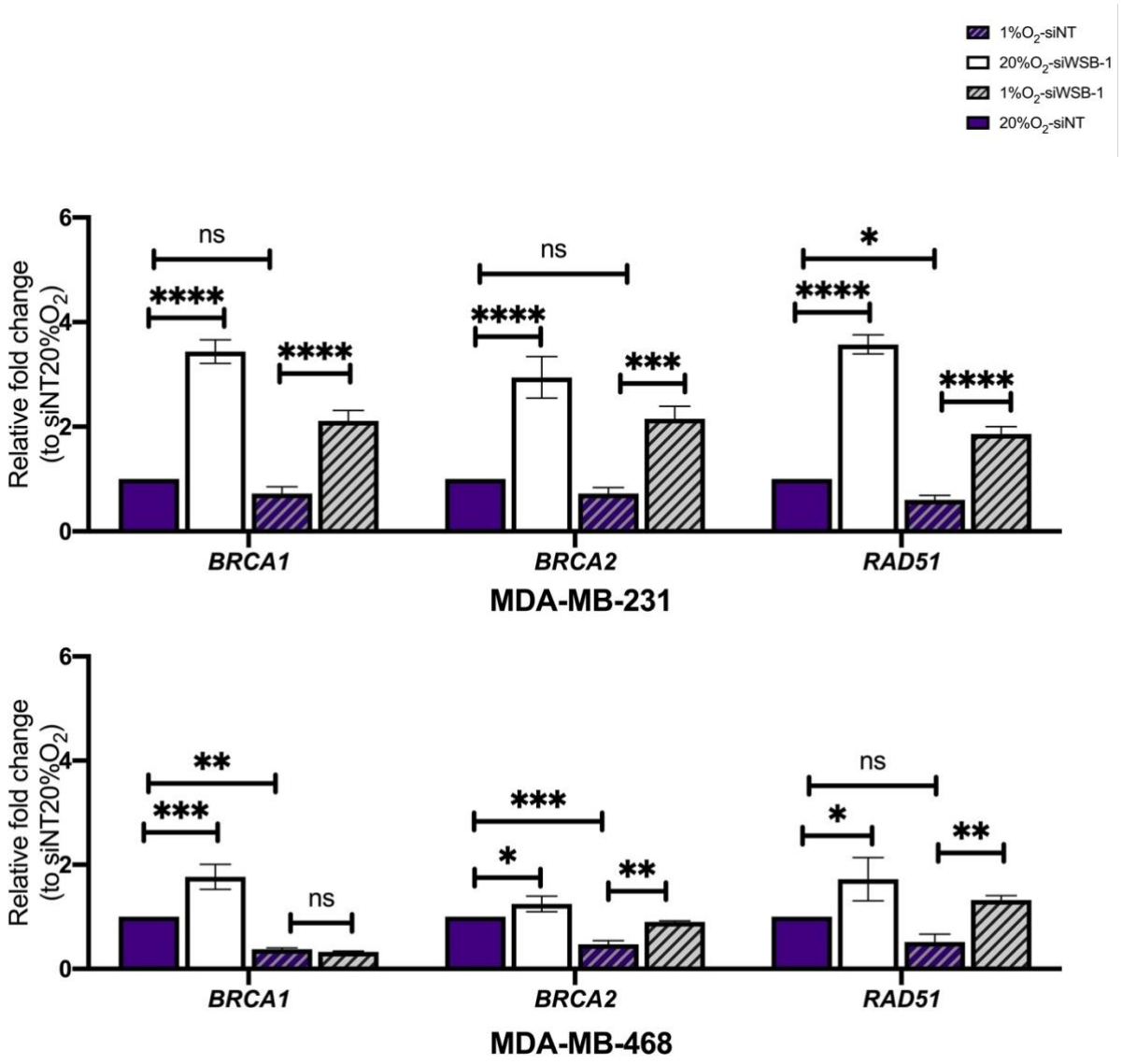

Figure 3. 8 WSB-1 depletion upregulated DNA repair factors in MDA-MB-231 and MDA-MB-468
MDA-MB-231 and MDA-MB-468 were transfected with WSB-1 (siWSB-1) or non-targeting siRNA (siNT) and exposed 24 h to 20% (normoxia) or 1% O_2 (hypoxia). mRNA samples were extracted, reversed into cDNA and analysed by qPCR for validation of expression levels of *BRCA1, BRCA2, RAD51.* n=3 independent biological repeats. * $p<0.05$; ** $p<0.01$; *** $p<0.001$; **** $p<0.0001$, ns: not significant, 2-Way ANOVA multiple comparison siNT vs siWSB-1, Error bars represent mean ± SEM.

In MDA-MB-231, WSB-1 depletion led to *E2F1* expression increase by 5.2-fold change under normoxia ($p<0.0001$) and 1.8-fold change under hypoxia ($p<0.01$) when compared to siNT. Under hypoxia alone, *E2F1* decreased by 0.6-fold change ($p<0.0001$) but this change is not statistic significant. Under normoxia, *RB1* increased by 1.6-fold change when depleted WSB-1 ($p<0.0001$) and increased 0.4 -fold change under hypoxia ($p<0.001$) compared to siNT control. Under hypoxia alone, *RB1* decreased by 0.9-fold change which is not statistically significant. When WSB-1 was depleted, *CDK6* increased by 3.2-fold change under normoxia ($p<0.001$) and by 2.8-fold change in hypoxia ($p<0.001$) compared to siNT. Under hypoxia alone, *CDK6* decreased by 0.8-fold change but this change is not statistic significant.

In MDA-MB-468 cells, WSB-1 depletion led to *E2F1* expression increase by 1.3 -fold change under normoxia and 0.2-fold change under hypoxia compared to siNT. However, these changes are not statistic significant. And under hypoxia alone, *E2F1* decreased by 0.16 -fold change ($p<0.001$), which suggested hypoxia could has a bigger impact on E2F1 expression than WSB-1 in MDA-MB-468 cells. Compared to siNT control, when WSB-1 was depleted, *CDK6* increased by 2.0 -fold change under normoxia and 5.2 -fold change under hypoxia compared to siNT. And under hypoxia, *CDK6* increased by 1.0 -fold change. However, these changes are not statistic significant. In MDA-MB-468 cells it was not possible to detect enough *RB1* transcripts, which aligned with other studies, which found that MDA-MB-468 could exhibit low or no RB1 expression (Robinson et al., 2013).

These data indicate that WSB-1 depletion mostly led to an increase in gene expression of the DDR factors analysed, with some cell line and oxygen tension-dependent variability, which will be discussed later in this chapter.

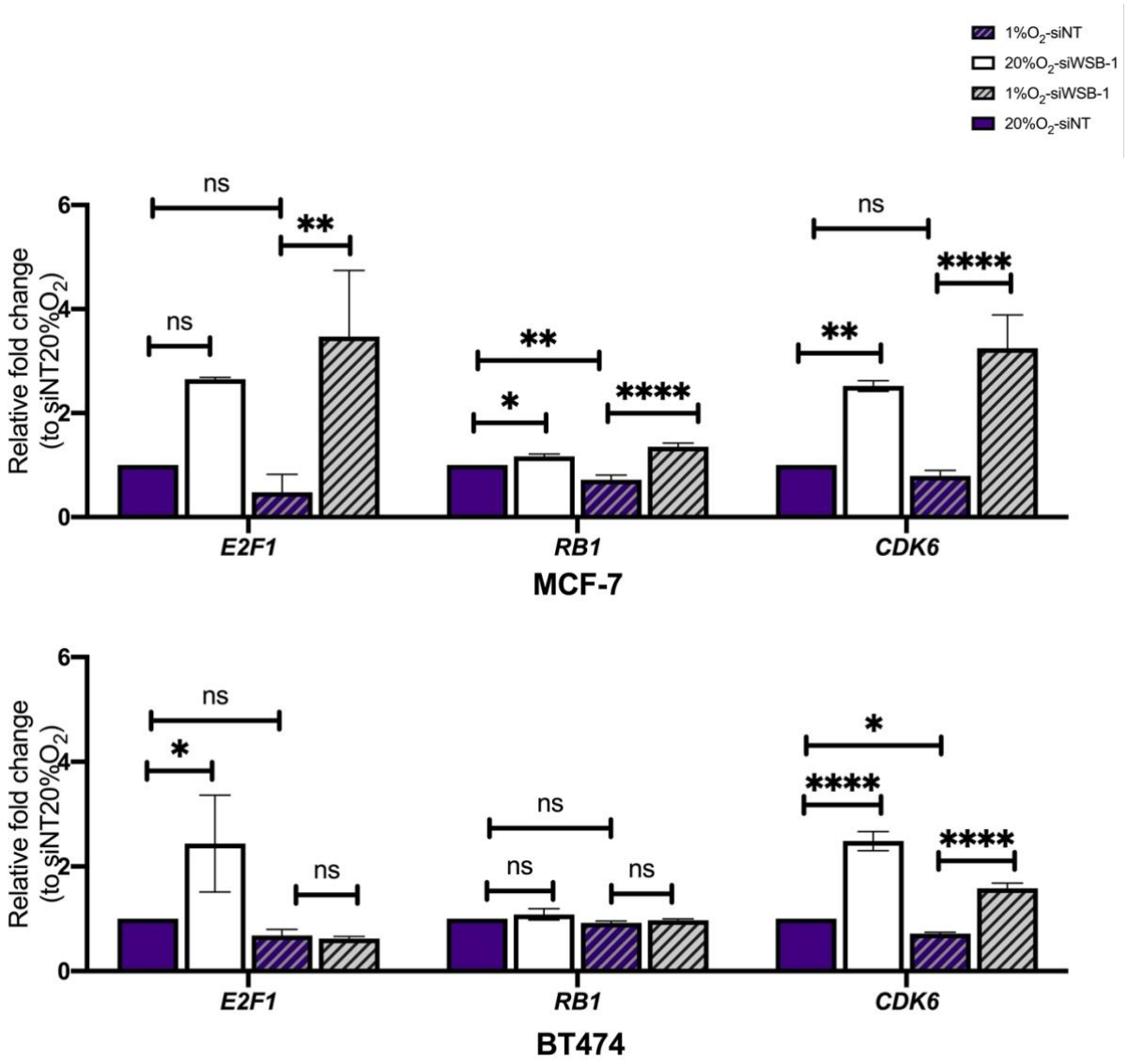

Figure 3. 9 The impact of WSB-1 depletion on cell cycle regulation in MCF-7 and BT474
MCF-7 and BT474 were transfected with WSB-1 (siWSB-1) or non-targeting siRNA (siNT) and exposed 24 h to 20% (normoxia) or 1% O_2 (hypoxia). mRNA samples were extracted, reversed into cDNA and analysed by qPCR for validation of expression levels of *E2F1*, *RB1*, *CDK6*. n=3 independent biological repeats. * $p<0.05$; ** $p<0.01$; *** $p<0.001$; **** $p<0.0001$, ns: not significant, 2-Way ANOVA multiple comparison siNT vs siWSB-1, Error bars represent mean ± SEM.

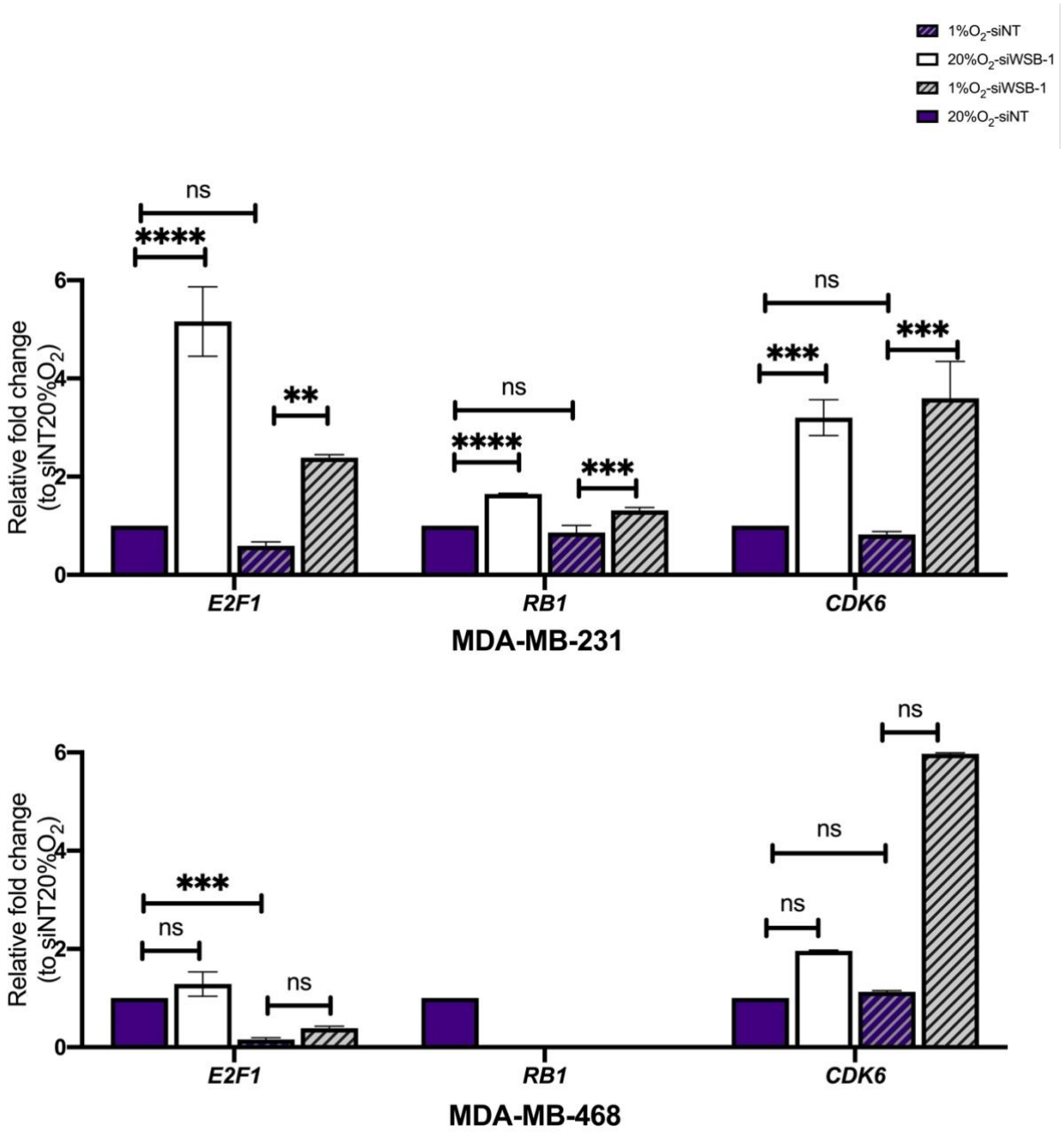

Figure 3. 10 The impact of WSB-1 depletion on cell cycle regulation in MDA-MB-231 and MDA-MB-468
MDA-MB-231, MDA-MB-468 were transfected with WSB-1 (siWSB-1) or non-targeting siRNA (siNT) and exposed 24 h to 20% (normoxia) or 1% O_2 (hypoxia). mRNA samples were extracted, reversed into cDNA and analysed by qPCR for validation of expression levels of *E2F1*, *RB1*, *CDK6.* n=3 independent biological repeats. * $p<0.05$; ** $p<0.01$; *** $p<0.001$; **** $p<0.0001$, 2-Way ANOVA multiple comparison siNT vs siWSB-1, Error bars represent mean ± SEM.

3.3.6 WSB-1 depletion upregulated some DNA repair and cell cycle regulation factors (Protein level)

In order to further evaluate how these DNA repair and cell cycle regulation factors respond to WSB-1 depletion at the protein level, MCF-7 and MDA-MB-231 cells were transfected with either WSB-1 siRNA (siWSB-1) or non-targeting control (siNT) in normoxic or hypoxic condition as described before. Analysis of protein samples for specific protein expression was conducted by western blotting. As shown in Figure 3.11 for MCF7 cells WSB-1 depletion mostly led to an increase in BRCA1 and RAD51 protein expression, albeit not significantly due to variability between samples. WSB-1 depletion also upregulated the protein expression of E2F1 under normoxic conditions, with more variable results in hypoxic conditions, and again not statistically significant. For RB1, a change in the intensity of the doublet bands was observed but again showed variability. For MDA-MB-231 (Figure 3.12) WSB-1 depletion led to more mixed results re impact on protein expression, with variability between samples, so no clear conclusions can be drawn. Analysis of BRCA2 and E2F1 expression in hypoxic conditions was challenging as expression was repressed. However, due to the variety of WSB-1 depletion efficiency, the quantification shows these changes are not statistic significant. protein expression results vary between these two cells lines especially the expression E2F1, possible reasons could be because MDA-MB-231 is a more aggressive TNBC cancer type and is also lack of RB1 expression (Robinson et al., 2013). These could be tested by overexpressed RB1 in MDA-MB-231 cells or deplete RB1 in MCF7.These results indicate that the gene expression changes are partially represented at protein level in terms of trends but require further confirmation due to sample-to-sample variability.

3.3.7 Overexpression of WSB-1 is associated with repression of gene expression of DNA repair and cell cycle regulation factors (RNA level)

To further test the impact of WSB-1 on the expression of these DDR factors, we used a flag-WSB-1 construct to ectopically overexpress WSB-1 in MCF-7, BT474, MDA-MB-231 and MDA-MB-468 cells to determine the effects of WSB-1 overexpression on DNA repair and cell cycle factor gene expression under normoxic (20% O_2) and hypoxic (1% O_2) conditions. As shown on Figure 3.13, *WSB-1* was significantly overexpressed in all cell lines in different degrees under normoxia and hypoxia. Compared to siNT, *WSB-1* was increased by 287.6-fold change under normoxia and 700.3-fold change under hypoxia in MCF-7 ($p<0.0001$). In BT474, *WSB-1* was increased by 50.7-fold change under normoxia and increased by 91.9-fold change under hypoxia in comparation to siNT ($p<0.0001$).

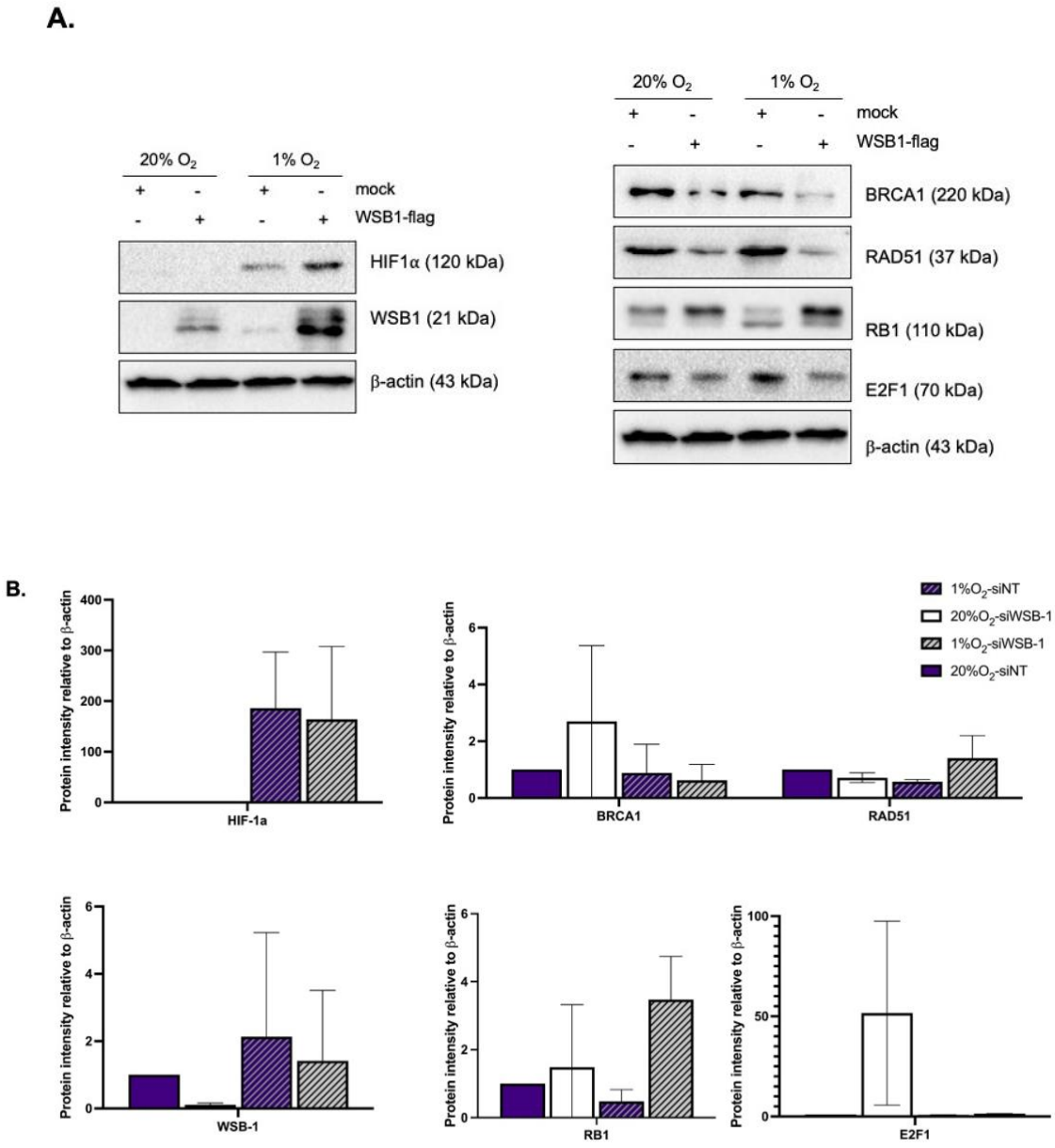

Figure 3. 11 Effect of WSB-1 depletion on DDR pathways regulators in MCF7

MCF7 cells were transfected with siWSB1(siWSB1) or non-targeting siRNA (siNT) and exposed to either 20% (normoxia) or 1% O_2 (hypoxia). Cells were lysed and 50 ug lysate were used to analyse different protein expression in samples by Western blotting. Representative images of experiments (n=3) are shown (A). Bar chart (B) shows quantification of protein levels compared to β-actin control in each condition. Error bars show standard deviation, * $p<0.05$; ** $p<0.01$; *** $p<0.001$; **** $p<0.0001$

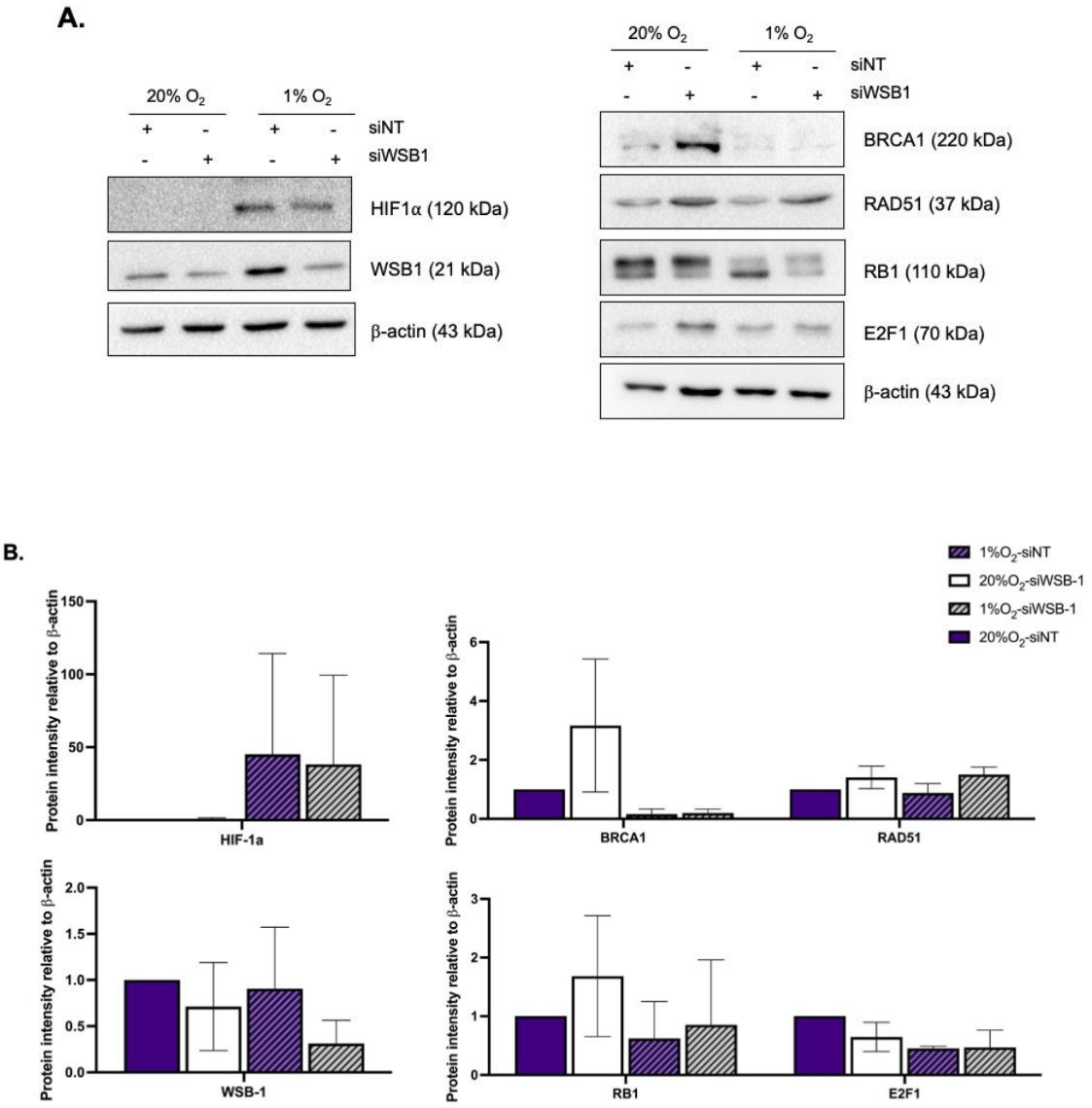

Figure 3. 12 Effect of WSB-1 depletion on DDR pathways regulators in MDA-MB-231
MDA-MB-231 cells were transfected with siWSB1 (siWSB-1) or non-targeting siRNA (siNT) and exposed to either 20% (normoxia) or 1% O_2 (hypoxia) for 24 hours. Cells were lysed and 50 ug lysate were used to analyse different protein expression in samples by Western blotting. Representative images of experiments (n=3) are shown (A). Bar chart (B) shows quantification of protein levels compared to β-actin control in each condition. Error bars show standard deviation, * $p<0.05$; ** $p<0.01$; *** $p<0.001$; **** $p<0.0001$

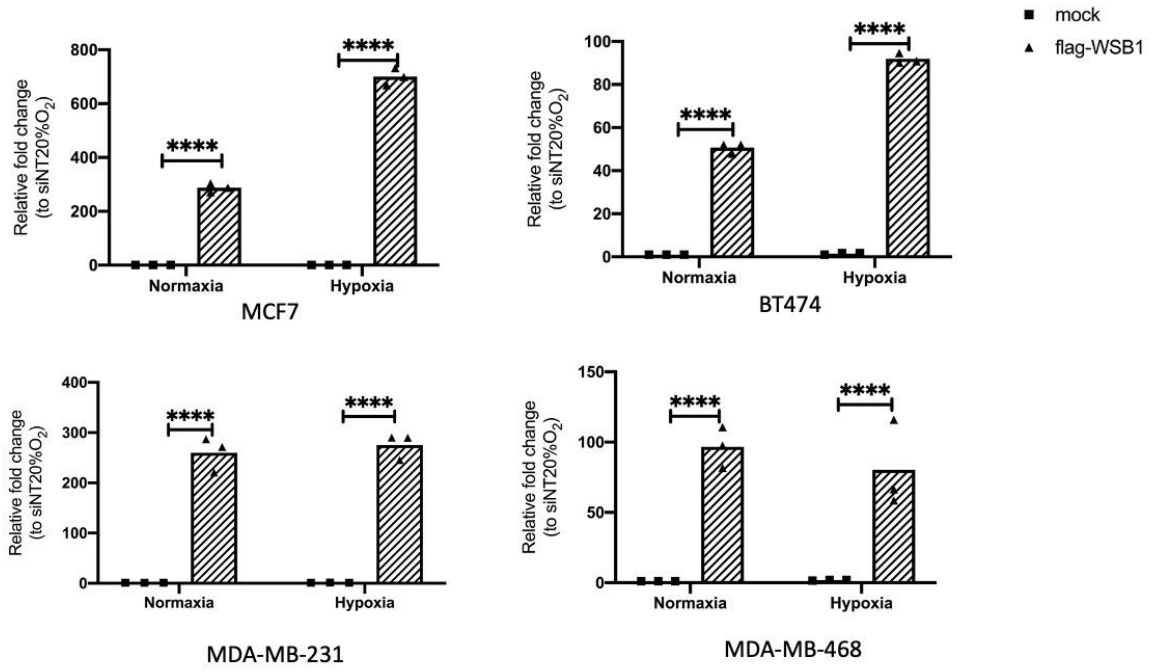

Figure 3. 13 The validation of WSB-1 overexpression
MCF-7, BT474, MDA-MB-231 and MDA-MB-468 cells were either transfected with DEPC water (mock) or transfected with a Flag-tagged WSB-1 (flag-WSB1) and exposed 24h to 20% or 1% O_2. 24 h to 20% (normoxia) or 1% O_2 (hypoxia). mRNA samples were extracted, reversed into cDNA analysed by qPCR for validation of expression levels of *WSB-1*. n=3. * $p<0.05$; ** $p<0.01$; *** $p<0.001$; **** $p<0.0001$; ns: not significant, 2-Way ANOVA comparison with mock 20% O2, Error bars represent mean ± SEM.

WSB-1 was increased by 260-fold change under normoxia and increased by 275 -fold change under hypoxia in MDA-MB-231($p<0.0001$). In MDA-MB-468, *WSB-1* was increased by 96.7 -fold change under normoxia and increased by 80.3-fold change under hypoxia in comparation to siNT control ($p<0.0001$). As can be observed in Figure 3.14 and Figure 3.15, a trend of downregulation of the DNA repair factors *BRCA1*, *BRCA2*, and *RAD51* can be observed for all cell lines, with some variability in the degree in which these changes occur between cell lines.

For MCF-7 cells (Figure 3.14), when WSB-1was overexpressed under normoxic conditions, *BRCA1* expression was decreased by 0.66-fold change ($p<0.0001$) and *BRCA2* expression was decreased by 0.74-fold under normoxia ($p<0.0001$). Hypoxia alone, significantly led to a decrease in *BRCA1 and* BRCA2 expression, 0.15-fold ($p<0.0001$) and 0.27-fold ($p<0.0001$) respectively. No further significant decrease in expression was observed for both these genes when WSB-1 was overexpressed under hypoxic conditions. WSB-1 overexpression led to a decrease in *RAD51* expression by 0.6-fold under normoxia ($p<0.05$). Hypoxia alone led to a 0.1-fold change decrease ($p<0.0001$), with no further significant changes with WSB-1 overexpression in hypoxic conditions. For BT474 cells (Figure 3.14), WSB-1 overexpression led to similar changes, with significant decrease in *BRCA1*, *BRCA2,* and *RAD51* expression in normoxia, respectively 0.5-fold ($p<0.0001$), 0.4-fold ($p<0.0001$), and 0.65-fold ($p<0.05$). As observed for MCF7, hypoxia alone led to significant decrease in *BRCA1*, *BRCA2,* and *RAD51* expression, respectively 0.6-fold ($p<0.0001$), 0.62-fold ($p<0.0001$), and 0.44-fold ($p<0.001$). For *BRCA1* and *BRCA2*, overexpression of WSB-1 led to even further decreases in expression under hypoxic conditions, 0.1-fold ($p<0.05$) and 0.23-fold ($p<0.0001$), with no significant changes in expression for *RAD51*.

For MDA-MB-231 cells (Figure 3.15), WSB-1 overexpression led to significant decrease in *BRCA1, BRCA2,* and *RAD51*, respectively 0.16-fold ($p<0.0001$) 0.068-fold ($p<0.0001$) and 0.30-fold ($p<0.01$), Hypoxia alone again led to significant decrease in the expression of *BRCA1* and *BRCA2*, respectively 0.88-fold ($p<0.0001$) 0.79-fold ($p<0.0001$), but not significantly for *RAD51*. For all three genes, overexpression under hypoxia led to significant decrease in expression, by 0.7-fold ($p<0.0001$), 0.71-fold ($p<0.0001$), and 0.77-fold ($p<0.01$) for *BRCA1*, *BRCA2,* and *RAD51* respectively.

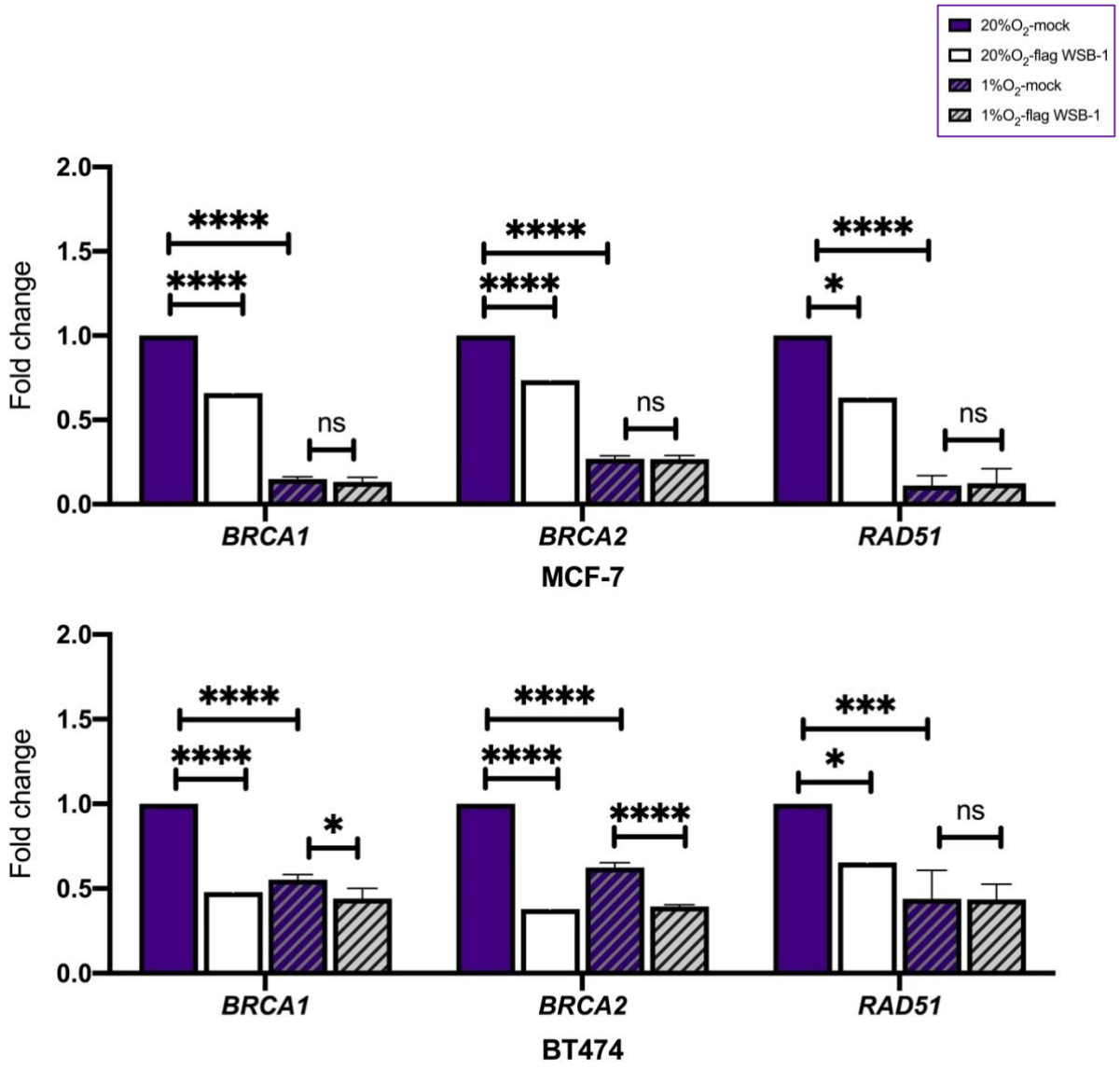

Figure 3. 14 WSB-1 overexpression repressed DNA repair factors in MCF7 and BT474
MCF-7, BT474 were either either transfected with DEPC water (mock) or transfected with a Flag-tagged WSB-1 (flag-WSB1) and exposed 24h to 20% or 1% O_2. 24 h to 20% (normoxia) or 1% O_2 (hypoxia). mRNA samples were extracted, reversed into cDNA and analysed by qPCR for validation of expression levels of *WSB-1*. n=3. * $p<0.05$; ** $p<0.01$; *** $p<0.001$; **** $p<0.0001$; ns: not significant, 2-Way ANOVA multiple comparisons were used, Error bars represent mean ± SEM.

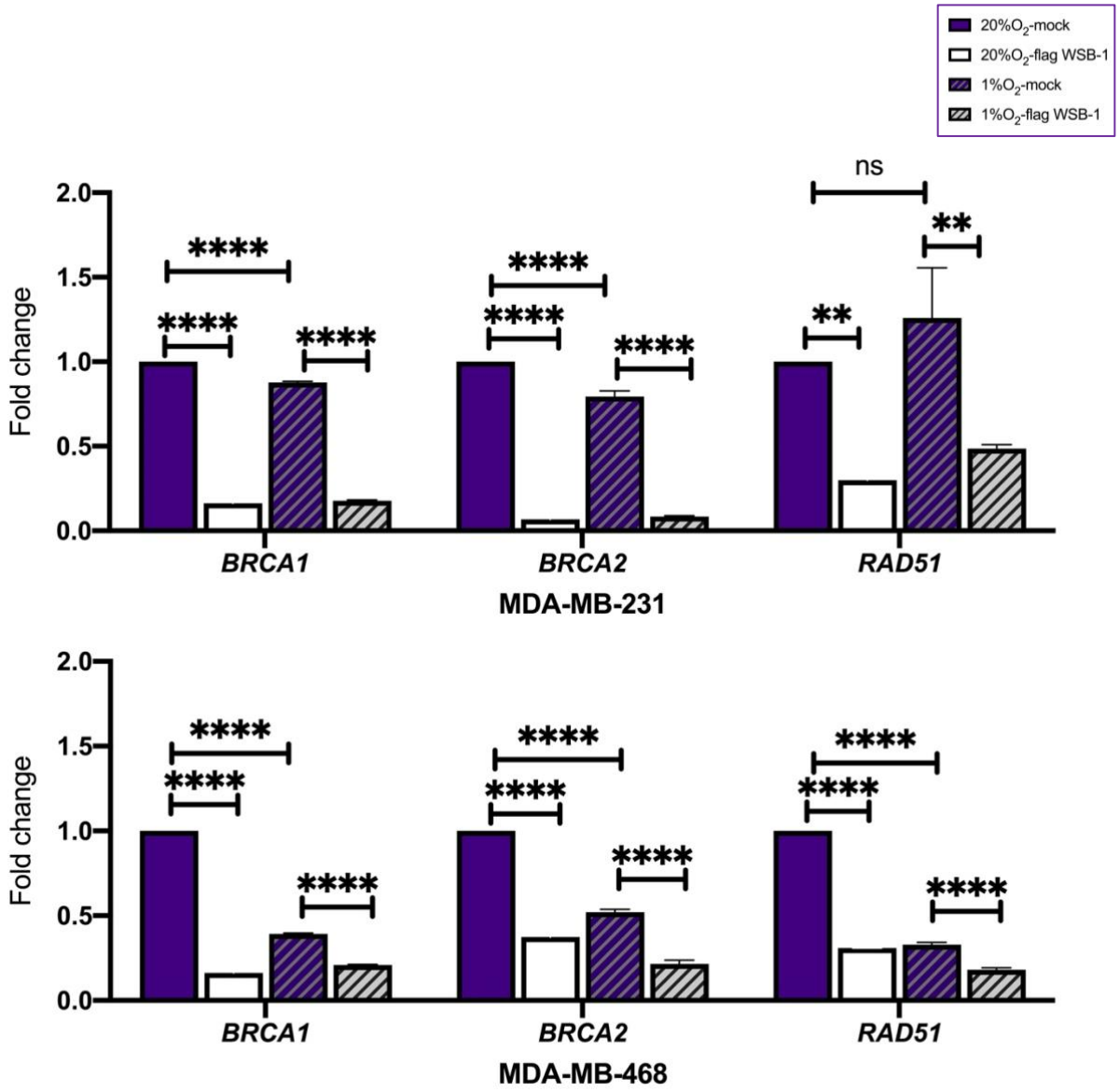

Figure 3. 15 WSB-1 overexpression repressed DNA reapir factors MDA-MB-231 and MDA-MB-468
MDA-MB-231, MDA-MB-468 were either transfected with DEPC water (mock) or transfected with a Flag-tagged WSB-1 (flag-WSB1) and exposed 24h to 20% or 1% O_2. 24 h to 20% (normoxia) or 1% O_2 (hypoxia). mRNA samples were extracted, reversed into cDNA and analysed by qPCR for validation of expression levels of *WSB-1*. n=3. * $p<0.05$; ** $p<0.01$; *** $p<0.001$; **** $p<0.0001$; ns: not significant, 2-Way ANOVA multiple comparisons were used, Error bars represent mean ± SEM.

For MDA-MB-468 cells (Figure 3.15) similar trends were again observed. WSB-1 overexpression in normoxia significantly decreased *BRCA1*, *BRCA2*, and *RAD51* expression, respectively by 0.16-fold ($p<0.0001$), 37-fold ($p<0.0001$) and 0.31-fold ($p<0.0001$). Hypoxia alone again repressed the expression of these genes by 0.18-fold ($p<0.0001$), 0.52-fold, ($p<0.0001$), and 0.15-fold ($p<0.0001$). Finally, expression of all three genes was also decreased by WSB-1 overexpression in hypoxia, respectively by 0.21-fold ($p<0.0001$), 0.30-fold ($p<0.0001$), and 0.33-fold ($p<0.0001$). Regarding *E2F1*, *RB1*, and *CDK6* expression (Figures 3.16 – 3.17), again a similar trend of decreased expression after WSB-1 overexpression was observed, more robust in normoxic conditions, with some variability depending on cell line and impact of hypoxia.

For MCF-7 cells (Figure 3.16), WSB-1 overexpression led to decrease in *E2F1*, *RB1*, and *CDK6* expression in normoxic conditions, respectively by 0.64-fold ($p<0.001$), 0.54-fold ($p<0.0001$), and 0.68-fold ($p<0.001$). Hypoxia alone led to significant repression of expression of all three genes, respectively by 0.25-fold $p<0.0001$), 0.65-fold, and ($p<0.001$) 0.55-fold ($p<0.0001$). However, overexpression of WSB-1 in hypoxia presented a much more varied picture: *E2F1* expression was not significantly changed, RB1 expression was significantly increased by 0.16 -fold ($p<0.05$), and CDK6 expression was significantly decreased by 0.16-fold change ($p<0.05$). For BT474 cells cells (Figure 3.16), WSB-1 overexpression led to decrease in *E2F1*, *RB1*, and *CDK6* expression in normoxic conditions, respectively by 0.67-fold ($p<0.001$), 0.60-fold ($p<0.01$) and 0.65-fold ($p<0.0001$). Hypoxia alone again led to a significant decrease in expression for all three genes, respectively 0.57-fold ($p<0.0001$), 0.66-fold ($p<0.05$), and 0.62-fold ($p<0.0001$). As for MCF7, WSB-1 overexpression led to variable results under hypoxia, with *E2F1* and *RB1* expression not significantly changed and *CDK6* expression decreased by 0.10-fold ($p<0.05$).

For MDA-MB-231 cells (Figure 3.17), WSB-1 overexpression in normoxic conditions again led to significant decrease in expression of *E2F1*, *RB1*, and *CDK6*, respectively by 0.27-fold ($p<0.0001$), 0.29-fold ($p<0.0001$), and 0.086-fold ($p<0.0001$). Hypoxia did not lead to as dramatic changes in gene expression as observed for all other cell lines, with some small albeit significant changes in expression for all three genes: 1.03-fold for *BRCA1*, 0.95-fold for *RB1* ($p<0.001$), and 0.84-fold ($p<0.05$) for *CDK6*. On the other hand, expression of of *E2F1*, *RB1*, and *CDK6* was clearly and significantly decreased when WSB-1 was overexpressed under hypoxia, respectively by 0.74 -fold ($p<0.0001$), 0.72-fold ($p<0.0001$),

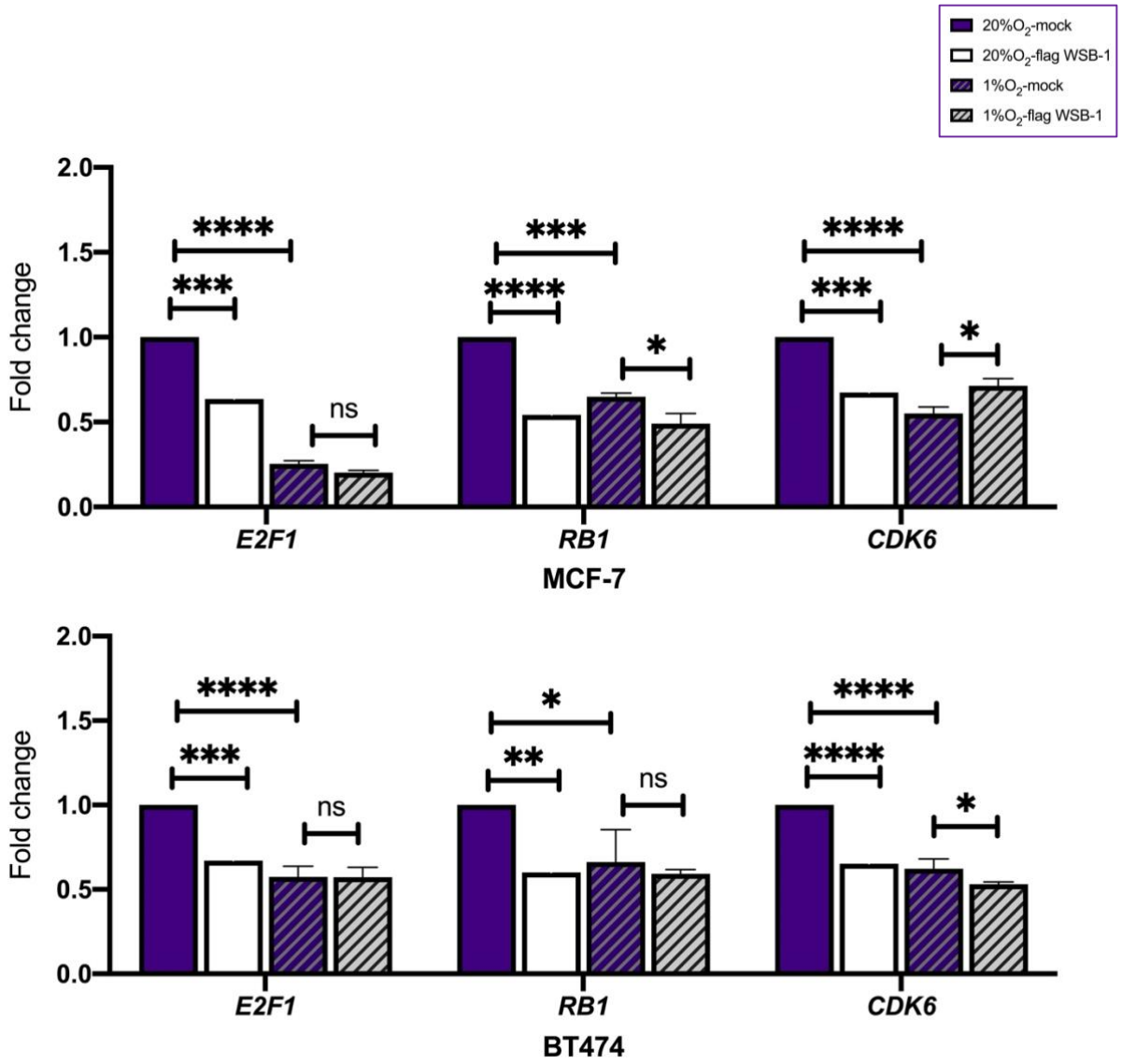

Figure 3. 16 WSB-1 overexpression repressed cell cycle genes in MCF7 and BT474
MCF-7, BT474 were either either transfected with DEPC water (mock) or transfected with a Flag-tagged WSB-1 (flag-WSB1) and exposed 24h to 20% or 1% O_2. 24 h to 20% (normoxia) or 1% O_2 (hypoxia). mRNA samples were extracted, reversed into cDNA and analysed by qPCR for validation of expression levels of *WSB-1*. n=3. * $p<0.05$; ** $p<0.01$; *** $p<0.001$; **** $p<0.0001$; ns: not significant, 2-Way ANOVA multiple comparisons were used, Error bars represent mean ± SEM.

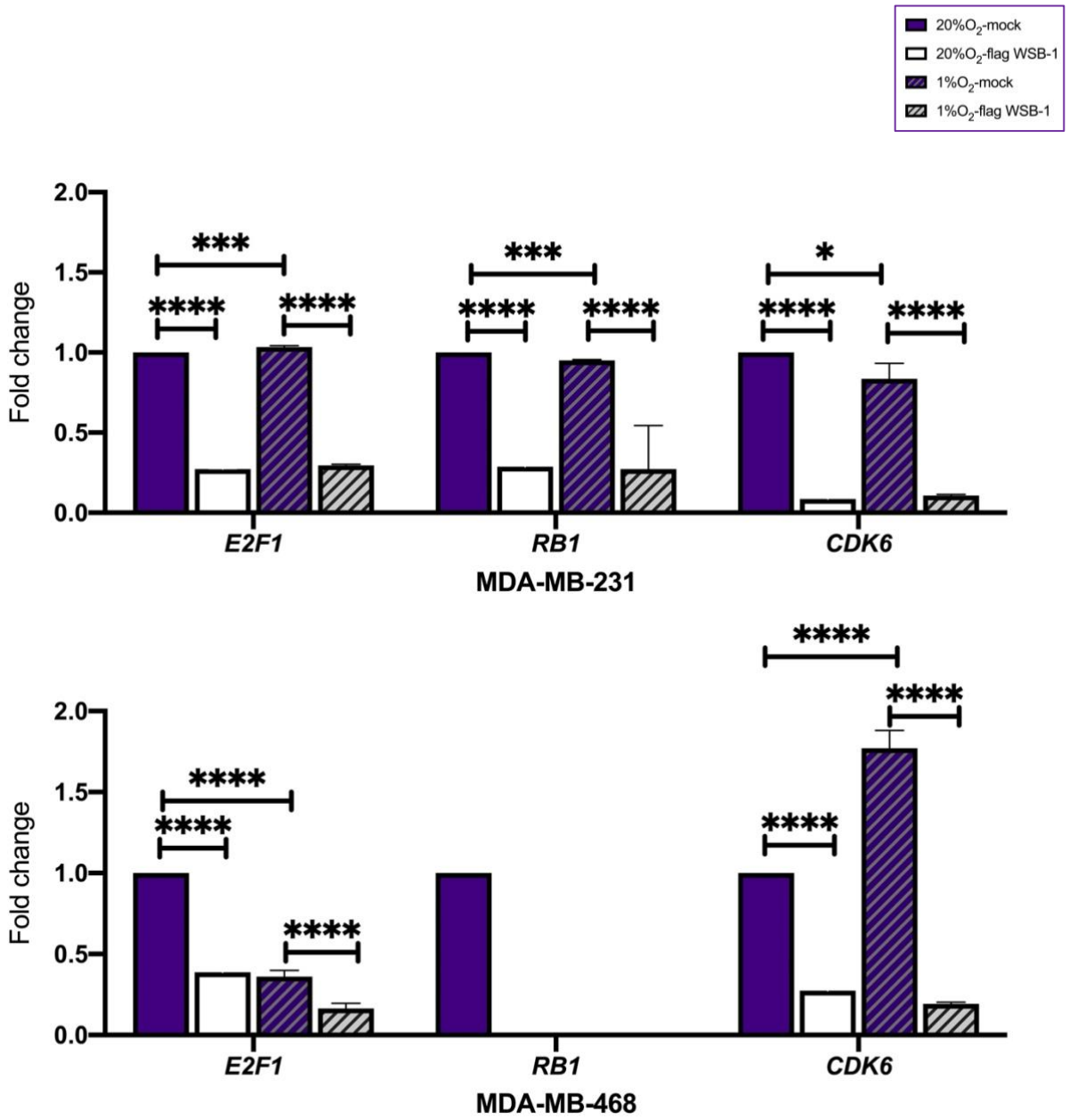

Figure 3. 17 WSB-1 overexpression repressed cell cycle regulation genes in MDA-MB-231 and MDA-MB-468

MDA-MB-231, MDA-MB-468 were either transfected with DEPC water (mock) or transfected with a Flag-tagged WSB-1 (flag-WSB1) and exposed 24h to 20% or 1% O_2. 24 h to 20% (normoxia) or 1% O_2 (hypoxia). mRNA samples were extracted, reversed into cDNA and analysed by qPCR for validation of expression levels of *WSB-1*. n=3. * p<0.05; ** p<0.01; *** p<0.001; **** p<0.0001; ns: not significant, 2-Way ANOVA multiple comparisons were used, Error bars represent mean ± SEM.

and 0.73-fold ($p<0.0001$). Finally, for MDA-MB-468 cells, WSB-1 overexpression led to decrease in expression for *E2F1* and *CDK6* by 0.39-fold ($p<0.0001$) and 0.28-fold ($p<0.0001$) respectively. Hypoxia alone led to repression of *E2F1* expression by 0.36-fold change ($p<0.0001$) but increase in *CDK6* expression by 1.77-fold ($p<0.0001$). When WSB-1 was overexpressed in hypoxic conditions, E2F-1 expression was decreased by 0.20-fold ($p<0.0001$) and CDK6 by 0.19-fold ($p<0.0001$). again, as noted before, no RB1 expression was detected in MDA-MB-468 cells.

In conclusion, these data indicate that, reciprocally to the trends observed for WSB-1 depletion, WSB-1 overexpression mostly led to a repression in gene expression of the DDR factors analysed, but again with some cell line and oxygen tension-dependent variability, which will be discussed later in this chapter.

3.3.8 The impact of WSB-1 overexpressed in breast cancer cells (protein level)

In order to evaluate how these DNA repair and cell cycle regulation factors respond to WSB-1 overexpression in protein level, again the WSB-1-Flag plasmid was used to transfect or not breast cancer cells MCF-7 and MDA-MB-231 cells under normoxic and hypoxic conditions and extracted protein samples were analysed by western blotting.

For MCF7 cells, as can be observed in Figure 3.18, overexpressing WSB-1 led to an overall albeit not significant decrease in expression of RAD51 and E2F1. Overexpressing WSB-1 led to a significant decrease in expression of BRCA1. Overexpressing WSB-1 upregulated BRCA1 expression by 53.7% compared to mock under normoxia ($p<0.05$). More clearly observed in normoxic conditions, but with variability between samples. RB1 doublet pattern also changed, but again with variability between samples, so no clear conclusion can be drawn at this stage.
For MDA-MB-231 (Figure 3.19), similar trends can also be observed, again with variability between samples. Overexpressing WSB-1 upregulated BRCA1 expression by 65.5% compare to mock under normoxia($p<0.05$).

These results indicate that the changes observed at mRNA level are partially represented as trends at protein level but again require further analysis to confirm them.

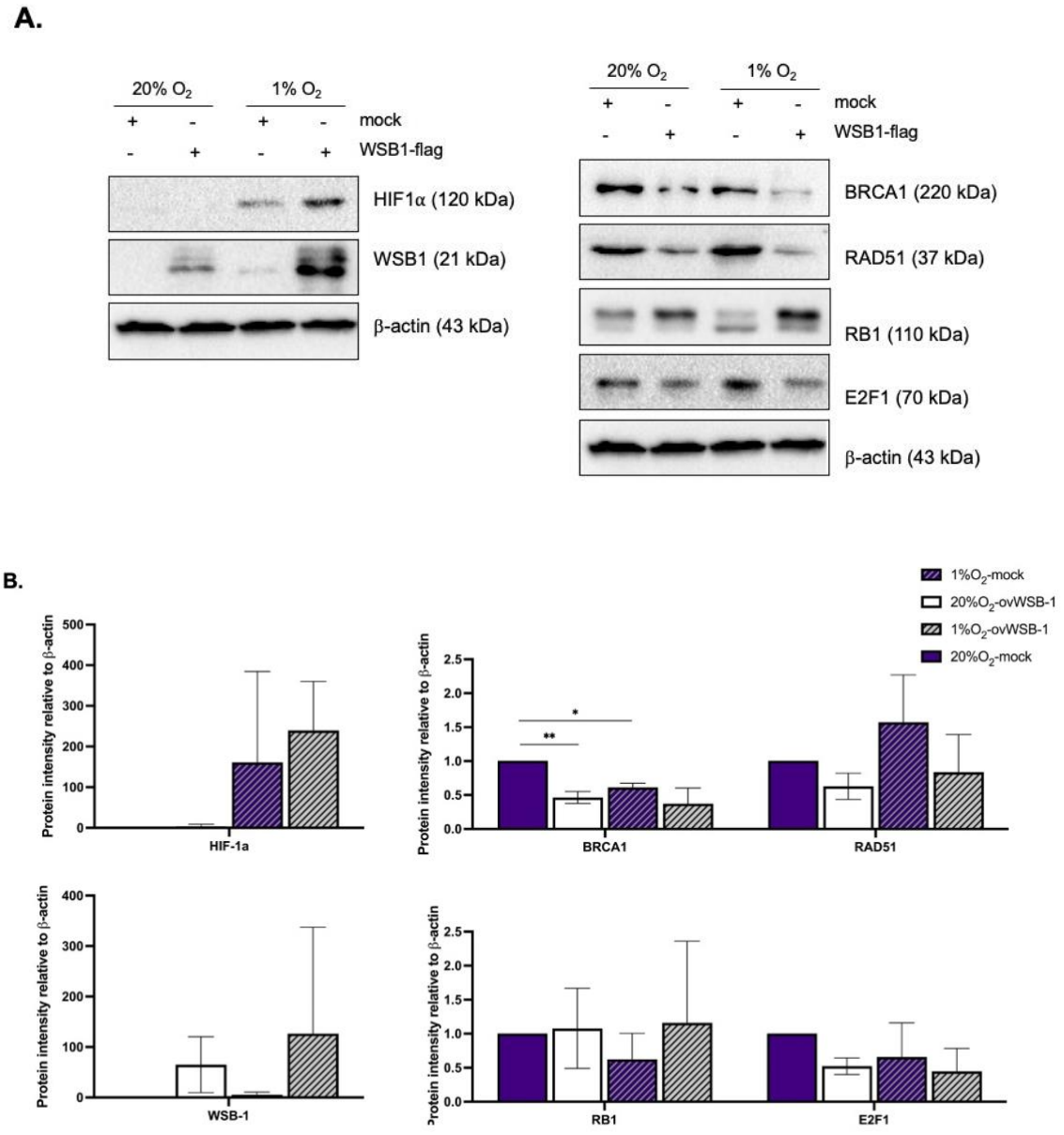

Figure 3. 18 Effect of WSB-1 overexpression on DDR pathways regulators in MCF-7
MCF7 cells were transfected with flag tagged WSB-1(WSB1-flag) or mock and exposed to either 20% (normoxia) or 1% O_2 (hypoxia). Cells were lysed and 50 ug lysate were used to analyse different protein expression in samples by Western blotting. Representative images of experiments (n=3) are shown (A). Bar chart (B) shows quantification of protein levels compared to β-actin control in each condition. Error bars show standard deviation, * $p<0.05$; ** $p<0.01$; *** $p<0.001$; **** $p<0.0001$

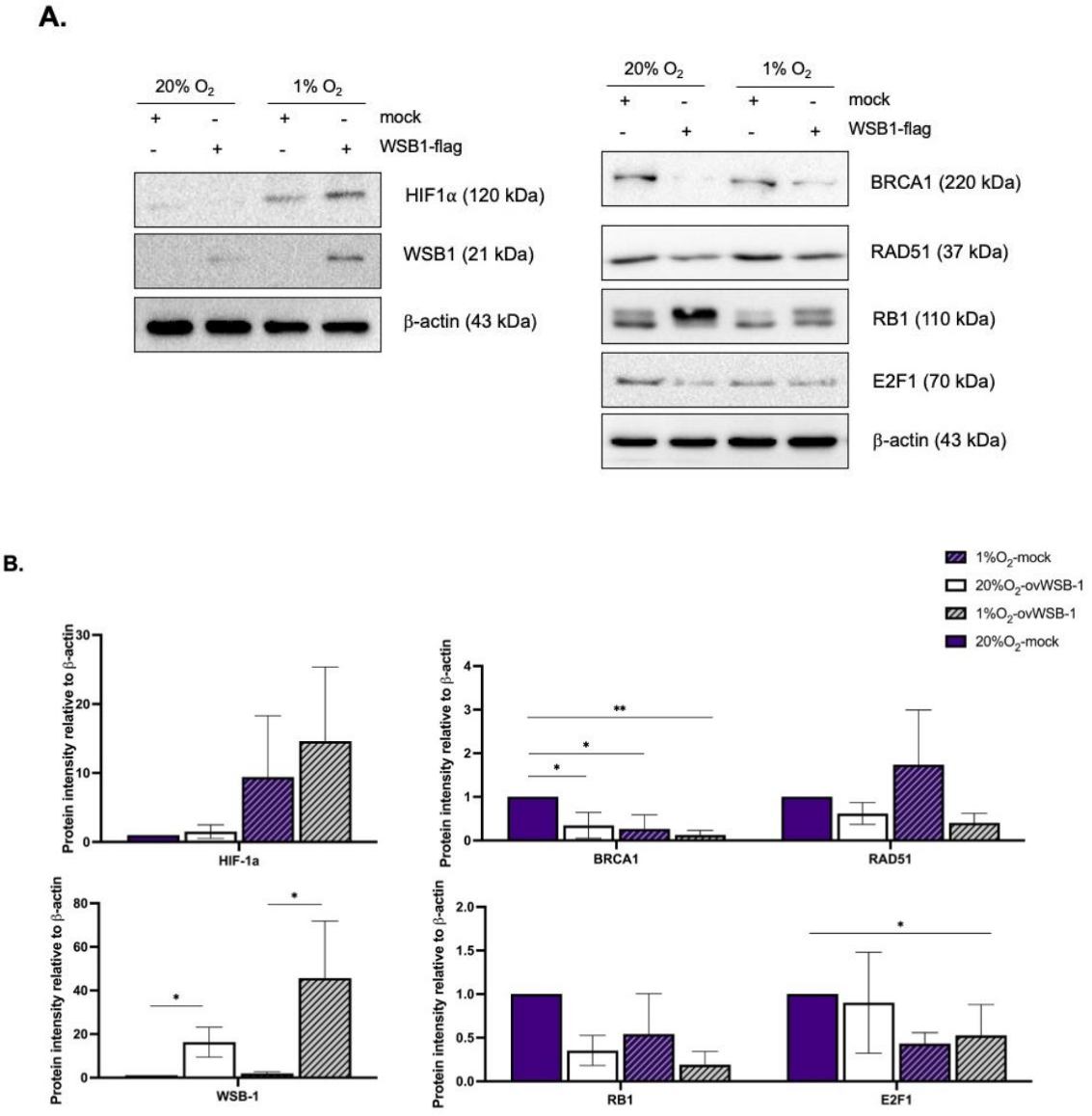

Figure 3. 19 Effect of WSB-1 overexpression on DDR pathways regulators in MDA-MB-231
MDA-MB-231 cells were transfected with flag tagged WSB-1(WSB1-flag) and exposed to either 20% (normoxia) or 1% O_2 (hypoxia). Cells were lysed and 50 ug lysate were used to analyse different protein expression in samples by Western blotting. Representative images of experiments (n=3) are shown (A). Bar chart (B) shows quantification of protein levels compared to β-actin control in each condition. Error bars show standard deviation, * p<0.05; ** p<0.01; *** p<0.001; **** p<0.0001

3.4 Discussion

In this chapter, the novel role of WSB-1 in breast cancer were investigated and validated in a panel of breast cancer cell lines in RNA level and protein level. Our results mostly achieved the specific aims stated in the beginning of this chapter as discussed below.

1. *Investigate novel pathways regulated by WSB-1 in hypoxic breast cancer by analysing WSB-1 regulated transcriptomic changes*

As mentioned in Section 1.6.4, studies showed WSB-1 as an E3 ligase has an impact on DNA damage signalling and cell cycle regulation via its E3 ligase activity. HIPK2 and ATM are both important regulators in DDR pathways, with HIPK2 shown to be ubiquitinated and degraded by WSB-1 (Choi et al., 2008). ATM has also been shown to be ubiquitinated by WSB-1, which resulted in the degradation of ATM during tumour initiation (Kim et al., 2017). However, the role of WSB-1 in DDR especially under tumour microenvironmental conditions such as hypoxia remains unclear. Our preliminary results indicate WSB-1 could play an important role in DNA damage response under hypoxia.

Bioinformatic analysis of RNA-seq on different pathway enrichments revealed that WSB-1 depletion in MDA-MB-231 cells under hypoxia upregulated genes in DDR pathways including cell cycle, DNA replication, and DNA damage repair. Interestingly, according to our results from WikiPathways enrichments of Metascape analysis, there were 39 genes enriched in DNA IR-damage and cellular response via ATR, which also indicate the connection between WSB-1 and ATR respond to IR-damage DNA. To our knowledge, there is no evidence showing the relationships between WSB-1 and ATR pathways so far. However, further investigations need to be done to validate the relationship between WSB-1 and ATR, which will be further discussed in the next two chapters.
In addition, WSB-1 has been shown related to several miRNA in the literature. For instance, it has been reported that WSB-1 may be a target of miRNA-191 (Guerau-de-Arellano et al., 2015). miR-191 has been shown to regulate cell cycle progression in breast cancer by promoting G1/S and G2/M transitions (Nagpal and Kulshreshtha, 2014). Our pathway enrichments analysis also showed 41 genes were enriched in miRNA regulation of DNA damage response when depleting WSB-1 under hypoxia. These results also indicated that WSB-1 depletion under hypoxia is associated to DNA damage response, and potentially via miRNA. However, further investigations need to be done to validate it.

However, these findings also lead to more questions. For example, how does DNA damage repair as well as cell cycle regulation change in respond to WSB-1 modulation, and how will some key proteins in IR-activated DDR signalling respond to WSB-1 expression? These will be further investigated in next chapter.

2. *Analysis of the transcriptional factor enrichments after WSB-1 depletion under hypoxia.*

Transcription factor (TF) enrichment analysis ChEA3 database analysis of the RNA-seq data showed that E2F family members, including *E2F8, E2F7, E2F2, E2F1, E2F4*, as well as *TP53* were enriched for the DEGs after WSB-1 depletion under hypoxia in MDA-MB-231 cells. These data again indicated that WSB-1 depletion under hypoxia in MDA-MB-231 cells is associated with DNA damage respond and could affect cell cycle regulation and DNA damage repair by regulating E2F family and *TP53* in a transcriptional level.

The E2F family of transcription factors can be divided into 4 subgroups based on their different functions and play critical roles in controlling cell cycle progression (Attwooll et al., 2004). Enriched E2F family when WSB-1 was depleted under hypoxia includes E2F1 and E2F2, which are transcriptional activators that are required for promoting transcription of target genes involved in the G1/S transition (Bertoli et al., 2013). And transcriptional repressors E2F7 and E2F8 (Li et al., 2008), as well as E2F4, which is also considered as repressor to possess cell cycle repressive activity. And for E2F4, more and more studies have discovered more novel regulation functions of E2F4 including differentiation, DNA damage response and apoptosis, etc (Hsu and Sage, 2016, Lee et al., 2011). Therefore, our TF enrichment analysis showed that WSB-1 could potentially impact on cell cycle progression by regulating E2F family; however, further investigation on the impact and its regulatory function on different E2Fs need to be done in future works. *TP53* is well known as one of the classical type tumour suppressors that plays vital role in the DDR, including induction of cell cycle arrest and/or apoptosis (Ozaki and Nakagawara, 2011). Therefore, our preliminary results suggested E2Fs and/or p53 could be regulated by WSB-1 to lead to the transcriptional changes observed in the RNA-seq data, but, especially for p53, there is no evidence this happens solely at a transcriptional level. However, there are unpublished preliminary data from our lab has indicated that E2F7, p53, and p53's co-factors such as STRAP were identified as potentially interacting with WSB-1 in a proteomic interactome analysis, which

suggests that E2F7 and/or p53 could potentially be directly regulated by WSB-1 at the protein level. Changes in protein level of p53 in response to WSB-1 modulation will be further investigated in next chapter.

3. *Validate the impact of WSB-1 modulation in regulation of expression of DDR signalling factors under hypoxia in breast cancer in vitro.*

Finally, interesting hits from the RNA-seq analysis such as key DNA damage repair factors *BRCA1, BRCA2, RAD51,* and cell cycle regulators *E2F1, RB1, CDK6* were validated in 4 different breast cancer cell lines from different backgrounds: MCF7, BT474, MDA-MB-231 and MDA-MB-468.

In work previously published from our lab, we showed that WSB-1 depletion impacted metastatic potential only in hormone receptor negative TNBC cell lines (Poujade et al., 2018). However, WSB-1 depletion led to a trend of upregulation at the transcript level of DNA repair genes *BRCA1, BRCA2,* and *RAD51,* and cell cycle regulation genes *E2F1, RB1* and *CDK6* in Luminal A breast cancer cell line MCF7 and Luminal B breast cancer cell line BT474 in normoxic and hypoxic conditions. Conversely, WSB-1 overexpression induces repression of the expression of these genes. The results were significant in normoxic conditions but, although the trend was still the same overall, less significant in hypoxic conditions. One reason for this is that hypoxia alone can significantly repress these DNA repair and cell cycle genes, as previously shown (Scanlon and Glazer, 2015, Hegan et al., 2010, Iida et al., 2002, Fanale et al., 2013). In this context, the impact of WSB-1 overexpression does not further repress the expression of these genes. Whether WSB-1 contributes or is uncoupled from this hypoxia-mediated repression remains unclear but will be investigated in subsequent studies. For TNBC MDA-MB-231 and MDA-MB-238 cell lines, WSB-1 depletion again led to a trend of *BRCA1, BRCA2, RAD51, E2F1, RB1* and *CDK6* upregulation under normoxia and hypoxia. WSB-1 overexpression again led to repression of the expression of these DNA repair and cell cycle regulation genes under normoxia and, as observed for the Luminal cell lines, some of these changes were also not significant in hypoxic conditions, as noted for the Luminal cell lines. Specifically for the MDA-MB-468 cell line, former studies found that the lack of RB1 expression is associated with a more aggressive form of breast cancer, and RB-deficient TNBC such as MDA-MB-468 would benefit from gamma-irradiation (Robinson et al., 2013), in our results, MDA-MB-

468 cells were also found lack of *RB1* expression, which might indicate high WSB-1 expression repressed *RB1* could modulate the efficiency of radiation treatments in TNBC.

Interestingly, although the trends were similar, depletion of WSB-1 lead to varied degrees of mRNA expression changes between the different cell lines. A potential reason for this is, as showed Figure 3.6, depletion of WSB-1 had different efficiency between cell lines, with MDA-MB-231 having the highest depletion efficiency at over 90%, and MCF7 and MDA-MB-468 only at 50%. This variability could lead to impact on downstream gene expression patterns between cell lines. Another possible reason is MDA-MB-231 and MDA-MB-468 are TNBC in origin, which are a more aggressive tumour type than Luminal A/B which MCF7 and BT474 are derived from. Therefore, genomic differences among these cell lines could also underpin these differences. Finally, there was some variation between cell lines for mRNA levels particularly for the hypoxic samples. This could be due to the fact already discussed that hypoxia alone already promotes repression of expression for these genes for most cell lines (MCF7, BT474, and MDA-MB-468), but for MDA-MB-231 hypoxia alone does not lead to as clear or significant repression of gene expression. It is unclear why this is the case, apart from the fact that some HIF1-alpha expression can be present in normoxic conditions in MDA-MB-231 (see Figures 3.19) and has also been observed elsewhere (Zhang et al., 2016).

Whereas gene expression patterns after WSB-1 depletion and overexpression were very consistent between independent repeats at mRNA level, there was a lot more variability between protein expression of BRCA1, RAD51, E2F1, and Rb between independent experiments. Although the overall trend from protein levels changes mostly supports the trends seen at mRNA level (increase for WSB-1 depletion and reduction for WSB-1 overexpression), these do vary between independent samples. Firstly, any observed changes at transcript level might not necessarily directly translate to changes at protein level due to impact of translational and post-translational changes. Also, the chosen timecourses could impact on this - protein samples were harvested in the same timeframe (24 hours) as the mRNA samples, and more time might have been needed to see clearer changes at protein level. Again, hypoxia-mediated repression of these factors also impeded seeing clearer effects for those sample sets. Finally, although effort was taken to use cells within a relative limited number of passages and with consistent confluency, it might be possible variability in these could impact inter-sample variability.

Interestingly, for Rb a doublet could be observed for most samples. This corresponds to non-phosphorylated (lower band) and phosphorylated Rb (higher band). CDK4/6 can initiate the mono-phosphorylation of Rb and the inactivation of the Rb release E2F transcription factors (Knudsen et al., 2019). In addition, Rb can be hyperphosphorylated by CDK2 which also released E2F family during the cell cycle control of cell proliferation (Thwaites et al., 2017). As WSB-1 modulation affected key CDK gene expression levels (CDK2 in RNA-seq dataset and CDK6 in RNA-seq and qPCR datasets), these could have affected Rb phosphorylation status; however as for the total protein blots, there is variability in the intensity of phosphorylated Rb band between samples and conditions, which makes it hard to conclude about the impact of WSB- on Rb phosphorylation.
In any case, further repeats must take place to conclusively validate these findings at the protein level.

Taken together, these data indicate that WSB-1 depletion upregulated genes expression in DDR pathways and reciprocally, WSB-1 overexpression downregulated these DDR factors. The results suggested that WSB-1 could play an important role in DDR pathways in breast cancer. However, more questions appeared, including does WSB-1modulation alter DNA repair capabilities and DDR signalling at a phenotypical level and could it related to HR deficiency to represent potential BRCAness biomarker in breast cancer? To answer these questions, further *in vitro* work as well as analyses of patient samples for the status of these factors vs WSB-1 was conducted in next two chapters.

Chapter 4

Investigating the impact of WSB-1 modulation on the DDR in breast cancer

4.1 Introduction

As described in the Introduction, ionising radiation (IR) induces a variety of DNA damage types, leading to activation of the DDR signalling cascades that control cell cycle arrest, DNA repair, DNA replication stress responses, and determine cells death (Chapter 1). Double-strand breaks (DSBs) are a major type of DNA damage caused by radiation, responsible for radiation-mediated cell death (Vignard et al., 2013). DSBs are repaired either by non-homologous end joining (NHEJ) pathways throughout the cell cycle or by homologous recombination (HR) pathways during the S phase and G2 phase (Haber, 2000, Mao et al., 2008, Shibata et al., 2011). DNA damage such as SSBs and base damage can be repaired by BER pathway (Hegde et al., 2008). IR also causes DNA replication stress associated DSBs, which activates the replication stress response (Nickoloff, 2022). Three kinases, ATM, ATR, and DNA-PKcs, are the central regulators of this DDR signalling pathways respond to DNA damage (Blackford and Jackson, 2017) and DNA replication stress (Liu et al., 2012a). For example, ATM and ATR are activated by DNA damage and DNA replication stress. The activation of ATM phosphorylates its downstream CHK2 kinase, which involved in DNA repair pathways by phosphorylate BRCA1/2, XRCC1 and regulate cell cycle in G1/S and G2/M as well as p53 activation (Zannini et al., 2014). The activation of ATR phosphorylates CHK1 kinase, which activates the G2/M cell cycle checkpoint through phosphorylation and inactivation of CDC25 phosphatases (Shimuta et al., 2002).

The ubiquitin-proteasome system has been shown to regulate the expression and function of numerous proteins and signalling pathways therefore determine DNA damage response. For example, in respond to DSBs, the ubiquitin E3 ligase RNF8 recruits key DDR proteins such as 53BP1 and BRCA1 to the DSB site thus mediates DSBs repair (Nakada, 2016). H2A is also found to be ubiquitinated on K13 and K15 by another E3 ubiquitin-protein ligase RNF168 which enabling 53BP1 and BRCA1 complexes recruited to DSBs sites (Brown and Jackson, 2015). Moreover, studies found that cullin ring ubiquitin ligases (CRLs) have crucial roles in regulating the cell cycle, hypoxia signalling, DNA repair and response to IR (Fouad et al., 2019). WSB-1 is also a ubiquitin E3 ligases, and act as the substrate recognition subunit of the ECS (Elongin BC-Cul5-Rbx1) ubiquitin ligase complexes that regulate and degrade key proteins involved in determine cell fate. For example, WSB-1 negatively regulates the pVHL protein by ubiquitinating pVHL and thereby stabilizing HIF-1α protein

(Chen et al., 2017, Kim et al., 2015). It is also suggested that WSB-1 negatively affects the cellular response to IR by regulating HIF-1α (Fouad et al., 2019).

As a ubiquitin E3 ligases, WSB-1 ubiquitinates a DNA damage-responsive serine/threonine kinase HIPK2 (Choi et al., 2008). HIPK2 is a tumour suppressor which is activated in respond to DNA damage and forms a complex with p53, which therefore phosphorylates p53 and initiates the apoptosis (D'Orazi et al., 2002). Siah-1 is another E3 ligase that mediates the degradation of HIPK2. In response to DNA damage, ATM and/or ATR is activated and phosphorylating Siah-1, which interrupts the interaction of Siah-1 and HIPK2, therefore stabilized HIPK2. Moreover, Kim et al found that ATM has also been shown to be ubiquitinated by WSB-1, resulting in ATM degradation (Kim et al., 2017b). In this study, they also identified that CDK2 or CDK4 phosphorylated WSB-1 to mediate ATM degradation (Kim et al., 2015). A more recent study found that WSB-1 is a direct target gene of c-Myc, and that WSB-1 in turn also regulates c-Myc expression through WNT/β-catenin pathway, which forms a positive feedback loop, leading to cancer initiation and development (Gao et al., 2022).

4.1.1. Hypothesis, aims, and objectives of this chapter

Alongside the evidence described above, we have also found, as described in Chapter 3 that WSB-1 modulation impacts on the expression of genes involved in DDR pathways under normoxia and hypoxia, specifically with WSB-1 depletion inducing expression of DDR factors and WSB-1 overexpression repressing their expression. Therefore, for this Chapter we hypothesised that changes in WSB-1 expression could impact the DDR directly, and therefore potentially lead to accumulation of DNA damage.

Therefore, the specific aims of this chapter are to:
1: Investigate the relationship between WSB-1 expression and DDR signalling
2. Validate the impact of WSB-1 on DNA repair and cell cycle progression

4.2 Experimental design

4.2.1 Investigation of the impact of WSB-1 modulation of DDR signalling after IR

In order to determine which protein in DDR signalling pathways could be influenced by WSB-1 with or without IR as well as hypoxia, different protein levels were investigated in this chapter by Western blot.

Firstly, As mentioned in Section 1.3.4, DSBs are the most common DNA damage lesions induced by ionising radiation exposure. H2AX is a member of histone H2A family and its phosphorylated form of the histone H2AX (γH2AX) is a biomarker for DSBs (Nagelkerke et al., 2011). p53 is a crucial factor in the function of DNA damage response includes cell cycle arrest, DNA repair and apoptosis (Ozaki and Nakagawara, 2011, Williams and Schumacher, 2016). Therefore, γH2AX and p53 protein status were evaluated by Western blot when overexpressed WSB-1 under normoxia and hypoxia to confirm the impact of WSB-1 on DNA damage response. In chapter 3, p53 was enriched in TF enrichment database when WSB-1 was depleted under hypoxia. p53 protein status was also tested when WSB-1 was depleted under normoxia and hypoxia.

The phosphorylation of BRCA1 (phospho BRCA1) is a critical step in respond to DNA double-strand breaks induced by irradiation and ATM is required during this process (Cortez et al., 1999). Moreover, the phosphorylation of BRCA1 especially at Ser1524 could indicate the activation of ATM (Gatei et al., 2001), therefore, BRCA1, phospho BRCA1 (Ser1524) were tested in this chapter to see if WSB-1 overexpressed with or without IR could activate ATM under normoxia and hypoxia. As data in Section 3.3.3 showed, when WSB-1 was depleted under hypoxia in MDA-MB-231 cells, the upregulated genes were found to be enriched in one of the pathways included DNA IR-damage and cellular response via ATR, so, in order to see whether the ATR pathway was activated, ATR downstream target pCHK1 (Ser345) was also tested by Western blot in this chapter. Moreover, to further confirmed WSB-1 overexpressed affects cell cycle with or without IR under nomoxia and hypoxia, phospho RB1 (Ser807/811) and phospho p53 (Ser 15) were assessed in this chapter by using western blotting.

4.2.2 Detection of DNA damage *in situ* by immunofluorescence (IF) staining for γ-H2AX and 53BP1 foci

Ionising radiation-induced foci (IRIF) refer to the DNA damage response protein clusters that form at the DNA DSBs sites and can be visualized through microscopic imaging following

including immunofluorescence staining (Rothkamm et al., 2015). H2AX is a member of histone H2A family and its phosphorylated form of the histone H2AX (γH2AX) is a biomarker for DSBs. Constitutive expression of γH2AX was suggested as an indicator of the DNA damage repair pathway disruption and genetic instability in breast cancer (Nagelkerke et al., 2011). In addition, the formation of DSBs also attract the DSB damage sensor p53-binding protein 1 (53BP1) to the DSB-containing chromatin (Lassmann et al., 2010). Previous studies found that DNA DSBs after exposure of cells to IR, γH2AX foci begin to form immediately and reach to maximum 60 min later and disappearing over the next several hours. However, residual foci may remain in some cells for days after exposure and may mark unrepaired or misrepaired sites (Banáth et al., 2010). Studies also suggested that repair-deficient cell lines retain more foci and more cells with foci when analysed 24 hours after irradiation (Kato et al., 2006). In addition, 53BP1 foci were evident 5 min after irradiation, by 15 min the entire cell population had developed foci, and by 30 min the average number of 53BP1 foci per cell had peaked. Thereafter, the number of 53BP1 foci decreased over time and returned to baseline levels about 16 h after irradiation.

Therefore, to investigate the impact of WSB-1 induce DNA damage, IF staining was conducted to detect DNA damage biomarkers γH2AX and 53BP1 in either MCF-7 and MDA-MB-231 cells with or without overexpressed WSB-1. To evaluate the impact of WSB-1 overexpression with IR on γH2AX and 53BP1 foci formation as a marker for DNA repair efficiency, we calculated the foci 4h and 24h after irradiation in 2Gy, as well as for non-irradiated cells. Scoring criteria was as follow: 100 cells were counted, and one cell with foci >5 was considered positive (Ramachandran et al., 2021).

4.2.3 Evaluation of the impact of WSB-1 overexpressed on cell cycle progression

The measurement of the DNA content by flow cytometry can distinguish a population of cells into different phases of the cell cycle: G0/G1 phase cells exhibit diploid (2N), cells in S-phase shows 2N>n<4N and tetraploid (4N) for those in G2/M phases(GM, 2000). Therefore, MCF7 and MDA-MB-231 cells were transfected either mock control with DEPC water or flag tagged WSB-1 plasmid for 24h then harvested and DNA content was staining by Propidium iodide (PI), then run on the BD Biosciences LSRFortessa^{TM} flow cytometer to investigate the impact of WSB-1 overexpression on cell cycle in MCF7 and MDA-MB-231 cells.

4.3 Results

4.3.1 Evaluation of the impact of WSB-1 modulation on DDR signalling - γH2AX and p53

Histone H2AX (γH2AX) is a biomarker for DNA damage such as DSBs and replication stress(Mah et al., 2010, Moeglin et al., 2019). Also, in Chapter 3 we indicated that p53 was one of the TFs enriched when depleting WSB-1 under hypoxia. Therefore, levels and expression of γH2AX and p53 after WSB-1 modulation were evaluated in this Section. For this, MCF7 and MDA-MB-231 cells were transfected with either mock control and flag WSB-1 plasmid under normoxia or siNT/siWSB-1 and placed in hypoxia for 24h.

In Figure 4.1 it can be observed that WSB-1 depletion led to a decrease, albeit with some variability, in p53 levels for both MCF7 and MDA-MB-231 cell lines independently of hypoxia. p53 level was decreased by 46.2% when depleted WSB-1 compared to control under normoxia ($p<0.05$) and was decreased by 46.4% when depleted WSB-1 compared to control under hypoxia ($P<0.05$). Although a similar trend can be seen in MDA-MB-231 cells, these results are not statistic significant due to sample variability. Reciprocally, in Figure 4.2 it can be observed that p53 levels increased when WSB-1 was overexpressed in MCF7 independently of hypoxia, however p53 level was decreased by 52.2% under hypoxia compared to normoxia in MDA-MB-231 ($p<0.05$), and p53 level was decreased by 65.7% under hypoxia after WSB-1 overexpression compared to normoxia ($p<0.01$) in MDA-MB-231 (Figure 4.3).

Interestingly, in Figure 4.3 it can be observed that γH2AX levels increased when WSB-1 was overexpressed in both MCF7 and MDA-MB-231 cells, independently of hypoxia, which indicates high levels of WSB-1 could increase endogenous DNA damage.

To evaluate the effect of WSB-1 overexpression on the changes of some key regulators in DDR signalling pathway when using IR treatments under normoxia and hypoxia, a preliminary experiment (n=1) was conducted for samples with overexpressed WSB-1, where western blot was conducted to determine the levels of γH2AX, phosphor-BRCA1 (pBRCA1, phospho-Chk1(Ser345), phospho-p53 (Ser15), and phospho RB1(pRB1) (Ser807/811) as DDR activation markers. Flag was used as a marker for efficient WSB-1 transfection using the Flag-WSB-1 construct.

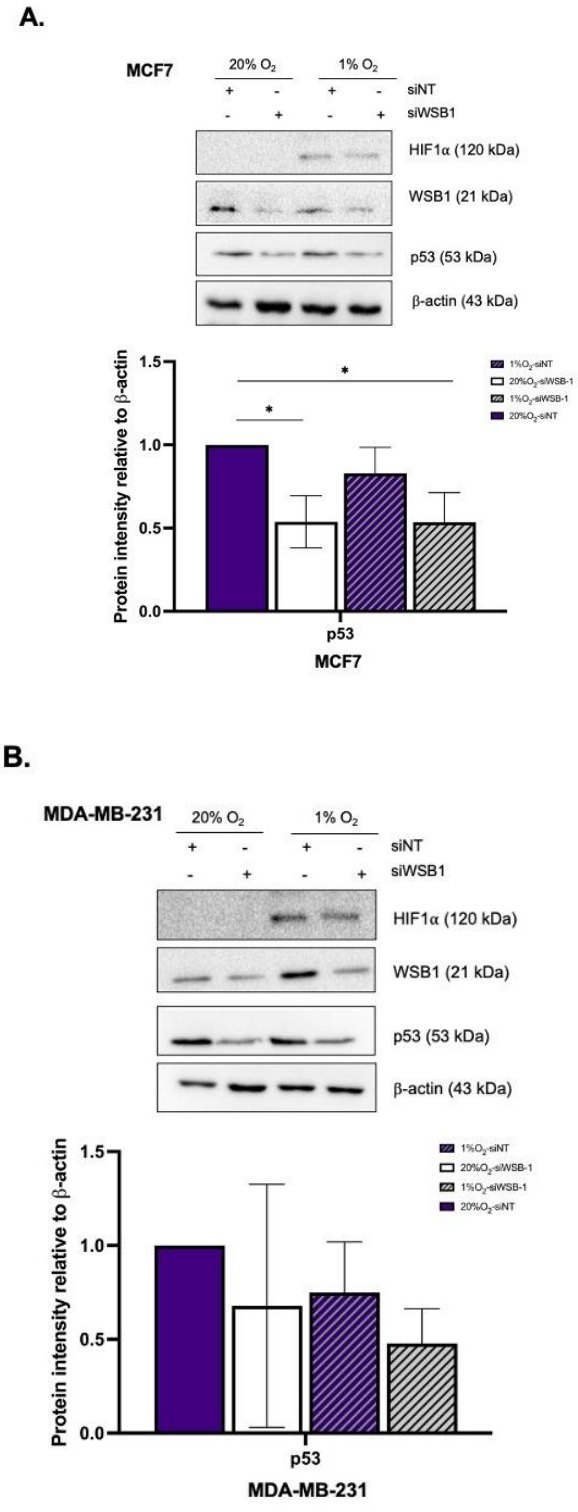

Figure 4. 1 WSB-1 depletion downregulated p53 in MCF-7 and MDA-MB-231 cells

MCF7(A) and MDA-MB-231(B) cells were transfected with siWSB1 (siWSB-1) or non-targeting siRNA (siNT) and exposed to either 20% (normoxia) or 1% O_2 (hypoxia) for 24 hours. Cells were lysed and 50 ug lysate were used to analyse different protein expression in samples by Western blotting. Representative images of experiments (n=3) are shown. These data are representative of experiments n=3. Bar chart shows quantification of protein levels compared to β-actin control in each condition. Error bars show standard deviation, * $p<0.05$; ** $p<0.01$; *** $p<0.001$; **** $p<0.0001$

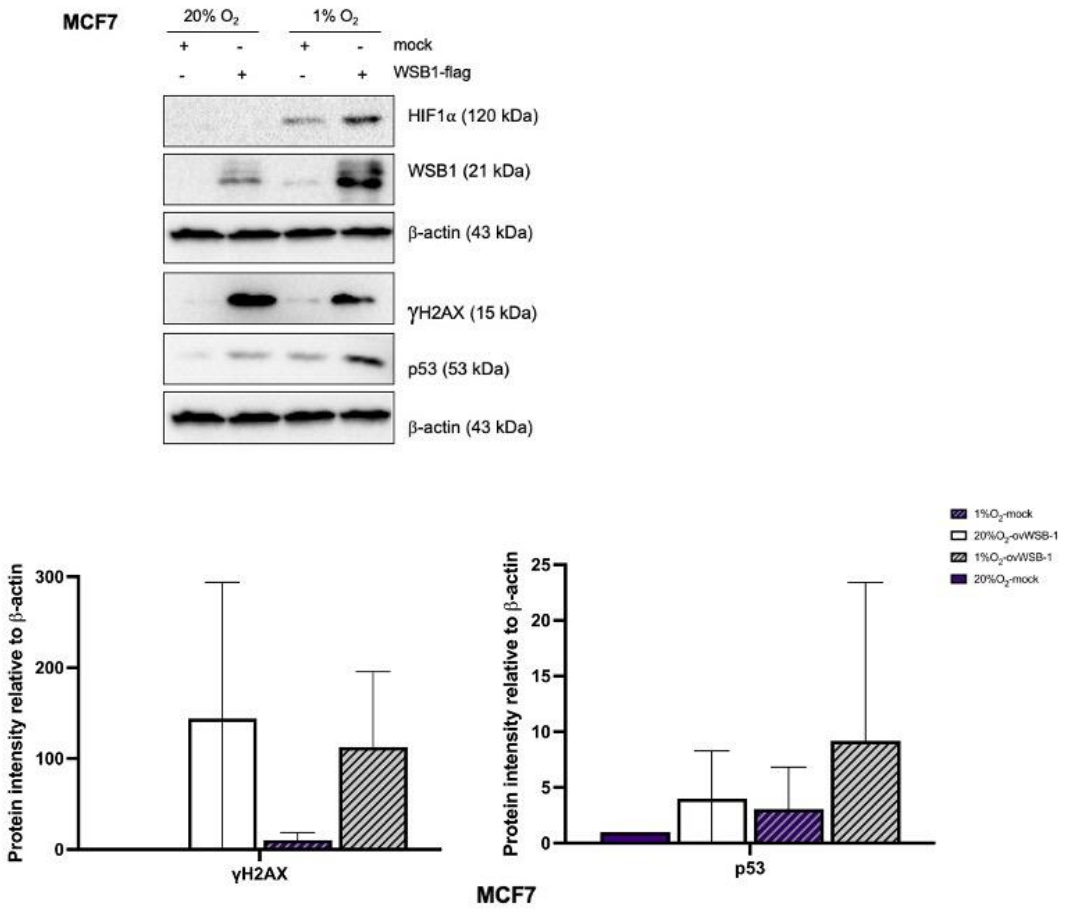

Figure 4. 2 γH2AX and p53 expression when WSB-1 is overexpressed in MCF-7 cells

MCF7 cells were transfected with either flag WSB-1 (WSB1-flag) or mock control (mock) for 24 hours and exposed to either 20% (normoxia) or 1% O_2 (hypoxia) for a further 24 hours. Cells were lysed and 50 ug lysate were used to analyse protein expression γH2AX and p53 in samples by Western blotting. These data are representative of experiments n=3. Bar chart shows quantification of protein levels compared to β-actin control in each condition. Error bars show standard deviation, * $p<0.05$; ** $p<0.01$; *** $p<0.001$; **** $p<0.0001$

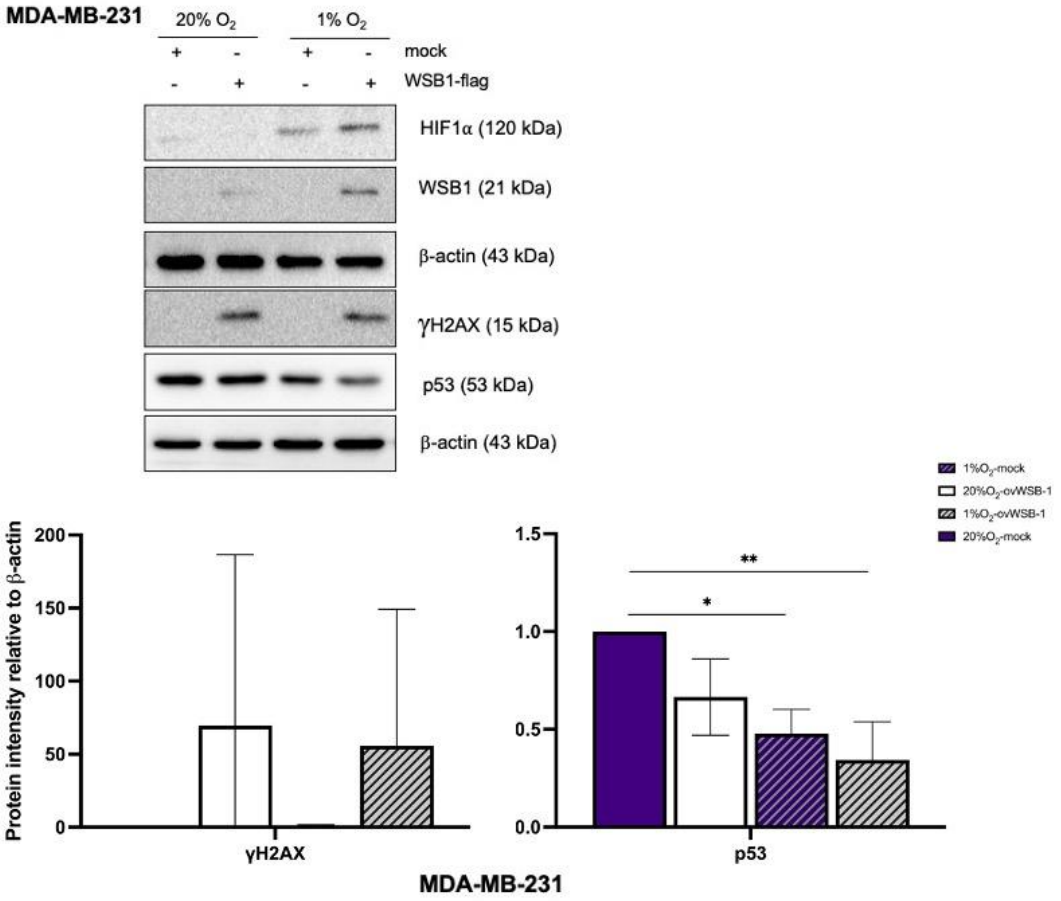

Figure 4. 3 γH2AX and p53 expression when WSB-1 is overexpressed in MAD-MB-231 cells

MDA-MB-231 cells were transfected with either flag WSB-1 (WSB1-flag) or mock control (mock) for 24 hours and exposed to either 20% (normoxia) or 1% O_2 (hypoxia) for a further 24 hours. Cells were lysed and 50 ug lysate were used to analyse protein expression γH2AX and p53 in samples by Western blotting. These data are representative of experiments n=3. Bar chart shows quantification of protein levels compared to β-actin control in each condition. Error bars show standard deviation, * $p<0.05$; ** $p<0.01$; *** $p<0.001$; **** $p<0.0001$

Figure 4.4 represents these preliminary data (n=1). Here, WSB-1 overexpression led to increased γH2AX levels for both cell lines, independently of oxygen tensions, and was also increased after irradiation, and again more dramatically in WSB-1 overexpressed samples. Total p53 levels were variable between samples but again increased after WSB-1 overexpression, with phospho-p53 levels increased overall after IR and increased by WSB-1 overexpression in the absence of irradiation.

WSB-1 overexpression decreased the protein expression of BRCA1 for MCF7 and MDA-MB-231 cells in non-irradiated samples (similar to observed in previous chapter but to variable degrees). Interestingly, for irradiated samples, total BRCA1 was increased with WSB-1 overexpression in normoxic conditions but repressed in hypoxic conditions. Regarding p-BRCA1, used here as an ATM activity marker, the pattern of change after WSB-1 overexpression was more variable depending on cell line, oxygen levels, and irradiation, so no clear conclusion can be drawn. For MCF7 cells, p-Chk1 levels, a marker of ATR activity, are increased with WSB-1 overexpression, independently of IR treatment of oxygen levels. pRb levels were decreased in MDA-MB-231 cells, again independently of IR.

These results indicate that overexpressing WSB-1 can lead to the occurrence of DNA damage, and suggested, albeit only preliminarily, that WSB-1 overexpression could activate ATM/pBRCA pathway, ATR/pCHK1 pathway, and p53/RB pathways. However, further work will need to be performed to confirm the occurrence of DNA damage and the impact of WSB-1 modulation on DNA repair.

4.3.2 WSB-1 overexpression induced DNA damage and reduced DNA repair capacity after IR in MCF7 cells

To further evaluate the impact of WSB-1 on the ability of cells to repair IR-mediated damage, MCF7 and MDA-MB-231 cells were transfected with either mock control or flag WSB-1 plasmid, and then cells were irradiated with 2 Gy, and fixed after 4h and 24h respectively for analysis of levels of γH2AX and 53BP1 foci.

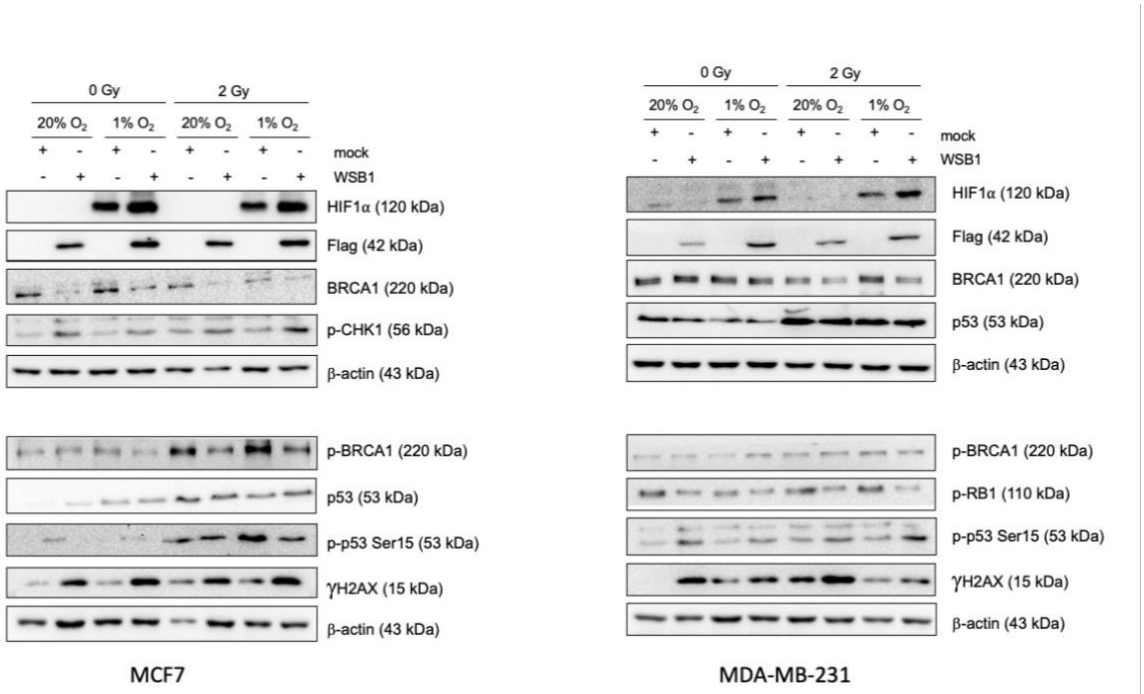

Figure 4. 4 The impact of WSB-1 overexpression on DDR signalling after IR in MCF-7 and MDA-MB 231 cells

MCF7 and MDA-MB-231 cells were transfected with either mock control (mock) or flag WSB-1 (WSB1) and exposed to either with or without irradiation treatments(2Gy) under 20% (normoxia) or 1% O_2 (hypoxia) for 24h post irradiation. Cells were lysed and various protein expression in samples were analysed by Western blotting for different proteins. These data represent n=1 experiments.

As showed in Figure 4.5, the average percentage of cells with γH2AX foci>5 in mock control (mock 0 Gy) in MCF-7 cell line without irradiation treatment was 14%. The average percentage of cells with γH2AX foci>5 in WSB-1 overexpression (WSB1 0 Gy) was 50%, which was approximately 3-fold higher than mock 0Gy ($p<0.0001$). This corroborates the findings from section 4.3.1. γH2AX foci levels were not much different between mock control (mock 2 Gy 4h) and overexpression WSB-1 (WSB1 2 Gy 4h) in MCF7 4 hours post irradiation, with average percentage of cells with γH2AX foci>5 being 99% in both conditions. To assess ability of cells to repair DNA damage, foci levels were also evaluated 24h post irradiation. Here, the average percentage of cells with γH2AX foci>5 in mock control (mock 2 Gy) was 54%, whereas it was 75% for WSB-1 overexpressing cells (WSB1 2 Gy), which was significantly ($p<0.0001$) higher (approx. 1.4-fold). A similar analysis for MCF7 cells was performed for 53BP1 foci (Figure 4.6). Similarly, to that observed for γH2AX, a significantly higher (approximately 3-fold) number of 53BP1 foci positive cells in the absence of irradiation were observed in cells with WSB-1 overexpression (WSB1 0 Gy) than mock 0 Gy ($p<0.0001$), respectively and 42% and 13%. 4 hours post irradiation, again not much difference was observed between mock and WSB-1 overexpression, with average again being 99% for both conditions. For samples fixed 24h post irradiation, average cells with 53BP1foci>5 in was 34% for mock control samples and 59% for WSB-1 overexpression samples, which was again significantly ($p<0.0001$) higher by about 1.8-fold.

Therefore, the key findings are that WSB-1 overexpression n MCF7 cells led to induction of DNA damage foci even in the absence of irradiation, and that DNA repair might also be downregulated in these cells, as foci number decrease 24 hours post irradiation was slower than for mock transfected cells.

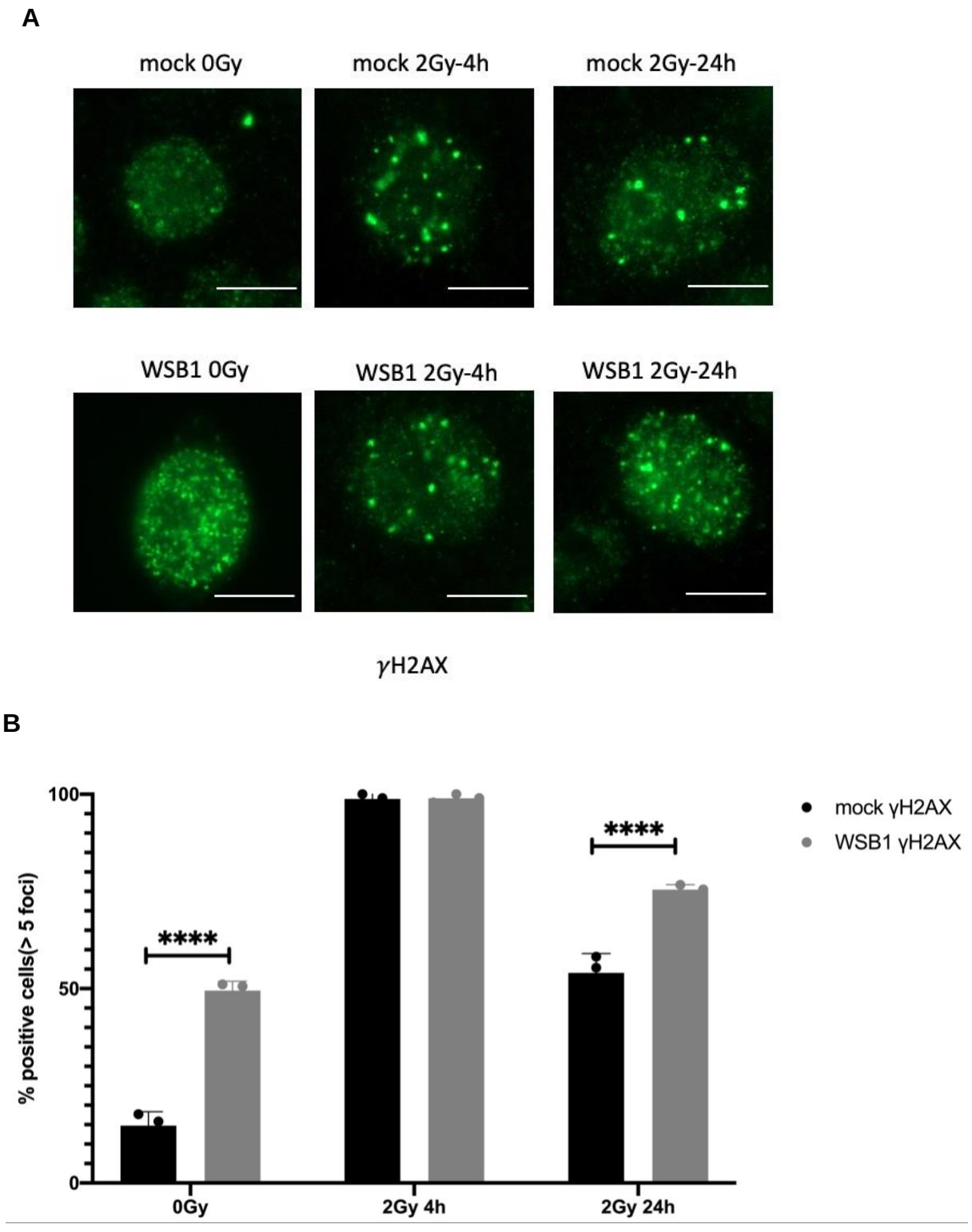

Figure 4. 5 γH2AX foci after WSB-1 overexpression and IR treatment in MCF-7 cells

MCF-7 cells were transfected with either mock (mock) or flag-tagged WSB1 (ovWSB1) for 24 hours then divided into 2 groups with or without irradiation (2 Gy) treatment, then cells were fixed 4h or 24h after irradiation. 100 cells were counted, and one cell with foci >5 was considered positive, N=3. A: representative images were taken after IF staining for γ-H2AX (green), n=3. Scale bar represents 100 μm. B: histograms show the average number of γ-H2AX positive cells. Statistical significance was determined using Student's t-test; error bars represent mean ± SEM * $p<0.05$; ** $p<0.01$; *** $p<0.001$; **** $p<0.0001$

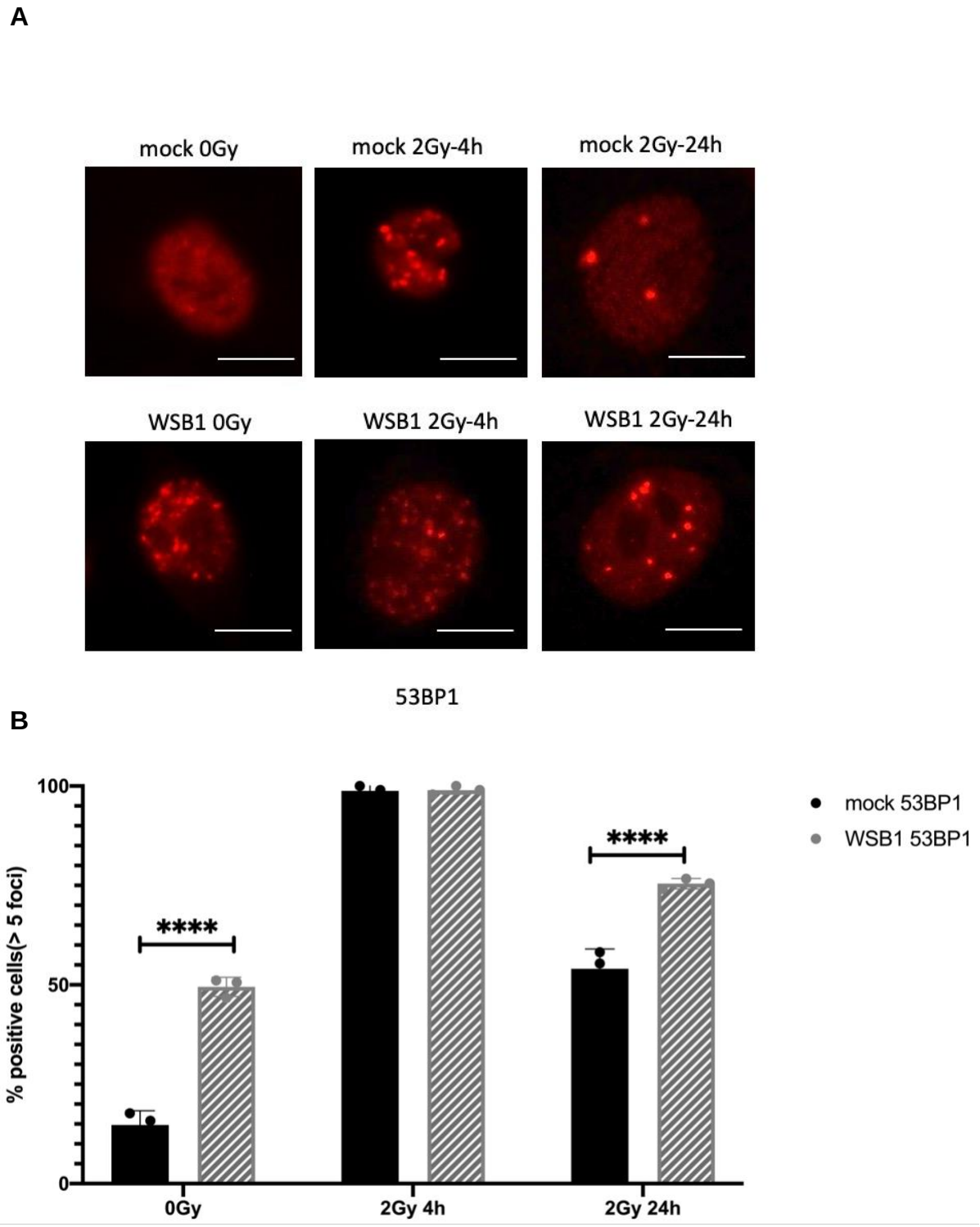

Figure 4. 6 53BP1 foci after WSB-1 overexpression and IR treatment in MCF7 cells

MCF-7 cells were transfected with either mock (mock) or flag-tagged WSB1 (ovWSB1) for 24 hours then divided into 2 groups with or without irradiation (2 Gy) treatment, then cells were fixed 4h or 24h after irradiation. 100 cells were counted, and one cell with foci >5 was considered positive, N=3. A: representative images were taken after IF staining for γ-H2AX (green), n=3. Scale bar represents 100 μm. B: histograms show the average number of γ-H2AX positive cells. Statistical significance was determined using Student's t-test; error bars represent mean ± SEM * $p<0.05$; ** $p<0.01$; *** $p<0.001$; **** $p<0.0001$

4.3.3 WSB-1 overexpression induced DNA damage and reduced DNA repair capacity after IR in MDA-MB-231 cells

As showed in Figure 4.7 showed, the average percentage of cells with γH2AX foci>5 in mock control without irradiation (mock 0 Gy) was 19.8% in MDA-MB-231 cells. The average percentage of cells with γH2AX foci>5 in WSB-1 overexpression without irradiation (WSB1 0 Gy) was 46.1%, which was 2.3 times higher than mock 0 Gy ($p<0.001$). γH2AX Foci were not much difference between mock control (mock 2 Gy 4h) with overexpression WSB-1 when used irradiation treatment after 4h (WSB1 2 Gy 4h) in MDA-MB-231, the average percentage of cells with γH2AX foci>5 in mock 0 Gy 4h was 99.3%. The average percentage of cells with γH2AX foci>5 in WSB1 2 Gy 4h was 99.6%. When used irradiation with overexpressed WSB-1 in MDA-MB-231, the average of cells with γH2AX foci>5 in mock control (mock 0 Gy) was 38.4% and average cells with γH2AX foci>5 in WSB-1 overexpressed with irradiation treatment after 24h (WSB1 2 Gy) was 62.9%, which was 1.64 times higher than mock 2 Gy ($p<0.001$).

A similar analysis for MDA-MB-231 cells was performed for 53BP1 foci (Figure 4.8). Similarly, to that observed for γH2AX, a significantly higher (approximately 5.27-fold) number of 53BP1 foci positive cells in the absence of irradiation were observed in cells with WSB-1 overexpression (WSB1 0 Gy) than mock 0 Gy ($p<0.0001$), respectively and 35.1% and 6.7%. 4 hours post irradiation, again not much difference was observed between mock and WSB-1 overexpression, with average percentage of cells in mock 0 Gy 4h was 98.3% and the average percentage of cells with 53BP1 foci>5 in WSB1 2 Gy 4h was 98.3%. For samples fixed 24h post irradiation, average cells with 53BP1 foci>5 in was 33.8% for mock control samples and 50.8% for WSB-1 overexpression samples, which was again significantly ($p<0.001$) higher by about 1.5-fold.

Taken together, WSB-1 overexpression in MDA-MB-231 cells led to induction of DNA damage foci including γH2AX and 53BP1 foci. and that DNA repair might also be downregulated in these cells, as foci number decrease 24 hours post irradiation was slower than for mock transfected cells.

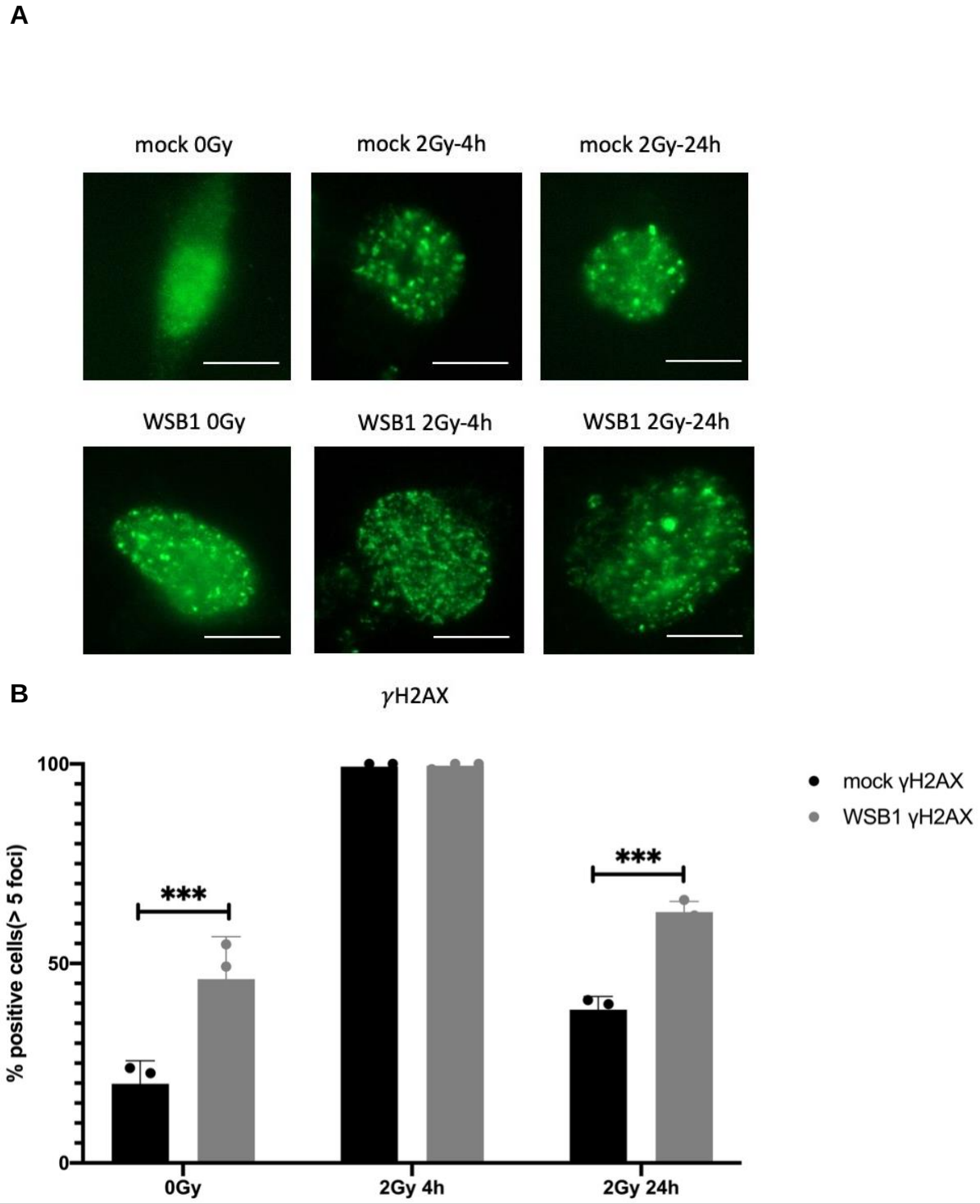

Figure 4. 7 γH2AX foci after WSB-1 overexpression and IR treatment in MDA-MB-231 cells

MDA-MB-231 cells were transfected with either mock (mock) or flag-tagged WSB1 (ovWSB1) for 24 hours then divided into 2 groups with or without irradiation (2 Gy) treatment, then cells were fixed 4h or 24h after irradiation. 100 cells were counted, and one cell with foci >5 was considered positive, N=3. A: representative images were taken after IF staining for γ-H2AX (green), n=3. Scale bar represents 100 μm. B: histograms show the average number of γ-H2AX positive cells. Statistical significance was determined using Student's t-test; error bars represent mean ± SEM * $p<0.05$; ** $p<0.01$; *** $p<0.001$; **** $p<0.0001$

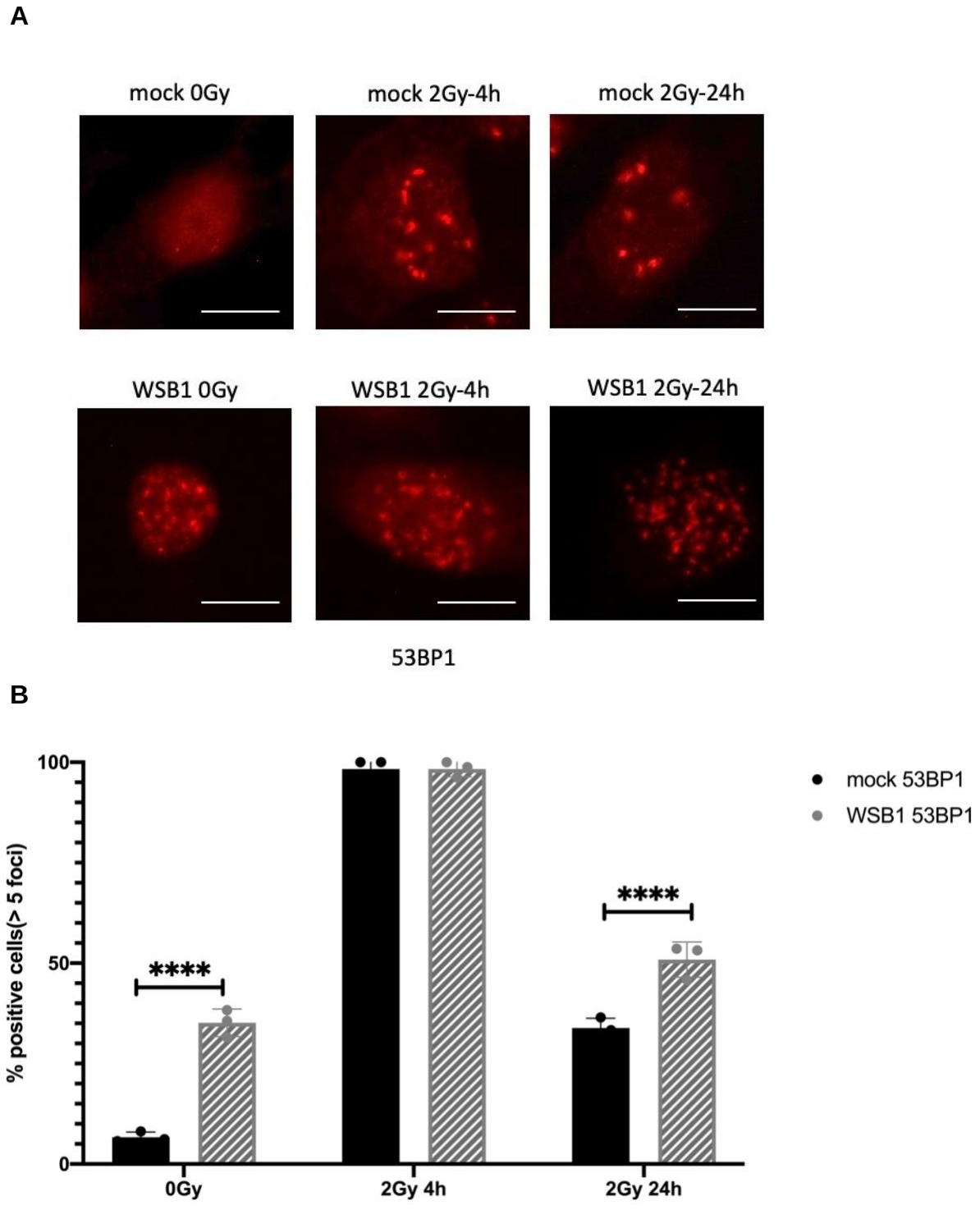

Figure 4. 8 53BP1 foci after WSB-1 overexpression and IR treatment in MDA-MB-231 cells
MDA-MB-231 cells were transfected with either mock (mock) or flag-tagged WSB1 (ovWSB1) for 24 hours then divided into 2 groups with or without irradiation (2 Gy) treatment, then cells were fixed 4h or 24h after irradiation. 100 cells were counted, and one cell with foci >5 was considered positive, N=3. A: representative images were taken after IF staining for 53BP1 (red), n=3. Scale bar represents 100 μm. B: histograms show the average number of 53BP1 positive cells. Statistical significance was determined using Student's t-test; error bars represent mean ± SEM * $p<0.05$; ** $p<0.01$; *** $p<0.001$; **** $p<0.0001$

4.3.4 WSB1 depletion reduced DNA damage foci after IR in MCF7 cells

The impact of WSB-1 on the ability of cells to repair IR-mediated damage was also evaluated by WSB-1 depleted, MCF7 and MDA-MB-231 cells were transfected with either siNT control or siWSB-1 for 24h then irradiated with 2 Gy, and again were fixed after 4h and 24h respectively for analysis of levels of γH2AX and 53BP1 foci.

As showed in Figure 4.9 and Figure 4.10, the average percentage of cells with γH2AX foci>5 in siNT control without irradiation (siNT 0 Gy) was 15.8%, the average percentage of cells with γH2AX foci>5 in WSB-1 depleted cells without irradiation (siWSB1 0 Gy) was 13.1%, and the difference between siNT 0 Gy and siWSB1 0 Gy is not statistic significant. γH2AX foci were not much difference between mock (mock 2 Gy 4h) and siWSB-1 (siWSB1 2 Gy 4h) when used irradiation treatment after 4h in MCF7 cells, with the average percentage of cells with γH2AX foci>5 both 99.7%. When used irradiation 2Gy in WSB-1 depleted cells after 24h, the average percentage of cells with γH2AX foci>5 in siNT control (siNT 2 Gy 24h) was 46.5% and the average percentage of cells with γH2AX foci>5 in depleted WSB-1 cells (siWSB1 2 Gy 24h) was 35.1%, which was 1.32 times lower than siNT 2 Gy ($p<0.01$).

The average percentage of cells with 53BP1 foci>5 in siNT control without irradiation (siNT 0 Gy) was 13.6%, and the average percentage of cells with 53BP1foci>5 in WSB-1 depleted cells without irradiation (siWSB1 0 Gy) was 14.3%, which was not much difference ($p>0.05$). 4h after irradiation, 53BP1 Foci were not much difference between siNT (siNT 2 Gy 4h) and siWSB-1 (siWSB-1 2 Gy 4h) either, which with the average percentage of 98.9 and 99.4% respectively. When used irradiation with WSB-1 depletion, the average percentage of cells with 53BP1foci>5 in siNT control (siNT 2 Gy 24h) was 33.4% and the average percentage of cells with 53BP1 foci>5 in depleted WSB-1 conditions (siWSB1 2 Gy 24h) was 22.6%, which was 1.5 times lower than siNT (siWSB1 2 Gy 24h) ($p<0.05$).

Taken together, WSB-1 depletion reduced irradiation induced DNA damage foci in MCF7 cells, which also indicated might improve DNA repair after 24h post irradiation when WSB-1 was depleted.

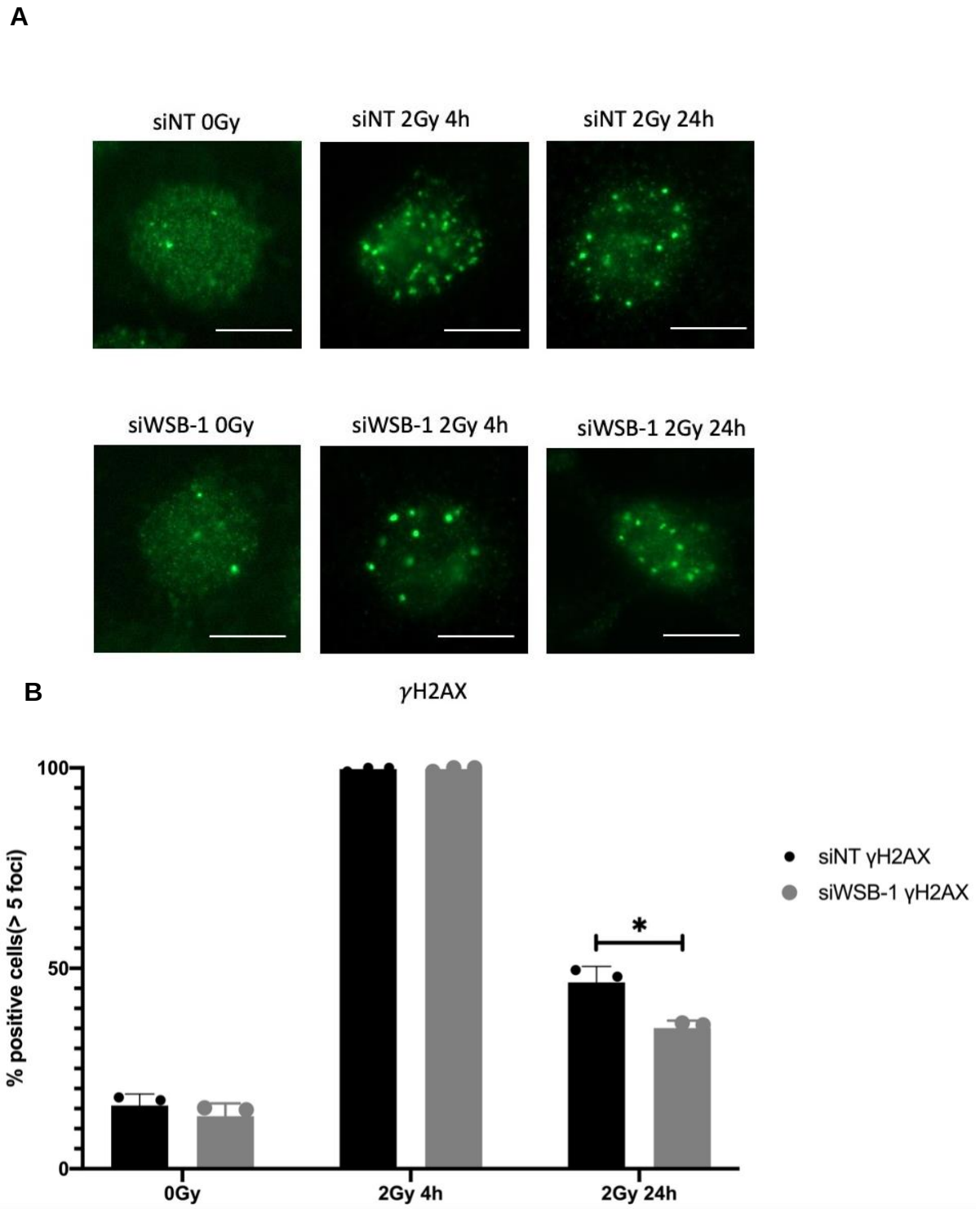

Figure 4. 9 γH2AX foci after WSB-1 depletion and IR treatment in MCF7 cells

MCF7 cells were transfected with either siNT or siWSB-1 for 24 hours then divided into 2 groups with or without irradiation (2 Gy) treatments, then cells were fixed 4h or 24h after irradiation. 100 cells were counted, and one cell with foci >5 was considered positive, N=3. A: representative images were taken after IF staining for γH2AX (green), n=3. Scale bar represents 100 μm. B: histograms show the average number of γH2AX positive cells. Statistical significance was determined using Student's t-test; error bars represent mean ± SEM * $p<0.05$; ** $p<0.01$; *** $p<0.001$; **** $p<0.0001$

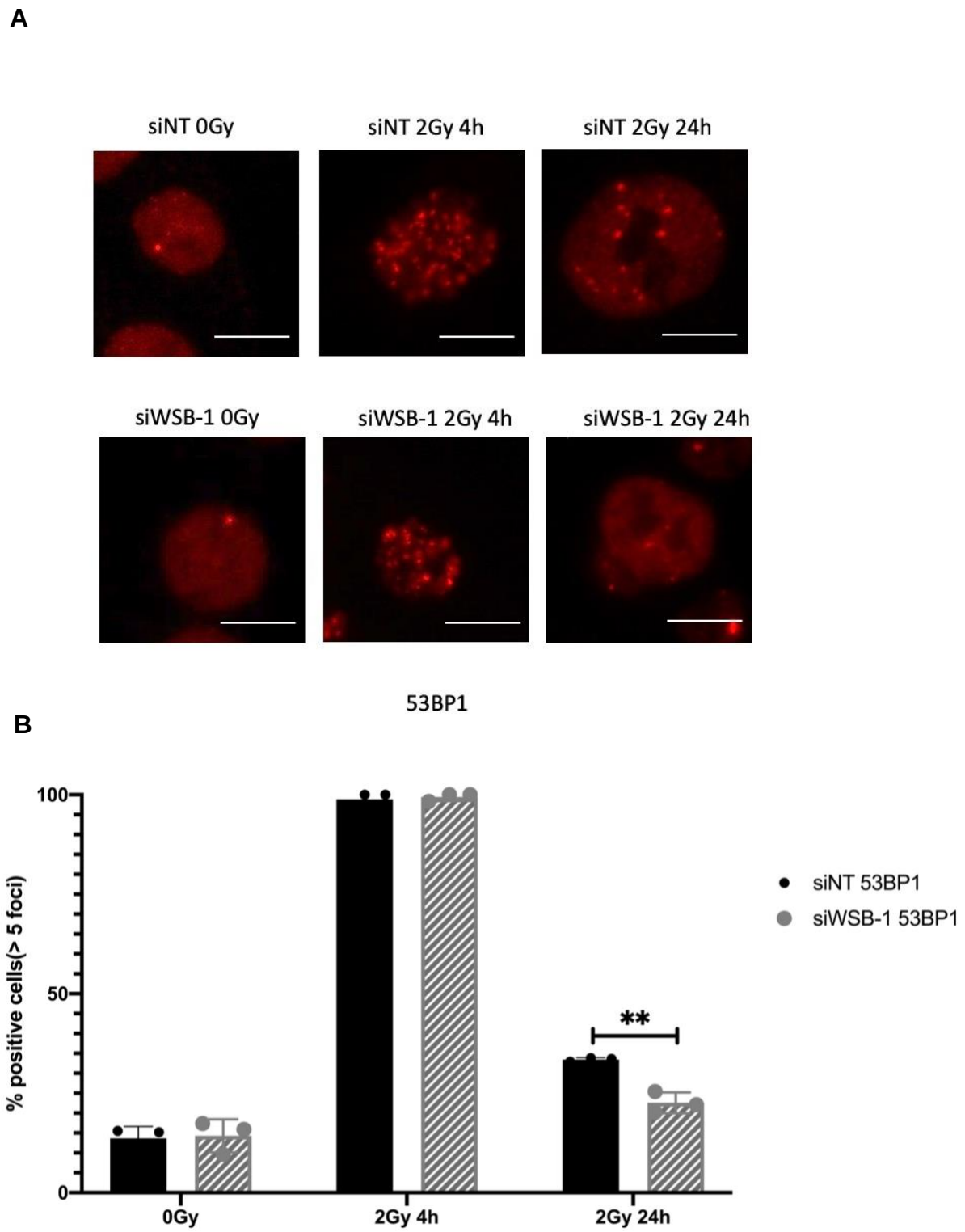

Figure 4. 10 53BP1 foci after WSB-1 depletion and IR treatment in MCF7 cells

MCF7 cells were transfected with either siNT or siWSB1 for 24 hours then divided into 2 groups with or MCF7 cells were transfected with either siNT or siWSB-1 for 24 hours then divided into 2 groups with or without irradiation (2 Gy) treatment, then cells were fixed 4h or 24h after irradiation. 100 cells were counted, and one cell with foci >5 was considered positive, N=3. A: representative images were taken after IF staining for 53BP1 (red), n=3. Scale bar represents 100 μm. B: histograms show the average number of 53BP1 positive cells. Statistical significance was determined using Student's t-test; error bars represent mean ± SEM * $p<0.05$; ** $p<0.01$; *** $p<0.001$; **** $p<0.0001$

4.3.5 WSB1 depletion reduced DNA damage foci after IR in MDA-MD-231 cells

As showed in Figure 4.11, in MDA-MB-231 cells, the average percentage of cells with γH2AX foci>5 in siNT control without irradiation (siNT 0Gy) was 18.7%, the average percentage of cells with γH2AX foci>5 with WSB-1 depletion without irradiation (siWSB-1 0Gy) was 19.5%, which was not much difference between these two groups ($p>0.05$). γH2AX foci levels were not much different between siNT control (siNT 2Gy 4h) and depleted WSB-1 condition (siWSB-1 2Gy 4h) in MDA-MB-231 4 hours post irradiation, with average percentage of cells with γH2AX foci>5 being 100% in both conditions. And again, to assess the ability of cells to repair DNA damage, foci levels were also evaluated 24h post irradiation. Here, the average percentage of cells with γH2AX foci>5 in siNT control (siNT 2Gy 24h) was 36.9%, whereas it was 21.8% for WSB-1 depleted cells (siWSB-1 2Gy), which was significantly ($p<0.001$) higher (approx. 1.7-fold).

53BP1 foci in MDA-MB-231 cells with and without irradiation were also calculated (Figure 4.12). The average percentage of cells with 53BP1 foci>5 in siNT control (siNT 0Gy) was 13.8%, and the average percentage of cells with 53BP1foci>5 in WSB-1 depleted cells without irradiation (siWSB1 0Gy) was 12.3%, which was not much difference ($p>0.05$). 4h after irradiation, 53BP1foci levels were not much different between siNT (siNT 2Gy 4h) and siWSB-1 (siWSB-1 2Gy 4h), with average percentage of cells with 53BP1foci>5 being 100% in both conditions.

24h after irradiation, the average percentage of cells with 53BP1foci>5 in siNT control (siNT 2 Gy 24h) was 33.3% and the average percentage of cells with 53BP1 foci>5 in WSB-1 depleted cells (siWSB1 2 Gy 24h) was 24.9%, which was 1.34 times lower than siNT (siWSB1 2 Gy 24h) ($p<0.05$).

Taken together, WSB-1 depletion reduced DNA damage foci including γH2AX and 53BP1 foci in MDA-MB-231 cells. When using irradiation, these changes were not appeared after 4h post irradiation, but after 24 h post irradiation, the ability of cells to repair DNA damage induced by irradiation seems improved significantly when WSB-1 is depleted.

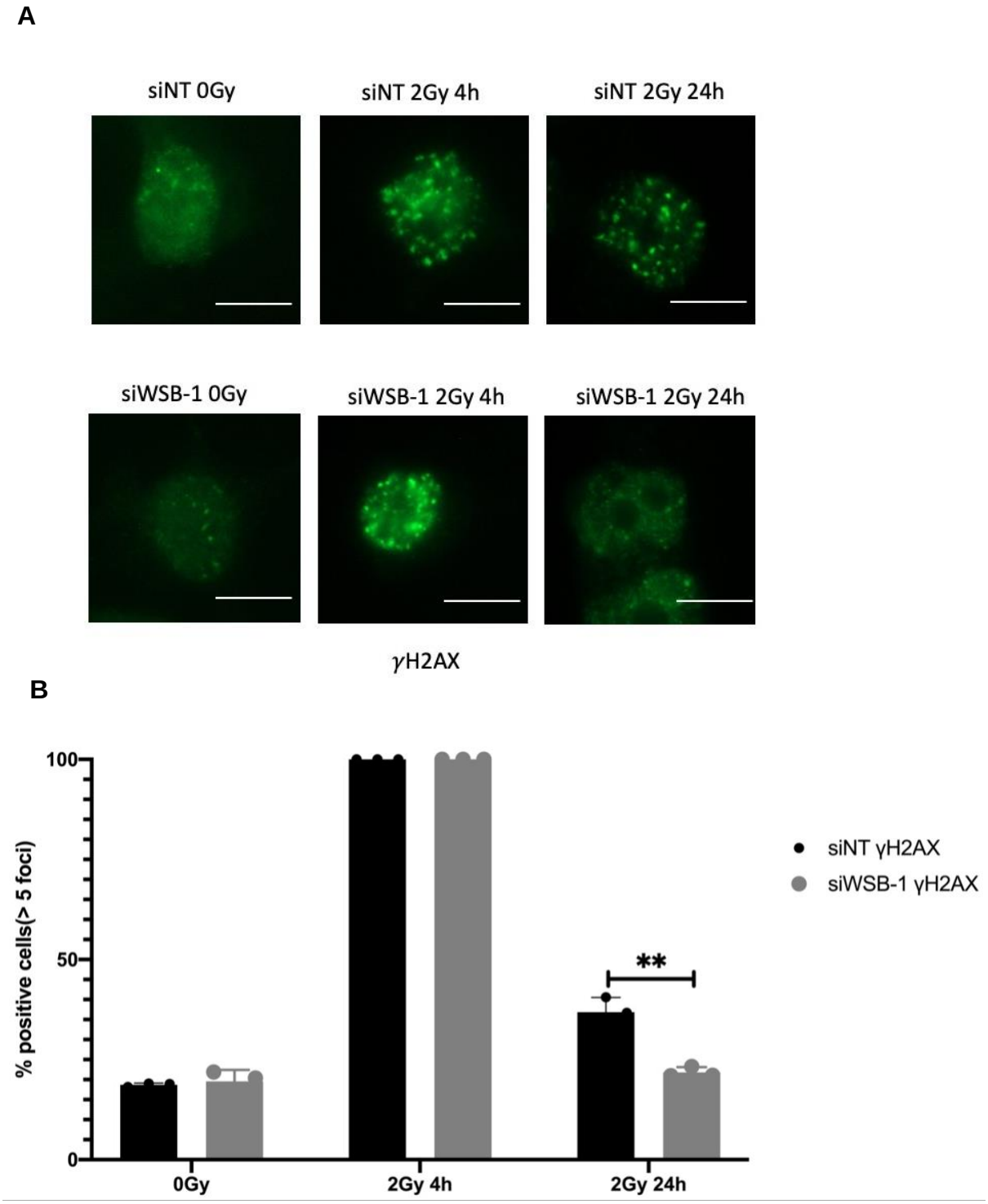

Figure 4. 11 γH2AX foci after WSB-1 depletion and IR treatment in MDA-MB-231 cells

MDA-MB-231 cells were transfected with either siNT or siWSB-1 for 24 hours then divided into 2 groups with or without irradiation (2 Gy) treatment, then cells were fixed 4h or 24h after irradiation. 100 cells were counted, and one cell with foci >5 was considered positive, N=3. A: representative images were taken after IF staining for γH2AX (green), n=3. Scale bar represents 100 μm. B: histograms show the average number of γH2AX positive cells. Statistical significance was determined using Student's t-test; error bars represent mean ± SEM * $p<0.05$; ** $p<0.01$; *** $p<0.001$; **** $p<0.0001$

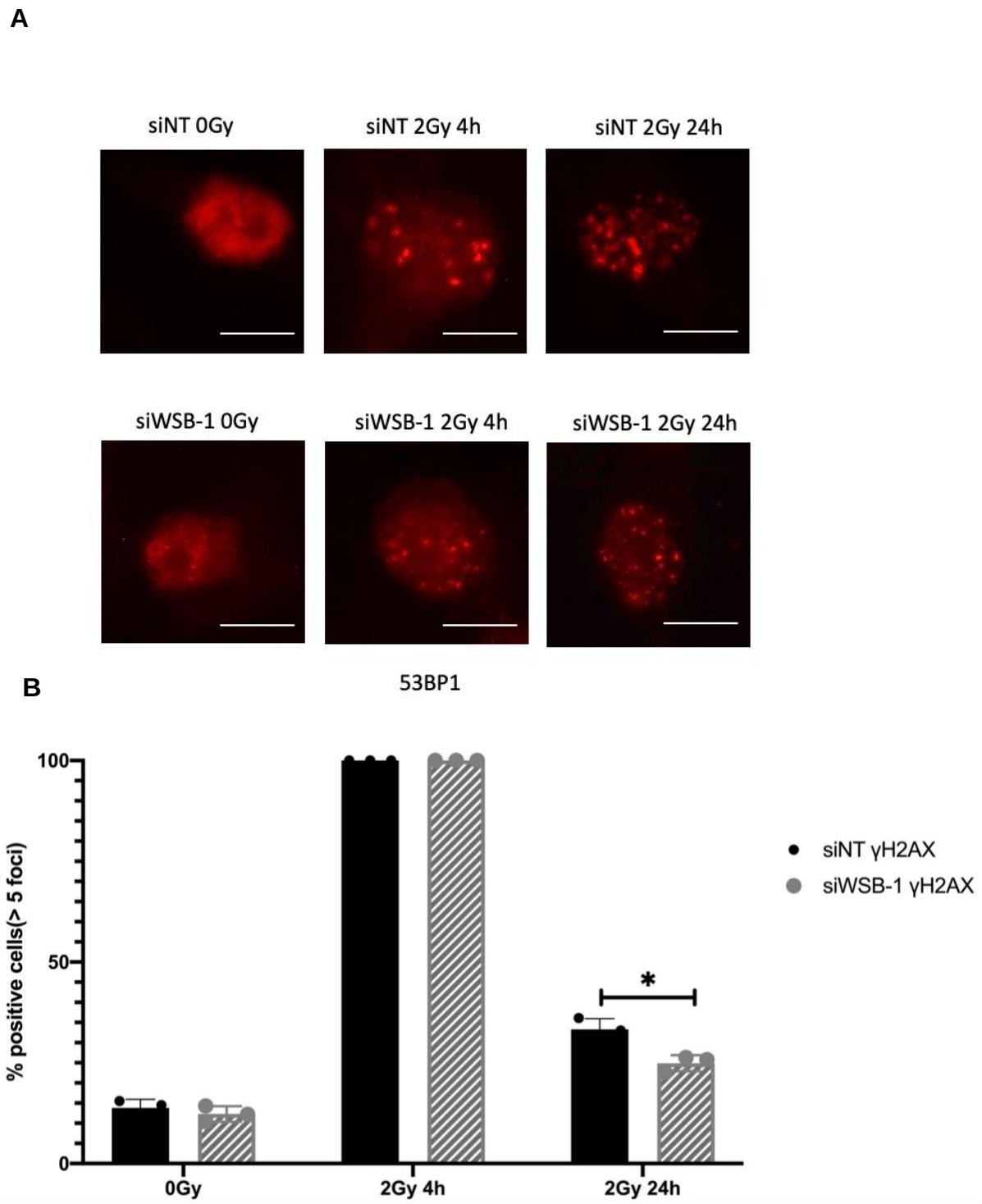

Figure 4. 12 53BP1 foci after WSB-1 depletion and IR treatment in MDA-MB-231 cells
MDA-MB-231 cells were transfected with either siNT or siWSB-1 for 24 hours then divided into 2 groups with or without irradiation (2 Gy) treatment, then cells were fixed 4h or 24h after irradiation. 100 cells were counted, and one cell with foci >5 was considered positive, N=3. A: representative images were taken after IF staining for 53BP1 (red), n=3. Scale bar represents 100 μm. B: histograms show the average number of 53BP1 positive cells. Statistical significance was determined using Student's t-test; error bars represent mean ± SEM * $p<0.05$; ** $p<0.01$; *** $p<0.001$; **** $p<0.0001$

4.3.6 Cell cycle arrest analysis of WSB-1 overexpression

As WSB-1 overexpression increased p53 and potentially increased phospho-p53 and phospho-Rb levels, we hypothesised that WSB-1 overexpression could impact cell cycle progression. To investigate this, the effect of WSB-1 overexpression on cell cycle arrest was tested *in vitro* using flow cytometric analysis after PI staining. MCF7 and MDA-MB-231 cells were transfected with either mock control or flag WSB-1 plasmid for 24h, then conduct the PI staining and flow cytometric analysis.

Figure 4.13 (MCF7) and Figure 4.14 (MDA-MB-231) represent graphs of cell cycle arrest for control mock and overexpressed WSB-1. And the percentages of cells in different cell cycle phases were quantified and summarised.

As can be seen in Figure 4.13, for MCF7 cells, there was not much difference between the average proportion of cells in the subG1 phase of the cell cycle for mock (1.73%) and overexpressed WSB-1 samples (1.4%). There was a significant ($p<0.001$) decrease on the average proportion of cells in the G1 phase of the cell cycle for overexpressed WSB-1 samples (15.53%) when compared to control mock (33.7%). The proportion of cells in the S phase following WSB-1 overexpression was also significantly ($p<0.01$) decreased, with an average of 24.4% when compared to mock control (32.7%). Conversely, proportion of cells in the G2/M phase of the cell cycle was significantly increased ($p<0.01$) when WSB-1 was overexpressed (58.97%) compared to mock (average 32.5%).

For MDA-MB-231 cells (Figure 4.14), a similar pattern was observed: the average proportion of cells in the subG1 phase of the cell cycle for overexpressed WSB-1 samples (1.77%) was higher than mock (0.53%) but this difference was not statistic significant. There was a significant ($p<0.01$) decrease on the average proportion of cells in the G1 phase of the cell cycle for overexpressed WSB-1 samples (22.3%) when compared to control mock (43.2%). The proportion of cells in the S phase was significantly different between WSB-1 overexpression with an average of 30.13% when compared to mock control (30.67%). Conversely, proportion of cells in the G2/M phase of the cell cycle was significantly increased ($p<0.01$) when WSB-1 was overexpressed (39.5%) compared to mock (average 24.7%).

In summary, flow cytometric detection revealed that WSB-1 overexpression was associated to a G2/M arrest in MCF7 and MDA-MB-231 cells.

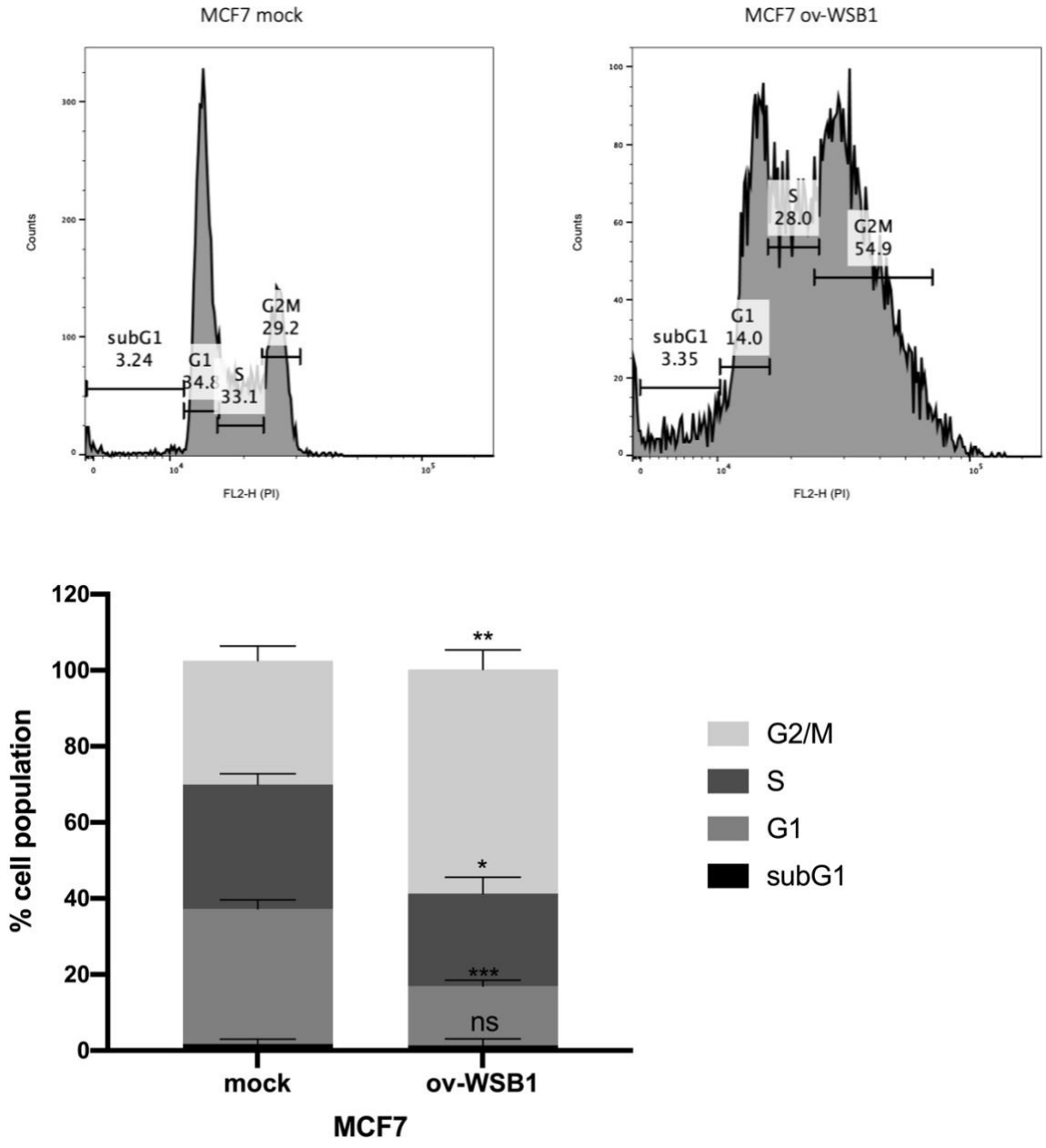

Figure 4. 13 The impact of WSB1 overexpression Cell cycle arrest in MCF7 cells

MCF7 cells were transfected with either mock(mock) or flag-tagged WSB-1(WSB1) for 24 hours, and original representative graphs were measured by PI staining, detected by LSRFortessa^{TM} flow cytometer, and analysed by FlowJo® V10 software (n=3). Bar charts showed comparisons of mock, WSB-1 overexpression (ov-WSB1) on cell cycle arrest. * $p<0.05$; ** $p<0.01$; *** $p<0.001$; **** $p<0.0001$; (Student's t-test) as compared to mock, Error bars represent mean ± SEM.

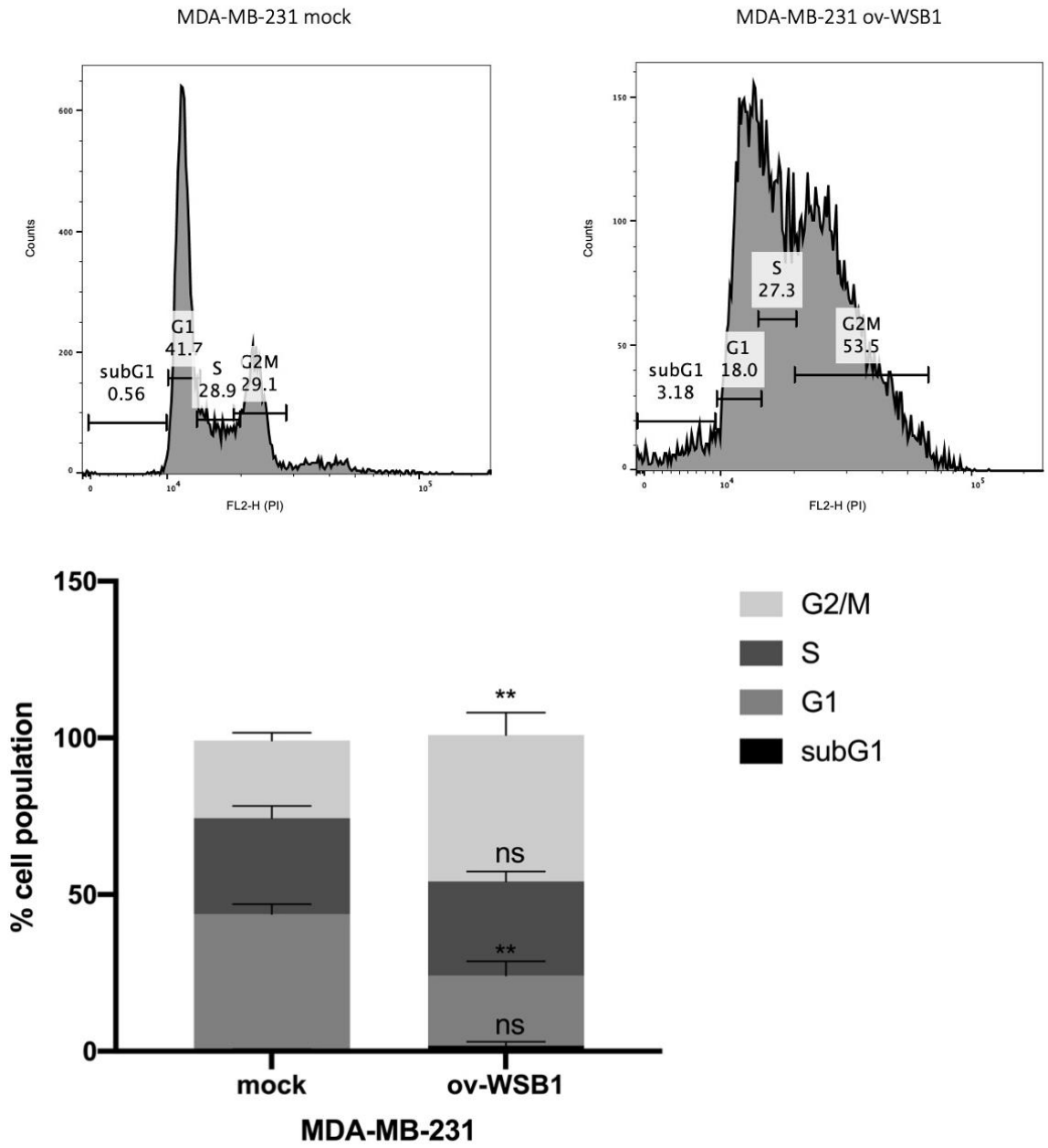

Figure 4. 14 The impact of WSB1 overexpression Cell cycle arrest in MDA-MB-231 cells
MDA-MB-231 cells were transfected with either mock(mock) or flag-tagged WSB-1(WSB1) for 24 hours, and original representative graphs were measured by PI staining, detected by LSRFortessa^{TM} flow cytometer, and analysed by FlowJo® V10 software (n=3). Bar charts showed comparisons of mock, WSB-1 overexpression (ov-WSB1) on cell cycle arrest. * $p<0.05$; ** $p<0.01$; *** $p<0.001$; **** $p<0.0001$; (Student's t-test) as compared to mock, Error bars represent mean ± SEM.

4.4 Discussion

In this chapter, the relationship between WSB-1 and some important protein in the DDR pathway were analysed when overexpressed WSB-1 under normoxia and hypoxia. In addition, the impact of WSB-1 overexpression as well as WSB-1 depletion on DNA damage markers such as γH2AX and 53BP1 were investigated. Finally, the impact of WSB-1 overexpression on chromosome instability and cell cycle arrest were also evaluated. Following the results we obtained, below is a discussion of these results to address the aims stated at the start of the Chapter.

1. *Investigate the relationship between WSB-1 expression and DDR signalling.*

Firstly, we found that overexpressing WSB-1 upregulated γH2AX and p53 independently of hypoxia. γH2AX is a biomarker of DNA damage especially DSBs (Redon et al., 2011). When DNA damage such as DSBs occurs, H2AX is phosphorylated, flagging the lesions and recruiting repair proteins to the site of damage. The upregulation of γH2AX after WSB-1 overexpression indicates that WSB-1 overexpression causes DNA damage such as DSBs in the absence of exogenous sources of DNA damage. Meanwhile, p53 levels were upregulated when WSB-1 was overexpressed and downregulated when WSB-1 was depleted under normoxia and hypoxia. As it is well known, in respond to DNA damage, p53 is phosphorylated and stabilised, which would be consistent with p53 stabilisation and γH2AX induction being evidence of the presence of damage after WSB-1 overexpression. Preliminary data indicated that phospho-p53 was also present after WSB-1 overexpression, further indicating that DNA damage was present in these conditions. p53 stabilisation also leads to increased p21 expression, causing cell cycle arrest to allow damaged DNA to be repaired, or apoptosis (Chen, 2016). In addition, p53 has also been directly implicated in the regulation and participation in HR pathways such as directly regulate RAD51 (Williams and Schumacher, 2016, Hine et al., 2014). Moreover, studies found that H2AX is required for cell cycle arrest via the p53/p21 (Fragkos et al., 2009). p21 (CDKN1A) was also upregulated by 1.10-fold change ($p<0.001$) from RNA-seq data for WSB-1 depleted samples under hypoxia. We attempted to evaluate p21 protein levels after WSB-1 modulation but unfortunately the antibody did not work.

As mentioned earlier in this chapter, the phosphorylation of BRCA1 especially at Ser1524 BRCA1 could indicate ATM activation (Gatei et al., 2001). As the study shown in (Kim et

al., 2017a) that ATM can be degraded by WSB-1, so a concurrent decrease in ATM activity could be predicted after WSB-1 overexpression. However, in our very preliminary results, phospho BRCA1 (Ser1524) levels after WSB-1 overexpression were variable between cell lines and conditions, so no clear conclusion can be drawn without further studies. Our preliminary data also indicates that that the ATR pathway downstream target pCHK1(Ser345) could be increased when WSB-1 was overexpressed in MCF7. The activation of CHK1 can be induced by DNA damage, in particular linked with replication stress, which then triggers the checkpoint signal such as the phosphorylation of cdc25 proteins, leads to the inhibition of cyclin-dependent kinase (CDK1/CDK2) activity, and promote cell cycle arrest and allow the damaged DNA to be repaired (Zhang and Hunter, 2014). Given its critical roles in DDR and cell cycle checkpoints, CHK1 was initially considered to function as a tumour suppressor. However, CHK1 was also found promotes tumour growth and may contribute to the resistance of anticancer therapies (Rundle et al., 2017). These data indicate that WSB-1 overexpression could possibly be inducing ATR signalling via replication stress, but further work needs to be performed to further validate this, as discussed later. Finally, the preliminary data indicates that phospho RB could be downregulated by WSB-1 overexpression in MDA-MB-231 cells but again the results are variable and clear conclusions cannot be drawn.

In summary, although further repeats of these protein expression analyses are needed, as well as analyses of other DDR makers such as p-CHK2, a target of ATM, our preliminary results indicate that WSB-1potentially effects DDr signalling factors after RT, which indicates WSB-1 could play an important role in DNA damage response pathway.

2. *Validate the impact of WSB-1 on DNA repair and cell cycle progression*

Prevalence of γH2AX and 53BP1 foci after IR were tested in order to confirm the effect of WSB-1 on DNA damage and repair. The data for both cell lines confirmed the western blotting data that overexpression of WSB-1 was linked with the presence of DNA damage as noted by increased γH2AX and 53BP1 foci even in the absence of external damage.
These data also showed that IR-induced foci were higher in WSB-1 overexpressed samples 24 hrs post IR, indicating that DNA repair was impaired/less efficient in these conditions. Conversely, depleting WSB-1 further reduced γH2AX and 53BP1 foci 24 hours post IR in both MCF-7 and MDA-MB-231 cells, indicating potentially more effective DNA repair.

These data indicated that 1) WSB-1 overexpression was linked with presence of DNA damage and 2) WSB-1 modulation potentially altered DNA repair post IR. To test more quantitatively and sensitively to evaluate which type of DNA repair pathway is affected by WSB-1 modulation, methodologies such as the DR-GFP assay for HR efficiency, or equivalent assays for NHEJ, can be used (Nakanishi et al., 2011, Seluanov et al., 2010). In these assays, GFP reporter constructs contain sites for the I-SceI endonuclease, leading to the induction of a DSB. In the absence of I-SceI expression of the GFP gene is inactivated. If repair is successful, repair of I-SceI-induced breaks by NHEJ or HR restores the functional GFP gene, and the proportion of florescent cells can be quantified by flow cytometry.

The IRIF data also indicates that different types of DNA damage could be caused by WSB-1 overexpression, both DSBs (detected by the presence of 53BP1 foci) and SSBs/replication stress (detected by a more diffuse γH2AX foci staining alongside larger foci). This would support the observations from the preliminary data discussed above where phospho-Chk1 levels are observed after WSB-1 overexpression, albeit preliminarily. However, due to time limitation, the impact of WSB-1 on the loss of HR capacity, chromosomal instability, and DNA replication stress was not investigated in this study, and will be included in future studies. To test the presence of different types of damage more clearly, other markers could be used. For example, the presence of RPA (replication protein A) foci or phosphorylated RPA could be evaluated to determine the presence of SSBs and replication stress (Pires et al., 2010). Further methodologies to evaluate the presence of replication stress include BRdU incorporation kinetics and DNA fiber assays (Pires et al., 2010). In addition, complex DNA damage (CDD), which has been defined as two or more DNA damage lesions occurs, can be detected by the enzyme-modified neutral comet (EMNC) assay (Fabbrizi et al., 2021). Therefore, EMNC assay could be conducted to detect CDD when overexpressing WSB-1. Finally, flow cytometric analysis of cell cycle progression indicates that WSB-1 overexpression caused a cell cycle arrest in G2/M, but not in G1, which again can be dependent on p53 activation downstream of DSBs and/or replications stress.

There are limitations to the scoring system used in this study, which considers a cell as positive if more than 5 γH2AX and 53BP1 foci are present. This does not allow for a determination of changes in foci number per cell beyond that threshold, and therefore could limit a more refined evaluation of DNA repair kinetics. An alternative more sensitive criteria is to score the total number of foci/cell and present this as a frequency plot or a violin plot, as

for example shown in this recent study by the Higgins group (Rodriguez-Berriguete et al., 2023).

In conclusion, in this chapter, our results shows that WSB-1 overexpression increased DNA damage markers including γH2AX and 53BP1 foci, and was linked with altered DNA repair, with WSB-1 overexpression also leading to a potential G2/M arrest linked with p53 stabilisation, causing cell cycle arrest.

The following chapter will evaluate if these findings can be translated to patient samples, and whether targeting the DDR in the context WSB-1 modulation is a potential valid therapeutic strategy.

Chapter 5

High WSB-1 expression increased sensitivity to DDRi and IR

5.1 Introduction

The DNA damage response (DDR) constitutes approximately 450 proteins that identify and sensing damaged DNA, signal, mediate DNA damage repair, and coordinates cell-cycle progression with DNA repair to minimize or prevent DNA damage being permanently passed through cell division (Gourley et al., 2019). PARP is a key regulator involved in DDR and is also the first clinically approved DDR inhibitor target. BRCA1 and/or BRCA2 are centrally involved in HR repair pathway and BRCA1 and/or BRCA2 deficiency determines the sensitivity to platinum-based chemotherapy and PARP inhibitors, which is based on the concept of synthetic lethality (Von Minckwitz, 2014). In addition, a growing body of evidence suggests that PARP inhibitors might also be used in the treatment of those cancer patients without germline mutation of BRCA1 or BRCA2 mutation but that still have deficiency in HR, a phenomenon has been termed BRCAness (Dedes et al., 2011). BRCAness can be defined as the alteration genes involved in DNA repair pathways, presenting a phenotype, which can mimic mutations of germline BRCA1/2 gene, thus lead to DNA repair, particularly HR, deficiency (Lord and Ashworth, 2016).

Tumours with BRCAness drivers such as deficiency of RAD51, ATR, ATM, CHK1/2, can also be sensitive to PARP inhibition (McCabe et al., 2006). The concept of BRCAness expands the application of PARP inhibition and highlights the importance of investigating other targets in DDR based on the concept of synthetic lethality. For example, ATR inhibitors is effective in ATM-deficient prostate cancer (Rafiei et al., 2020), in human lung and colorectal cancer cells, the silenced of the B-family of DNA polymerases was found sensitized CHK1 inhibition (Rogers et al., 2020). Therefore, numerous DDR kinase inhibitors have been discovered by targeting key regulators involved in DDR pathways including but not limited to ATR, ATM, DNA-PK, CHK1, CHK2 and WEE1 (Gourley et al., 2019). Moreover, exploiting the concept of synthetic lethality, specifically targeting DSBs repair pathways, has become one of the most effective approaches for radioresistance. As discussed in Chapter 1, various DNA damage induced by radiation triggers a series of cellular DNA damage responses, including the activation of DNA damage sensing, mediation of DNA damage repair pathways and cell cycle arrest, and help cells recover from radiation injuries (Huang and Zhou, 2020). The DNA base damage and SSBs are mainly repaired by BER pathway, and DSBs is mainly repaired by HR, and NHEJ pathways. Cell cycle checkpoints are also activated in response to DNA damage during these processes. ATM, ATR and DNA-PKcs play viral role in DDR pathways. Key regulators in the DDR pathway are also crucial

targets for cancer therapy. While ATM is initially activated in respond to radiation-induced DNA DSBs, subsequently the activation of ATR contributes to the response of cell cycle checkpoint (Morgan and Lawrence, 2015). Apparently, these protective DDRs can cause tumour radioresistance. For example, the activation of ATM protein and its mediation of DNA repair pathways signalling and/or cell cycle responses are reported to induce radioresistance (Enns et al., 2015). In addition, Shimura et, al found that Cyclin D1-dependent DNA damage activated DNA-PK/AKT/GSK3β signalling which in turn increased Cyclin D1 expression. The overexpression of Cyclin D1 led to the activation of ATM/CHK1 signalling and HR pathways thus cause acquired radioresistance of human tumour cells(Shimura et al., 2010). Therefore, targeting DDR signalling pathways has become one of the attractive strategies for overcoming tumour radioresistance, summarised in Figure 5.1. As Chapter 1 discussed, there are several preclinical and clinical studies focus on the combination of DDR inhibitors and radiation to improve patience outcomes.

5.1.1. Hypothesis, aims, and objectives of this chapter

As Chapter 3 showed, depleting WSB-1 increased the expression of genes in DNA repair pathways, WSB-1 overexpression decreased BRCA1/2 expression and HR genes such as RAD51, in Chapter 4 we found that overexpressed WSB-1 increased DNA damage and modulated DNA repair and DDR signalling. Therefore, we hypothesise that WSB-1 could be a BRCAness biomarker. Therefore, overexpression of WSB-1 could increase the sensitivity to PARP inhibitors or other DDR inhibitor, as single agents and potentially in combination with radiation treatment.

The aims and objectives of this chapter is to evaluate the impact of WSB-1 respond to DDRi or the combination with radiotherapy, and the potential of WSB-1 as a BRCAness biomarker in breast cancer.

The specific aims of this chapter are to:
1: Evaluate the relationship between WSB-1 expression and DNA repair signatures in patient samples
2. Assess the impact of overexpressing WSB-1 on the response to DDRis as single agent or in combination with IR

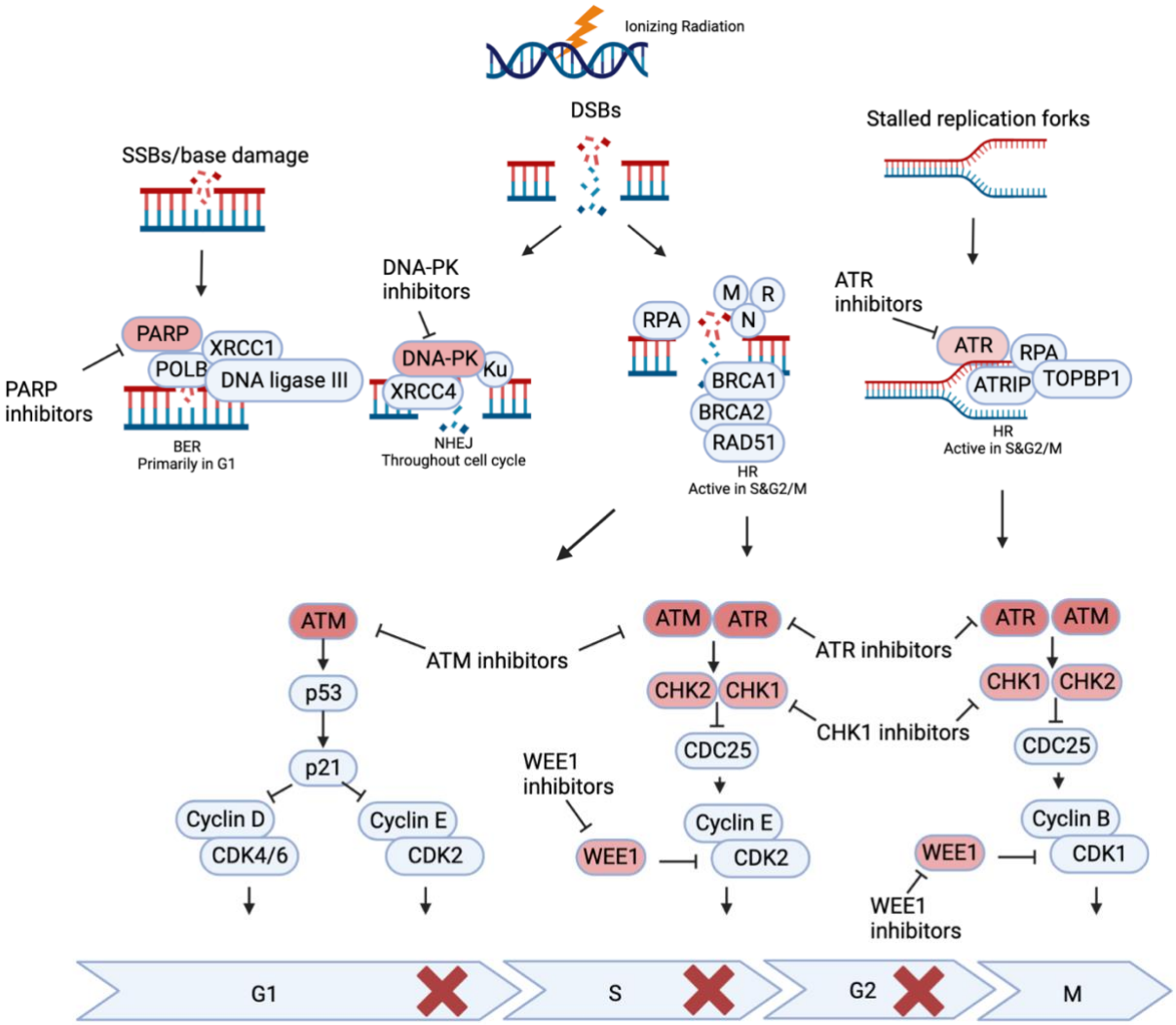

Figure 5. 1 Radiation induced DNA damage respond and clinically relevant DDR targets
Radiation induces SSB, DSB and stalled replication forks and triggers BER, NHEJ, and HR pathways, which activate ATM/ATR and their downstream and cause cell cycle arrest.
SSBs: single-strand DNA breaks; DSBs: double-strand DNA breaks; PARP: Poly (ADP-ribose) polymerase; MRN: MRE11, RAD50 and NBS1 complex; BER: base-excision repair; NHEJ: non-homologous end joining; HR: homologous recombination; ATRIP: ATR-interacting protein; POLB: DNA polymerase-β; RPA: replication protein A; TOPBP1: DNA topoisomerase 2-binding protein. (Created using Biorender.com)

5.2 Experimental design

5.2.1. Exploration of the clinical relevance of WSB-1 expression on patient samples

To evaluate the relationship between WSB-1 transcript levels with DNA repair pathway signatures on patient samples, RNA-sequencing datasets (RNA Seq V2 RSEM) for breast invasive carcinoma tumours were downloaded from the TCGA project accessed through cBioportal (http://www.cbioportal.org) to examine WSB1 expression against DNA repair signature and DNA repair pathways including HR, NHEJ, MMR, and BER. cBioPortal is an online tool provides multidimensional cancer genomics data which including molecular profiles and clinical patients data (Cerami et al., 2012). This approach has been used in our lab before to determine the relationship between WSB-1 expression and hypoxic signatures (Poujade et al., 2018).

For this, gene sets were initially downloaded from GSEA (https://www.gsea-msigdb.org/). These gene sets included DNA repair gene signature with systematic name M5898, HR pathway with systematic name M27570, BER pathway with systematic name M2158, MMR pathway with systematic name M27442, NHEJ pathway with systematic name M27587. Raw gene expression datasets for each sequenced gene were downloaded using datasets Breast Cancer METABRIC dataset (Curtis et al., 2012) (n = 2509) from cBioportal. The median expression of *WSB1* were determined. Expression values for DNA repair genes were also calculated by quantifying the median expression of different gene sets from GSEA respectively. Log10 transformed values of the median DNA repair genes expression values were plotted against Log10 conversion of the median expression of *WSB1* genes by R studio (R studio, USA). A two-tailed test, non-parametric Spearman's correlation coefficient, non-parametric Pearson 's correlation coefficient were carried out in was calculated with p-value <0.05 considered significant.

5.2.2 Evaluation of the effects of WSB-1 overexpression on cell viability and respond to DDR inhibitors *in vitro* (short term viability)

In order to evaluate the effect of WSB-1 overexpressed using different DDRi including PARPi (Olaparib); ATMi (KU-559933) and ATRi (VE-822) in cell viability *in vitro*, the short-term viability assay MTS viability assay was used alongside with WSB-1 overexpression in 4 different cell lines MCF7, BT474, MDA-MB-231 and MDA-MB-468 under hypoxia. The use of Olaparib and KU-559933 with concentration follows the dilution

ratios of 1:3 range from 300nM to 1.2nM. The use of VE-822 with concentration follows the dilution ratios of 1:3 range from 100nM to 0.4nM.

5.2.3 Evaluation of the effects of WSB-1 overexpression on cell viability and respond to DDR inhibitors and radiation treatment *in vitro* (long term viability)

To evaluate the effect of the combination of DDR inhibitor with radiation treatments when WSB-1 was ovexpressed, the long-term viability assay clonogenic survival assays were used.

5.2.3.1 Test of the efficiency of hypoxic boxes to sustain hypoxia conditions during irradiation

Firstly, to make sure the plates are remained kept in hypoxic condition, 6 carrying boxes were used to carry the plates to the radiator in order to be irradiated in hypoxic conditions, as described before (Pires et al., 2012, Anbalagan et al., 2012). Validation of their ability to retain hypoxic conditions was tested as follows. For all samples MCF7 cells were seeded in 25cm dishes overnight. Then the following samples were prepared for protein extraction for HIF1α western blotting (Figure 5.2):

1. Normoxic control sample: remained in incubator at 20% O_2 until harvesting.
2. Hypoxic control sample: placed in the hypoxic chamber at 1% O_2 and harvested in the chamber after 4 hours.
3. Hypoxia boxes (box 1-6) test samples: placed in the hypoxic chamber at 1% O_2 for 3 hours, then placed in the hypoxia boxes (1-6) and sealed within the chamber and placed in normoxic conditions for 1 hour before harvesting.
4. Reox (reoxygenation) control sample: placed in the hypoxic chamber at 1% O_2 for 3 hour and reoxygenated outside boxes for 1 hour alongside test samples in boxes in normoxic conditions.

As all samples in boxes retained HIF1α expression, these boxes could be used for subsequent hypoxia irradiation experiments.

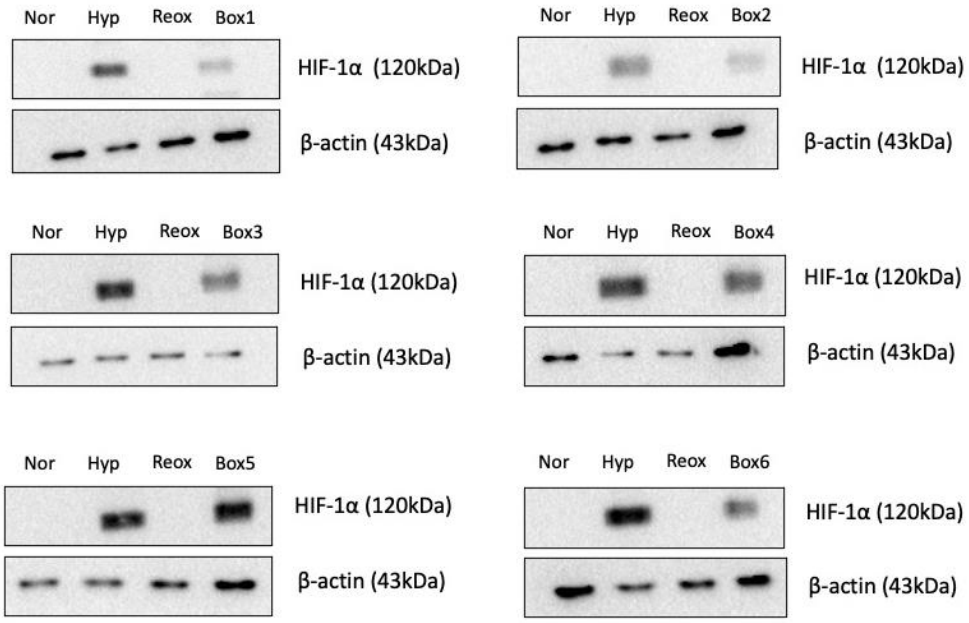

Figure 5. 2 The HIF-1a expression of 6 carrying boxes

Nor: MCF7 cells were placed in normoxia (20% O2) for 4h; Hyp: MCF7 cells were placed in hypoxia (1% O_2) for 4h; Reox, MCF7 cells were brought out in normoxia to re oxygen for 1h; Box1-6: MCF7 cells were placed in hypoxia for 4h and brought out in normoxia to re oxygen for 1h alongside with Reox. Cells were lysed and HIF1α protein expression was analysed by Western blotting.

5.2.3.2 Optimization of cell seeding densities with WSB-1 overexpressed response to RT in vitro

MCF7 cell lines were seeded in 6 well plates. 6 well plates at seeding densities optimised for the clonogenic assay (Table 5.1). Cells were treated with exposed to irradiation 2 Gy, 4 Gy and 6 Gy respectively 12 h post seeding. Non-irradiated (0 Gy) mock control plates were also transported to the irradiator but not exposed to irradiation. Plates were placed back in the cell culture incubator and incubated for a further 14 days undisturbed.

Table 5. 1 Optimised seeding densities for the clonogenic assay with WSB-1 overexpression and IR treatments

Irradiation	0 Gy	2 Gy	4 Gy	6 Gy
MCF7(mock)	200 cells/well	1000 cells/well	8000 cells/well	10000 cells/well
MCF7(WSB-1)	200 cells/well	2000 cells/well	10000 cells/well	20000 cells/well

5.2.3.3 Optimization of PARP1i, ATMi, and ATRi concentration in combination with IR

MCF7 cell lines were seeded in 6 well plates at seeding densities from Table 5.1. Cells were treated with different ranges of DDRi concentrations after 8h of seeding. Cells were exposed to irradiation 2 Gy, 4 Gy and 6 Gy respectively 4 h post drug treatments/12 h post seeding. Non-irradiated (0 Gy) mock control plates were also transported to the irradiator but not exposed to irradiation. Plates were placed back in the cell cultural incubator and incubated for 14days. Optimised DDRi concentrations are as below: 80 nM PARPi (Olaparib); 800 nM ATMi (KU-559933); 10 nM ATRi (VE-822).

5.2.4 Evaluation of the effects of overexpressed WSB-1 on cell viability respond to DDR inhibitors and radiation treatment *in vitro*

MCF7 cell lines were transfected with either mock control (mock) or WSB-1 plasmid (WSB1). After 24 h post transfection, cells were re seeded in 6 well plates. Cells were treated with 80 nM PARPi (Olaparib) /800 nM ATMi (KU-559933) /10 nM ATRi (VE-822) after 8 h post seeding then exposed to irradiation with 2 Gy, 4 Gy and 6 Gy respectively 4h post drug treatments/12 h post seeding. Non-irradiated (0 Gy) mock control dishes were also transported to the irradiator but not exposed to irradiation. Plates were placed back in the cell cultural incubator and incubated for 14 days. Optimised seeding densities for the clonogenic

assay are shown in Table 5.2. Cells seeding, transfection, re seeding, DDRi treatments, irradiation and staining schedule is shown in Figure 5.3.

Table 5. 2 Optimised seeding densities for the clonogenic assay with DDRi with IR treatments in MCF7

Irradiation	0Gy	2Gy	4Gy	6Gy
MCF7(mock)	200 cells/well	4000 cells/well	10000 cells/well	20000 cells/well
MCF7(WSB-1)	200 cells/well	8000 cells/well	20000 cells/well	40000 cells/well

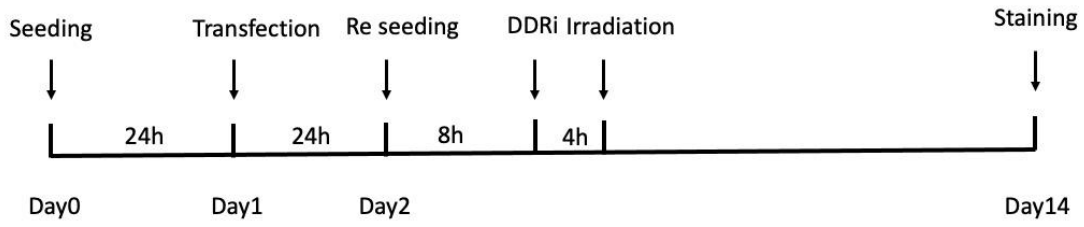

Figure 5. 3 Timelines for transfection, DDRi treatment and irradiation for the clonogenic assay

MCF7 cells were seeded overnight and transfected for 24h, then cells were re seeded and treated with 80nM PARPi (Olaparib) /800nM ATMi (KU-559933) /10nM ATRi (VE-822) after 8h post seeding then exposed to irradiation with 2 Gy, 4Gy and 6Gy respectively 4h post drug treatments/12h post seeding. Cells were stained in Day 14 by crystal violet.

5.3 Results

5.3.1 *WSB1* expression is negatively associated with DNA repair gene expression signature in breast cancer patient datasets

Breast cancer patient gene expression data (n=2509) were used to investigate whether the observed relationship between WSB-1 and the DDR in cell line models (Chapters 3 and 4), specifically with DNA repair factors, is reflected in patients. Specifically, *WSB1* expression was compared with that of DNA repair signatures.

As Figure 5.4 shows, *WSB1* expression is significantly ($p<0.0001$) negatively correlated with the expression of generic DNA repair gene expression signature (Hallmark DNA repair) (Liberzon et al., 2015) with Spearman r = -0.3847, Pearson r = -0.3723. Moreover, *WSB1* expression is also significantly negatively correlated in these samples with the expression of genes involved in individual DNA repair pathways. For example, *WSB1* expression is significantly ($p<0.0001$) negatively correlated with the median expression of HR pathway genes with Spearman r = -0.2798, Pearson r = -0.2559 (Figure 5.5), which indicates high *WSB1* expression could be associated with HR pathway deficiency/downregulation. *WSB1* expression also was negatively correlated with the median expression of genes involved in BER pathway with Spearman r = -0.3122, Pearson r = -0.2841, ($p<0.001$) and MMR pathway with Spearman r = -0.2084, Pearson r = -0.1728, ($p<0.0001$) (Figure 5.5-5.7). In Figure 5.8, although *WSB1* expression is negatively correlated with the expression of genes in NHEJ pathway ($p<0.05$), this correlation is very weak, according to the Spearman r = -0.09452 and Pearson r = -0.1111.

Taken together, these results indicate that *WSB1* expression in patients is indeed inversely correlated with DNA repair gene expression signatures in breast cancer patient datasets, including HR, indicating that high WSB1 expression could indeed represent a potential BRCAness-like biomarker.

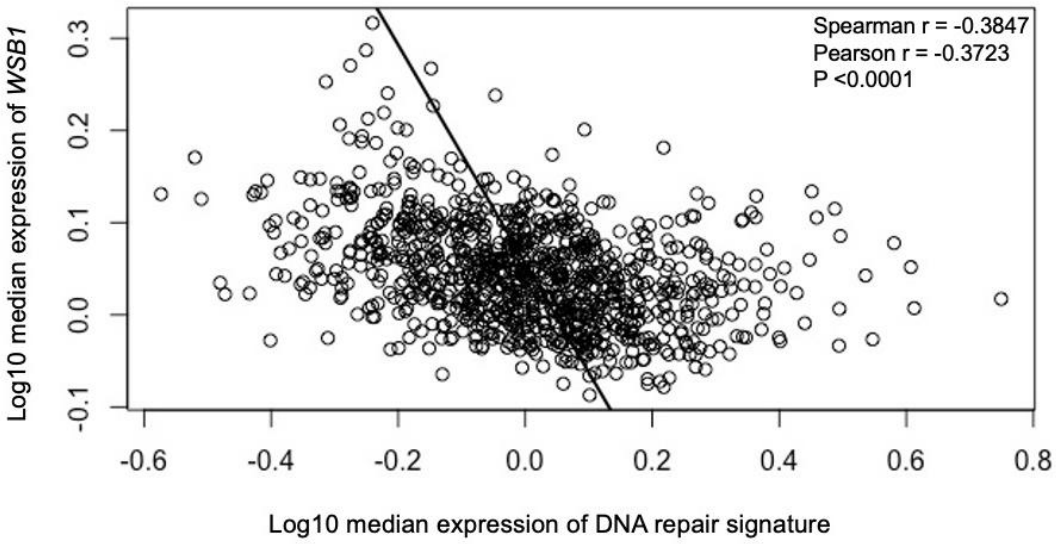

Figure 5. 4 The correlation of WSB1 and DNA repair signature
WSB1 expression is negatively correlated with DNA repair signatures (M5898) in breast invasive carcinoma patient samples (TCGA datasets). Log10 conversions of *WSB1* median expression against log 10 conversion median expression of DNA repair signatures (M5898) from GSEA, Spearman's and Pearson's rho rank correlation coefficients, and two-tailed p values were inset, n = 2509

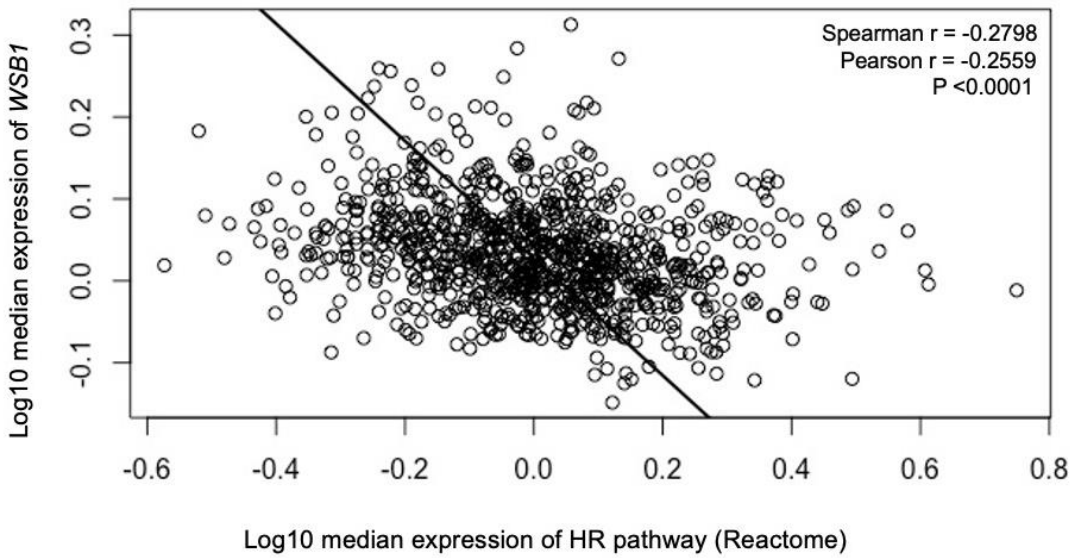

Figure 5. 5 The correlation of WSB1 and HR pathway (M27570)
WSB1 expression is negatively correlated with HR repair pathway (M27570) in breast invasive carcinoma patient samples (TCGA datasets). Log10 conversions of *WSB1* median expression against log 10 conversion median expression of HR repair pathway (M27570) from GSEA, Spearman's and Pearson's rho rank correlation coefficients, and two-tailed p values were inset, n = 2509

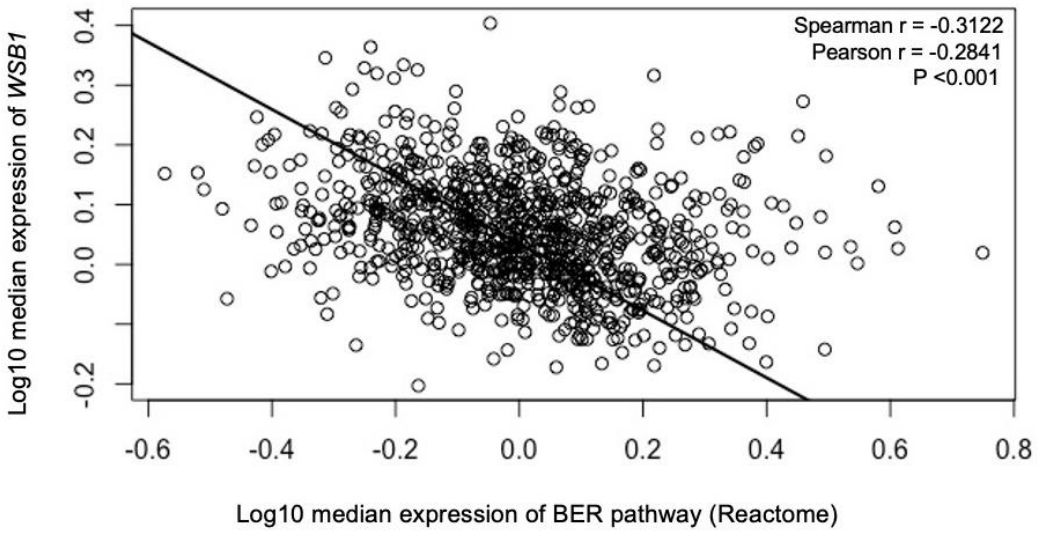

Figure 5. 6 The correlation of WSB1 and BER pathway (M2158)
WSB1 expression is negatively correlated with BER pathway (M2158) in breast invasive carcinoma patient samples (TCGA datasets). Log10 conversions of *WSB1* median expression against log 10 conversion median expression of BER pathway (M2158) from GSEA, Spearman's and Pearson's rho rank correlation coefficients, and two-tailed p values were inset, n = 2509

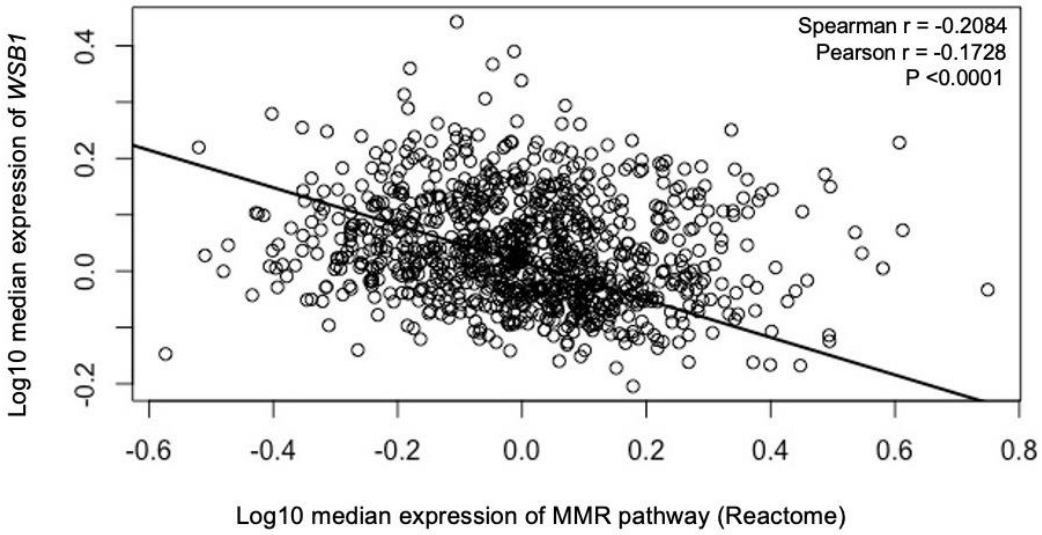

Figure 5. 7 The correlation of WSB1 and MMR pathway (M27442)
WSB1 expression is negatively correlated with MMR pathway (M27442) in breast invasive carcinoma patient samples (TCGA datasets). Log10 conversions of *WSB1* median expression against log 10 conversion median expression of MMR pathway (M27442) from GSEA, Spearman's and Pearson's rho rank correlation coefficients, and two-tailed p values were inset, n = 2509

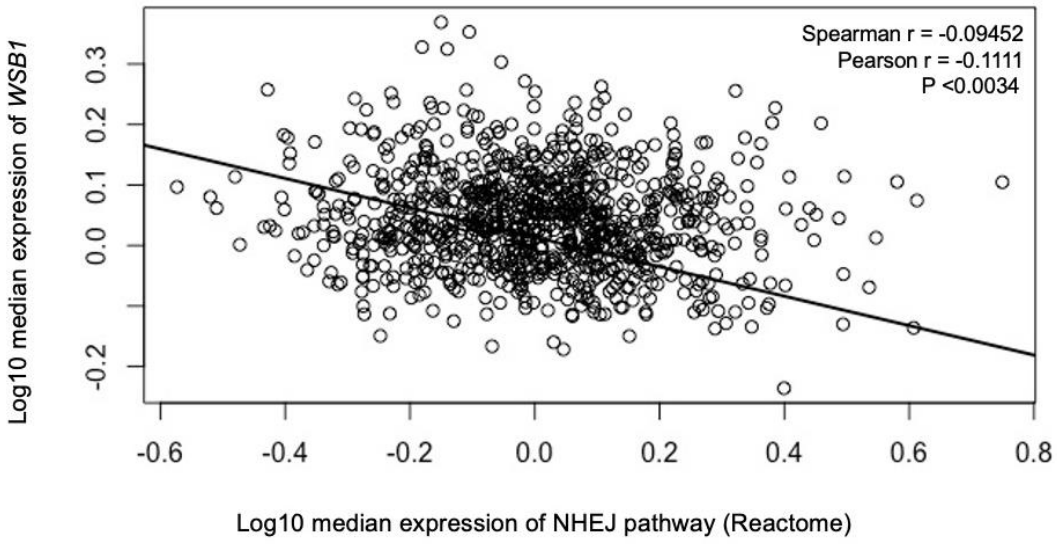

Figure 5. 8 The correlation of WSB1 and NHEJ pathway (M27587)
WSB1 expression is negatively correlated with NHEJ pathway (M27587) in breast invasive carcinoma patient samples (TCGA datasets). Log10 conversions of *WSB1* median expression against log 10 conversion median expression of NHEJ pathway (M27587) from GSEA, Spearman's and Pearson's rho rank correlation coefficients, and two-tailed p values were inset, n = 2509

5.3.2 WSB-1 overexpression might increase sensitivity of DDR inhibitors (DDRi) under hypoxia in breast cancer cells

As previously noted, BRCA1/2 deficient breast cancer was associated with sensitivity to PARP1 inhibitors, with genes alterations that mirror BRCA1/2 mutation and cause DNA repair deficiency could also lead to sensitivity to PARP1 inhibitors, a concept named BRCAness. Therefore, we hypothesised that, as WSB-1 overexpression led to repression of several DDR factors including HR factors and is linked with decreased DNA repair capacity *in vitro* (Chapter 3 and 4) and that high *WSB1* expression is negatively correlated with DNA repair signatures (section 5.3.2), WSB-1 overexpression would sensitise to treatment with PARPi.

In order to test this, initially four breast cancer cell lines, two luminal A/B cell lines (MCF-7 and BT474) and two TNBC cell lines (MDA-MB-231 and MDA-MB-468) were transfected with Flag-tagged WSB-1 as well as mock transfected as a negative control, as previously described. After 24 hours, cells were exposed to 20% O_2 (normoxia) or 1% O_2 (hypoxia) and treated with a range of concentrations of Olaparib (PARPi), KU-55933 (ATMi), or VE-822 (ATRi), for 72 hours, after which short term relative cell viability/proliferation was determined using the MTS assay.

Figures 5.9 and 5.10 showed in that all cell lines, overexpressing WSB-1 increased the sensitivity to higher doses of Olaparib in hypoxic conditions, with the biggest effect observed for BT474 cells, with about 40% decrease in cell viability vehicle vs Olaparib highest dose. However, there was variability of this effect between cell lines, with a maximum decrease in viability of approximately 40% for BT474, 10% for MCF7 and MDA-MB-468, and approximately 20% for MDA-MB-231 cells.

It is important to note that effect was not as pronounced as it would be predicted for BRCA1/2 deficiency effect, where a dramatic effect was previously reported with several log kill sensitisation observed (Bryant et al., 2005). This will be discussed later in this chapter.

We also investigated the impact of WSB-1 overexpression on sensitivity to other DDRis, such as ATRi and ATMi, as we have shown that a DNA damage response is likely to be activated in WSB-1 overexpressing *in vitro* models (Chapter 4).

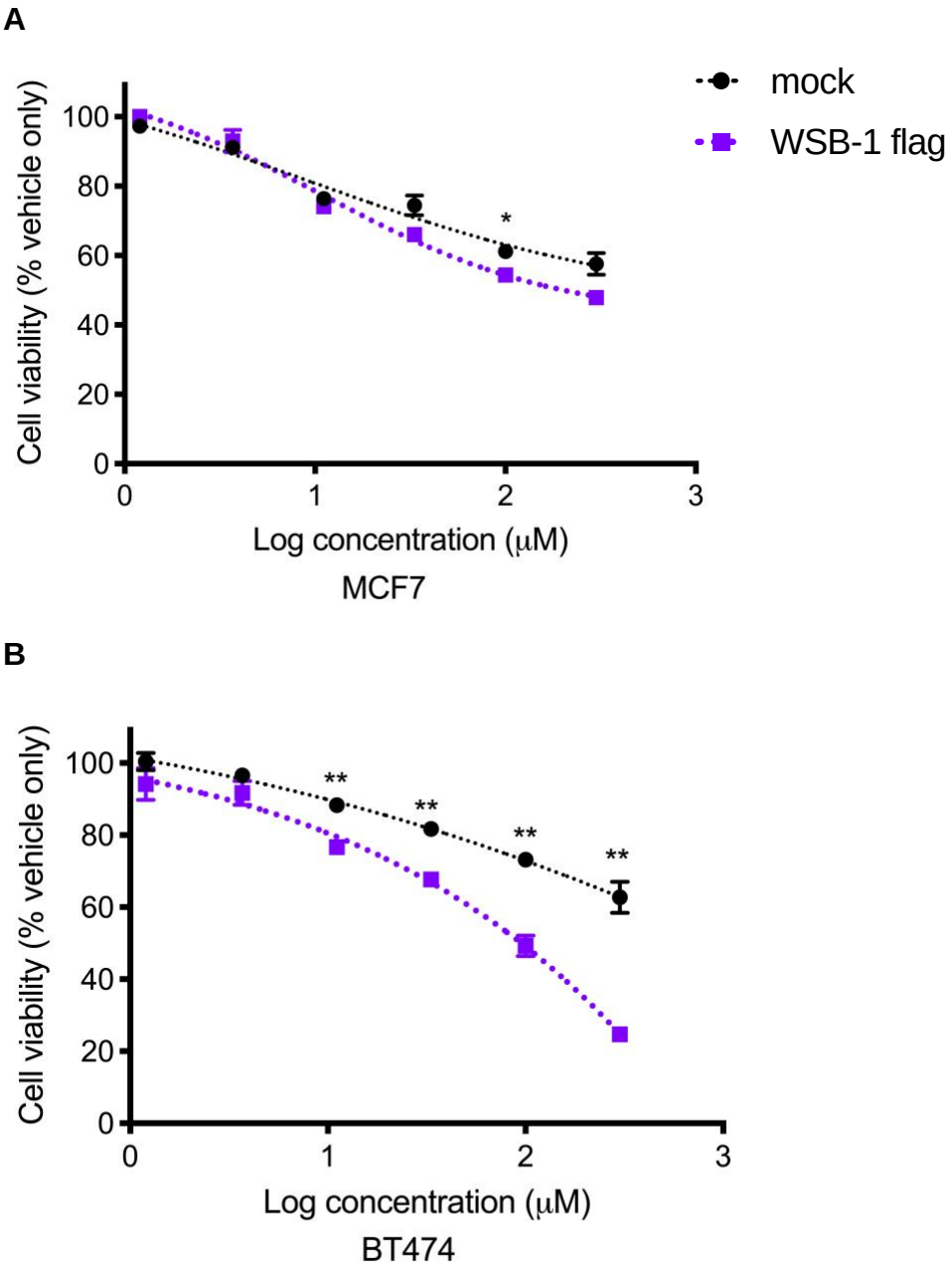

Figure 5. 9 Overexpressed WSB-1 increased the sensitivity to PARPi in MCF7 and BT474 under hypoxia

$2x10^5$ MCF7 (A) and BT474 (B) cells were either mock transfected (mock) or transfected with a Flag-tagged WSB-1 (WSB-1 flag), exposed 24 h to 1% O_2, and treated with a range of concentrations of Olaparib PARPi for 72 h, after which MTS assay was used to determine the relative cell viability and cell viability is noted as relative to vehicle control (DMSO), and plots note n=3 independent experiments. * $p<0.05$; ** $p<0.01$; *** $p<0.001$; **** $p<0.0001$ (student t-test for each PARPi concentration, Error bars represent mean ± SEM).

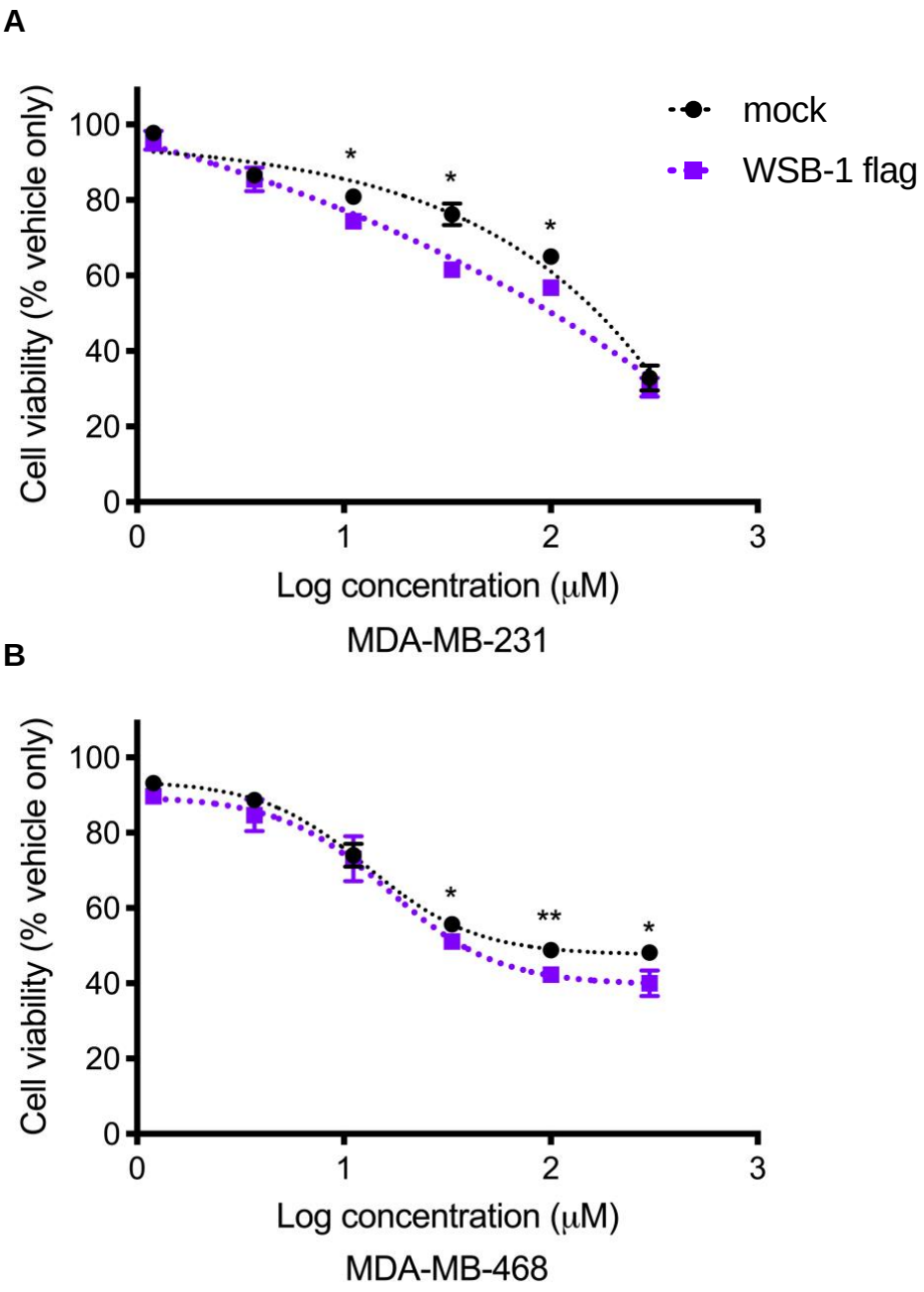

Figure 5. 10 Overexpressed WSB-1 potentially sensitized PARPi in MDA-MB-231 and MDA-MB-468 under hypoxia

$2x10^5$ MDA-MB-231 (A) and MDA-MB-468 (B) cells were either mock transfected (mock) or transfected with a Flag-tagged WSB-1 (WSB-1 flag), exposed 24 h to 1% O_2, and treated with a range of concentrations of Olaparib PARPi for 72 h, after which MTS assay was used to determine the relative cell viability and cell viability is noted as relative to vehicle control (DMSO), and plots note n=3 independent experiments. * $p<0.05$; ** $p<0.01$; *** $p<0.001$; **** $p<0.0001$ (student t-test for each PARPi concentration, Error bars represent mean ± SEM).

Figures 5.11 and 5.12 show that overexpressing WSB-1 also increased the sensitivity to ATM inhibitors (KU-55933) in hypoxic conditions for some of the cell lines, with a maximum decrease in cell viability of approximately 20% and 15% for MCF7 and MDA-MB-231 cells, respectively. However, no clear sensitising effect was observed for WSB-1 overexpression for BT474 and MDA-MB-468.

A similar trend was observed for ATR inhibitor (VE-822) treatment (Figures 5.13 – 5.14), with WSB-1 overexpression leading to increase sensitisation to VE-822 for most cell lines. Specifically, a maximum decrease in cell viability of approximately 30% was observed for MCF7 and MDA-MB-468 cells, and about 15% for MDA-MB-231 cells.

Therefore, these results showed that overall, cells with increased WSB-1 levels could be more sensitive to DDRi, including PARP inhibitors (Olaparib), ATM inhibitors (KU-55933) and ATR inhibitors (VE-822) under hypoxia, but that sensitisation is variable depending on the cell line background.

5.3.3 High WSB-1 expression is associated with increased sensitivity to the combination of PARP/ATM/ATR inhibitors and/or IR

As the MTS assay used in the previous section was a short-term assay, long-term assay clonogenic survival assays were used in this Section to assess the longer-term impact of WSB-1 overexpression on response to DDRi treatment, either as a single agent or in combination with radiation. DDRi compounds again included PARP1i (Olaparib), ATMi (KU-55933) and ATRi (VE-822) were used to treat either mock control (mock) transfected, or flag tagged WSB-1 (WSB-1) transfected MCF7 cells with or without IR treatments with different X-ray doses includes 2 Gy, 4 Gy and 6 Gy.

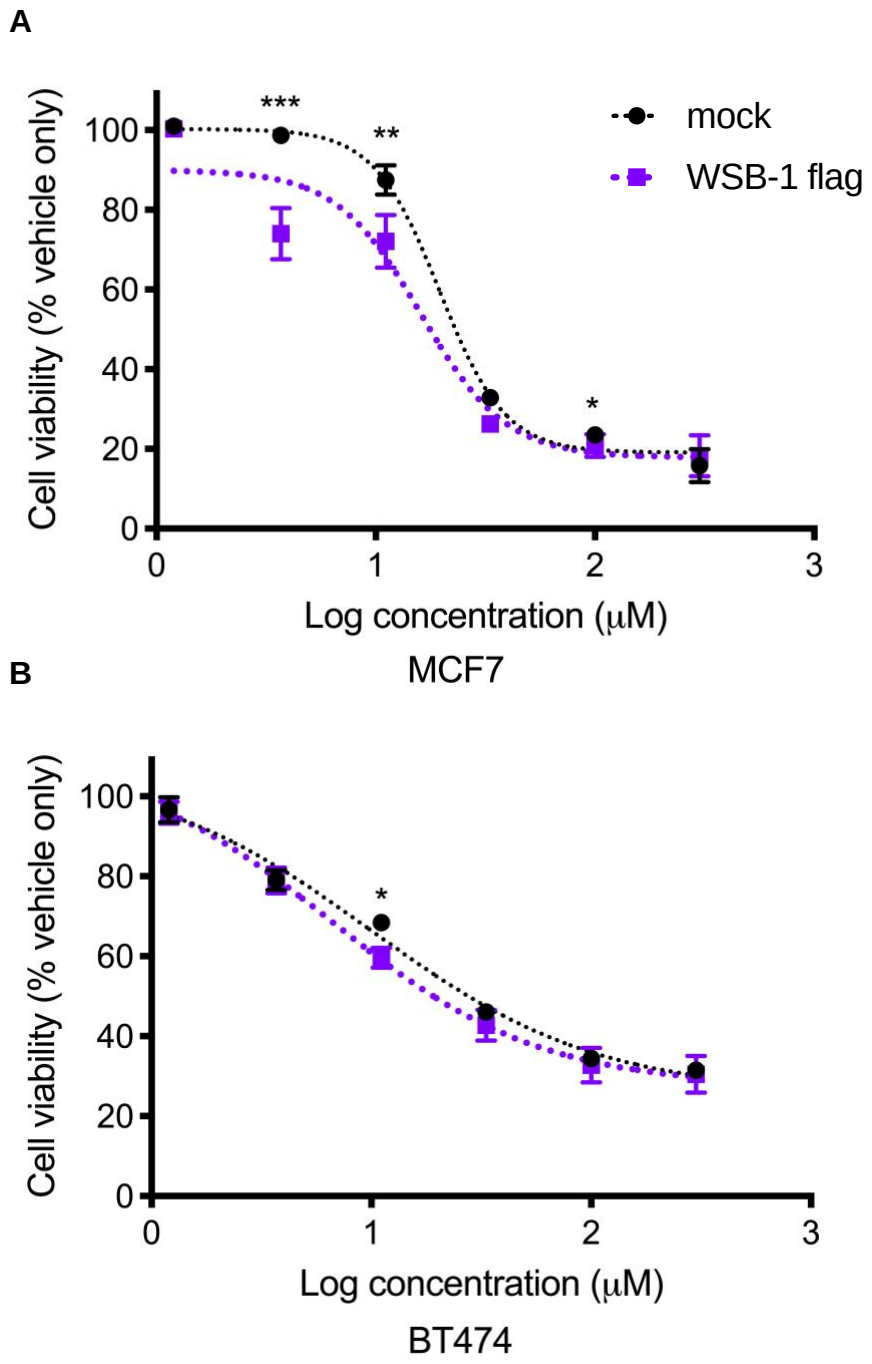

Figure 5. 11 Overexpressed WSB-1 potentially sensitized ATMi in MCF7 and BT474 under hypoxia

$2x10^5$ MCF7 (A) and BT474 (B) cells were either mock transfected (mock) or transfected with a Flag-tagged WSB-1 (WSB-1 flag), exposed 24 h to 1% O_2, and treated with a range of concentrations of KU-55933 ATMi for 72 h, after which MTS assay was used to determine the relative cell viability and cell viability is noted as relative to vehicle control (DMSO), and plots note n=3 independent experiments. * $p<0.05$; ** $p<0.01$; *** $p<0.001$; **** $p<0.0001$ (student t-test for each ATMi concentration, Error bars represent mean ± SEM).

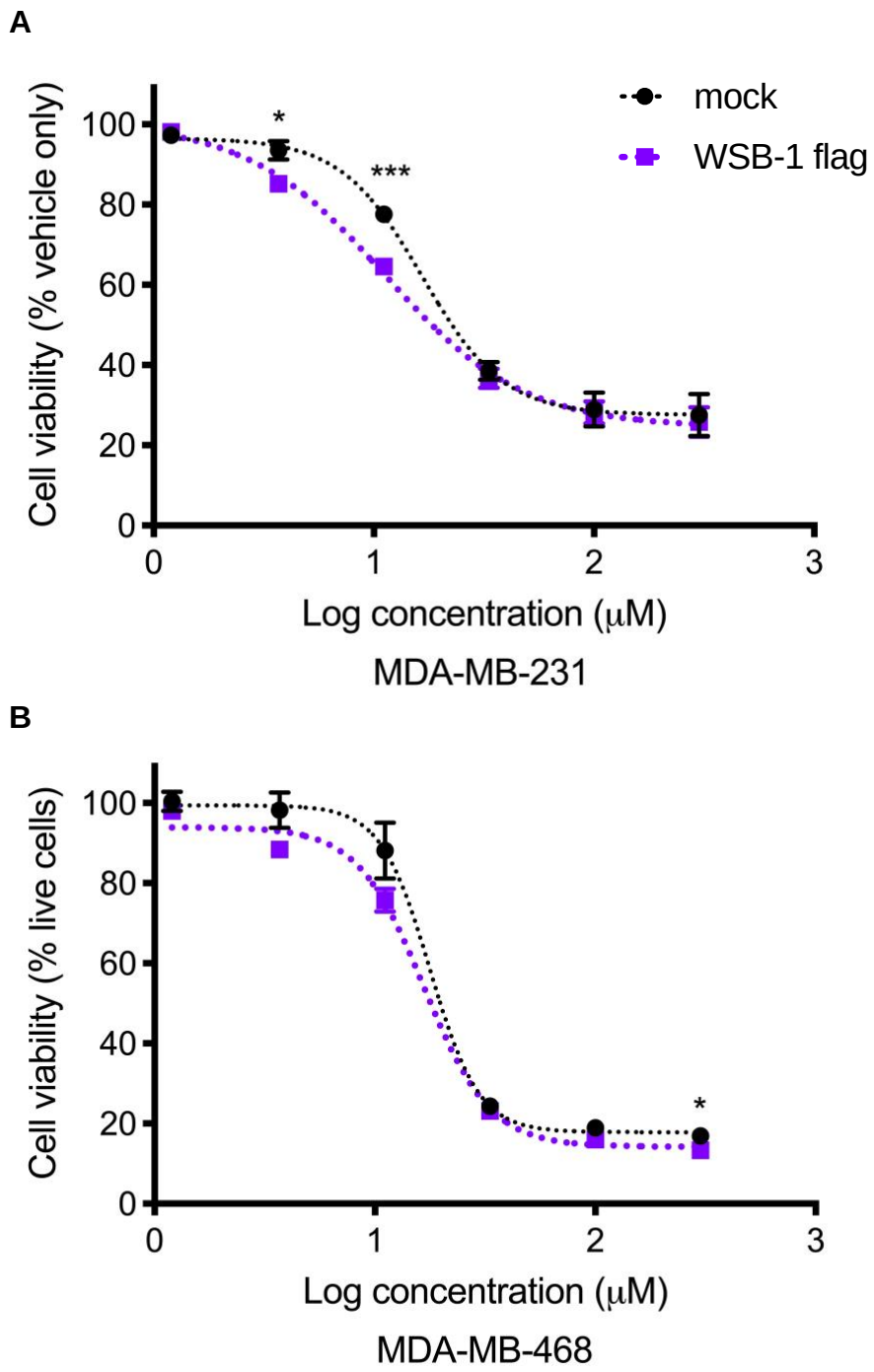

Figure 5. 12 Overexpressed WSB-1 potentially sensitized ATMi in MDA-MB-231 and MDA-MB-468 under hypoxia

$2x10^5$ MDA-MB-231 (A) and MDA-MB-468 (B) cells were either mock transfected (mock) or transfected with a Flag-tagged WSB-1 (WSB-1 flag), exposed 24 h to 1% O_2, and treated with a range of concentrations of KU-55933 ATMi for 72 h, after which MTS assay was used to determine the relative cell viability and cell viability is noted as relative to vehicle control (DMSO), and plots note n=3 independent experiments. * $p<0.05$; ** $p<0.01$; *** $p<0.001$; **** $p<0.0001$ (student t-test for each ATMi concentration, Error bars represent mean ± SEM).

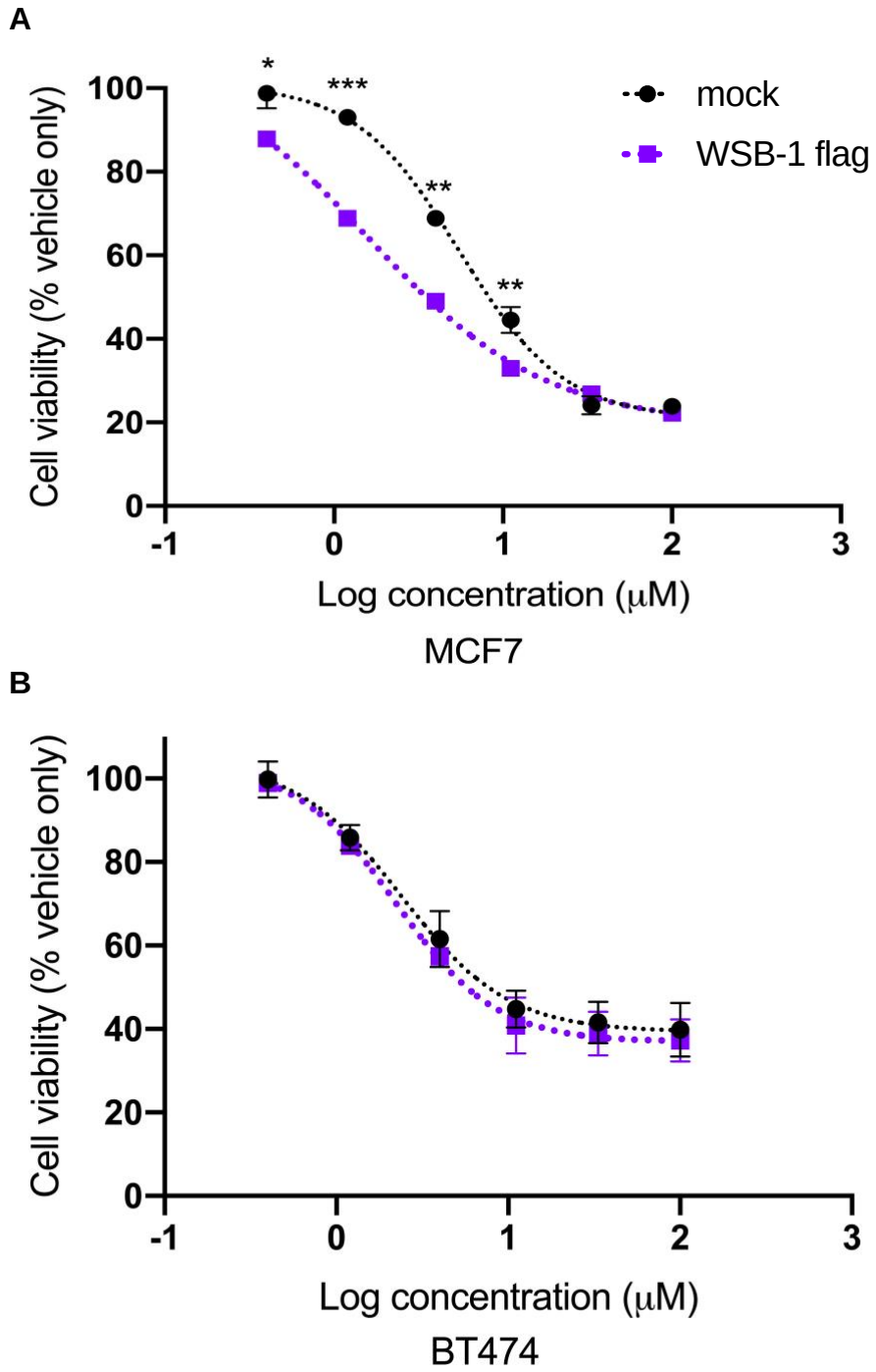

Figure 5. 13 Overexpressed WSB-1 potentially sensitized ATRi in MCF7 and BT474 under hypoxia

$2x10^5$ MCF7 (A) and BT474 (B) cells were either mock transfected (mock) or transfected with a Flag-tagged WSB-1 (WSB-1 flag), exposed 24 h to 1% O_2, and treated with a range of concentrations of VE-822 ATRi for 72 h, after which MTS assay was used to determine the relative cell viability and cell viability is noted as relative to vehicle control (DMSO), and plots note n=3 independent experiments. * $p<0.05$; ** $p<0.01$; *** $p<0.001$; **** $p<0.0001$ (student t-test for each ATRi concentration, Error bars represent mean ± SEM).

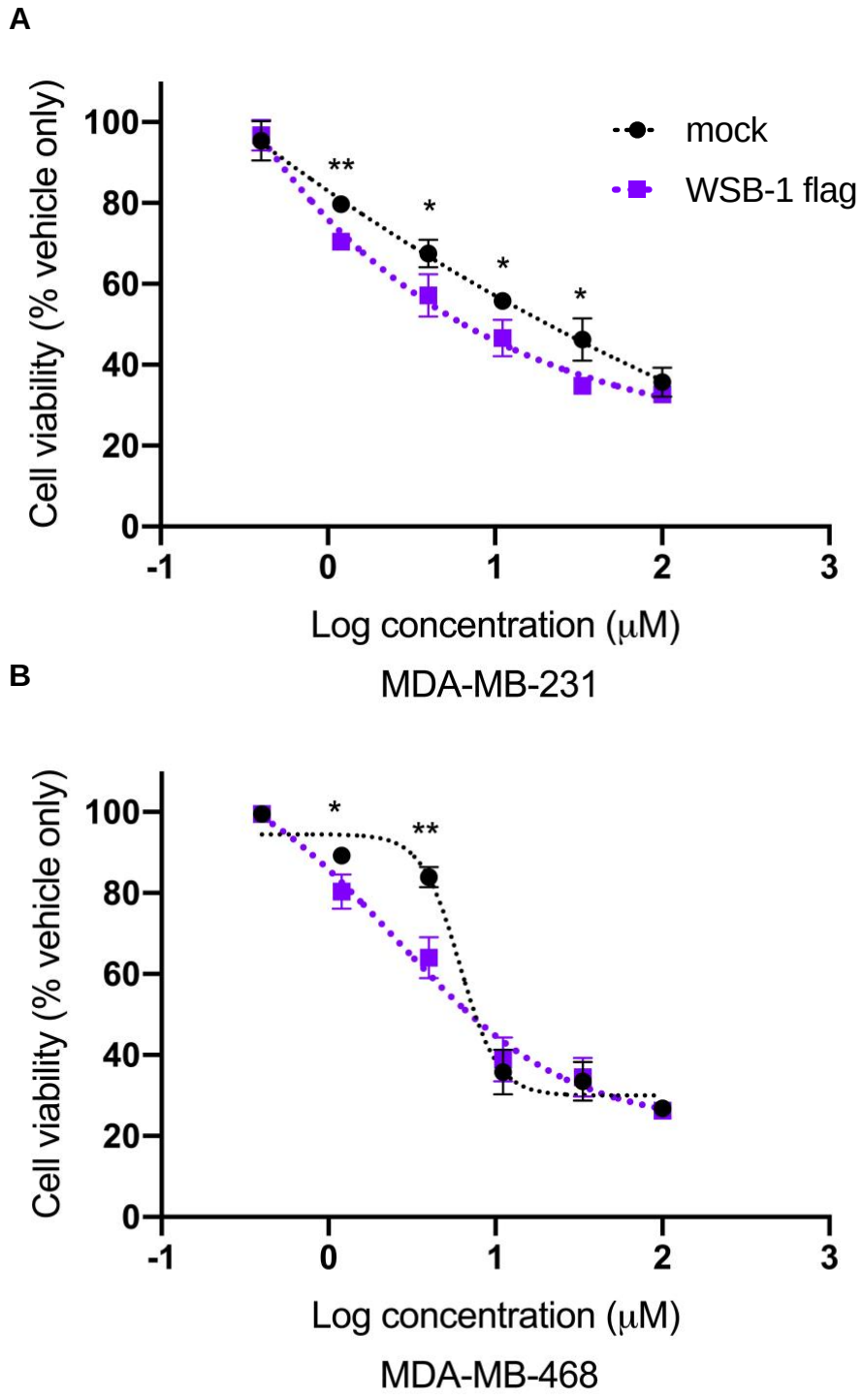

Figure 5. 14 Overexpressed WSB-1 potentially sensitized ATRi in MDA-MB-231 and MDA-MB-468 under hypoxia

$2x10^5$ MDA-MB-231 (A) and MDA-MB-468 (B) cells were either mock transfected (mock) or transfected with a Flag-tagged WSB-1 (WSB-1 flag), exposed 24 h to 1% O_2, and treated with a range of concentrations of VE-822 ATRi for 72 h, after which MTS assay was used to determine the relative cell viability and cell viability is noted as relative to vehicle control (DMSO), and plots note n=3 independent experiments. * $p<0.05$; ** $p<0.01$; *** $p<0.001$; **** $p<0.0001$ (student t-test for each ATRi concentration, Error bars represent mean ± SEM).

As can be seen in Figures 5.15 and 5.16, the survival curves indicate that WSB-1 overexpression sensitised PARPi combined with IR in 2 Gy ($p<0.001$) under normoxia (Figures 5.15 A). A similar trend can be observed under hypoxic conditions; however, it is not statistically significant (Figures 5.16 A). The survival fraction was significancy decreased at lower IR doses (2 Gy) by WSB-1 overexpression alone in normoxic conditions ($p<0.0001$), with a reduced clonogenic survival from 18.1% to 11.24% compared to mock control. When comparing the impact of Olaparib treatment for WSB-1 overexpressing cells, this was significant at 2 Gy ($p<0.0001$) with a reduced clonogenic survival from 15.6% to 6.6% compared to mock control at 2 Gy in normoxia ($p<0.0001$). WSB-1 overexpressing cells Olaparib treatment reduced clonogenic survival from 11.0% to 5.8% compared to WSB-1 overexpressing cells without treatments at 2 Gy in normoxia ($p<0.001$).There are trends that WSB-1 overexpression reduced clonogenic survival in 4 Gy and 6 Gy even but not statistically significant (Figures 5.15 B). In addition, higher doses (4Gy) combined with Olaparib is sensitized than 2Gy with Olaparib($p<0.001$) under normoxia. Under hypoxia, PARPi mock vs PARPi WSB1 has the survival fraction significantly decreased from with 19.5% to 6.3% ($p<0.01$) in 2 Gy. There are trends that WSB-1 overexpression reduced clonogenic survival in 4 Gy and 6 Gy even with statistic not significant (Figures 5.16 B).

For ATM inhibition, as can be seen in Figures 5.17 A, the survival curves indicate that WSB-1 overexpression sensitised ATMi (KU-55933) combined with IR in 2 Gy ($p<0.01$) under normoxia. There are trends shown under hypoxic condition in different doses. However, it is not significant (Figures 5.18 A). As the histograms Figures show, WSB-1 overexpression sensitised 2 Gy IR treatment under normoxia (Figure 5.17 B) and hypoxia (Figure 5.18 B). after IR treatment at 2 Gy, WSB-1 overexpression significantly reduced clonogenic survival from 35.14% to 27.3% compared to mock control at normoxia ($p<0.001$), and reduced clonogenic survival from 15.9% to 14% under hypoxia ($p<0.05$). When combining KU-55933 with IR, although WSB-1 overexpression also reduced clonogenic survival in different degrees in normoxia and hypoxia, the differences were not statistic significant. However, when compared to KU-55933 treatments alone, WSB-1 overexpression significantly reduced clonogenic survival with the combination of KU-55933 with IR under normoxia ($p<0.0001$) and hypoxia ($p<0.0001$). Moreover, higher doses (4 Gy) combined with KU-55933 was sensitized than 2 Gy with KU-55933 ($p<0.001$) under normoxia ($p<0.0001$) and hypoxia ($p<0.001$).

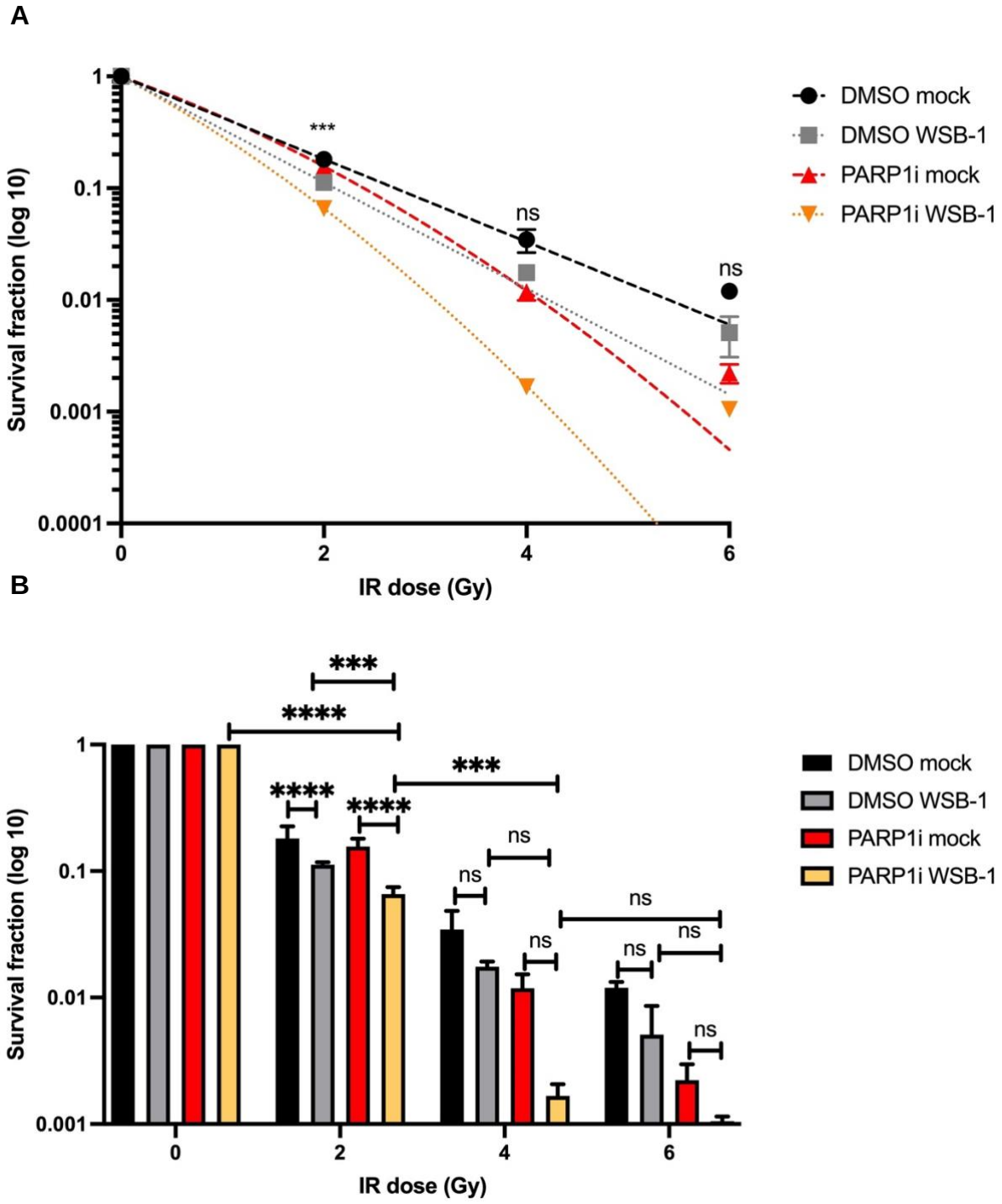

Figure 5. 15 WSB-1 overexpression sensitized PARPi after IR under normoxia

MCF7 were either mock transfected (mock) or transfected with a Flag-tagged WSB-1 (WSB-1) for 24h. Cells were kept in nomoxic condition (20% O_2). Cells were treated with PARP1i Olaparib (80nM) alongside with DMSO control then exposed to different IR doses (2Gy, 4Gy, 6Gy). Clonogenic survival was measured 10 days after IR; cells survival fraction (log 10) was showed in fitting curve (A) and histogram (B); n=3 independent biological repeats. * $p<0.05$; ** $p<0.01$; *** $p<0.001$; **** $p<0.0001$, ns: not significant, 2-Way ANOVA comparison to mock nonirradiated cells, Error bars represent mean ± SEM.

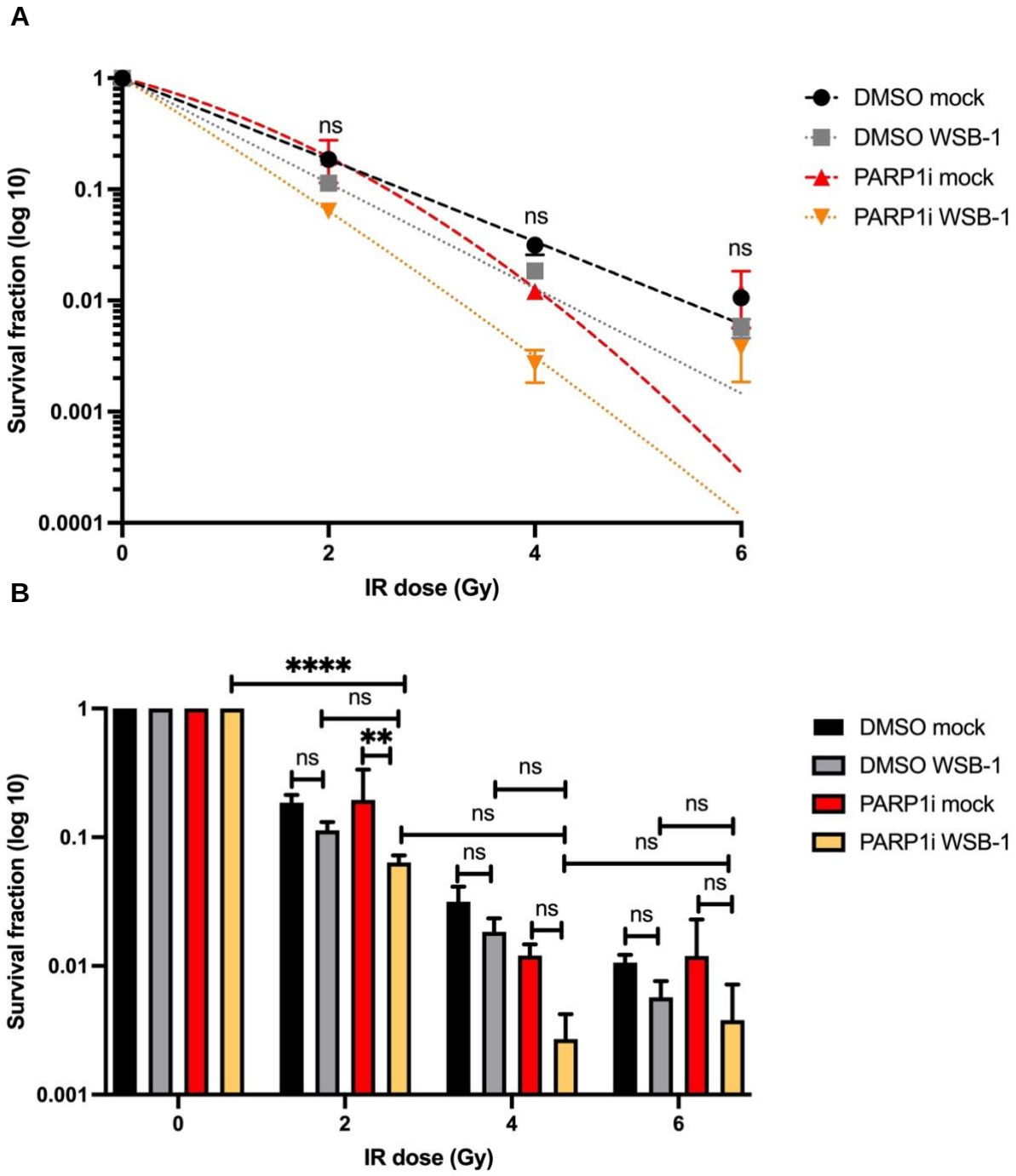

Figure 5. 16 WSB-1 overexpression sensitized PARPi after IR under hypoxia

MCF7 were either mock transfected (mock) or transfected with a Flag-tagged WSB-1 (WSB-1) for 24h. Cells were kept in hypoxic condition (1% O_2). Cells were treated with PARP1i Olaparib (80nM) alongside with DMSO control then exposed to different IR doses (2Gy, 4Gy, 6Gy). Clonogenic survival was measured 10 days after IR; cells survival fraction (log 10) was showed in fitting curve (A) and histogram (B); n=3 independent biological repeats. * $p<0.05$; ** $p<0.01$; *** $p<0.001$; **** $p<0.0001$, ns: not significant, 2-Way ANOVA comparison to mock nonirradiated cells, Error bars represent mean ± SEM.

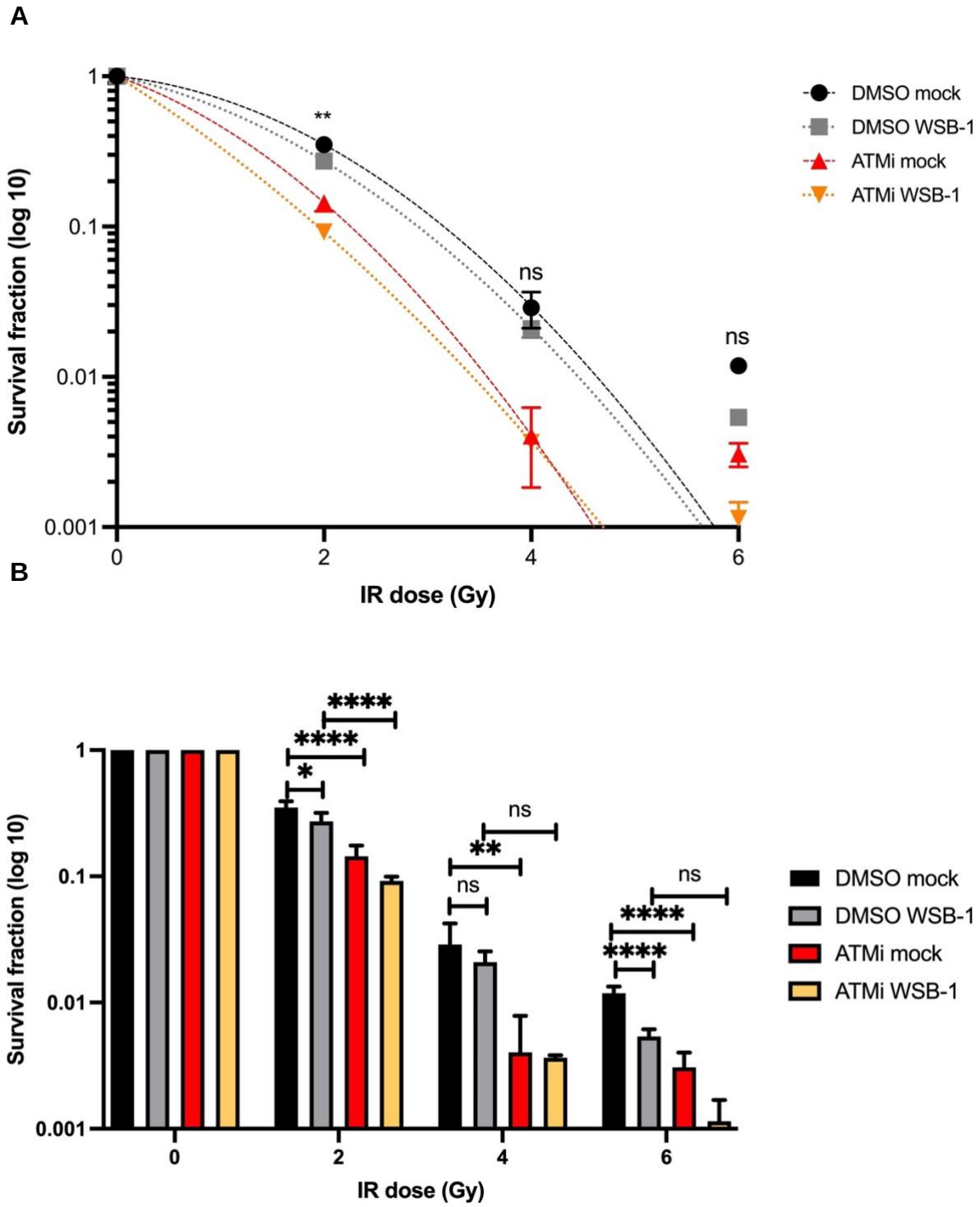

Figure 5. 17 WSB-1 overexpression sensitized ATMi after IR under normoxia

MCF7 were either mock transfected (mock) or transfected with a Flag-tagged WSB-1 (WSB-1) for 24h. Cells were kept in nomoxic condition (20% O_2). Cells were treated with ATMi KU-55933 (800nM) alongside with DMSO control then exposed to different IR doses (2Gy, 4Gy, 6Gy). Clonogenic survival was measured 10 days after IR; cells survival fraction (log 10) was showed in fitting curve (A) and histogram (B); n=3 independent biological repeats. * $p<0.05$; ** $p<0.01$; *** $p<0.001$; **** $p<0.0001$, ns: not significant, 2-Way ANOVA comparison to mock nonirradiated cells, Error bars represent mean ± SEM.

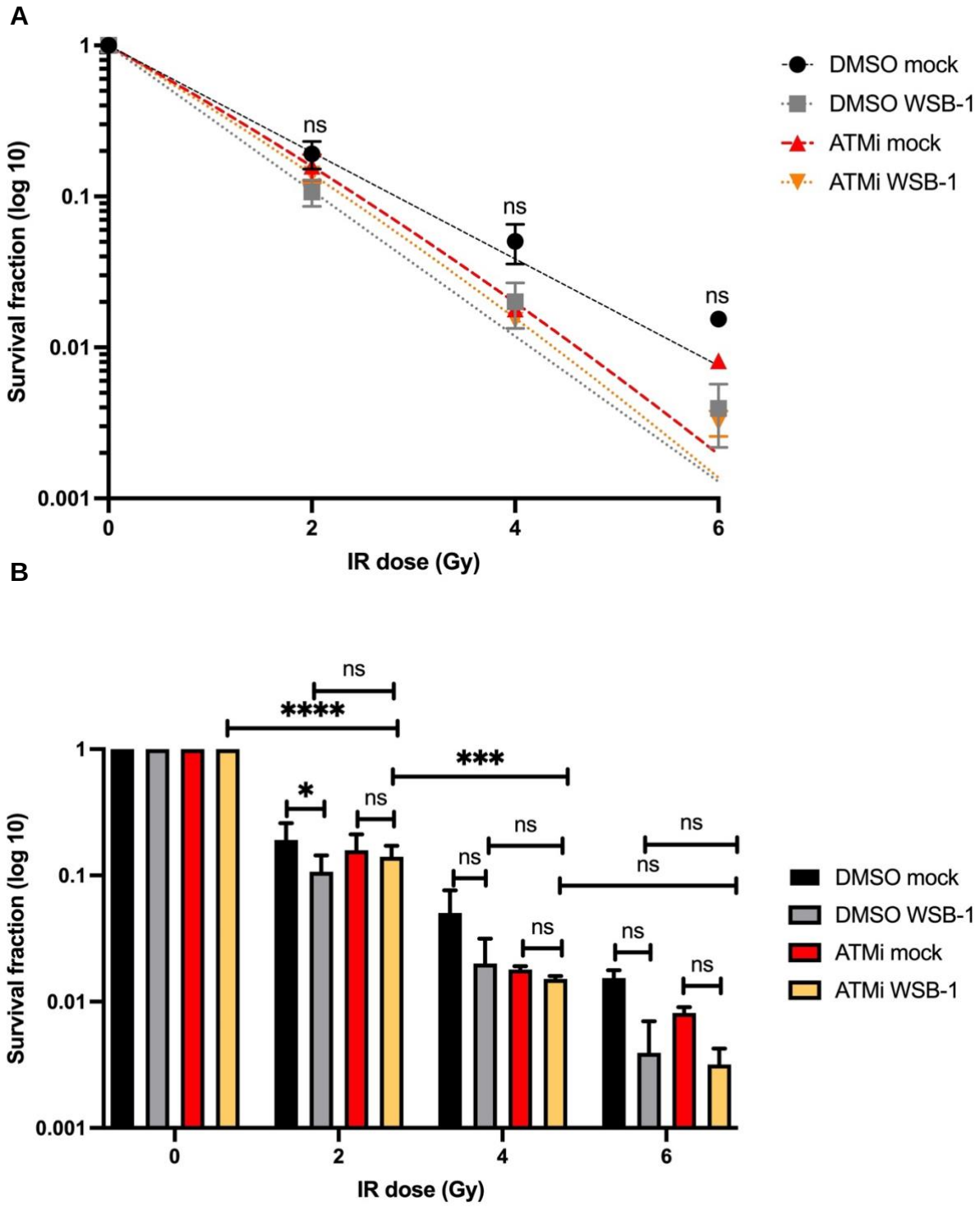

Figure 5. 18 WSB-1 overexpression sensitized ATMi after IR under hypoxia

MCF7 were either mock transfected (mock) or transfected with a Flag-tagged WSB-1 (WSB-1) for 24h. Cells were kept in hypoxic condition (1% O_2). Cells were treated with ATMi KU-55933 (800nM) alongside with DMSO control then exposed to different IR doses (2Gy, 4Gy, 6Gy). Clonogenic survival was measured 10 days after IR; cells survival fraction (log 10) was showed in fitting curve (A) and histogram (B); n=3 independent biological repeats. * $p<0.05$; ** $p<0.01$; *** $p<0.001$; **** $p<0.0001$, ns: not significant, 2-Way ANOVA comparison to mock nonirradiated cells, Error bars represent mean ± SEM.

For ATR inhibition, the fitting curve showed the trend of WSB-1 overexpression increased sensitivity to the combination with IR and ATRi (VE-822) under normoxia. WSB-1 overexpression sensitised ATMi (KU-55933) combined with IR in 2Gy($p<0.01$) under normoxia (Figure 5.19 A). There are trends shown under hypoxic condition in different doses. However, the data is not statistic significant (Figures 5.20 A). As the histograms showed, under normoxia (Figure 5.20 B), although WSB-1 overexpression reduced clonogenic survival compared to mock control at different doses alone or combine with VE-822, the differences were not significant. Under hypoxia, WSB-1 overexpression significantly ($p<0.0001$) sensitized IR (2 Gy) alone with reduction of survival from 18.8% to 12.7% compared to mock control with IR (2 Gy) treatment, as well as significantly ($p<0.0001$) sensitized the combination of IR (2 Gy) with VE-822 with reduction of survival from 12.22% to 2.3% compared to mock control with IR (2 Gy) and VE-822 treatments. Moreover, when compared to using VE-822 treatments alone, WSB-1 overexpression significantly reduced clonogenic survival with the combination of IR (2 Gy) and VE-822 under normoxia ($p<0.0001$) and hypoxia ($p<0.0001$). Higher doses (4 Gy) combined with VE-822 sensitised cells compared to 2 Gy with VE-822 under normoxic conditions ($p<0.05$).

In conclusion, these data indicate that overexpression of WSB-1 sensitises cells for treatment with DDRi, particularly in normoxic conditions. The results look the most promising for ATRi and IR combinations in hypoxic conditions, which will be discussed later.

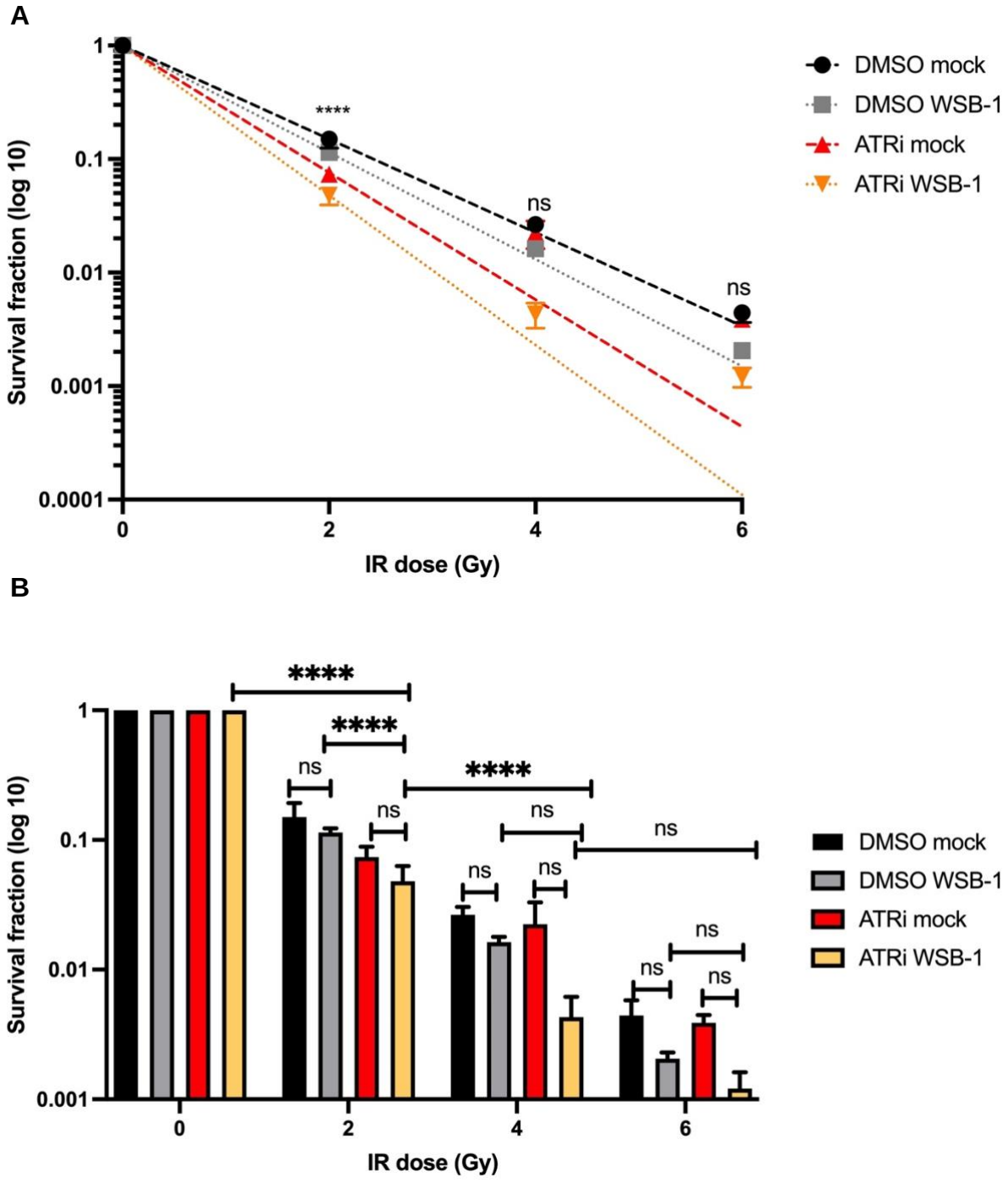

Figure 5. 19 WSB-1 overexpression sensitized ATRi after IR under normoxia

MCF7 were either mock transfected (mock) or transfected with a Flag-tagged WSB-1 (WSB-1) for 24h. Cells were kept in normoxic condition (20% O_2). Cells were treated with ATRi VE-822 (10nM) alongside with DMSO control then exposed to different IR doses (2Gy, 4Gy, 6Gy). Clonogenic survival was measured 10 days after IR; cells survival fraction (log 10) was showed in fitting curve (A) and histogram (B); n=3 independent biological repeats. * $p<0.05$; ** $p<0.01$; *** $p<0.001$; **** $p<0.0001$, ns: not significant, 2-Way ANOVA comparison to mock nonirradiated cells, Error bars represent mean ± SEM.

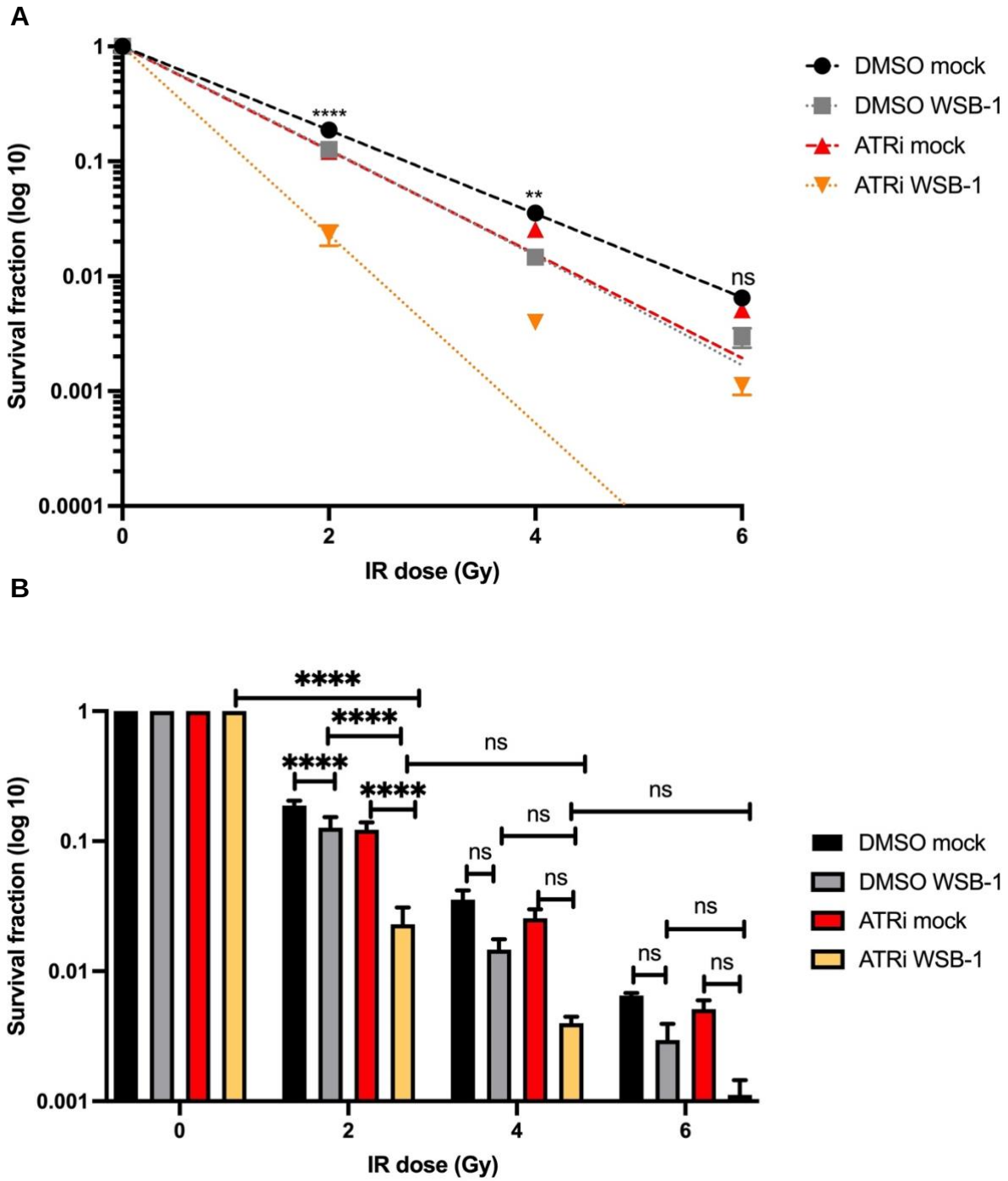

Figure 5. 20 WSB-1 overexpression sensitized ATRi after IR under hypoxia

MCF7 were either mock transfected (mock) or transfected with a Flag-tagged WSB-1 (WSB-1) for 24h. Cells were kept in hypoxic condition (1% O_2). Cells were treated with ATRi VE-822 (10nM) alongside with DMSO control then exposed to different IR doses (2Gy, 4Gy, 6Gy). Clonogenic survival was measured 10 days after IR; cells survival fraction (log 10) was showed in fitting curve (A) and histogram (B); n=3 independent biological repeats. * $p<0.05$; ** $p<0.01$; *** $p<0.001$; **** $p<0.0001$, ns: not significant, 2-Way ANOVA comparison to mock nonirradiated cells, Error bars represent mean ± SEM.

5.4 Discussion

In this chapter, we firstly showed that WSB-1 expression was negatively correlated with DNA repair signatures, as well as individual DNA repair pathways including HR pathways, BER pathways, and MMR pathways significantly.
Further, we examined WSB-1 overexpression respond to DDR inhibitors including PARPi (Olaparib), ATMi (KU-55933) and ATRi (VE-822) in a short-term MTS assay and the results showed that WSB-1 overexpression could potentially increase the sensitivity to these DDRi, but effects varied in a cell line dependent manner.
Finally, clonogenic assay where these DDRi were combined or not with IR when overexpressed WSB-1 under normoxia and hypoxia were investigated and the results showed that increased WSB-1 expression can at least partially sensitised DDR inhibitors PARPi (Olaparib) and ATRi (VE-822) alone as well as the combination with radiation under normoxia and hypoxia, but results were not as clear for ATMi (KU-55933).
Following the results we obtained, achieved the aims that we stated in the beginning of this chapter:

1. *Evaluate the relationship between WSB-1 expression and DNA repair signature in patient samples*

WSB-1 expression was negatively associated with DNA repair signatures in breast cancer patient samples. WSB-1 expression was also negatively correlated with DNA repair pathways including HR pathways, BER pathways, and MMR pathways significantly. Although the correlation between WSB-1 expression with NHEJ pathways was statistic significant ($p<0.05$), however this correlation was very weak (Spearman r = -0.09452 and Pearson r = -0.1111). High WSB-1 expression could therefore indicate DNA repair deficiency, such as HR deficiency (HRD). HRD tumours has been shown to be sensitive to PARP inhibition (McCabe et al., 2006, Chopra et al., 2020). These results support our hypothesis that WSB-1 could act as a BRCAness biomarker but investigating correlation in protein expression in patient samples would further support this hypothesis. Also, the patient datasets analysed comprised a large cohort of patients with different breast cancer types, so further analyses separating this larger cohort by hormone receptor positivity, for example, would also clarify some of the variability observed for different cell lines *in vitro*.

2. *Assess the impact of overexpressing WSB-1 on the response to DDRis as single agents or in combination with IR*

In this study, the overall trend observed was a moderate to mild reduction of cell viability/proliferation for PARPi when WSB-1 was overexpressed, and with different levels between cell lines. As noted earlier, even the largest decrease in viability observed was only around 40%, which is not as dramatic as the several fold change decreased in viability observed when PARPi was used in cells with deficient BRCA1/2 backgrounds when compared to wild type cells (Farmer et al., 2005) (Bryant et al., 2005). This could be due to the level of impact of BRCA1/2 downregulation has when WSB-1 is overexpressed is not directly comparable with BRCA/1 deficient cell. As observed in Chapter 3, in hypoxic conditions *BRCA1* and *BRCA2* mRNA levels were decreased by approximately 0-90% (depending on cell line). This variability could have also impacted the response to the other DDRi after WSB-1 overexpression, noting that, especially for ATMi, WSB-1 overexpression did not lead to any significant sensitisation. Sensitisation to ATRi was again observed in most cell lines but to different degrees. A key point to note is that some of the observed sensitisation phenotypes observed are only mild albeit being significant, so the longer-term translation of these effects needs to be further investigated using complementary models. It is important to remember that the cell populations used in these experiments will have a variable expression of WSB-1 after transfection as they are not monoclonal lines, and therefore this can also impact on the robustness of the results observed.

Finally, recent studies found that ATRi and PARPi synergistically kill tumour cells and their sensitivity upon inactivation of RAD51 (Zimmermann et al., 2022). In Chapter 3, WSB-1 overexpression was shown to repress RAD51, which means WSB-1 could also sensitise the combination of ATRi with PARPi combination. Therefore, the sensitivity of ATRi and PARPi combination could be tested in future work.

There are trends observed in long-term survival clonogenic assays that when WSB-1 is overexpressed it increased sensitivities to DDRi including PARP1 inhibitor (Olaparib), ATMi (KU-55933) and ATRi (VE-822) combined with IR under normoxia and hypoxia. As the results in Chapter 4 showed, WSB-1 overexpression potentially (albeit preliminarily) increased pCHK1 with and without IR under normoxia and hypoxia. Studies have shown that CHK1 inhibitor MK-8776 can promote radiation-induced cell death (Suzuki et al., 2017).

Therefore, CHK1 inhibitors have the potential to be used in WSB-1 overexpression alone and/or in combination with IR. Moreover, DNA damage can also be signalled via the ATR-CHK1-WEE1 pathway and prevent G2/M progression (Do et al., 2015). Therefore, other types of DDRi such as WEE1 inhibitors could be examined with overexpression of WSB-1 with/without IR in the future work.

In addition, 3D spheroid and even patient derived organoids model are more clinically relevant tumour models than traditional 2D models, which has been generally accepted (Zanoni et al., 2020). The sensitivity of WSB-1 overexpression to different DDRi could be tested by using 3D sphenoid models in future work.

In conclusion, this chapter we found that increased WSB-1 expression and associated DNA repair deficiency could potentially increase sensitivity to DDRi includes PARP1 inhibitor (Olaparib), ATMi (KU-55933) and ATRi (VE-822) alone or combine with IR under normoxia and hypoxia. Therefore, WSB-1 could be a BRCAness/HRD biomarker predict the sensitivity of DDRi and IR treatments in high WSB-1 expressed breast cancer.

Chapter 6

Discussion

6. General Discussion

6.1 Summary of previous chapters

Breast cancer is the most common cancer in women worldwide (Loibl et al., 2021). Treatment for breast cancer currently includes conventional therapies, such as local treatments surgery and radiotherapy, and systemic treatments like chemotherapy, targeted therapy, and immunotherapy (Costa et al., 2020). Moreover, combination therapies approaches can achieve a better outcomes, such as the combination of radiotherapy with targeted therapy (Elbanna et al., 2021) or immunotherapy (Simone II et al., 2015). However, the acquired therapeutic resistance and the selections of different therapeutic strategies as well as the concept of personalised treatments revealed the importance of the discoveries of reliable biomarkers that can predict and/or monitor different therapeutic treatments alone or their combination.

Radiotherapy is one of the major therapeutic approaches in the treatments for cancers. It can also be used in combination with surgery or chemotherapy, which has become a highly effective treatment. However, hypoxia induces radioresistance through a number of molecular pathways, such as the activation of HIFs, which leads to the transcriptional activation of HIFs downstream genes and plays a role in radioresistance (Bouleftour et al., 2021). WSB1 as a E3 ubiquitin ligase can degrade pVHL, therefore stabilising HIF-1. Moreover, WSB-1 expression is induced by HIF1, which is a positive feedback loop (Kim et al., 2015). WSB-1 has also been shown to play a role in DDR pathway, including the ubiquitination and degradation of HIPK2 (Choi et al., 2008) and ATM (Kim et al., 2017a). However, the role of WSB-1 in DDR signalling pathways and response to radiotherapy in breast cancer, especially in the context of hypoxia remains unknown. Therefore, the aims of this thesis were to evaluate the use of WSB-1 expression as a 'BRCAness' biomarker, both in terms of signalling changes, response to RT, and response to DDR inhibitors.

To do this, initially in Chapter 3 we investigated the new role of WSB-1 in DDR signalling pathway in hypoxic breast cancer. WSB-1 depletion is associated with transcriptional changes, including cell cycle regulation, DNA replication, and DNA repair. Modulation of expression of DNA repair factors *BRCA1, BRCA2, RAD51*, as well as cell cycle control factors *E2F1, RB1, CDK4/6* were validated at mRNA level and BRCA1, RAD51, E2F1 and

RB1 were validated at the protein level *in vitro* as being upregulated after WSB-1 depletion. Reciprocally, WSB-1 overexpression downregulated these DDR factors.

In Chapter 4 the role of WSB-1 in DNA damage and cell cycle as well as radiotherapy response in breast cancer under normoxia and hypoxia was investigated. DSBs biomarkers γH2AX and 53BP1 foci were increased when overexpressed WSB-1 and/or after IR 24h. Reciprocally, WSB-1 depletion reduced the occurrence of these foci. WSB-1 overexpression also caused cell cycle arrest in MCF7 and MDA-MB-231 cells. These results indicated that overexpressed WSB-1 caused DNA damage and repressed DNA repair and could be a BRCAness biomarker.

As studies already found that BRCAness tumours can be sensitive to PARPi treatments, therefore, the sensitivities of PARPi as well as other DDRi including ATMi and ATRi were investigated in Chapter 5 when overexpressed WSB-1 under normoxia and hypoxia *in vitro.*

In conclusion, this study investigated the new role of WSB-1 in DDR in hypoxic breast cancer and could be used as a BRCAness biomarker for the treatments of DDRi including PARPi, ATMi and ATRi as well as the combination of radiation treatments. The role of WSB-1 in DDR pathways investigated in this study and its potential role as BRCAness biomarker for the treatments of PARPi, ATMi and ATRi are summarised in Figure 6.1.

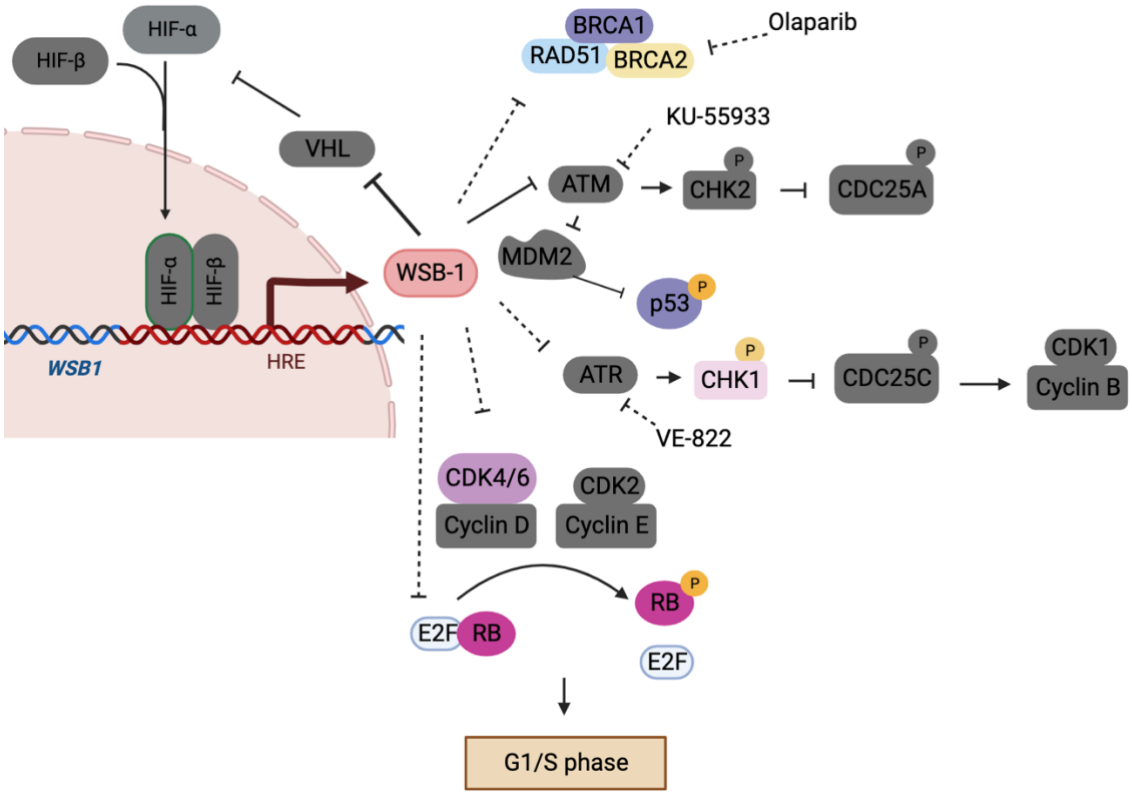

Figure 6. 1 Summary of the effect of WSB-1 on DDR

HIF-1α promotes the transcription of WSB-1. WSB-1 inhibit BRCA1/2, RAD51 expression which could be sensitive to Olaparib; WSB-1 degrade ATM which could be sensitive to KU-55933, and VE-822 could also be used based on the impact of WSB-1 on ATR/CHK1 pathway. WSB-1 effect cell cycle by influencing the expression of CDK4/6, E2F1 and RB. Molecules noted in colour have been investigated in this study. (Created using Biorender.com)

6.2 WSB-1 and DDR signalling

6.2.1 WSB-1 and DNA damage and repair

6.2.1.1 DSB repair

γH2AX and 53BP1 are biomarkers for the presence of DSBs (Nagelkerke et al., 2011, Djuzenova et al., 2015). Increased levels of γ-H2AX foci are indicator of DNA repair pathway deficiency, whereas 53BP1 is a DNA double-strand breaks sensor, and both expression is correlated with radiation therapy-induced outcome (Djuzenova et al., 2015). In Chapter 4, overexpressed WSB-1 increased γH2AX and 53BP1 foci and/or after IR 24h, whereas WSB-1 depletion reduced γH2AX and 53BP1 foci and/or after IR 24h. These results showed that WSB-1 overexpression could potentially repress DDR signalling such as DSBs repair capacity, as seen by the impact on the foci number after IR. Moreover, WSB-1 overexpression alone also increased γH2AX and 53BP1 foci, which suggested WSB-1 overexpression could repress DNA damage repair and high WSB-1 could represented the sensitivities to radiation. However, these foci assay only detected the impact of WSB-1 on DSBs. Whether there are other types of DNA damage induced by WSB-1 overexpression is still unclear.

6.2.1.2 Other repair pathways

In the pathway enrichments, WSB-1 depletion can also upregulated BER pathways and among the top 30 upregulated genes in DDR pathways, DNA glycosylases genes *NEIL3*, *POLE* were also upregulated genes when WSB-1 was depleted. These indicated BER could also participate the repair of WSB-1, which means SSBs could be also induced when WSB-1 is overexpressed. Moreover, the pathways enrichments also showed that Fanconi anaemia pathway which mainly respond to interstrand crosslink DNA lesions (Ceccaldi et al., 2016), were enriched when WSB-1 was depleted under hypoxia, and *FANCD2, FANCI,* etc. were also the top 30 upregulated genes in DDR pathway after WSB-1 depletion under hypoxia. Therefore, WSB-1 could induce different types of DNA damage including DSBs, SSBs, and interstrand crosslink DNA lesions, but more evidence needs to be investigated. And as mentioned in Chapter 5, The XRCC1 protein could be tested in our future works (London, 2015). In addition, the complex DNA damage (CDD), which can be detected by the enzyme-modified neutral comet (EMNC) assay (Fabbrizi et al., 2021), could also be conducted when

overexpressed WSB-1 to investigate different DNA damages caused by WSB-1 overexpression.

As stated above, if WSB-1 could induce various types of DNA damage including DSBs, SSBs, and interstrand crosslink DNA lesions, in respond to these DNA damages, WSB-1 could also activate different DNA repair pathways such as MMR, BER, HR as well as Fanconi anemia pathway. In Chapter 3, RNA-seq WSB-1 depletion under hypoxia in MDA-MB-231 cells was used to perform different pathways and functions enrichments, different DNA repair pathways including BER, MMR, HR, etc. were enriched. According to KEGG pathways enrichments from ExpressAnalyst, when depletion of WSB-1 under hypoxia in MDA-MB-231 cells, there were 15 hits out of 33 genes enriched in BER pathways, 12 hits out of 23 genes MMR pathways. Fanconi anemia pathway has 18 hits out of 54 genes, and HR pathway has 15 hits out of 41 genes. And NHEJ pathways seems exclusive for WSB-1 depletion under hypoxia. These results were confirmed in Chapter 5 where WSB-1 expression is found negatively correlated with MMR, BER, HR, and NHEJ pathways showed weak correlation with WSB-1 expression.

6.2.1.3 ATM and ATR signalling

For the impact of WSB-1 on ATM signalling, ATM has been showed to degraded by WSB1 in different tumours types including breast cancer (Kim et al., 2017a). Gatei et al also demonstrated that rapid ionising radiation-induced phosphorylation of BRCA1 *in vivo,* the presence of functional ATM protein is required for the phosphorylation of BRCA1 in breast cancer (Gatei et al., 2000). Although we did not test the expression of ATM respond to WSB-1 in this study, in chapter 4, pBRCA1 was decreased when overexpressed WSB-1 after IR in MCF7.

For the impact of WSB-1 on ATR signalling, the enrichments analysis also indicated the potential connection between WSB-1 and ATR pathways in Chapter 3 and Chapter 4. In chapter 3, depleting WSB-1 under hypoxia in MDA-MB-231 cells upregulated genes in DNA IR-damage and cellular response via ATR pathways. In Chapter 4, we found that pCHK1 and phosphorated p53 was upregulated by WSB-1 respond to IR under normoxia and hypoxia. p53 were increase when overexpressed WSB-1 and decreased after WSB-1 depletion in Chapter 4. Among the upregulated genes from RNA-seq, *CDC25, CDK2, CDK1* were increased when WSB-1 was depleted under hypoxia in Chapter 3. These results suggest WSB-1 could activate ATR/pCDK1 pathways. In general, DNA damage or stressed

replication forks creates single-strand DNA (ssDNA) which activates ATR. ATR downstream factor CHK1 is phosphorylated by ATR and the release of pCHK1 activate the effectors CDC25, therefore promote the mitotic cell G2/M transition by activating the cyclin B1/CDK1 complex, cyclin E/ CDK2 complex or via p53-mediated signal transduction (Qiu et al., 2018, Gralewska et al., 2020). According to literature, there is no evidence showing the impact of WSB-1 on ATR pathways to date. We also did not test the direct connection between ATR and WSB-1. Therefore, more confirmations and detailed mechanisms of the impact of WSB-1 on ATR pathways need to be fully studied in the future. For example, the ATR protein expression after WSB-1 overexpression or depletion. And Co-IP to detect if WSB-1 could have a direct interaction with ATR protein.

As TF enrichments showed E2F family including E2F1 were enriched when WSB-1 was depleted under hypoxia. E2F1 was regulated respond to the modulation of WSB-1 under normoxia and hypoxia in RNA and protein levels. Studies found both ATM and ATR can phosphorylate E2F1 in response to DNA damage, such DSBs. E2F1 is phosphorylated by ATM, which is associated with the induction of apoptosis, while E2F1 is phosphorylated by ATR (Manickavinayaham et al., 2020). The relationships between E2F1, ATM, ATR and WSB-1 could be further evaluated in further works.

6.2.2 WSB-1 and cell cycle arrest

WSB-1 isoforms 1 and 2 has been found to promote cancer progression in the human pancreatic cancer cell lines (Archange et al., 2008). c-Myc is a multifunctional transcription factor which drives the multiple synthetic functions including cell proliferation and cell cycle regulation (Miller et al., 2012). Recent study found that WSB1 is a direct target gene of c-Myc, WSB1 also regulates c-Myc expression through WNT/β-catenin pathway, which forms a positive feedback loop (Gao et al., 2022). In addition, in an integrative analysis of the cancer transcriptome, ATF5 have been seen to activate and bind to the WSB-1 promoter (Rhodes and Chinnaiyan, 2005). ATF5 has been showed to regulates stress responses, cell survival, differentiation and plays a vital role in cell cycle (Liu et al., 2012b, Madarampalli et al., 2015, Paerhati et al., 2022). WSB-1 has been reported may be a target of miRNA-191 in Multiple Sclerosis (Guerau-de-Arellano et al., 2015). miRNA-191 has been shown to regulates cell proliferation, differentiation, apoptosis, and targeting cell cycle associated genes such as CDK6 and CCND2 (Nagpal and Kulshreshtha, 2014). These findings indicate the potential regulation of WSB-1 in cell cycle regulation.

In Chapter 3, WSB-1 depletion upregulated key cell cycle regulation genes, such as CDK2, CDK6, CDK1 and WEE1 which also have been studies as clinically relevant DDR therapeutic targets. In chapter 4, we also found that WSB-1 overexpression cause cell cycle arrest in phrase G1, S and G2/M in MCF7, and in phrase G1 and G2/M in MDA-MB-231. Therefore, WSB-1 participates in the regulation of cell cycle arrest.

WSB-1 has been shown to cause ubiquitination of DNA damage-responsive serine/threonine kinase HIPK2 (Choi et al., 2008) and ATM (Kim et al., 2017b). In respond to DNA damage, both HIPK2 and ATM can phosphorylate p53 (Liebl and Hofmann, 2019). In Chapter 3, the pathways enrichments also indicated the impact of WSB-1 on p53 signalling pathways. Moreover, WSB-1 depletion under hypoxia could affect cell cycle regulation and DNA damage repair by regulating p53 expression from the TFs enrichments analysis. Kim et al. also found that overexpressed WSB-1 decreased p53 expression whereas WSB-1 depletion stabilised p53 (Kim et al., 2017a). The TF enrichments also found that E2F family members *E2F8, E2F7, E2F2, E2F1, E2F4* were enriched. E2F1 was upregulated after WSB-1 depletion and decreased when overexpressed WSB-1 in mRNA and protein level under normoxia and hypoxia. To our knowledge, there's no evidence showing the direct impact of WSB-1 on E2F family members and to date. These results indicated that WSB-1 could directly regulating E2F family and *Tp53* in a transcriptional level under hypoxia.

6.2.3 WSB-1 and DNA replication stress

As foci images shown in Section 4.3.3, the formation of γH2AX foci when overexpressed WSB-1 is a wide spread pattern, which is also called pan-nuclear γ-H2AX pattern, and pan-nuclear γ-H2AX formation has been suggested is an indicator of replication stress induced cell death(Moeglin et al., 2019). Therefore, WSB-1 overexpression could induce DNA replication stress. In Chapter 3, E2F1 was showed regulated respond to the modulation of WSB-1, although the impact of WSB-1 of E2F1 could be DNA damage, recent studies suggests that dysregulation of E2F1 is caused and consequences of DNA replication stress(Fouad et al., 2021). Moreover, in Chapter 4, WSB-1 overexpression caused abnormal changes in chromosome. Studies have found that the major source of structural chromosome instability (s-CIN) and leading to structural chromosome aberrations is DNA replication stress(Wilhelm et al., 2020). Therefore, high WSB-1 expression could have impacts on DNA replication stress and further validation needed. To validate this hypothesis, IF staining for RAP foci could be tested when overexpressed WSB-1 to see if RPA has the similar pan-

nuclear staining pattern, as well as γH2AX and RPA Foci colocalize as described in (Gagou et al., 2010) to test DNA replication stress. Moreover, phosphorylation of RPA (Ser33) or CHK1 (Ser345) which are ATR-dependent as well as the detection of ssDNA by BrdU staining described in (Pires et al., 2010) could also be used to detect if DNA replication stress is induced by WSB-1.

6.3 WSB-1 as a biomarker in the treatments of DDRi/IR

Several biomarkers have been proposed for DDR Inhibitors. For example, for PARP inhibitors, the expressions of *BRCA1* and *BRCA2*, the status of homologous recombination deficiency (HRD), and the phosphorylation status of H2AX proteins (Ganguly et al., 2016). However, the validation and clinical utility of these biomarkers are still under investigation, and additional studies are needed to fully understand their role in the development and assessment of DDR inhibitors. In this studyWSB-1 overexpression repressed BRCA1/2 and RAD51 (Chapter 3), and in Chapter 5 WSB-1 expression was shown to be negatively correlated with DNA repair pathways such as HR pathways. This indicates that high WSB-1 expression could be associated with DNA repair dysregulation, such as HR repair deficiency. These results show that WSB-1 could represent BRCAness and DNA repair deficiency. Therefore, in Chapter 5 we also used DDRi, including PARPi, ATMi, and ATRi, to treat WSB-1 overexpressed MCF7 cells as well as the combination of IR treatments under normoxia and hypoxia. Our data showed that high WSB-1 expression sensitized these DDRi with IR especially when using high doses of X ray. Among these DDRi, ATR inhibition and/or IR in WSB-1 overexpressed MCF-7 under hypoxia seems was the most effective, which further indicated WSB-1 overexpression could active ATRi-pCHK1 pathways. In addition, WSB-1 overexpression upregulated pCHK1 with IR under normoxia and hypoxia. Therefore, CHK1 inhibitors such as V158411, PF-477736 and AZD7762 which have been shown that can inhibit cell proliferation of TNBC and ovarian cancers(Bryant et al., 2014), could also potentially sensitise cells with high WSB-1 expression either as single agents or in combination with RT. Moreover, recent study found that ATRi and PARPi can synergistically kill tumour cells and their sensitivity upon the inactivation of RAD51(Zimmermann et al., 2022). In Chapter 3, WSB-1 overexpression was shown to repress RAD51, which means WSB-1 could also sensitized the combination of ATRi with PARPi combination. Therefore, the sensitivity of ATRi and PARPi combination could be tested in future works.

6.4 Study Limitations

Although this study identified WSB-1 as a potential BRCAness biomarkers for DDRi and DDRi/IR combination treatment, we noticed there are several limitations in our study. Firstly, some alteration of genes expression after WSB-1 depletion were not validated such as *p21*, *CDC25, CDK2, CDK1*, etc, which could give us more confirmations about the impact of WSB-1 on ATM/ATR signalling pathways and cell cycle pathways. But the impact of WSB-1 on ATM/ATR signalling pathways and cell cycle pathways will be further investigated in our future works (these will be discussed in detail in the next Section). Secondly, in western blot experiments (Section 4.3.2), some of the protein statuses were not repeated 3 times such as pCHK1(n=1), p-p53 (n=1) due to time limitation, and pCHK2 was not working in this study. Possible reason could be pCHK2 was degraded during the process of sample preparation. Different cell lysis that might prevent the degradation described in (Matsuoka et al., 2000) could be used in our future work. In addition, the foci assay and flow cytometer were also only evaluated in MCF7 and MDA-MB-231 and only evaluated under normoxic condition, therefore, these will be further validated in our future work. Finally, the clonogenic assays were only evaluated in one cell line and we did not investigate the response to DDRi and DDRi/IR combination treatment *in vivo* which will be put in our future works (will be further discussed in the next Section).

6.5 Future directions

According to the results obtained in this study, there are several aspects could be investigated further, which includes the different DNA damages and the damage repair pathways induced by WSB-1; The detailed mechanisms of direct regulation of E2F family or p53; the impact of WSB-1 on ATR-pCHK1 pathways; the impact of WSB-1 on more DDRi and/or IR with more clinically relevant models, in vivo or clinical patience samples works, WSB-1 in different tumour types and its inhibitions. The approaches are detailed below.

6.5.1 Different DNA damages and damage repair induced by WSB-1

As stated above, WSB-1 overexpression could induce not only DSBs repaired by HR pathway, but also SSBs repaired by BER pathways, and interstrand crosslink DNA lesions repaired by Fanconi anaemia pathway. The further validation of DSBs damage and the repair by HR could be achieved by metaphrase spread assays which tested in chromosome levels. The repair of SSBs through BER pathway may be evaluated using the comet assay(Fabbrizi

et al., 2021) and the examination of XRCC1 protein(London, 2015). For interstrand crosslink DNA lesions repaired by Fanconi anaemia pathway, key regulators in Fanconi anaemia pathway such as FANCA, FANCB, FANCC, FANCE, FANCF, FANCG and FANCL(Niraj et al., 2019) could be tested when overexpressed WSB-1.

6.5.2 The direct regulation of E2F family or TP53

We propose to directly evaluate role of E2F family or p53 in the upregulation of WSB-1 after DNA damage at the transcript and protein level. Firstly, the evaluation E2F family or TP53 expression could be achieved when WSB-1 was depleted and overexpressed. Secondly, we will also search for *p53/ E2F1* binding motifs in the WSB-1 promoter using bioinformatic tools for identification of conserved regulatory sequences, and subsequently validate these using reported assays could be used to evaluate the expression levels of E2F1 (Ingram et al., 2011) and p53 (Leszczynska et al., 2015). Furthermore, the analysis of the WSB-1 interactome with E2F family and/or p53, and its co-factors as potential binding partners will be further investigated by using pull down assays in vitro. We propose to use in vitro ubiquitylation assays, as described in (Pires et al., 2014), to evaluate whether E2F family and/or p53 is ubiquitylated in response to the presence or absence of WSB-1. From this aim we expect to determine the mechanism behind the WSB-1-mediated repression of error-free DNA repair, and its link with p53 and E2F-mediated changes in gene expression downstream of WSB-1.

6.5.3 The impact of WSB-1 on ATR-CHK1 pathways

In Chapter 5, only pCHK1 protein was tested when overexpressed WSB-1 with or IR treatment under nomoxia and hypoxia. Protein expression including phosphorylation of RPA (Ser33), ATR and pCHK1 downstream CDC25, CDK1 and CDK2 can also be evaluated when overexpressed/depleted WSB-1 to validate if WSB-1 can regulate the ATR-pCHK1 pathway as well as its downstream. DNA replication stress can activate the protective ATR-Chk1 signalling(Zeman and Cimprich, 2014). As described in 6.2.3, high WSB-1 could cause DNA replication stress, therefore, RAP foci, γH2AX and RPA Foci colocalize, and BrdU experiments with overexpressed WSB-1 could also be conducted in our future works.

6.5.4 WSB-1 on other DDRi and IR

Other DDRi such as CHK1 inhibitors, WEE1 inhibitors, CDK4/6 inhibitors (supplemental data) could be tested in WSB-1 overexpression with or without IR to test the potential wider

application of WSB-1 on other DDRi. Moreover, 3D sphenoid and even patience derived organoids model which are more clinically relevant Tumour cells are surrounded by cells such as stromal cells, endothelial cells immune cells, metabolites, growth factors, etc, which constitute the tumour microenvironments. Taking this into account, in vitro 3D culture models 3D sphenoid method has been used more and more (Zanoni et al., 2020). Therefore, the impact of WSB-1 on the formation of 3D sphenoid with the treatments of DDRi and/or IR could be tested in the future works. Moreover, *in vivo* work on mice or even examination of WSB-1 expression on clinical patience will also be the future direction.

6.5.5 WSB-1 in other tumour types and its inhibition

In this thesis, the role of WSB-1 on DDR were solely studied in breast cancer cells. However, as chapter 1 stated, WSB-1 also plays important role in various types of cancer with different regulation function such as the regulation of cell proliferation in pancreatic cancer(Archange et al., 2008), the promotion of tumour initiation and development in hepatocellular carcinoma cell, ovarian cancer cell and colon cancer cell(Gao et al., 2022). Therefore, the role of WSB-1 on DDR pathways in different cancer types could be investigated, which could forward the application DDRi and/or IR treatments not limited in breast cancer.

As WSB-1 plays pivotal roles in DDR(Choi et al., 2008), cell proliferation(Archange et al., 2008, Shichrur et al., 2014), and immune regulation(Nara et al., 2011a) etc. In addition, in this study such as Chapter 3, WSB-1 repressed *BRCA1/2*, *RAD51*, and *RB1* which are all well-known tumour suppressors genes. WSB-1 could be considered as an oncogene. Moreover, as we known E3 ubiquitin ligases mediate the degradation of various regulatory protein including tumour suppressor proteins. Protein degrader including targeting E3 ligase has been considered as a new approach to cancer therapy and there are 18 protein degraders are in clinical trials (Chirnomas et al., 2023). Given WSB-1 as a E3 ubiquitin ligase and its different regulatory functions in various tumour types, WSB-1 inhibition and degradation will be the future direction. Moreover, there are studies of WSB-1 inhibitors provides relevant information of the WSB1 inhibitor drugs in future drug design. Recent studies discovered a WSB1 Degrader 5,6-Bis(4-methoxy-3-methylphenyl)pyridin-2-amine can potentially inhibit the metastasis of lung cancer cells (Che et al., 2021). Weng et al also identified a stable structure of WSB1 inhibitors G490-0341 which provide promising information for further development of WSB1 inhibitors (Weng et al., 2022). Therefore, the validation of WSB-1

inhibitors firstly on cell levels, 3D models, as well as in vivo works and move to further clinical trials will be the future direction.

In conclusion, this study investigated the new role of WSB-1 in DDR in hypoxic breast cancer and demonstrated the WSB-1 could be used as a BRCAness biomarker for the treatments of DDRi including PARPi, ATMi and ATRi as well as the combination of radiation treatments. This study expands our knowledge of how high WSB-1 levels are associated with aggressive breast cancers, and whether these cells have a similar behaviour to cells with BRCAness or DNA repair deficiency. This will allow us to understand the biology of advanced breast cancers and develop effective and specific therapy strategies to target these cells, either alone or in combination with treatment strategies already available in the clinic. Secondly, establishing high WSB-1 levels as a novel marker for 'BRCAness', will allow us to develop new tests or biological markers for determining the presence of these aggressive tumours, and whether they are likely, or not, rot respond to therapy. This would result in more adequate and specific treatment earlier, leading to increased likeliness of survival and better quality of life.

References

AL TAMEEMI, W., DALE, T. P., AL-JUMAILY, R. M. K. & FORSYTH, N. R. 2019. Hypoxia-Modified Cancer Cell Metabolism. *Front Cell Dev Biol,* 7**,** 4.

ALEXANDER, B. M., AHLUWALIA, M. S., DESAI, A. S., DIETRICH, J., KALEY, T. J., PEEREBOOM, D. M., TAKEBE, N., SUPKO, J. G., DESIDERI, S., FISHER, J. D., SIMS, M., YE, X., NABORS, L. B., GROSSMAN, S. A. & WEN, P. Y. 2017. Phase I study of AZD1775 with radiation therapy (RT) and temozolomide (TMZ) in patients with newly diagnosed glioblastoma (GBM) and evaluation of intratumoral drug distribution (IDD) in patients with recurrent GBM. *Journal of Clinical Oncology,* 35**,** 2005-2005.

ALI, R., AOUIDA, M., ALHAJ SULAIMAN, A., MADHUSUDAN, S. & RAMOTAR, D. 2022. Can Cisplatin Therapy Be Improved? Pathways That Can Be Targeted. *Int J Mol Sci,* 23.

ALMANDOZ, J. P. & GHARIB, H. 2012. Hypothyroidism: etiology, diagnosis, and management. *Med Clin North Am,* 96**,** 203-21.

ANBALAGAN, S., BIASOLI, D., LESZCZYNSKA, K. B., MUKHERJEE, S. & HAMMOND, E. M. 2015. In Vitro Radiosensitization of Esophageal Cancer Cells with the Aminopeptidase Inhibitor CHR-2797. *Radiat Res,* 184**,** 259-65.

ANBALAGAN, S., PIRES, I. M., BLICK, C., HILL, M. A., FERGUSON, D. J., CHAN, D. A. & HAMMOND, E. M. 2012. Radiosensitization of renal cell carcinoma in vitro through the induction of autophagy. *Radiother Oncol,* 103**,** 388-93.

ANDREOPOULOU, E. & SPARANO, J. A. 2013. Chemotherapy in Patients with Anthracycline- and Taxane-Pretreated Metastatic Breast Cancer: An Overview. *Curr Breast Cancer Rep,* 5**,** 42-50.

ARCHANGE, C., NOWAK, J., GARCIA, S., MOUTARDIER, V., CALVO, E. L., DAGORN, J. C. & IOVANNA, J. L. 2008. The WSB1 gene is involved in pancreatic cancer progression. *PLoS One,* 3**,** e2475.

ARGIRIS, A., MIAO, J., CRISTEA, M. C., CHEN, A. M., SANDS, J., DECKER, R. H., GETTINGER, S. N., DALY, M. E., FALLER, B. A., ALBAIN, K. S., YANAGIHARA, R. H., GARLAND, L. L., BYERS, L. A., WANG, D., KOCZYWAS, M., REDMAN, M. W., KELLY, K. & GANDARA, D. R. 2019. S1206: A dose-finding study followed by a phase II randomized placebo-controlled trial of chemoradiotherapy (CRT) with or without veliparib in stage III non-small cell lung cancer (NSCLC). *Journal of Clinical Oncology,* 37**,** 8523-8523.

ARNOLD, M., MORGAN, E., RUMGAY, H., MAFRA, A., SINGH, D., LAVERSANNE, M., VIGNAT, J., GRALOW, J. R., CARDOSO, F., SIESLING, S. & SOERJOMATARAM, I. 2022. Current and future burden of breast cancer: Global statistics for 2020 and 2040. *The Breast,* 66**,** 15-23.

ATTWOOLL, C., LAZZERINI DENCHI, E. & HELIN, K. 2004. The E2F family: specific functions and overlapping interests. *Embo j,* 23**,** 4709-16.

AUGEREAU, P., PATSOURIS, A., BOURBOULOUX, E., GOURMELON, C., ABADIE LACOURTOISIE, S., BERTON RIGAUD, D., SOULIÉ, P., FRENEL, J. S. & CAMPONE, M. 2017. Hormonoresistance in advanced breast cancer: a new revolution in endocrine therapy. *Ther Adv Med Oncol,* 9**,** 335-346.

BALAKRISHNAN, L. & STEWART, J. A. 2019. *DNA Repair: Methods and Protocols*, Springer.

BANÁTH, J. P., KLOKOV, D., MACPHAIL, S. H., BANUELOS, C. A. & OLIVE, P. L. 2010. Residual γH2AX foci as an indication of lethal DNA lesions. *BMC Cancer,* 10**,** 4.

BANIN, S., MOYAL, L., SHIEH, S., TAYA, Y., ANDERSON, C. W., CHESSA, L., SMORODINSKY, N. I., PRIVES, C., REISS, Y., SHILOH, Y. & ZIV, Y. 1998. Enhanced phosphorylation of p53 by ATM in response to DNA damage. *Science,* 281**,** 1674-7.

BARCELLINI, A., LOAP, P., MURATA, K., VILLA, R., KIROVA, Y., OKONOGI, N. & ORLANDI, E. 2021. PARP Inhibitors in Combination with Radiotherapy: To Do or Not to Do? *Cancers (Basel),* 13.

BARNES, D. E., TOMKINSON, A. E., LEHMANN, A. R., WEBSTER, A. D. & LINDAHL, T. 1992. Mutations in the DNA ligase I gene of an individual with immunodeficiencies and cellular hypersensitivity to DNA-damaging agents. *Cell,* 69**,** 495-503.

BASKAR, R., DAI, J., WENLONG, N., YEO, R. & YEOH, K. W. 2014. Biological response of cancer cells to radiation treatment. *Front Mol Biosci,* 1**,** 24.

BAUER, N. C., CORBETT, A. H. & DOETSCH, P. W. 2015. The current state of eukaryotic DNA base damage and repair. *Nucleic acids research,* 43**,** 10083-10101.

BAXTER, P. A., SU, J. M., ONAR-THOMAS, A., BILLUPS, C. A., LI, X. N., POUSSAINT, T. Y., SMITH, E. R., THOMPSON, P., ADESINA, A., ANSELL, P., GIRANDA, V., PAULINO, A., KILBURN, L., QUADDOUMI, I., BRONISCER, A., BLANEY, S. M., DUNKEL, I. J. & FOULADI, M. 2020. A phase I/II study of veliparib (ABT-888) with radiation and temozolomide in newly diagnosed diffuse pontine glioma: a Pediatric Brain Tumor Consortium study. *Neuro Oncol,* 22**,** 875-885.

BEDFORD, J. S. 1991. Sublethal damage, potentially lethal damage, and chromosomal aberrations in mammalian cells exposed to ionizing radiations. *Int J Radiat Oncol Biol Phys,* 21**,** 1457-69.

BENCOKOVA, Z., KAUFMANN, M. R., PIRES, I. M., LECANE, P. S., GIACCIA, A. J. & HAMMOND, E. M. 2009. ATM activation and signaling under hypoxic conditions. *Mol Cell Biol,* 29**,** 526-37.

BENDELL, J. C., SHAFIQUE, M. R., PEREZ, B., CHENNOUFI, S., BEIER, F., TRANG, K. & ANTONIA, S. J. 2019. Phase 1, open-label, dose-escalation study of M3814 + avelumab ± radiotherapy (RT) in patients (pts) with advanced solid tumors. *Journal of Clinical Oncology,* 37**,** TPS3169-TPS3169.

BENDER, M. A. & PRESCOTT, D. M. 1962. DNA synthesis and mitosis in cultures of human peripheral leukocytes. *Experimental Cell Research,* 27**,** 221-229.

BERMEJO, R., LAI, M. S. & FOIANI, M. 2012. Preventing replication stress to maintain genome stability: resolving conflicts between replication and transcription. *Molecular cell,* 45**,** 710-718.

BERTI, M. & VINDIGNI, A. 2016. Replication stress: getting back on track. *Nature Structural & Molecular Biology,* 23**,** 103-109.

BERTOLI, C., SKOTHEIM, J. M. & DE BRUIN, R. A. 2013. Control of cell cycle transcription during G1 and S phases. *Nat Rev Mol Cell Biol,* 14**,** 518-28.

BESSON, A., DOWDY, S. F. & ROBERTS, J. M. 2008. CDK Inhibitors: Cell Cycle Regulators and Beyond. *Developmental Cell,* 14**,** 159-169.

BLACKFORD, A. N. & JACKSON, S. P. 2017. ATM, ATR, and DNA-PK: The Trinity at the Heart of the DNA Damage Response. *Molecular Cell,* 66**,** 801-817.

BLAKELEY, J. O., GROSSMAN, S. A., MIKKELSEN, T., ROSENFELD, M. R., PEEREBOOM, D., NABORS, L. B., CHI, A. S., EMMONS, G., GARCIA RIBAS, I.,

SUPKO, J. G., DESIDERI, S. & YE, X. 2015. Phase I study of iniparib concurrent with monthly or continuous temozolomide dosing schedules in patients with newly diagnosed malignant gliomas. *J Neurooncol,* 125**,** 123-31.
BOSACKI, C., BOULEFTOUR, W., SOTTON, S., VALLARD, A., DAGUENET, E., OUAZ, H., COJOCARU, I., MOSLEMI, D., MOLEKZADEHMOGHANI, M. & MAGNÉ, N. 2021. CDK 4/6 inhibitors combined with radiotherapy: A review of literature. *Clinical and Translational Radiation Oncology,* 26**,** 79-85.
BOULEFTOUR, W., ROWINSKI, E., LOUATI, S., SOTTON, S., WOZNY, A. S., MORENO-ACOSTA, P., MERY, B., RODRIGUEZ-LAFRASSE, C. & MAGNE, N. 2021. A Review of the Role of Hypoxia in Radioresistance in Cancer Therapy. *Med Sci Monit,* 27**,** e934116.
BOUQUET, F., OUSSET, M., BIARD, D., FALLONE, F., DAUVILLIER, S., FRIT, P., SALLES, B. & MULLER, C. 2011. A DNA-dependent stress response involving DNA-PK occurs in hypoxic cells and contributes to cellular adaptation to hypoxia. *Journal of Cell Science,* 124**,** 1943-1951.
BOUSTANI, J., GRAPIN, M., LAURENT, P. A., APETOH, L. & MIRJOLET, C. 2019. The 6th R of Radiobiology: Reactivation of Anti-Tumor Immune Response. *Cancers (Basel),* 11.
BREASTCANCERNOW 2022. Facts and Statistics 2021. *breastcancernow.org*.
BRIGHAM, HOSPITAL, W. S., 13, H. M. S. C. L. P. P. J. K. R., 25, G. D. A. B. C. O. M. C. C. J. D. L. A. & ILYA, I. F. S. B. R. S. K. R. B. B. B. B. R. E. T. L. J. T. V. Z. W. S. 2012. Comprehensive molecular portraits of human breast tumours. *Nature,* 490**,** 61-70.
BROWN, J. M., CARLSON, D. J. & BRENNER, D. J. 2014. The Tumor Radiobiology of SRS and SBRT: Are More Than the 5 Rs Involved? *International Journal of Radiation Oncology*Biology*Physics,* 88**,** 254-262.
BROWN, J. S. & JACKSON, S. P. 2015. Ubiquitylation, neddylation and the DNA damage response. *Open Biology,* 5**,** 150018.
BROWN, S., BANFILL, K., AZNAR, M. C., WHITEHURST, P. & FAIVRE FINN, C. 2019. The evolving role of radiotherapy in non-small cell lung cancer. *Br J Radiol,* 92**,** 20190524.
BRUNER, S. D., NORMAN, D. P. & VERDINE, G. L. 2000. Structural basis for recognition and repair of the endogenous mutagen 8-oxoguanine in DNA. *nature,* 403**,** 859-866.
BRYANT, A. K., BANEGAS, M. P., MARTINEZ, M. E., MELL, L. K. & MURPHY, J. D. 2017. Trends in Radiation Therapy among Cancer Survivors in the United States, 2000–2030. *Cancer Epidemiology, Biomarkers & Prevention,* 26**,** 963-970.
BRYANT, C., RAWLINSON, R. & MASSEY, A. J. 2014. Chk1 Inhibition as a novel therapeutic strategy for treating triple-negative breast and ovarian cancers. *BMC Cancer,* 14**,** 570.
BRYANT, H. E., PETERMANN, E., SCHULTZ, N., JEMTH, A. S., LOSEVA, O., ISSAEVA, N., JOHANSSON, F., FERNANDEZ, S., MCGLYNN, P. & HELLEDAY, T. 2009. PARP is activated at stalled forks to mediate Mre11-dependent replication restart and recombination. *The EMBO journal,* 28**,** 2601-2615.
BRYANT, H. E., SCHULTZ, N., THOMAS, H. D., PARKER, K. M., FLOWER, D., LOPEZ, E., KYLE, S., MEUTH, M., CURTIN, N. J. & HELLEDAY, T. 2005. Specific killing of BRCA2-deficient tumours with inhibitors of poly (ADP-ribose) polymerase. *Nature,* 434**,** 913-917.
BRYANT, H. E. & SHALL, S. 2015. Synthetic Lethality with Homologous Recombination Repair Defects. *PARP Inhibitors for Cancer Therapy***,** 315-344.

BUSCHTA-HEDAYAT, N., BUTERIN, T., HESS, M. T., MISSURA, M. & NAEGELI, H. 1999. Recognition of nonhybridizing base pairs during nucleotide excision repair of DNA. *Proc Natl Acad Sci U S A,* 96**,** 6090-5.

BYERS, K. F. 2021. Ribociclib and Abemaciclib: CDK4/6 Inhibitors for the Treatment of Hormone Receptor-Positive Metastatic Breast Cancer. *J Adv Pract Oncol,* 12**,** 100-107.

BYRSKI, T., GRONWALD, J., HUZARSKI, T., GRZYBOWSKA, E., BUDRYK, M., STAWICKA, M., MIERZWA, T., SZWIEC, M., WIŚNIOWSKI, R., SIOLEK, M., DENT, R., LUBINSKI, J. & NAROD, S. 2010. Pathologic Complete Response Rates in Young Women With BRCA1-Positive Breast Cancers After Neoadjuvant Chemotherapy. *Journal of Clinical Oncology,* 28**,** 375-379.

BYRUM, A. K., VINDIGNI, A. & MOSAMMAPARAST, N. 2019. Defining and modulating 'BRCAness'. *Trends in cell biology,* 29**,** 740-751.

BYUN, T. S., PACEK, M., YEE, M.-C., WALTER, J. C. & CIMPRICH, K. A. 2005. Functional uncoupling of MCM helicase and DNA polymerase activities activates the ATR-dependent checkpoint. *Genes & development,* 19**,** 1040-1052.

CAI, M. Y., DUNN, C. E., CHEN, W., KOCHUPURAKKAL, B. S., NGUYEN, H., MOREAU, L. A., SHAPIRO, G. I., PARMAR, K., KOZONO, D. & D'ANDREA, A. D. 2020. Cooperation of the ATM and Fanconi Anemia/BRCA Pathways in Double-Strand Break End Resection. *Cell Rep,* 30**,** 2402-2415.e5.

CALDECOTT, K. W. 2008. Single-strand break repair and genetic disease. *Nat Rev Genet,* 9**,** 619-31.

CANCERRESEARCHUK 2022. Breast cancer statistics. *Cancer research UK*.

CÁNEPA, E. T., SCASSA, M. E., CERUTI, J. M., MARAZITA, M. C., CARCAGNO, A. L., SIRKIN, P. F. & OGARA, M. F. 2007. INK4 proteins, a family of mammalian CDK inhibitors with novel biological functions. *IUBMB Life,* 59**,** 419-26.

CANNAN, W. J. & PEDERSON, D. S. 2016. Mechanisms and Consequences of Double-Strand DNA Break Formation in Chromatin. *J Cell Physiol,* 231**,** 3-14.

CAO, J., WANG, Y., DONG, R., LIN, G., ZHANG, N., WANG, J., LIN, N., GU, Y., DING, L., YING, M., HE, Q. & YANG, B. 2015. Hypoxia-Induced WSB1 Promotes the Metastatic Potential of Osteosarcoma Cells. *Cancer Res,* 75**,** 4839-51.

CECCALDI, R., SARANGI, P. & D'ANDREA, A. D. 2016. The Fanconi anaemia pathway: new players and new functions. *Nature Reviews Molecular Cell Biology,* 17**,** 337-349.

CERAMI, E., GAO, J., DOGRUSOZ, U., GROSS, B. E., SUMER, S. O., AKSOY, B. A., JACOBSEN, A., BYRNE, C. J., HEUER, M. L., LARSSON, E., ANTIPIN, Y., REVA, B., GOLDBERG, A. P., SANDER, C. & SCHULTZ, N. 2012. The cBio cancer genomics portal: an open platform for exploring multidimensional cancer genomics data. *Cancer Discov,* 2**,** 401-4.

CHABOT, P., HSIA, T. C., RYU, J. S., GORBUNOVA, V., BELDA-INIESTA, C., BALL, D., KIO, E., MEHTA, M., PAPP, K., QIN, Q., QIAN, J., HOLEN, K. D., GIRANDA, V. & SUH, J. H. 2017. Veliparib in combination with whole-brain radiation therapy for patients with brain metastases from non-small cell lung cancer: results of a randomized, global, placebo-controlled study. *J Neurooncol,* 131**,** 105-115.

CHANG, H. H. Y., PANNUNZIO, N. R., ADACHI, N. & LIEBER, M. R. 2017. Non-homologous DNA end joining and alternative pathways to double-strand break repair. *Nature Reviews Molecular Cell Biology,* 18**,** 495-506.

CHATTERJEE, N. & WALKER, G. C. 2017. Mechanisms of DNA damage, repair, and mutagenesis. *Environ Mol Mutagen,* 58**,** 235-263.

CHAUDHARY, L. N. 2020. Early stage triple negative breast cancer: Management and future directions. *Semin Oncol,* 47**,** 201-208.

CHE, J., JIN, Z., YAN, F., YOU, J., XIE, J., CHEN, B., CHENG, G., ZHU, H., HE, Q., HU, Y., YANG, B., CAO, J. & DONG, X. 2021. Discovery of 5,6-Bis(4-methoxy-3-methylphenyl)pyridin-2-amine as a WSB1 Degrader to Inhibit Cancer Cell Metastasis. *Journal of Medicinal Chemistry,* 64**,** 8621-8643.

CHEN, J. 2016. The Cell-Cycle Arrest and Apoptotic Functions of p53 in Tumor Initiation and Progression. *Cold Spring Harb Perspect Med,* 6**,** a026104.

CHEN, L., NIEVERA, C. J., LEE, A. Y. & WU, X. 2008. Cell cycle-dependent complex formation of BRCA1.CtIP.MRN is important for DNA double-strand break repair. *J Biol Chem,* 283**,** 7713-20.

CHEN, M. C., HSU, W. L., CHANG, W. L. & CHOU, T. C. 2017. Antiangiogenic activity of phthalides-enriched Angelica Sinensis extract by suppressing WSB-1/pVHL/HIF-1alpha/VEGF signaling in bladder cancer. *Sci Rep,* 7**,** 5376.

CHEN, Q. R., BILKE, S., WEI, J. S., GREER, B. T., STEINBERG, S. M., WESTERMANN, F., SCHWAB, M. & KHAN, J. 2006. Increased WSB1 copy number correlates with its over-expression which associates with increased survival in neuroblastoma. *Genes Chromosomes Cancer,* 45**,** 856-62.

CHEN, T., STEPHENS, P. A., MIDDLETON, F. K. & CURTIN, N. J. 2012. Targeting the S and G2 checkpoint to treat cancer. *Drug discovery today,* 17**,** 194-202.

CHIRNOMAS, D., HORNBERGER, K. R. & CREWS, C. M. 2023. Protein degraders enter the clinic — a new approach to cancer therapy. *Nature Reviews Clinical Oncology*.

CHOI, D. W., SEO, Y. M., KIM, E. A., SUNG, K. S., AHN, J. W., PARK, S. J., LEE, S. R. & CHOI, C. Y. 2008. Ubiquitination and degradation of homeodomain-interacting protein kinase 2 by WD40 repeat/SOCS box protein WSB-1. *J Biol Chem,* 283**,** 4682-9.

CHOPRA, N., TOVEY, H., PEARSON, A., CUTTS, R., TOMS, C., PROSZEK, P., HUBANK, M., DOWSETT, M., DODSON, A., DALEY, F., KRIPLANI, D., GEVENSLEBEN, H., DAVIES, H. R., DEGASPERI, A., ROYLANCE, R., CHAN, S., TUTT, A., SKENE, A., EVANS, A., BLISS, J. M., NIK-ZAINAL, S. & TURNER, N. C. 2020. Homologous recombination DNA repair deficiency and PARP inhibition activity in primary triple negative breast cancer. *Nature Communications,* 11**,** 2662.

CHOWDHARY, M., SEN, N., CHOWDHARY, A., USHA, L., COBLEIGH, M. A., WANG, D., PATEL, K. R., BARRY, P. N. & RAO, R. D. 2019. Safety and Efficacy of Palbociclib and Radiation Therapy in Patients With Metastatic Breast Cancer: Initial Results of a Novel Combination. *Adv Radiat Oncol,* 4**,** 453-457.

COLEMAN, C. N. & TURRISI, A. T. 1990. Radiation and chemotherapy sensitizers and protectors. *Crit Rev Oncol Hematol,* 10**,** 225-52.

CORTESI, L., RUGO, H. S. & JACKISCH, C. 2021. An Overview of PARP Inhibitors for the Treatment of Breast Cancer. *Target Oncol,* 16**,** 255-282.

CORTEZ, D., WANG, Y., QIN, J. & ELLEDGE, S. J. 1999. Requirement of ATM-Dependent Phosphorylation of Brca1 in the DNA Damage Response to Double-Strand Breaks. *Science,* 286**,** 1162-1166.

COSTA, B., AMORIM, I., GÄRTNER, F. & VALE, N. 2020. Understanding Breast cancer: from conventional therapies to repurposed drugs. *European Journal of Pharmaceutical Sciences,* 151**,** 105401.

COSTANZO, V., ROBERTSON, K., BIBIKOVA, M., KIM, E., GRIECO, D., GOTTESMAN, M., CARROLL, D. & GAUTIER, J. 2001. Mre11 protein complex prevents double-strand break accumulation during chromosomal DNA replication. *Molecular cell,* 8**,** 137-147.

CRABTREE, H. G., CRAMER, W. & MURRAY, J. A. 1933. The action of radium on cancer cells. II.—Some factors determining the susceptibility of cancer cells to radium. *Proceedings of the Royal Society of London. Series B, Containing Papers of a Biological Character,* 113**,** 238-250.

CUNEO, K. C., MORGAN, M. A., SAHAI, V., SCHIPPER, M. J., PARSELS, L. A., PARSELS, J. D., DEVASIA, T., AL-HAWARAY, M., CHO, C. S., NATHAN, H., MAYBAUM, J., ZALUPSKI, M. M. & LAWRENCE, T. S. 2019. Dose Escalation Trial of the Wee1 Inhibitor Adavosertib (AZD1775) in Combination With Gemcitabine and Radiation for Patients With Locally Advanced Pancreatic Cancer. *J Clin Oncol,* 37**,** 2643-2650.

CURTIS, C., SHAH, S. P., CHIN, S.-F., TURASHVILI, G., RUEDA, O. M., DUNNING, M. J., SPEED, D., LYNCH, A. G., SAMARAJIWA, S., YUAN, Y., GRÄF, S., HA, G., HAFFARI, G., BASHASHATI, A., RUSSELL, R., MCKINNEY, S., CALDAS, C., APARICIO, S., CURTIS†, C., SHAH, S. P., CALDAS, C., APARICIO, S., BRENTON, J. D., ELLIS, I., HUNTSMAN, D., PINDER, S., PURUSHOTHAM, A., MURPHY, L., CALDAS, C., APARICIO, S., CALDAS, C., BARDWELL, H., CHIN, S.-F., CURTIS, C., DING, Z., GRÄF, S., JONES, L., LIU, B., LYNCH, A. G., PAPATHEODOROU, I., SAMMUT, S. J., WISHART, G., APARICIO, S., CHIA, S., GELMON, K., HUNTSMAN, D., MCKINNEY, S., SPEERS, C., TURASHVILI, G., WATSON, P., ELLIS, I., BLAMEY, R., GREEN, A., MACMILLAN, D., RAKHA, E., PURUSHOTHAM, A., GILLETT, C., GRIGORIADIS, A., PINDER, S., DE RINALDIS, E., TUTT, A., MURPHY, L., PARISIEN, M., TROUP, S., CALDAS, C., CHIN, S.-F., CHAN, D., FIELDING, C., MAIA, A.-T., MCGUIRE, S., OSBORNE, M., SAYALERO, S. M., SPITERI, I., HADFIELD, J., APARICIO, S., TURASHVILI, G., BELL, L., CHOW, K., GALE, N., HUNTSMAN, D., KOVALIK, M., NG, Y., PRENTICE, L., CALDAS, C., TAVARÉ, S., CURTIS, C., DUNNING, M. J., GRÄF, S., LYNCH, A. G., RUEDA, O. M., RUSSELL, R., SAMARAJIWA, S., SPEED, D., MARKOWETZ, F., YUAN, Y., BRENTON, J. D., APARICIO, S., SHAH, S. P., BASHASHATI, A., HA, G., et al. 2012. The genomic and transcriptomic architecture of 2,000 breast tumours reveals novel subgroups. *Nature,* 486**,** 346-352.

CZITO, B. G., DEMING, D. A., JAMESON, G. S., MULCAHY, M. F., VAGHEFI, H., DUDLEY, M. W., HOLEN, K. D., DELUCA, A., MITTAPALLI, R. K., MUNASINGHE, W., HE, L., ZALCBERG, J. R., NGAN, S. Y., KOMARNITSKY, P. & MICHAEL, M. 2017. Safety and tolerability of veliparib combined with capecitabine plus radiotherapy in patients with locally advanced rectal cancer: a phase 1b study. *Lancet Gastroenterol Hepatol,* 2**,** 418-426.

D'ORAZI, G., CECCHINELLI, B., BRUNO, T., MANNI, I., HIGASHIMOTO, Y., SAITO, S. I., GOSTISSA, M., COEN, S., MARCHETTI, A. & DEL SAL, G. 2002. Homeodomain-interacting protein kinase-2 phosphorylates p53 at Ser 46 and mediates apoptosis. *Nature cell biology,* 4**,** 11-19.

DALMAU, E., ARMENGOL-ALONSO, A., MUÑOZ, M. & SEGUÍ-PALMER, M. Á. 2014. Current status of hormone therapy in patients with hormone receptor positive (HR+) advanced breast cancer. *The Breast,* 23**,** 710-720.

DARZYNKIEWICZ, Z., SHARPLESS, T., STAIANO-COICO, L. & MELAMED, M. R. 1980. Subcompartments of the G1 phase of cell cycle detected by flow cytometry. *Proceedings of the National Academy of Sciences,* 77**,** 6696-6699.

DE HAAN, R., VAN WERKHOVEN, E., VAN DEN HEUVEL, M. M., PEULEN, H. M. U., SONKE, G. S., ELKHUIZEN, P., VAN DEN BREKEL, M. W. M., TESSELAAR, M. E. T., VENS, C., SCHELLENS, J. H. M., VAN TRIEST, B. & VERHEIJ, M.

2019. Study protocols of three parallel phase 1 trials combining radical radiotherapy with the PARP inhibitor olaparib. *BMC Cancer,* 19**,** 901.

DEDES, K. J., WILKERSON, P. M., WETTERSKOG, D., WEIGELT, B., ASHWORTH, A. & REIS-FILHO, J. S. 2011. Synthetic lethality of PARP inhibition in cancers lacking BRCA1 and BRCA2 mutations. *Cell Cycle,* 10**,** 1192-9.

DENTICE, M., BANDYOPADHYAY, A., GEREBEN, B., CALLEBAUT, I., CHRISTOFFOLETE, M. A., KIM, B. W., NISSIM, S., MORNON, J. P., ZAVACKI, A. M., ZEOLD, A., CAPELO, L. P., CURCIO-MORELLI, C., RIBEIRO, R., HARNEY, J. W., TABIN, C. J. & BIANCO, A. C. 2005. The Hedgehog-inducible ubiquitin ligase subunit WSB-1 modulates thyroid hormone activation and PTHrP secretion in the developing growth plate. *Nat Cell Biol,* 7**,** 698-705.

DEWIRE, M., FULLER, C., HUMMEL, T., CHOW, L., SALLOUM, R., PATER, L., DRISSI, R., LU, Q., STEVENSON, C., LANE, A., BRENEMAN, J., WITTE, D., LEACH, J. & FOULADI, M. 2018. DIPG-73. CLEE011XUS17T (NCT 02607124): A PHASE I/II STUDY OF RIBOCICLIB (LEE011) FOLLOWING RADIATION THERAPY (RT) IN CHILDREN AND YOUNG ADULTS WITH NEWLY DIAGNOSED NON-BIOPSIED DIFFUSE PONTINE GLIOMAS (DIPG) AND RB+ BIOPSIED DIPG AND HIGH GRADE GLIOMAS (HGG). *Neuro-Oncology,* 20**,** i64-i64.

DIANOV, G., BISCHOFF, C., PIOTROWSKI, J. & BOHR, V. A. 1998. Repair Pathways for Processing of 8-Oxoguanine in DNA by Mammalian Cell Extracts*. *Journal of Biological Chemistry,* 273**,** 33811-33816.

DILALLA, V., CHAPUT, G., WILLIAMS, T. & SULTANEM, K. 2020. Radiotherapy Side Effects: Integrating a Survivorship Clinical Lens to Better Serve Patients. *Current Oncology,* 27**,** 107-112.

DILLON, M. T., BOYLAN, Z., SMITH, D., GUEVARA, J., MOHAMMED, K., PECKITT, C., SAUNDERS, M., BANERJI, U., CLACK, G., SMITH, S. A., SPICER, J. F., FORSTER, M. D. & HARRINGTON, K. J. 2018. PATRIOT: A phase I study to assess the tolerability, safety and biological effects of a specific ataxia telangiectasia and Rad3-related (ATR) inhibitor (AZD6738) as a single agent and in combination with palliative radiation therapy in patients with solid tumours. *Clin Transl Radiat Oncol,* 12**,** 16-20.

DJUZENOVA, C. S., ZIMMERMANN, M., KATZER, A., FIEDLER, V., DISTEL, L. V., GASSER, M., WAAGA-GASSER, A.-M., FLENTJE, M. & POLAT, B. 2015. A prospective study on histone γ-H2AX and 53BP1 foci expression in rectal carcinoma patients: correlation with radiation therapy-induced outcome. *BMC Cancer,* 15**,** 856.

DO, K., WILSKER, D., JI, J., ZLOTT, J., FRESHWATER, T., KINDERS, R. J., COLLINS, J., CHEN, A. P., DOROSHOW, J. H. & KUMMAR, S. 2015. Phase I study of single-agent AZD1775 (MK-1775), a Wee1 kinase inhibitor, in patients with refractory solid tumors. *Journal of Clinical Oncology,* 33**,** 3409.

DO, K. T., KOCHUPURAKKAL, B., KELLAND, S., DE JONGE, A., HEDGLIN, J., POWERS, A., QUINN, N., GANNON, C., VUONG, L., PARMAR, K., LAZARO, J. B., D'ANDREA, A. D. & SHAPIRO, G. I. 2021. Phase 1 Combination Study of the CHK1 Inhibitor Prexasertib and the PARP Inhibitor Olaparib in High-grade Serous Ovarian Cancer and Other Solid Tumors. *Clin Cancer Res,* 27**,** 4710-4716.

DOETSCH, P. W. & CUNNINGHAM, R. P. 1990. The enzymology of apurinic/apyrimidinic endonucleases. *Mutation Research/DNA Repair,* 236**,** 173-201.

DUDÁS, A. & CHOVANEC, M. 2004. DNA double-strand break repair by homologous recombination. *Mutat Res,* 566**,** 131-67.

DUNNE-DALY, C. F. 1999. Principles of radiotherapy and radiobiology. *Seminars in Oncology Nursing,* 15**,** 250-259.
EGRI, P. & GEREBEN, B. 2014. Minimal requirements for ubiquitination-mediated regulation of thyroid hormone activation. *J Mol Endocrinol,* 53**,** 217-26.
ELBANNA, M., CHOWDHURY, N. N., RHOME, R. & FISHEL, M. L. 2021. Clinical and Preclinical Outcomes of Combining Targeted Therapy With Radiotherapy. *Frontiers in Oncology,* 11.
ENNS, L., RASOULI-NIA, A., HENDZEL, M., MARPLES, B. & WEINFELD, M. 2015. Association of ATM activation and DNA repair with induced radioresistance after low-dose irradiation. *Radiat Prot Dosimetry,* 166**,** 131-6.
ERKELAND, S. J., AARTS, L. H., IRANDOUST, M., ROOVERS, O., KLOMP, A., VALKHOF, M., GITS, J., EYCKERMAN, S., TAVERNIER, J. & TOUW, I. P. 2007. Novel role of WD40 and SOCS box protein-2 in steady-state distribution of granulocyte colony-stimulating factor receptor and G-CSF-controlled proliferation and differentiation signaling. *Oncogene,* 26**,** 1985-94.
EWING, D. 1998. The oxygen fixation hypothesis: a reevaluation. *Am J Clin Oncol,* 21**,** 355-61.
FABBRIZI, M. R., HUGHES, J. R. & PARSONS, J. L. 2021. The Enzyme-Modified Neutral Comet (EMNC) Assay for Complex DNA Damage Detection. *Methods Protoc,* 4.
FALCK, J., MAILAND, N., SYLJUÅSEN, R. G., BARTEK, J. & LUKAS, J. 2001. The ATM–Chk2–Cdc25A checkpoint pathway guards against radioresistant DNA synthesis. *Nature,* 410**,** 842-847.
FANALE, D., BAZAN, V., CARUSO, S., CASTIGLIA, M., BRONTE, G., ROLFO, C., CICERO, G. & RUSSO, A. 2013. Hypoxia and human genome stability: downregulation of BRCA2 expression in breast cancer cell lines. *Biomed Res Int,* 2013**,** 746858.
FARMER, H., MCCABE, N., LORD, C. J., TUTT, A. N., JOHNSON, D. A., RICHARDSON, T. B., SANTAROSA, M., DILLON, K. J., HICKSON, I. & KNIGHTS, C. 2005. Targeting the DNA repair defect in BRCA mutant cells as a therapeutic strategy. *Nature,* 434**,** 917-921.
FENG, W., DI RIENZI, S. C., RAGHURAMAN, M. K. & BREWER, B. J. 2011. Replication Stress-Induced Chromosome Breakage Is Correlated with Replication Fork Progression and Is Preceded by Single-Stranded DNA Formation. *G3 Genes|Genomes|Genetics,* 1**,** 327-335.
FIGURA, N. B., POTLURI, T. K., MOHAMMADI, H., OLIVER, D. E., ARRINGTON, J. A., ROBINSON, T. J., ETAME, A. B., TRAN, N. D., LIU, J. K., SOLIMAN, H., FORSYTH, P. A., SAHEBJAM, S., YU, H. M., HAN, H. S. & AHMED, K. A. 2019. CDK 4/6 inhibitors and stereotactic radiation in the management of hormone receptor positive breast cancer brain metastases. *Journal of Neuro-Oncology,* 144**,** 583-589.
FINN, R. S., BOER, K., BONDARENKO, I., PATEL, R., PINTER, T., SCHMIDT, M., SHPARYK, Y. V., THUMMALA, A., VOITKO, N., BANANIS, E., MCROY, L., WILNER, K., HUANG, X., KIM, S., SLAMON, D. J. & ETTL, J. 2020. Overall survival results from the randomized phase 2 study of palbociclib in combination with letrozole versus letrozole alone for first-line treatment of ER+/HER2- advanced breast cancer (PALOMA-1, TRIO-18). *Breast Cancer Res Treat,* 183**,** 419-428.
FOK, J. H. L., RAMOS-MONTOYA, A., VAZQUEZ-CHANTADA, M., WIJNHOVEN, P. W. G., FOLLIA, V., JAMES, N., FARRINGTON, P. M., KARMOKAR, A., WILLIS, S. E., CAIRNS, J., NIKKILÄ, J., BEATTIE, D., LAMONT, G. M., FINLAY, M. R. V., WILSON, J., SMITH, A., O'CONNOR, L. O., LING, S., FAWELL, S. E., O'CONNOR, M. J., HOLLINGSWORTH, S. J., DEAN, E.,

GOLDBERG, F. W., DAVIES, B. R. & CADOGAN, E. B. 2019. AZD7648 is a potent and selective DNA-PK inhibitor that enhances radiation, chemotherapy and olaparib activity. *Nature Communications,* 10**,** 5065.

FORSTER, M. D., MENDES, R., HARRINGTON, K. J., URBANO, T. G., BAINES, H., SPANSWICK, V. J., ENSELL, L., HARTLEY, J. A., ADELEKE, S., GOUGIS, P., LEADER, D., MCDOWELL, C., LOPES, A., TEAGUE, J., FORSYTH, S. & BEARE, S. 2016. ORCA-2: A phase I study of olaparib in addition to cisplatin-based concurrent chemoradiotherapy for patients with high risk locally advanced squamous cell carcinoma of the head and neck. *Journal of Clinical Oncology,* 34**,** TPS6108-TPS6108.

FORTINI, P. & DOGLIOTTI, E. 2007. Base damage and single-strand break repair: mechanisms and functional significance of short-and long-patch repair subpathways. *DNA repair,* 6**,** 398-409.

FOUAD, S., HAUTON, D. & D'ANGIOLELLA, V. 2021. E2F1: Cause and Consequence of DNA Replication Stress. *Frontiers in Molecular Biosciences,* 7.

FOUAD, S., WELLS, O. S., HILL, M. A. & D'ANGIOLELLA, V. 2019. Cullin Ring Ubiquitin Ligases (CRLs) in Cancer: Responses to Ionizing Radiation (IR) Treatment. *Frontiers in Physiology,* 10.

FOWLER, J. F. 1989. The linear-quadratic formula and progress in fractionated radiotherapy. *Br J Radiol,* 62**,** 679-94.

FRADET-TURCOTTE, A., SITZ, J., GRAPTON, D. & ORTHWEIN, A. 2016. BRCA2 functions: from DNA repair to replication fork stabilization. *Endocr Relat Cancer,* 23**,** T1-t17.

FRAGKOS, M., JURVANSUU, J. & BEARD, P. 2009. H2AX Is Required for Cell Cycle Arrest via the p53/p21 Pathway. *Molecular and Cellular Biology,* 29**,** 2828-2840.

FRANKEN, N. A., OEI, A. L., KOK, H. P., RODERMOND, H. M., SMINIA, P., CREZEE, J., STALPERS, L. J. & BARENDSEN, G. W. 2013. Cell survival and radiosensitisation: modulation of the linear and quadratic parameters of the LQ model (Review). *Int J Oncol,* 42**,** 1501-15.

FRIT, P., BARBOULE, N., YUAN, Y., GOMEZ, D. & CALSOU, P. 2014. Alternative end-joining pathway (s): bricolage at DNA breaks. *DNA repair,* 17**,** 81-97.

FU, D., CALVO, J. A. & SAMSON, L. D. 2012. Balancing repair and tolerance of DNA damage caused by alkylating agents. *Nature Reviews Cancer,* 12**,** 104-120.

FULTON, B., SHORT, S. C., JAMES, A., NOWICKI, S., MCBAIN, C., JEFFERIES, S., KELLY, C., STOBO, J., MORRIS, A., WILLIAMSON, A. & CHALMERS, A. J. 2018. PARADIGM-2: Two parallel phase I studies of olaparib and radiotherapy or olaparib and radiotherapy plus temozolomide in patients with newly diagnosed glioblastoma, with treatment stratified by MGMT status. *Clinical and Translational Radiation Oncology,* 8**,** 12-16.

GAGOU, M. E., ZUAZUA-VILLAR, P. & MEUTH, M. 2010. Enhanced H2AX phosphorylation, DNA replication fork arrest, and cell death in the absence of Chk1. *Mol Biol Cell,* 21**,** 739-52.

GANGULY, B., DOLFI, S. C., RODRIGUEZ-RODRIGUEZ, L., GANESAN, S. & HIRSHFIELD, K. M. 2016. Role of Biomarkers in the Development of PARP Inhibitors. *Biomark Cancer,* 8**,** 15-25.

GAO, X., YOU, J., GONG, Y., YUAN, M., ZHU, H., FANG, L., ZHU, H., YING, M., HE, Q., YANG, B. & CAO, J. 2022. WSB1 regulates c-Myc expression through β-catenin signaling and forms a feedforward circuit. *Acta Pharmaceutica Sinica B,* 12**,** 1225-1239.

GATEI, M., SCOTT, S. P., FILIPPOVITCH, I., SORONIKA, N., LAVIN, M. F., WEBER, B. & KHANNA, K. K. 2000. Role for ATM in DNA Damage-induced Phosphorylation of BRCA11. *Cancer Research,* 60**,** 3299-3304.

GATEI, M., ZHOU, B. B., HOBSON, K., SCOTT, S., YOUNG, D. & KHANNA, K. K. 2001. Ataxia telangiectasia mutated (ATM) kinase and ATM and Rad3 related kinase mediate phosphorylation of Brca1 at distinct and overlapping sites. In vivo assessment using phospho-specific antibodies. *J Biol Chem,* 276**,** 17276-80.

GENG, W., TIAN, D., WANG, Q., SHAN, S., ZHOU, J., XU, W. & SHAN, H. 2019. DNA-PKcs inhibitor increases the sensitivity of gastric cancer cells to radiotherapy. *Oncol Rep,* 42**,** 561-570.

GIAQUINTO, A. N., SUNG, H., MILLER, K. D., KRAMER, J. L., NEWMAN, L. A., MINIHAN, A., JEMAL, A. & SIEGEL, R. L. 2022. Breast Cancer Statistics, 2022. *CA: A Cancer Journal for Clinicians,* 72**,** 524-541.

GM, C. 2000. The Eukaryotic Cell Cycle. *The Cell: A Molecular Approach. 2nd edition. Sunderland (MA): Sinauer Associates,* Sunderland (MA): Sinauer Associates;.

GODA, N., RYAN, H. E., KHADIVI, B., MCNULTY, W., RICKERT, R. C. & JOHNSON, R. S. 2003. Hypoxia-inducible factor 1alpha is essential for cell cycle arrest during hypoxia. *Mol Cell Biol,* 23**,** 359-69.

GORDHANDAS, S. B., MANNING-GEIST, B., HENSON, C., IYER, G., GARDNER, G. J., SONODA, Y., MOORE, K. N., AGHAJANIAN, C., CHUI, M. H. & GRISHAM, R. N. 2022. Pre-clinical activity of the oral DNA-PK inhibitor, peposertib (M3814), combined with radiation in xenograft models of cervical cancer. *Scientific Reports,* 12**,** 974.

GÖTTGENS, E.-L., BUSSINK, J., LESZCZYNSKA, K. B., PETERS, H., SPAN, P. N. & HAMMOND, E. M. 2019. Inhibition of CDK4/CDK6 Enhances Radiosensitivity of HPV Negative Head and Neck Squamous Cell Carcinomas. *International Journal of Radiation Oncology*Biology*Physics,* 105**,** 548-558.

GOURLEY, C., BALMAÑA, J., LEDERMANN, J. A., SERRA, V., DENT, R., LOIBL, S., PUJADE-LAURAINE, E. & BOULTON, S. J. 2019. Moving From Poly (ADP-Ribose) Polymerase Inhibition to Targeting DNA Repair and DNA Damage Response in Cancer Therapy. *J Clin Oncol,* 37**,** 2257-2269.

GRALEWSKA, P., GAJEK, A., MARCZAK, A. & ROGALSKA, A. 2020. Participation of the ATR/CHK1 pathway in replicative stress targeted therapy of high-grade ovarian cancer. *Journal of Hematology & Oncology,* 13**,** 39.

GUERAU-DE-ARELLANO, M., LIU, Y., MEISEN, W. H., PITT, D., RACKE, M. K. & LOVETT-RACKE, A. E. 2015. Analysis of miRNA in Normal Appearing White Matter to Identify Altered CNS Pathways in Multiple Sclerosis. *J Autoimmune Disord,* 1.

HABER, J. E. 2000. Partners and pathways: repairing a double-strand break. *Trends in Genetics,* 16**,** 259-264.

HALL, E. J. & GIACCIA, A. J. 2006. *Radiobiology for the Radiologist,* Philadelphia.

HALLIWELL, B. & GUTTERIDGE, J. M. C. 1990. [1] Role of free radicals and catalytic metal ions in human disease: An overview. *Methods in Enzymology.* Academic Press.

HAMMOND, E. M., DENKO, N. C., DORIE, M. J., ABRAHAM, R. T. & GIACCIA, A. J. 2002. Hypoxia links ATR and p53 through replication arrest. *Mol Cell Biol,* 22**,** 1834-43.

HANNA, J. A., DRUMMOND, C. J., GARCIA, M. R., GO, J. C., FINKELSTEIN, D., REHG, J. E. & HATLEY, M. E. 2017. Biallelic Dicer1 Loss Mediated by aP2-Cre Drives Angiosarcoma. *Cancer Res,* 77**,** 6109-6118.

HARPER, J. W., ELLEDGE, S. J., KEYOMARSI, K., DYNLACHT, B., TSAI, L.-H., ZHANG, P., DOBROWOLSKI, S., BAI, C., CONNELL-CROWLEY, L. & SWINDELL, E. 1995. Inhibition of cyclin-dependent kinases by p21. *Molecular biology of the cell,* 6**,** 387-400.

HARTMAN, A. R., KALDATE, R. R., SAILER, L. M., PAINTER, L., GRIER, C. E., ENDSLEY, R. R., GRIFFIN, M., HAMILTON, S. A., FRYE, C. A. & SILBERMAN, M. A. 2012. Prevalence of BRCA mutations in an unselected population of triple-negative breast cancer. *Cancer,* 118**,** 2787-2795.

HAUSSMANN, J., CORRADINI, S., NESTLE-KRAEMLING, C., BÖLKE, E., NJANANG, F. J. D., TAMASKOVICS, B., ORTH, K., RUCKHAEBERLE, E., FEHM, T., MOHRMANN, S., SIMIANTONAKIS, I., BUDACH, W. & MATUSCHEK, C. 2020. Recent advances in radiotherapy of breast cancer. *Radiation Oncology,* 15**,** 71.

HE, Z., CHEN, Z., TAN, M., ELINGARAMI, S., LIU, Y., LI, T., DENG, Y., HE, N., LI, S., FU, J. & LI, W. 2020. A review on methods for diagnosis of breast cancer cells and tissues. *Cell Prolif,* 53**,** e12822.

HEGAN, D. C., LU, Y., STACHELEK, G. C., CROSBY, M. E., BINDRA, R. S. & GLAZER, P. M. 2010. Inhibition of poly(ADP-ribose) polymerase down-regulates BRCA1 and RAD51 in a pathway mediated by E2F4 and p130. *Proceedings of the National Academy of Sciences,* 107**,** 2201-2206.

HEGDE, M. L., HAZRA, T. K. & MITRA, S. 2008. Early steps in the DNA base excision/single-strand interruption repair pathway in mammalian cells. *Cell Res,* 18**,** 27-47.

HILL, J. W., HAZRA, T. K., IZUMI, T. & MITRA, S. 2001. Stimulation of human 8-oxoguanine-DNA glycosylase by AP-endonuclease: potential coordination of the initial steps in base excision repair. *Nucleic acids research,* 29**,** 430-438.

HILTON, D. J., RICHARDSON, R. T., ALEXANDER, W. S., VINEY, E. M., WILLSON, T. A., SPRIGG, N. S., STARR, R., NICHOLSON, S. E., METCALF, D. & NICOLA, N. A. 1998. Twenty proteins containing a C-terminal SOCS box form five structural classes. *Proc Natl Acad Sci U S A,* 95**,** 114-9.

HINE, C. M., LI, H., XIE, L., MAO, Z., SELUANOV, A. & GORBUNOVA, V. 2014. Regulation of Rad51 promoter. *Cell Cycle,* 13**,** 2038-2045.

HOWARD-FLANDERS, P. & MOORE, D. 1958. The time interval after pulsed irradiation within which injury to bacteria can be modified by dissolved oxygen. I. A search for an effect of oxygen 0.02 second after pulsed irradiation. *Radiat Res,* 9**,** 422-37.

HSU, J. & SAGE, J. 2016. Novel functions for the transcription factor E2F4 in development and disease. *Cell Cycle,* 15**,** 3183-3190.

HUANG, R.-X. & ZHOU, P.-K. 2020. DNA damage response signaling pathways and targets for radiotherapy sensitization in cancer. *Signal Transduction and Targeted Therapy,* 5**,** 60.

HUERTAS, P. & JACKSON, S. P. 2009. Human CtIP mediates cell cycle control of DNA end resection and double strand break repair. *J Biol Chem,* 284**,** 9558-65.

HUSSAIN, R. N., COUPLAND, S. E., KHZOUZ, J., KALIRAI, H. & PARSONS, J. L. 2020. Inhibition of ATM Increases the Radiosensitivity of Uveal Melanoma Cells to Photons and Protons. *Cancers,* 12**,** 1388.

IIDA, T., MINE, S., FUJIMOTO, H., SUZUKI, K., MINAMI, Y. & TANAKA, Y. 2002. Hypoxia-inducible factor-1α induces cell cycle arrest of endothelial cells. *Genes to Cells,* 7**,** 143-149.

INGRAM, L., MUNRO, S., COUTTS, A. S. & LA THANGUE, N. B. 2011. E2F-1 regulation by an unusual DNA damage-responsive DP partner subunit. *Cell Death Differ,* 18**,** 122-32.

IONOV, Y., PEINADO, M. A., MALKHOSYAN, S., SHIBATA, D. & PERUCHO, M. 1993. Ubiquitous somatic mutations in simple repeated sequences reveal a new mechanism for colonic carcinogenesis. *Nature,* 363**,** 558-561.

IPPOLITO, E., GRECO, C., SILIPIGNI, S., DELL'AQUILA, E., PETRIANNI, G. M., TONINI, G., FIORE, M., D'ANGELILLO, R. M. & RAMELLA, S. 2019. Concurrent radiotherapy with palbociclib or ribociclib for metastatic breast cancer patients: Preliminary assessment of toxicity. *Breast,* 46**,** 70-74.

JACKMAN, M. & PINES, J. 1997. Cyclins and the G2/M transition. *Cancer surveys,* 29**,** 47-73.

JAFARI, S. H., SAADATPOUR, Z., SALMANINEJAD, A., MOMENI, F., MOKHTARI, M., NAHAND, J. S., RAHMATI, M., MIRZAEI, H. & KIANMEHR, M. 2018. Breast cancer diagnosis: Imaging techniques and biochemical markers. *J Cell Physiol,* 233**,** 5200-5213.

JAGODINSKY, J. C., HARARI, P. M. & MORRIS, Z. S. 2020. The Promise of Combining Radiation Therapy With Immunotherapy. *International Journal of Radiation Oncology*Biology*Physics,* 108**,** 6-16.

JAGSI, R., GRIFFITH, K. A., BELLON, J. R., WOODWARD, W. A., HORTON, J. K., HO, A., FENG, F. Y., SPEERS, C., OVERMOYER, B., SABEL, M., SCHOTT, A. F. & PIERCE, L. 2018. Concurrent Veliparib With Chest Wall and Nodal Radiotherapy in Patients With Inflammatory or Locoregionally Recurrent Breast Cancer: The TBCRC 024 Phase I Multicenter Study. *J Clin Oncol,* 36**,** 1317-1322.

JARUGA, P. & DIZDAROGLU, M. 1996. Repair of Products of Oxidative DNA Base Damage in Human Cells. *Nucleic Acids Research,* 24**,** 1389-1394.

JELINEK, M. J., FOSTER, N. R., ZOROUFY, A. J., DE SOUZA, J. A., SCHWARTZ, G. K., MUNSTER, P. N., SEIWERT, T. Y. & VOKES, E. E. 2018. A phase I/II trial adding poly(ADP-ribose) polymerase (PARP) inhibitor veliparib to induction carboplatin-paclitaxel (Carbo-Tax) in patients with head and neck squamous cell carcinoma (HNSCC) Alliance A091101. *Journal of Clinical Oncology,* 36**,** 6031-6031.

JIA, Y. Y., ZHAO, J. Y., LI, B. L., GAO, K., SONG, Y., LIU, M. Y., YANG, X. J., XUE, Y., WEN, A. D. & SHI, L. 2016. miR-592/WSB1/HIF-1alpha axis inhibits glycolytic metabolism to decrease hepatocellular carcinoma growth. *Oncotarget,* 7**,** 35257-69.

JOHNSON, K. S., CONANT, E. F. & SOO, M. S. 2020. Molecular Subtypes of Breast Cancer: A Review for Breast Radiologists. *Journal of Breast Imaging,* 3**,** 12-24.

JUTZY, J. M. S., LEMONS, J. M., LUKE, J. J. & CHMURA, S. J. 2018. The Evolution of Radiation Therapy in Metastatic Breast Cancer: From Local Therapy to Systemic Agent. *International Journal of Breast Cancer,* 2018**,** 4786819.

KAMEL, D., GRAY, C., WALIA, J. S. & KUMAR, V. 2018. PARP Inhibitor Drugs in the Treatment of Breast, Ovarian, Prostate and Pancreatic Cancers: An Update of Clinical Trials. *Curr Drug Targets,* 19**,** 21-37.

KARANAM, K., KAFRI, R., LOEWER, A. & LAHAV, G. 2012. Quantitative live cell imaging reveals a gradual shift between DNA repair mechanisms and a maximal use of HR in mid S phase. *Molecular cell,* 47**,** 320-329.

KATO, T. A., NAGASAWA, H., WEIL, M. M., LITTLE, J. & BEDFORD, J. 2006. Levels of γ-H2AX foci after low-dose-rate irradiation reveal a DNA DSB rejoining defect in cells from human ATM heterozygotes in two AT families and in another apparently normal individual. *Radiation research,* 166**,** 443-453.

KEENAN, A. B., TORRE, D., LACHMANN, A., LEONG, A. K., WOJCIECHOWICZ, M. L., UTTI, V., JAGODNIK, K. M., KROPIWNICKI, E., WANG, Z. & MA'AYAN, A.

2019. ChEA3: transcription factor enrichment analysis by orthogonal omics integration. *Nucleic Acids Res,* 47**,** W212-w224.
KIM, C., PAULUS, B. F. & WOLD, M. S. 1994. Interactions of human replication protein A with oligonucleotides. *Biochemistry,* 33**,** 14197-14206.
KIM, J. J., LEE, S. B., JANG, J., YI, S. Y., KIM, S. H., HAN, S. A., LEE, J. M., TONG, S. Y., VINCELETTE, N. D., GAO, B., YIN, P., EVANS, D., CHOI, D. W., QIN, B., LIU, T., ZHANG, H., DENG, M., JEN, J., ZHANG, J., WANG, L. & LOU, Z. 2015. WSB1 promotes tumor metastasis by inducing pVHL degradation. *Genes Dev,* 29**,** 2244-57.
KIM, J. J., LEE, S. B., YI, S.-Y., HAN, S.-A., KIM, S.-H., LEE, J.-M., TONG, S.-Y., YIN, P., GAO, B., ZHANG, J. & LOU, Z. 2017a. WSB1 overcomes oncogene-induced senescence by targeting ATM for degradation. *Cell Research,* 27**,** 274-293.
KIM, J. J., LEE, S. B., YI, S. Y., HAN, S. A., KIM, S. H., LEE, J. M., TONG, S. Y., YIN, P., GAO, B., ZHANG, J. & LOU, Z. 2017b. WSB1 overcomes oncogene-induced senescence by targeting ATM for degradation. *Cell Res,* 27**,** 274-293.
KIROVA, Y. M., LOIRAT, D., BERGER, F., RODRIGUES, M., BAZIRE, L., PIERGA, J.-Y., RICCI, F., CAO, K., -SALOMON, A. V., LAKI, F., EZZILI, C., RAIZONVILLE, L., MOSSERI, V., NEFFATI, S., EZZALFANI, M. & FOURQUET, A. 2020. Radioparp: A phase I of olaparib with radiation therapy (RT) in patients with inflammatory, locoregionally advanced or metastatic triple-negative breast cancer (TNBC) or patient with operated TNBC with residual disease—Preliminary results. *Journal of Clinical Oncology,* 38**,** 571-571.
KITSERA, N., RODRIGUEZ-ALVAREZ, M., EMMERT, S., CARELL, T. & KHOBTA, A. 2019. Nucleotide excision repair of abasic DNA lesions. *Nucleic Acids Res,* 47**,** 8537-8547.
KLEIN, M. E., KOVATCHEVA, M., DAVIS, L. E., TAP, W. D. & KOFF, A. 2018. CDK4/6 Inhibitors: The Mechanism of Action May Not Be as Simple as Once Thought. *Cancer Cell,* 34**,** 9-20.
KNUDSEN, E. S., PRUITT, S. C., HERSHBERGER, P. A., WITKIEWICZ, A. K. & GOODRICH, D. W. 2019. Cell Cycle and Beyond: Exploiting New RB1 Controlled Mechanisms for Cancer Therapy. *Trends Cancer,* 5**,** 308-324.
KODYM, E., KODYM, R., REIS, A. E., HABIB, A. A., STORY, M. D. & SAHA, D. 2009. The small-molecule CDK inhibitor, SNS-032, enhances cellular radiosensitivity in quiescent and hypoxic non-small cell lung cancer cells. *Lung cancer,* 66**,** 37-47.
KONG, A., GOOD, J., KIRKHAM, A., SAVAGE, J., MANT, R., LLEWELLYN, L., PARISH, J., SPRUCE, R., FORSTER, M., SCHIPANI, S., HARRINGTON, K., SACCO, J., MURRAY, P., MIDDLETON, G., YAP, C. & MEHANNA, H. 2020. Phase I trial of WEE1 inhibition with chemotherapy and radiotherapy as adjuvant treatment, and a window of opportunity trial with cisplatin in patients with head and neck cancer: the WISTERIA trial protocol. *BMJ Open,* 10**,** e033009.
KOZLOV, S. V. 2017. *ATM Kinase: Methods and Protocols,* Springer.
KOZONO, D. E., STINCHCOMBE, T., SALAMA, J. K., BOGART, J., PETTY, W. J., GUARINO, M. J., BAZHENOVA, L., LARNER, J. M., WEISS, J., DIPETRILLO, T. A., FEIGENBERG, S. J., HU, B., NUTHALAPATI, S., LUO, Y. & VOKES, E. E. 2019. Veliparib (Vel) in combination with chemoradiotherapy (CRT) of carboplatin/paclitaxel (C/P) plus radiation in patients (pts) with stage III non-small cell lung cancer (NSCLC) (M14-360/AFT-07). *Journal of Clinical Oncology,* 37**,** 8510-8510.

KRAJEWSKA, M., FEHRMANN, R. S. N., DE VRIES, E. G. E. & VAN VUGT, M. A. T. M. 2015. Regulators of homologous recombination repair as novel targets for cancer treatment. *Frontiers in Genetics,* 6.

KROKAN, H. E. & BJØRÅS, M. 2013. Base excision repair. *Cold Spring Harb Perspect Biol,* 5**,** a012583.

KUBAICHUK, K. & KIETZMANN, T. 2019. Involvement of E3 Ligases and Deubiquitinases in the Control of HIF-α Subunit Abundance. *Cells,* 8.

KUCHENBAECKER, K. B., HOPPER, J. L., BARNES, D. R., PHILLIPS, K. A., MOOIJ, T. M., ROOS-BLOM, M. J., JERVIS, S., VAN LEEUWEN, F. E., MILNE, R. L., ANDRIEU, N., GOLDGAR, D. E., TERRY, M. B., ROOKUS, M. A., EASTON, D. F., ANTONIOU, A. C., MCGUFFOG, L., EVANS, D. G., BARROWDALE, D., FROST, D., ADLARD, J., ONG, K. R., IZATT, L., TISCHKOWITZ, M., EELES, R., DAVIDSON, R., HODGSON, S., ELLIS, S., NOGUES, C., LASSET, C., STOPPA-LYONNET, D., FRICKER, J. P., FAIVRE, L., BERTHET, P., HOONING, M. J., VAN DER KOLK, L. E., KETS, C. M., ADANK, M. A., JOHN, E. M., CHUNG, W. K., ANDRULIS, I. L., SOUTHEY, M., DALY, M. B., BUYS, S. S., OSORIO, A., ENGEL, C., KAST, K., SCHMUTZLER, R. K., CALDES, T., JAKUBOWSKA, A., SIMARD, J., FRIEDLANDER, M. L., MCLACHLAN, S. A., MACHACKOVA, E., FORETOVA, L., TAN, Y. Y., SINGER, C. F., OLAH, E., GERDES, A. M., ARVER, B. & OLSSON, H. 2017. Risks of Breast, Ovarian, and Contralateral Breast Cancer for BRCA1 and BRCA2 Mutation Carriers. *Jama,* 317**,** 2402-2416.

LAINÉ, J.-P. & EGLY, J.-M. 2006. Initiation of DNA repair mediated by a stalled RNA polymerase IIO. *The EMBO Journal,* 25**,** 387-397.

LAKOMY, D. S., URBAUER, D. L., WESTIN, S. N. & LIN, L. L. 2020. Phase I study of the PARP inhibitor talazoparib with radiation therapy for locally recurrent gynecologic cancers. *Clin Transl Radiat Oncol,* 21**,** 56-61.

LASSMANN, M., HÄNSCHEID, H., GASSEN, D., BIKO, J., MEINEKE, V., REINERS, C. & SCHERTHAN, H. 2010. In vivo formation of gamma-H2AX and 53BP1 DNA repair foci in blood cells after radioiodine therapy of differentiated thyroid cancer. *J Nucl Med,* 51**,** 1318-25.

LEE, B. K., BHINGE, A. A. & IYER, V. R. 2011. Wide-ranging functions of E2F4 in transcriptional activation and repression revealed by genome-wide analysis. *Nucleic Acids Res,* 39**,** 3558-73.

LEE, Y.-Y., CHO, Y.-J., SHIN, S.-W., CHOI, C., RYU, J.-Y., JEON, H.-K., CHOI, J.-J., HWANG, J. R., CHOI, C. H., KIM, T.-J., KIM, B.-G., BAE, D.-S., PARK, W. & LEE, J.-W. 2019. Anti-Tumor Effects of Wee1 Kinase Inhibitor with Radiotherapy in Human Cervical Cancer. *Scientific Reports,* 9**,** 15394.

LEONG, A. S. Y. & ZHUANG, Z. 2011. The Changing Role of Pathology in Breast Cancer Diagnosis and Treatment. *Pathobiology,* 78**,** 99-114.

LESUEUR, P., CHEVALIER, F., AUSTRY, J.-B., WAISSI, W., BURCKEL, H., NOEL, G., HABRAND, J.-L., SAINTIGNY, Y. & JOLY, F. 2017. Poly-(ADP-ribose)-polymerase inhibitors as radiosensitizers: a systematic review of pre-clinical and clinical human studies. *Oncotarget,* 8**,** 69105.

LESUEUR, P., LEQUESNE, J., GRELLARD, J. M., DUGUÉ, A., COQUAN, E., BRACHET, P. E., GEFFRELOT, J., KAO, W., EMERY, E., BERRO, D. H., CASTERA, L., GOARDON, N., LACROIX, J., LANGE, M., CAPEL, A., LECONTE, A., ANDRE, B., LÉGER, A., LELAIDIER, A., CLARISSE, B. & STEFAN, D. 2019. Phase I/IIa study of concomitant radiotherapy with olaparib and temozolomide in unresectable or partially resectable glioblastoma: OLA-TMZ-RTE-01 trial protocol. *BMC Cancer,* 19**,** 198.

LESZCZYNSKA, K. B., FOSKOLOU, I. P., ABRAHAM, A. G., ANBALAGAN, S., TELLIER, C., HAIDER, S., SPAN, P. N., O'NEILL, E. E., BUFFA, F. M. & HAMMOND, E. M. 2015. Hypoxia-induced p53 modulates both apoptosis and radiosensitivity via AKT. *J Clin Invest,* 125**,** 2385-98.

LI, C., WISEMAN, L., OKOH, E., LIND, M., ROY, R., BEAVIS, A. W. & PIRES, I. M. 2022. Exploring hypoxic biology to improve radiotherapy outcomes. *Expert Rev Mol Med,* 24**,** e21.

LI, J., BRAGANZA, A. & SOBOL, R. W. 2013. Base excision repair facilitates a functional relationship between Guanine oxidation and histone demethylation. *Antioxid Redox Signal,* 18**,** 2429-43.

LI, J. & KUROKAWA, M. 2015. Regulation of MDM2 Stability After DNA Damage. *J Cell Physiol,* 230**,** 2318-27.

LI, J., RAN, C., LI, E., GORDON, F., COMSTOCK, G., SIDDIQUI, H., CLEGHORN, W., CHEN, H. Z., KORNACKER, K., LIU, C. G., PANDIT, S. K., KHANIZADEH, M., WEINSTEIN, M., LEONE, G. & DE BRUIN, A. 2008. Synergistic function of E2F7 and E2F8 is essential for cell survival and embryonic development. *Dev Cell,* 14**,** 62-75.

LIBERZON, A., BIRGER, C., THORVALDSDÓTTIR, H., GHANDI, M., MESIROV, J. P. & TAMAYO, P. 2015. The Molecular Signatures Database (MSigDB) hallmark gene set collection. *Cell Syst,* 1**,** 417-425.

LIEBL, M. C. & HOFMANN, T. G. 2019. Cell Fate Regulation upon DNA Damage: p53 Serine 46 Kinases Pave the Cell Death Road. *Bioessays,* 41**,** e1900127.

LIN, C.-S., LIU, T.-C., LEE, M.-T., YANG, S.-F. & TSAO, T. C.-Y. 2017. Independent Prognostic Value of Hypoxia-inducible Factor 1-alpha Expression in Small Cell Lung Cancer. *International Journal of Medical Sciences,* 14**,** 785-790.

LINDAHL, T. 2001a. Keynote: past, present, and future aspects of base excision repair. *Progress in nucleic acid research and molecular biology,* 68**,** xvii-xxx.

LINDAHL, T. 2001b. Keynote: Past, present, and future aspects of base excision repair. *Progress in Nucleic Acid Research and Molecular Biology.* Academic Press.

LINDAHL, T. & WOOD, R. D. 1999. Quality control by DNA repair. *Science,* 286**,** 1897-905.

LINOSSI, E. M. & NICHOLSON, S. E. 2012. The SOCS box-adapting proteins for ubiquitination and proteasomal degradation. *IUBMB Life,* 64**,** 316-23.

LIU, S., OPIYO, S. O., MANTHEY, K., GLANZER, J. G., ASHLEY, A. K., AMERIN, C., TROKSA, K., SHRIVASTAV, M., NICKOLOFF, J. A. & OAKLEY, G. G. 2012a. Distinct roles for DNA-PK, ATM and ATR in RPA phosphorylation and checkpoint activation in response to replication stress. *Nucleic Acids Res,* 40**,** 10780-94.

LIU, X., LIU, D., QIAN, D., DAI, J., AN, Y., JIANG, S., STANLEY, B., YANG, J., WANG, B., LIU, X. & LIU, D. X. 2012b. Nucleophosmin (NPM1/B23) interacts with activating transcription factor 5 (ATF5) protein and promotes proteasome- and caspase-dependent ATF5 degradation in hepatocellular carcinoma cells. *J Biol Chem,* 287**,** 19599-609.

LIU, Z.-J., SEMENZA, G. L. & ZHANG, H.-F. 2015. Hypoxia-inducible factor 1 and breast cancer metastasis. *Journal of Zhejiang University-SCIENCE B,* 16**,** 32-43.

LIVAK, K. J. & SCHMITTGEN, T. D. 2001. Analysis of Relative Gene Expression Data Using Real-Time Quantitative PCR and the 2−ΔΔCT Method. *Methods,* 25**,** 402-408.

LOAP, P., LOIRAT, D., BERGER, F., CAO, K., RICCI, F., JOCHEM, A., RAIZONVILLE, L., MOSSERI, V., FOURQUET, A. & KIROVA, Y. 2021. Combination of olaparib with radiotherapy for triple-negative breast cancers: one-year toxicity report of the RADIOPARP phase I trial. *International Journal of Cancer,* 149**,** 1828-1832.

LOHBERGER, B., GLÄNZER, D., ECK, N., STASNY, K., FALKNER, A., LEITHNER, A. & GEORG, D. 2023. The ATR Inhibitor VE-821 Enhances the Radiosensitivity and Suppresses DNA Repair Mechanisms of Human Chondrosarcoma Cells. *International Journal of Molecular Sciences,* 24**,** 2315.
LOIBL, S., POORTMANS, P., MORROW, M., DENKERT, C. & CURIGLIANO, G. 2021. Breast cancer. *The Lancet,* 397**,** 1750-1769.
LONDON, R. E. 2015. The structural basis of XRCC1-mediated DNA repair. *DNA Repair (Amst),* 30**,** 90-103.
LORD, C. J. & ASHWORTH, A. 2012. The DNA damage response and cancer therapy. *Nature,* 481**,** 287-294.
LORD, C. J. & ASHWORTH, A. 2016. BRCAness revisited. *Nature Reviews Cancer,* 16**,** 110-120.
LORD, C. J. & ASHWORTH, A. 2017. PARP inhibitors: Synthetic lethality in the clinic. *Science,* 355**,** 1152-1158.
LUNDBERG, A. S. & WEINBERG, R. A. 1998. Functional inactivation of the retinoblastoma protein requires sequential modification by at least two distinct cyclin-cdk complexes. *Molecular and cellular biology,* 18**,** 753-761.
MADARAMPALLI, B., YUAN, Y., LIU, D., LENGEL, K., XU, Y., LI, G., YANG, J., LIU, X., LU, Z. & LIU, D. X. 2015. ATF5 Connects the Pericentriolar Materials to the Proximal End of the Mother Centriole. *Cell,* 162**,** 580-92.
MAH, L. J., EL-OSTA, A. & KARAGIANNIS, T. C. 2010. γH2AX: a sensitive molecular marker of DNA damage and repair. *Leukemia,* 24**,** 679-686.
MANICKAVINAYAHAM, S., VELEZ-CRUZ, R., BISWAS, A. K., CHEN, J., GUO, R. & JOHNSON, D. G. 2020. The E2F1 transcription factor and RB tumor suppressor moonlight as DNA repair factors. *Cell Cycle,* 19**,** 2260-2269.
MAO, Z., BOZZELLA, M., SELUANOV, A. & GORBUNOVA, V. 2008. DNA repair by nonhomologous end joining and homologous recombination during cell cycle in human cells. *Cell Cycle,* 7**,** 2902-6.
MARÉCHAL, A. & ZOU, L. 2013. DNA damage sensing by the ATM and ATR kinases. *Cold Spring Harb Perspect Biol,* 5.
MARÉCHAL, A. & ZOU, L. 2015. RPA-coated single-stranded DNA as a platform for post-translational modifications in the DNA damage response. *Cell research,* 25**,** 9-23.
MATHESON, C. J., BACKOS, D. S. & REIGAN, P. 2016. Targeting WEE1 Kinase in Cancer. *Trends in Pharmacological Sciences,* 37**,** 872-881.
MATSUOKA, S., ROTMAN, G., OGAWA, A., SHILOH, Y., TAMAI, K. & ELLEDGE, S. J. 2000. Ataxia telangiectasia-mutated phosphorylates Chk2 in vivo and in vitro. *Proc Natl Acad Sci U S A,* 97**,** 10389-94.
MCCABE, N., TURNER, N. C., LORD, C. J., KLUZEK, K., BIAŁKOWSKA, A., SWIFT, S., GIAVARA, S., O'CONNOR, M. J., TUTT, A. N., ZDZIENICKA, M. Z., SMITH, G. C. M. & ASHWORTH, A. 2006. Deficiency in the Repair of DNA Damage by Homologous Recombination and Sensitivity to Poly(ADP-Ribose) Polymerase Inhibition. *Cancer Research,* 66**,** 8109-8115.
MCMAHON, S. J. 2018. The linear quadratic model: usage, interpretation and challenges. *Physics in Medicine & Biology,* 64**,** 01TR01.
MEHTA, M. P., WANG, D., WANG, F., KLEINBERG, L., BRADE, A., ROBINS, H. I., TURAKA, A., LEAHY, T., MEDINA, D., XIONG, H., MOSTAFA, N. M., DUNBAR, M., ZHU, M., QIAN, J., HOLEN, K., GIRANDA, V. & CURRAN, W. J. 2015. Veliparib in combination with whole brain radiation therapy in patients with brain metastases: results of a phase 1 study. *J Neurooncol,* 122**,** 409-17.

MERCIER, G. 2022. *Enhancing Anaphase Promoting Complex Activity to Counter Multiple Drug Resistant Breast Cancer.* University of Saskatchewan.
MICHMERHUIZEN, A. R., PESCH, A. M., MOUBADDER, L., CHANDLER, B. C., WILDER-ROMANS, K., CAMERON, M., OLSEN, E., THOMAS, D. G., ZHANG, A., HIRSH, N., RITTER, C. L., LIU, M., NYATI, S., PIERCE, L. J., JAGSI, R. & SPEERS, C. 2019. PARP1 Inhibition Radiosensitizes Models of Inflammatory Breast Cancer to Ionizing Radiation. *Mol Cancer Ther,* 18**,** 2063-2073.
MILANO, M. T., KATZ, A. W., ZHANG, H. & OKUNIEFF, P. 2012. Oligometastases Treated With Stereotactic Body Radiotherapy: Long-Term Follow-Up of Prospective Study. *International Journal of Radiation Oncology*Biology*Physics,* 83**,** 878-886.
MILLER, D. M., THOMAS, S. D., ISLAM, A., MUENCH, D. & SEDORIS, K. 2012. c-Myc and cancer metabolism. *Clin Cancer Res,* 18**,** 5546-53.
MITTENDORF, E. A., ZHANG, H., BARRIOS, C. H., SAJI, S., JUNG, K. H., HEGG, R., KOEHLER, A., SOHN, J., IWATA, H., TELLI, M. L., FERRARIO, C., PUNIE, K., PENAULT-LLORCA, F., PATEL, S., DUC, A. N., LISTE-HERMOSO, M., MAIYA, V., MOLINERO, L., CHUI, S. Y. & HARBECK, N. 2020. Neoadjuvant atezolizumab in combination with sequential nab-paclitaxel and anthracycline-based chemotherapy versus placebo and chemotherapy in patients with early-stage triple-negative breast cancer (IMpassion031): a randomised, double-blind, phase 3 trial. *The Lancet,* 396**,** 1090-1100.
MODRICH, P. & LAHUE, R. 1996. MISMATCH REPAIR IN REPLICATION FIDELITY, GENETIC RECOMBINATION, AND CANCER BIOLOGY. *Annual Review of Biochemistry,* 65**,** 101-133.
MOEGLIN, E., DESPLANCQ, D., CONIC, S., OULAD-ABDELGHANI, M., STOESSEL, A., CHIPER, M., VIGNERON, M., DIDIER, P., TORA, L. & WEISS, E. 2019. Uniform Widespread Nuclear Phosphorylation of Histone H2AX Is an Indicator of Lethal DNA Replication Stress. *Cancers (Basel),* 11.
MOISEEVA, T. N., QIAN, C., SUGITANI, N., OSMANBEYOGLU, H. U. & BAKKENIST, C. J. 2019. WEE1 kinase inhibitor AZD1775 induces CDK1 kinase-dependent origin firing in unperturbed G1- and S-phase cells. *Proceedings of the National Academy of Sciences,* 116**,** 23891-23893.
MORGAN, M. A. & LAWRENCE, T. S. 2015. Molecular Pathways: Overcoming Radiation Resistance by Targeting DNA Damage Response Pathways. *Clin Cancer Res,* 21**,** 2898-904.
MORGAN, M. A., PARSELS, L. A., ZHAO, L., PARSELS, J. D., DAVIS, M. A., HASSAN, M. C., ARUMUGARAJAH, S., HYLANDER-GANS, L., MOROSINI, D., SIMEONE, D. M., CANMAN, C. E., NORMOLLE, D. P., ZABLUDOFF, S. D., MAYBAUM, J. & LAWRENCE, T. S. 2010. Mechanism of radiosensitization by the Chk1/2 inhibitor AZD7762 involves abrogation of the G2 checkpoint and inhibition of homologous recombinational DNA repair. *Cancer Res,* 70**,** 4972-81.
MOSLY, D., TURNBULL, A., SIMS, A., WARD, C. & LANGDON, S. 2018. Predictive markers of endocrine response in breast cancer. *World J Exp Med,* 8**,** 1-7.
MOWERY, Y. M., NIEDZWIECKI, D., CHOE, J. H., KIRSCH, D. G. & BRIZEL, D. M. 2022. Phase I trial of the ATR inhibitor BAY 1895344 combined with stereotactic body radiation therapy and pembrolizumab for recurrent head and neck squamous cell carcinoma. *Journal of Clinical Oncology,* 40**,** TPS6108-TPS6108.
MOYNAHAN, M. E., PIERCE, A. J. & JASIN, M. 2001. BRCA2 is required for homology-directed repair of chromosomal breaks. *Mol Cell,* 7**,** 263-72.
NAGELKERKE, A., VAN KUIJK, S. J., SWEEP, F. C., NAGTEGAAL, I. D., HOOGERBRUGGE, N., MARTENS, J. W., TIMMERMANS, M. A., VAN

LAARHOVEN, H. W., BUSSINK, J. & SPAN, P. N. 2011. Constitutive expression of γ-H2AX has prognostic relevance in triple negative breast cancer. *Radiother Oncol,* 101**,** 39-45.
NAGPAL, N. & KULSHRESHTHA, R. 2014. miR-191: an emerging player in disease biology. *Front Genet,* 5**,** 99.
NAKADA, S. 2016. Opposing roles of RNF8/RNF168 and deubiquitinating enzymes in ubiquitination-dependent DNA double-strand break response signaling and DNA-repair pathway choice. *Journal of Radiation Research,* 57**,** i33-i40.
NAKANISHI, K., CAVALLO, F., BRUNET, E. & JASIN, M. 2011. Homologous Recombination Assay for Interstrand Cross-Link Repair. *In:* TSUBOUCHI, H. (ed.) *DNA Recombination: Methods and Protocols.* Totowa, NJ: Humana Press.
NANDA, R., LIU, M. C., YAU, C., SHATSKY, R., PUSZTAI, L., WALLACE, A., CHIEN, A. J., FORERO-TORRES, A., ELLIS, E., HAN, H., CLARK, A., ALBAIN, K., BOUGHEY, J. C., JASKOWIAK, N. T., ELIAS, A., ISAACS, C., KEMMER, K., HELSTEN, T., MAJURE, M., STRINGER-REASOR, E., PARKER, C., LEE, M. C., HADDAD, T., COHEN, R. N., ASARE, S., WILSON, A., HIRST, G. L., SINGHRAO, R., STEEG, K., ASARE, A., MATTHEWS, J. B., BERRY, S., SANIL, A., SCHWAB, R., SYMMANS, W. F., VAN 'T VEER, L., YEE, D., DEMICHELE, A., HYLTON, N. M., MELISKO, M., PERLMUTTER, J., RUGO, H. S., BERRY, D. A. & ESSERMAN, L. J. 2020. Effect of Pembrolizumab Plus Neoadjuvant Chemotherapy on Pathologic Complete Response in Women With Early-Stage Breast Cancer: An Analysis of the Ongoing Phase 2 Adaptively Randomized I-SPY2 Trial. *JAMA Oncology,* 6**,** 676-684.
NARA, H., ONODA, T., RAHMAN, M., ARAKI, A., JULIANA, F. M., TANAKA, N. & ASAO, H. 2011a. WSB-1, a novel IL-21 receptor binding molecule, enhances the maturation of IL-21 receptor. *Cell Immunol,* 269**,** 54-9.
NARA, H., ONODA, T., RAHMAN, M., ARAKI, A., JULIANA, F. M., TANAKA, N. & ASAO, H. 2011b. WSB-1, a novel IL-21 receptor binding molecule, enhances the maturation of IL-21 receptor. *Cellular Immunology,* 269**,** 54-59.
NARAYAN, P., PROWELL, T. M., GAO, J. J., FERNANDES, L. L., LI, E., JIANG, X., QIU, J., FAN, J., SONG, P., YU, J., ZHANG, X., KING-KALLIMANIS, B. L., CHEN, W., RICKS, T. K., GONG, Y., WANG, X., WINDSOR, K., RHIEU, S. Y., GEISER, G., BANERJEE, A., CHEN, X., REYES TURCU, F., CHATTERJEE, D. K., PATHAK, A., SEIDMAN, J., GHOSH, S., PHILIP, R., GOLDBERG, K. B., KLUETZ, P. G., TANG, S., AMIRI-KORDESTANI, L., THEORET, M. R., PAZDUR, R. & BEAVER, J. A. 2021. FDA Approval Summary: Alpelisib Plus Fulvestrant for Patients with HR-positive, HER2-negative, PIK3CA-mutated, Advanced or Metastatic Breast Cancer. *Clin Cancer Res,* 27**,** 1842-1849.
NGUYEN, N. P., SALLAH, S., KARLSSON, U. & ANTOINE, J. E. 2002. Combined chemotherapy and radiation therapy for head and neck malignancies: quality of life issues. *Cancer,* 94**,** 1131-41.
NICKOLOFF, J. A. 2022. Targeting Replication Stress Response Pathways to Enhance Genotoxic Chemo- and Radiotherapy. *Molecules,* 27.
NICKOLOFF, J. A., BOSS, M.-K., ALLEN, C. P. & LARUE, S. M. 2017. Translational research in radiation-induced DNA damage signaling and repair. *Translational Cancer Research***,** S875-S891.
NIRAJ, J., FÄRKKILÄ, A. & D'ANDREA, A. D. 2019. The Fanconi Anemia Pathway in Cancer. *Annu Rev Cancer Biol,* 3**,** 457-478.
NUCIFORA, F. C., NUCIFORA, L. G., NG, C.-H., ARBEZ, N., GUO, Y., ROBY, E., SHANI, V., ENGELENDER, S., WEI, D., WANG, X.-F., LI, T., MOORE, D. J.,

PLETNIKOVA, O., TRONCOSO, J. C., SAWA, A., DAWSON, T. M., SMITH, W., LIM, K.-L. & ROSS, C. A. 2016. Ubiqutination via K27 and K29 chains signals aggregation and neuronal protection of LRRK2 by WSB1. *Nature Communications,* 7**,** 11792.
ORII, K. E., LEE, Y., KONDO, N. & MCKINNON, P. J. 2006. Selective utilization of nonhomologous end-joining and homologous recombination DNA repair pathways during nervous system development. *Proc Natl Acad Sci U S A,* 103**,** 10017-22.
OTTO, T. & SICINSKI, P. 2017. Cell cycle proteins as promising targets in cancer therapy. *Nat Rev Cancer,* 17**,** 93-115.
OZAKI, T. & NAKAGAWARA, A. 2011. Role of p53 in Cell Death and Human Cancers. *Cancers (Basel),* 3**,** 994-1013.
PAERHATI, P., LIU, J., JIN, Z., JAKOŠ, T., ZHU, S., QIAN, L., ZHU, J. & YUAN, Y. 2022. Advancements in Activating Transcription Factor 5 Function in Regulating Cell Stress and Survival. *Int J Mol Sci,* 23.
PAGANO, M., PEPPERKOK, R., LUKAS, J., BALDIN, V., ANSORGE, W., BARTEK, J. & DRAETTA, G. 1993. Regulation of the cell cycle by the cdk2 protein kinase in cultured human fibroblasts. *The Journal of cell biology,* 121**,** 101-111.
PANNUNZIO, N. R., WATANABE, G. & LIEBER, M. R. 2018. Nonhomologous DNA end-joining for repair of DNA double-strand breaks. *J Biol Chem,* 293**,** 10512-10523.
PARSONS, C. A., BAUMANN, P., VAN DYCK, E. & WEST, S. C. 2000. Precise binding of single-stranded DNA termini by human RAD52 protein. *Embo j,* 19**,** 4175-81.
PAUL-KONIETZKO, K., THOMALE, J., ARAKAWA, H. & ILIAKIS, G. 2015. DNA Ligases I and III Support Nucleotide Excision Repair in DT40 Cells with Similar Efficiency. *Photochem Photobiol,* 91**,** 1173-80.
PAULL, T. T. & GELLERT, M. 1999. Nbs1 potentiates ATP-driven DNA unwinding and endonuclease cleavage by the Mre11/Rad50 complex. *Genes Dev,* 13**,** 1276-88.
PAYNE, S. J., BOWEN, R. L., JONES, J. L. & WELLS, C. A. 2008. Predictive markers in breast cancer--the present. *Histopathology,* 52**,** 82-90.
PEĆINA-ŠLAUS, N., KAFKA, A., SALAMON, I. & BUKOVAC, A. 2020. Mismatch Repair Pathway, Genome Stability and Cancer. *Front Mol Biosci,* 7**,** 122.
PERNAS, S., TOLANEY, S. M., WINER, E. P. & GOEL, S. 2018. CDK4/6 inhibition in breast cancer: current practice and future directions. *Therapeutic Advances in Medical Oncology,* 10**,** 1758835918786451.
PFEIFFER, P., GOEDECKE, W. & OBE, G. 2000. Mechanisms of DNA double-strand break repair and their potential to induce chromosomal aberrations. *Mutagenesis,* 15**,** 289-302.
PILIÉ, P. G., TANG, C., MILLS, G. B. & YAP, T. A. 2019. State-of-the-art strategies for targeting the DNA damage response in cancer. *Nat Rev Clin Oncol,* 16**,** 81-104.
PIRES, I. M., BENCOKOVA, Z., MILANI, M., FOLKES, L. K., LI, J. L., STRATFORD, M. R., HARRIS, A. L. & HAMMOND, E. M. 2010. Effects of acute versus chronic hypoxia on DNA damage responses and genomic instability. *Cancer Res,* 70**,** 925-35.
PIRES, I. M., BLOKLAND, N. J., BROOS, A. W., POUJADE, F.-A., SENRA, J. M., ECCLES, S. A., SPAN, P. N., HARVEY, A. J. & HAMMOND, E. M. 2014. HIF-1α-independent hypoxia-induced rapid PTK6 stabilization is associated with increased motility and invasion. *Cancer biology & therapy,* 15**,** 1350-1357.
PIRES, I. M., OLCINA, M. M., ANBALAGAN, S., POLLARD, J. R., REAPER, P. M., CHARLTON, P. A., MCKENNA, W. G. & HAMMOND, E. M. 2012. Targeting radiation-resistant hypoxic tumour cells through ATR inhibition. *Br J Cancer,* 107**,** 291-9.

POLGÁR, C., KAHÁN, Z., IVANOV, O., CHORVÁTH, M., LIGAČOVÁ, A., CSEJTEI, A., GÁBOR, G., LANDHERR, L., MANGEL, L., MAYER, Á. & FODOR, J. 2022. Radiotherapy of Breast Cancer-Professional Guideline 1st Central-Eastern European Professional Consensus Statement on Breast Cancer. *Pathol Oncol Res,* 28**,** 1610378.

POMMIER, Y., O'CONNOR, M. J. & DE BONO, J. 2016. Laying a trap to kill cancer cells: PARP inhibitors and their mechanisms of action. *Science Translational Medicine,* 8**,** 362ps17-362ps17.

POSTHUMADEBOER, J., WÜRDINGER, T., GRAAT, H. C. A., VAN BEUSECHEM, V. W., HELDER, M. N., VAN ROYEN, B. J. & KASPERS, G. J. L. 2011. WEE1 inhibition sensitizes osteosarcoma to radiotherapy. *BMC Cancer,* 11**,** 156.

POTHARAJU, M., MATHAVAN, A., MANGALESWARAN, B., PATIL, S., JOHN, R., GHOSH, S., KALAVAKONDA, C., GHOSH, M. & VERMA, R. S. 2019. Clinicopathological Analysis of HIF-1alpha and TERT on Survival Outcome in Glioblastoma Patients: A Prospective, Single Institution Study. *Journal of Cancer,* 10**,** 2397-2406.

POUJADE, F.-A. 2016. Investigating the Role of WSB-1 in Breast Cancer. *PhD thesis*.

POUJADE, F. A., MANNION, A., BRITTAIN, N., THEODOSI, A., BEEBY, E., LESZCZYNSKA, K. B., HAMMOND, E. M., GREENMAN, J., CAWTHORNE, C. & PIRES, I. M. 2018. WSB-1 regulates the metastatic potential of hormone receptor negative breast cancer. *Br J Cancer,* 118**,** 1229-1237.

PRITZKER, K. P. H. 2015. Predictive and prognostic cancer biomarkers revisited. *Expert Review of Molecular Diagnostics,* 15**,** 971-974.

QIU, Z., OLEINICK, N. L. & ZHANG, J. 2018. ATR/CHK1 inhibitors and cancer therapy. *Radiother Oncol,* 126**,** 450-464.

QUAN, L., QIU, T., LIANG, J., LI, M., ZHANG, Y. & TAO, K. 2015. Identification of Target Genes Regulated by KSHV miRNAs in KSHV-Infected Lymphoma Cells. *Pathol Oncol Res,* 21**,** 875-80.

RABIONET DIAZ, M. 2021. Design and fabrication of three-dimensional scaffolds for breast cancer stem cell expansion and molecular characterization.

RAFIEI, S., FITZPATRICK, K., LIU, D., CAI, M. Y., ELMARAKEBY, H. A., PARK, J., RICKER, C., KOCHUPURAKKAL, B. S., CHOUDHURY, A. D., HAHN, W. C., BALK, S. P., HWANG, J. H., VAN ALLEN, E. M. & MOUW, K. W. 2020. ATM Loss Confers Greater Sensitivity to ATR Inhibition Than PARP Inhibition in Prostate Cancer. *Cancer Res,* 80**,** 2094-2100.

RAGHAVAN, P., TUMATI, V., YU, L., CHAN, N., TOMIMATSU, N., BURMA, S., BRISTOW, R. G. & SAHA, D. 2012. AZD5438, an inhibitor of Cdk1, 2, and 9, enhances the radiosensitivity of non-small cell lung carcinoma cells. *Int J Radiat Oncol Biol Phys,* 84**,** e507-14.

RAMACHANDRAN, S., MA, T. S., GRIFFIN, J., NG, N., FOSKOLOU, I. P., HWANG, M.-S., VICTORI, P., CHENG, W.-C., BUFFA, F. M., LESZCZYNSKA, K. B., EL-KHAMISY, S. F., GROMAK, N. & HAMMOND, E. M. 2021. Hypoxia-induced SETX links replication stress with the unfolded protein response. *Nature Communications,* 12**,** 3686.

RAMAKRISHNAN GEETHAKUMARI, P., SCHIEWER, M. J., KNUDSEN, K. E. & KELLY, W. K. 2017. PARP Inhibitors in Prostate Cancer. *Curr Treat Options Oncol,* 18**,** 37.

RAMPIONI VINCIGUERRA, G. L., SONEGO, M., SEGATTO, I., DALL'ACQUA, A., VECCHIONE, A., BALDASSARRE, G. & BELLETTI, B. 2022. CDK4/6 Inhibitors in Combination Therapies: Better in Company Than Alone: A Mini Review. *Frontiers in Oncology,* 12.

REDDY, G. P. V. 1994. Cell cycle: Regulatory events in G1 → S transition of mammalian cells. *Journal of Cellular Biochemistry,* 54**,** 379-386.
REDDY, V. P., SYKES, A., COLCLOUGH, N., DURANT, S. T., CONNOR, L. O., HOCH, M., BRUNA, N. B., VITA, S. D., MERCHANT, M. & PASS, M. 2019. Abstract 4868: A preclinical PK/PD model based on a mouse glioblastoma survival model for AZD1390, a novel, brain-penetrant ATM kinase inhibitor, to predict the inhibition of DNA damage response induced by radiation and the human efficacious dose. *Cancer Research,* 79**,** 4868.
REDON, C. E., NAKAMURA, A. J., MARTIN, O. A., PAREKH, P. R., WEYEMI, U. S. & BONNER, W. M. 2011. Recent developments in the use of γ-H2AX as a quantitative DNA double-strand break biomarker. *Aging (Albany NY),* 3**,** 168-74.
REISS, K. A., HERMAN, J. M., ARMSTRONG, D., ZAHURAK, M., FYLES, A., BRADE, A., MILOSEVIC, M., DAWSON, L. A., SCARDINA, A., FISCHER, P., HACKER-PRIETZ, A., KINDERS, R. J., WANG, L., CHEN, A., TEMKIN, S., HORIBA, N., STAYNER, L. A., SIU, L. L. & AZAD, N. S. 2017. A final report of a phase I study of veliparib (ABT-888) in combination with low-dose fractionated whole abdominal radiation therapy (LDFWAR) in patients with advanced solid malignancies and peritoneal carcinomatosis with a dose escalation in ovarian and fallopian tube cancers. *Gynecol Oncol,* 144**,** 486-490.
RHODES, D. R. & CHINNAIYAN, A. M. 2005. Integrative analysis of the cancer transcriptome. *Nature Genetics,* 37**,** S31-S37.
ROBERT, N., LEYLAND-JONES, B., ASMAR, L., BELT, R., ILEGBODU, D., LOESCH, D., RAJU, R., VALENTINE, E., SAYRE, R., COBLEIGH, M., ALBAIN, K., MCCULLOUGH, C., FUCHS, L. & SLAMON, D. 2006. Randomized Phase III Study of Trastuzumab, Paclitaxel, and Carboplatin Compared With Trastuzumab and Paclitaxel in Women With HER-2–Overexpressing Metastatic Breast Cancer. *Journal of Clinical Oncology,* 24**,** 2786-2792.
ROBERTSON, A., KLUNGLAND, A., ROGNES, T. & LEIROS, I. 2009. DNA repair in mammalian cells: Base excision repair: the long and short of it. *Cellular and molecular life sciences,* 66**,** 981-993.
ROBINSON, T. J., LIU, J. C., VIZEACOUMAR, F., SUN, T., MACLEAN, N., EGAN, S. E., SCHIMMER, A. D., DATTI, A. & ZACKSENHAUS, E. 2013. RB1 status in triple negative breast cancer cells dictates response to radiation treatment and selective therapeutic drugs. *PLoS One,* 8**,** e78641.
RODLER, E., SHARMA, P., BARLOW, W. E., GRALOW, J. R., PUHALLA, S. L., ANDERS, C. K., GOLDSTEIN, L., TRIPATHY, D., BROWN-GLABERMAN, U. A., HUYNH, T.-T., SZYARTO, C. S., GODWIN, A. K., PATHAK, H. B., SWISHER, E. M., RADKE, M. R., TIMMS, K. M., LEW, D. L., MIAO, J., PUSZTAI, L., HAYES, D. F. & HORTOBAGYI, G. N. 2023. Cisplatin with veliparib or placebo in metastatic triple-negative breast cancer and BRCA mutation-associated breast cancer (S1416): a randomised, double-blind, placebo-controlled, phase 2 trial. *The Lancet Oncology,* 24**,** 162-174.
RODRIGUEZ-BERRIGUETE, G., RANZANI, M., PREVO, R., PULIYADI, R., MACHADO, N., BOLLAND, H. R., MILLAR, V., EBNER, D., BOURSIER, M., CERUTTI, A., CICCONI, A., GALBIATI, A., GRANDE, D., GRINKEVICH, V., MAJITHIYA, J. B., PISCITELLO, D., RAJENDRA, E., STOCKLEY, M. L., BOULTON, S. J., HAMMOND, E. M., HEALD, R. A., SMITH, G. C. M., ROBINSON, H. M. R. & HIGGINS, G. S. 2023. Small-Molecule Polθ Inhibitors Provide Safe and Effective Tumor Radiosensitization in Preclinical Models. *Clinical Cancer Research,* 29**,** 1631-1642.

ROGERS, R. F., WALTON, M. I., CHERRY, D. L., COLLINS, I., CLARKE, P. A., GARRETT, M. D. & WORKMAN, P. 2020. CHK1 Inhibition Is Synthetically Lethal with Loss of B-Family DNA Polymerase Function in Human Lung and Colorectal Cancer Cells. *Cancer Research,* 80**,** 1735-1747.

ROMESSER, P., HOLLIDAY, E., PHILIP, T., SARHOLZ, B., KUIPERS, M., RODRIGUEZ-GUTIERREZ, A., DIAZ-PADILLA, I. & MILLER, E. 2020. A multicenter phase Ib/II study of DNA-PK inhibitor peposertib (M3814) in combination with capecitabine and radiotherapy in patients with locally advanced rectal cancer. *Journal of Clinical Oncology,* 38**,** TPS4117-TPS4117.

ROMESSER, P. B., HOLLIDAY, E. B., PHILIP, T., GARCIA-CARBONERO, R., CAPDEVILA, J., TULI, R., SARHOLZ, B., KUIPERS, M., RODRIGUEZ, A., DIAZ-PADILLA, I. & MILLER, E. D. 2021. A multicenter phase Ib/II study of DNA-PK inhibitor peposertib (M3814) in combination with capecitabine and radiotherapy in patients with locally advanced rectal cancer. *Journal of Clinical Oncology,* 39**,** TPS144-TPS144.

ROTHKAMM, K., BARNARD, S., MOQUET, J., ELLENDER, M., RANA, Z. & BURDAK-ROTHKAMM, S. 2015. DNA damage foci: Meaning and significance. *Environmental and Molecular Mutagenesis,* 56**,** 491-504.

RUNDLE, S., BRADBURY, A., DREW, Y. & CURTIN, N. J. 2017. Targeting the ATR-CHK1 Axis in Cancer Therapy. *Cancers,* 9**,** 41.

SABATIER, R., LOPEZ, M., GUILLE, A., BILLON, E., CARBUCCIA, N., GARNIER, S., ADELAIDE, J., EXTRA, J.-M., CAPPIELLO, M.-A., CHARAFE-JAUFFRET, E., PAKRADOUNI, J., VIENS, P., GONÇALVES, A., CHAFFANET, M., BIRNBAUM, D. & BERTUCCI, F. 2019. High Response to Cetuximab in a Patient With EGFR-Amplified Heavily Pretreated Metastatic Triple-Negative Breast Cancer. *JCO Precision Oncology***,** 1-8.

SACHS, R. K., HAHNFELD, P. & BRENNER, D. J. 1997. The link between low-LET dose-response relations and the underlying kinetics of damage production/repair/misrepair. *Int J Radiat Biol,* 72**,** 351-74.

SAITO, S., GOODARZI, A. A., HIGASHIMOTO, Y., NODA, Y., LEES-MILLER, S. P., APPELLA, E. & ANDERSON, C. W. 2002. ATM mediates phosphorylation at multiple p53 sites, including Ser(46), in response to ionizing radiation. *J Biol Chem,* 277**,** 12491-4.

SARKARIA, J. N., BUSBY, E. C., TIBBETTS, R. S., ROOS, P., TAYA, Y., KARNITZ, L. M. & ABRAHAM, R. T. 1999. Inhibition of ATM and ATR kinase activities by the radiosensitizing agent, caffeine. *Cancer research,* 59**,** 4375-4382.

SCANLON, S. E. & GLAZER, P. M. 2015. Multifaceted control of DNA repair pathways by the hypoxic tumor microenvironment. *DNA Repair,* 32**,** 180-189.

SCHEIDEMANN, E. R. & SHAJAHAN-HAQ, A. N. 2021. Resistance to CDK4/6 Inhibitors in Estrogen Receptor-Positive Breast Cancer. *Int J Mol Sci,* 22.

SCHLACHER, K., CHRIST, N., SIAUD, N., EGASHIRA, A., WU, H. & JASIN, M. 2011. Double-strand break repair-independent role for BRCA2 in blocking stalled replication fork degradation by MRE11. *Cell,* 145**,** 529-542.

SCHWARTZ, G. K. 2003. Flavopiridol Plus Radiation Therapy Followed By Gemcitabine Hydrochloride in Treating Patients With Locally Advanced, Unresectable Pancreatic Cancer.

SELUANOV, A., MAO, Z. & GORBUNOVA, V. 2010. Analysis of DNA double-strand break (DSB) repair in mammalian cells. *J Vis Exp*.

SENDEROWICZ, A. M. 1999. Flavopiridol: the first cyclin-dependent kinase inhibitor in human clinical trials. *Invest New Drugs,* 17**,** 313-20.

SHAH, M., NUNES, M. R. & STEARNS, V. 2018. CDK4/6 Inhibitors: Game Changers in the Management of Hormone Receptor–Positive Advanced Breast Cancer? *Oncology (Williston Park),* 32**,** 216-22.

SHIBATA, A., CONRAD, S., BIRRAUX, J., GEUTING, V., BARTON, O., ISMAIL, A., KAKAROUGKAS, A., MEEK, K., TAUCHER-SCHOLZ, G., LÖBRICH, M. & JEGGO, P. A. 2011. Factors determining DNA double-strand break repair pathway choice in G2 phase. *The EMBO Journal,* 30**,** 1079-1092.

SHICHRUR, K., FEINBERG-GORENSHTEIN, G., LURIA, D., ASH, S., YANIV, I. & AVIGAD, S. 2014. Potential role of WSB1 isoforms in growth and survival of neuroblastoma cells. *Pediatr Res,* 75**,** 482-6.

SHIMURA, T., KAKUDA, S., OCHIAI, Y., NAKAGAWA, H., KUWAHARA, Y., TAKAI, Y., KOBAYASHI, J., KOMATSU, K. & FUKUMOTO, M. 2010. Acquired radioresistance of human tumor cells by DNA-PK/AKT/GSK3β-mediated cyclin D1 overexpression. *Oncogene,* 29**,** 4826-4837.

SHIMUTA, K., NAKAJO, N., UTO, K., HAYANO, Y., OKAZAKI, K. & SAGATA, N. 2002. Chk1 is activated transiently and targets Cdc25A for degradation at the Xenopus midblastula transition. *Embo j,* 21**,** 3694-703.

SHRIVASTAV, M., DE HARO, L. P. & NICKOLOFF, J. A. 2008. Regulation of DNA double-strand break repair pathway choice. *Cell Res,* 18**,** 134-47.

SIM, H.-W., MCDONALD, K. L., LWIN, Z., BARNES, E. H., ROSENTHAL, M., FOOTE, M. C., KOH, E.-S., BACK, M., WHEELER, H. & SULMAN, E. P. 2021. A randomized phase II trial of veliparib, radiotherapy, and temozolomide in patients with unmethylated MGMT glioblastoma: the VERTU study. *Neuro-Oncology,* 23**,** 1736-1749.

SIMONE II, C. B., BURRI, S. H. & HEINZERLING, J. H. 2015. Novel radiotherapy approaches for lung cancer: combining radiation therapy with targeted and immunotherapies. *Translational Lung Cancer Research,* 4**,** 545-552.

SINCLAIR, W. K. 1968. Cyclic x-ray responses in mammalian cells in vitro. *Radiation research,* 33**,** 620-643.

SOLAYMANI-MOHAMMADI, S., ECKMANN, L. & SINGER, S. M. 2019. Interleukin (IL)-21 in Inflammation and Immunity During Parasitic Diseases. *Front Cell Infect Microbiol,* 9**,** 401.

SONG, E. & HU, H. 2021. *Translational research in breast cancer*, Springer.

SPAGNOLO, L., RIVERA-CALZADA, A., PEARL, L. H. & LLORCA, O. 2006. Three-dimensional structure of the human DNA-PKcs/Ku70/Ku80 complex assembled on DNA and its implications for DNA DSB repair. *Mol Cell,* 22**,** 511-9.

SPRING, L. M., WANDER, S. A., ANDRE, F., MOY, B., TURNER, N. C. & BARDIA, A. 2020. Cyclin-dependent kinase 4 and 6 inhibitors for hormone receptor-positive breast cancer: past, present, and future. *The Lancet,* 395**,** 817-827.

STEEL, G. G., MCMILLAN, T. J. & PEACOCK, J. 1989. The 5Rs of radiobiology. *International journal of radiation biology,* 56**,** 1045-1048.

STRACKER, T. H., USUI, T. & PETRINI, J. H. 2009. Taking the time to make important decisions: the checkpoint effector kinases Chk1 and Chk2 and the DNA damage response. *DNA Repair (Amst),* 8**,** 1047-54.

SUGASAWA, K., NG, J. M., MASUTANI, C., IWAI, S., VAN DER SPEK, P. J., EKER, A. P., HANAOKA, F., BOOTSMA, D. & HOEIJMAKERS, J. H. 1998. Xeroderma pigmentosum group C protein complex is the initiator of global genome nucleotide excision repair. *Mol Cell,* 2**,** 223-32.

SUZUKI, M., YAMAMORI, T., BO, T., SAKAI, Y. & INANAMI, O. 2017. MK-8776, a novel Chk1 inhibitor, exhibits an improved radiosensitizing effect compared to UCN-01 by exacerbating radiation-induced aberrant mitosis. *Transl Oncol,* 10**,** 491-500.
SWANSON, R. L., MOREY, N. J., DOETSCH, P. W. & JINKS-ROBERTSON, S. 1999. Overlapping specificities of base excision repair, nucleotide excision repair, recombination, and translesion synthesis pathways for DNA base damage in Saccharomyces cerevisiae. *Molecular and cellular biology*.
SY, S. M., HUEN, M. S. & CHEN, J. 2009. PALB2 is an integral component of the BRCA complex required for homologous recombination repair. *Proceedings of the National Academy of Sciences,* 106**,** 7155-7160.
TAVARES, E. M., WRIGHT, W. D., HEYER, W.-D., LE CAM, E. & DUPAIGNE, P. 2019. In vitro role of Rad54 in Rad51-ssDNA filament-dependent homology search and synaptic complexes formation. *Nature Communications,* 10**,** 4058.
TAYLOR, A., LAM, Z., LAST, J. & BYRD, P. 2015. Ataxia telangiectasia: more variation at clinical and cellular levels. *Clinical genetics,* 87**,** 199-208.
THANGAVEL, S., BERTI, M., LEVIKOVA, M., PINTO, C., GOMATHINAYAGAM, S., VUJANOVIC, M., ZELLWEGER, R., MOORE, H., LEE, E. H., HENDRICKSON, E. A., CEJKA, P., STEWART, S., LOPES, M. & VINDIGNI, A. 2015. DNA2 drives processing and restart of reversed replication forks in human cells. *J Cell Biol,* 208**,** 545-62.
THWAITES, M. J., CECCHINI, M. J., PASSOS, D. T., WELCH, I. & DICK, F. A. 2017. Interchangeable Roles for E2F Transcriptional Repression by the Retinoblastoma Protein and p27^{KIP1}–Cyclin-Dependent Kinase Regulation in Cell Cycle Control and Tumor Suppression. *Molecular and Cellular Biology,* 37**,** e00561-16.
TONG, Y., LI, Q. G., XING, T. Y., ZHANG, M., ZHANG, J. J. & XIA, Q. 2013. HIF1 regulates WSB-1 expression to promote hypoxia-induced chemoresistance in hepatocellular carcinoma cells. *FEBS Lett,* 587**,** 2530-5.
TRIEST, B. V., DAMSTRUP, L., FALKENIUS, J., BUDACH, V., TROOST, E., SAMUELS, M., DEBUS, J., SØRENSEN, M. M., BERGHOFF, K., STROTMAN, R., BUSSEL, M. V., GOEL, S. & GEERTSEN, P. F. 2018. A phase Ia/Ib trial of the DNA-PK inhibitor M3814 in combination with radiotherapy (RT) in patients (pts) with advanced solid tumors: Dose-escalation results. *Journal of Clinical Oncology,* 36**,** 2518-2518.
TSUTSUI, T., HESABI, B., MOONS, D. S., PANDOLFI, P. P., HANSEL, K. S., KOFF, A. & KIYOKAWA, H. 1999. Targeted disruption of CDK4 delays cell cycle entry with enhanced p27Kip1 activity. *Molecular and cellular biology,* 19**,** 7011-7019.
TSUZUKI, T., KAWATE, H. & IWAKUMA, T. 1998. Study on carcinogenesis and mutation suppression: repair of alkylation DNA damage and suppression of tumors. *Fukuoka igaku zasshi= Hukuoka acta medica,* 89**,** 1-10.
TULI, R., SHIAO, S. L., NISSEN, N., TIGHIOUART, M., KIM, S., OSIPOV, A., BRYANT, M., RISTOW, L., PLACENCIO-HICKOK, V., HOFFMAN, D., ROKHSAR, S., SCHER, K., KLEMPNER, S. J., NOE, P., DAVIS, M. J., WACHSMAN, A., LO, S., JAMIL, L., SANDLER, H., PIANTADOSI, S. & HENDIFAR, A. 2019. A phase 1 study of veliparib, a PARP-1/2 inhibitor, with gemcitabine and radiotherapy in locally advanced pancreatic cancer. *EBioMedicine,* 40**,** 375-381.
UBHI, T. & BROWN, G. W. 2019. Exploiting DNA Replication Stress for Cancer Treatment. *Cancer Research,* 79**,** 1730-1739.

VAN OERS, J. M., ROA, S., WERLING, U., LIU, Y., GENSCHEL, J., HOU, H., JR., SELLERS, R. S., MODRICH, P., SCHARFF, M. D. & EDELMANN, W. 2010. PMS2 endonuclease activity has distinct biological functions and is essential for genome maintenance. *Proc Natl Acad Sci U S A,* 107**,** 13384-9.

VAN WERKHOVEN, E., HINSLEY, S., FRANGOU, E., HOLMES, J., DE HAAN, R., HAWKINS, M., BROWN, S. & LOVE, S. B. 2020. Practicalities in running early-phase trials using the time-to-event continual reassessment method (TiTE-CRM) for interventions with long toxicity periods using two radiotherapy oncology trials as examples. *BMC Med Res Methodol,* 20**,** 162.

VASAN, K., SATGUNASEELAN, L., ANAND, S., ASHER, R., SELINGER, C., LOW, T. H., PALME, C. E., CLARK, J. R. & GUPTA, R. 2019. Tumour mismatch repair protein loss is associated with advanced stage in oral cavity squamous cell carcinoma. *Pathology,* 51**,** 688-695.

VAUPEL, P., KALLINOWSKI, F. & OKUNIEFF, P. 1989. Blood flow, oxygen and nutrient supply, and metabolic microenvironment of human tumors: a review. *Cancer Res,* 49**,** 6449-65.

VIGNARD, J., MIREY, G. & SALLES, B. 2013. Ionizing-radiation induced DNA double-strand breaks: A direct and indirect lighting up. *Radiotherapy and Oncology,* 108**,** 362-369.

VOLKER, M., MONÉ, M. J., KARMAKAR, P., VAN HOFFEN, A., SCHUL, W., VERMEULEN, W., HOEIJMAKERS, J. H., VAN DRIEL, R., VAN ZEELAND, A. A. & MULLENDERS, L. H. 2001. Sequential assembly of the nucleotide excision repair factors in vivo. *Molecular cell,* 8**,** 213-224.

WANG, T., AMEMIYA, Y., HENRY, P., SETH, A., HANNA, W. & HSIEH, E. T. 2015. Multiplex Ligation-dependent Probe Amplification Can Clarify HER2 Status in Gastric Cancers with "Polysomy 17". *J Cancer,* 6**,** 403-8.

WAQAR, S. N., ROBINSON, C., OLSZANSKI, A. J., SPIRA, A., HACKMASTER, M., LUCAS, L., SPONTON, L., JIN, H., HERING, U., CRONIER, D., GRINBERG, M., SEITHEL-KEUTH, A., DIAZ-PADILLA, I. & BERLIN, J. 2022. Phase I trial of ATM inhibitor M3541 in combination with palliative radiotherapy in patients with solid tumors. *Investigational New Drugs,* 40**,** 596-605.

WARREN, N. J. H., DONAHUE, K. L. & EASTMAN, A. 2019. Differential Sensitivity to CDK2 Inhibition Discriminates the Molecular Mechanisms of CHK1 Inhibitors as Monotherapy or in Combination with the Topoisomerase I Inhibitor SN38. *ACS Pharmacology & Translational Science,* 2**,** 168-182.

WENG, Y., PAN, C., SHEN, Z., CHEN, S., XU, L., DONG, X. & CHEN, J. 2022. Identification of Potential WSB1 Inhibitors by AlphaFold Modeling, Virtual Screening, and Molecular Dynamics Simulation Studies. *Evid Based Complement Alternat Med,* 2022**,** 4629392.

WENZL, T. & WILKENS, J. J. 2011. Theoretical analysis of the dose dependence of the oxygen enhancement ratio and its relevance for clinical applications. *Radiation Oncology,* 6**,** 171.

WERNECK DE CASTRO, J. P., FONSECA, T. L., UETA, C. B., MCANINCH, E. A., ABDALLA, S., WITTMANN, G., LECHAN, R. M., GEREBEN, B. & BIANCO, A. C. 2015. Differences in hypothalamic type 2 deiodinase ubiquitination explain localized sensitivity to thyroxine. *J Clin Invest,* 125**,** 769-81.

WHITEWAY, S. L., HARRIS, P. S., VENKATARAMAN, S., ALIMOVA, I., BIRKS, D. K., DONSON, A. M., FOREMAN, N. K. & VIBHAKAR, R. 2013. Inhibition of cyclin-dependent kinase 6 suppresses cell proliferation and enhances radiation sensitivity in medulloblastoma cells. *Journal of Neuro-Oncology,* 111**,** 113-121.

WILHELM, T., SAID, M. & NAIM, V. 2020. DNA Replication Stress and Chromosomal Instability: Dangerous Liaisons. *Genes,* 11**,** 642.
WILLIAMS, A. B. & SCHUMACHER, B. 2016. p53 in the DNA-Damage-Repair Process. *Cold Spring Harb Perspect Med,* 6.
WILLIAMS, A. D., PAYNE, K. K., POSEY, A. D., JR., HILL, C., CONEJO-GARCIA, J., JUNE, C. H. & TCHOU, J. 2017. Immunotherapy for Breast Cancer: Current and Future Strategies. *Curr Surg Rep,* 5.
WIN, A. K., YOUNG, J. P., LINDOR, N. M., TUCKER, K. M., AHNEN, D. J., YOUNG, G. P., BUCHANAN, D. D., CLENDENNING, M., GILES, G. G., WINSHIP, I., MACRAE, F. A., GOLDBLATT, J., SOUTHEY, M. C., ARNOLD, J., THIBODEAU, S. N., GUNAWARDENA, S. R., BAPAT, B., BARON, J. A., CASEY, G., GALLINGER, S., LE MARCHAND, L., NEWCOMB, P. A., HAILE, R. W., HOPPER, J. L. & JENKINS, M. A. 2012. Colorectal and other cancer risks for carriers and noncarriers from families with a DNA mismatch repair gene mutation: a prospective cohort study. *J Clin Oncol,* 30**,** 958-64.
WITHERS, H. R. 1975. The four R's of radiotherapy. *Advances in radiation biology.* Elsevier.
WOOD, R. D. 1997. Nucleotide Excision Repair in Mammalian Cells*. *Journal of Biological Chemistry,* 272**,** 23465-23468.
XU, X. Q., PAN, X. H., WANG, T. T., WANG, J., YANG, B., HE, Q. J. & DING, L. 2021. Intrinsic and acquired resistance to CDK4/6 inhibitors and potential overcoming strategies. *Acta Pharmacol Sin,* 42**,** 171-178.
YIN, L., DUAN, J.-J., BIAN, X.-W. & YU, S.-C. 2020. Triple-negative breast cancer molecular subtyping and treatment progress. *Breast Cancer Research,* 22**,** 61.
YOSHIMURA, N., MASUMOTO, N., AMIOKA, A., KAJITANI, K., SHIGEMATSU, H., EMI, A. & KADOYA, T. 2014 San Antonio Breast Cancer Symposium.
ZANGHERI, B., MESSA, C., PICCHIO, M., GIANOLLI, L., LANDONI, C. & FAZIO, F. 2004. PET/CT and breast cancer. *European Journal of Nuclear Medicine and Molecular Imaging,* 31**,** S135-S142.
ZANNINI, L., DELIA, D. & BUSCEMI, G. 2014. CHK2 kinase in the DNA damage response and beyond. *J Mol Cell Biol,* 6**,** 442-57.
ZANONI, M., CORTESI, M., ZAMAGNI, A., ARIENTI, C., PIGNATTA, S. & TESEI, A. 2020. Modeling neoplastic disease with spheroids and organoids. *Journal of Hematology & Oncology,* 13**,** 97.
ZEMAN, M. K. & CIMPRICH, K. A. 2014. Causes and consequences of replication stress. *Nat Cell Biol,* 16**,** 2-9.
ZENG, L., BEGGS, R. R., COOPER, T. S., WEAVER, A. N. & YANG, E. S. 2017. Combining Chk1/2 Inhibition with Cetuximab and Radiation Enhances In Vitro and In Vivo Cytotoxicity in Head and Neck Squamous Cell Carcinoma. *Mol Cancer Ther,* 16**,** 591-600.
ZHANG, C., SAMANTA, D., LU, H., BULLEN, J. W., ZHANG, H., CHEN, I., HE, X. & SEMENZA, G. L. 2016. Hypoxia induces the breast cancer stem cell phenotype by HIF-dependent and ALKBH5-mediated m⁶A-demethylation of NANOG mRNA. *Proceedings of the National Academy of Sciences,* 113**,** E2047-E2056.
ZHANG, F., FAN, Q., REN, K. & ANDREASSEN, P. R. 2009. PALB2 functionally connects the breast cancer susceptibility proteins BRCA1 and BRCA2. *Molecular Cancer Research,* 7**,** 1110-1118.
ZHANG, Y. & HUNTER, T. 2014. Roles of Chk1 in cell biology and cancer therapy. *Int J Cancer,* 134**,** 1013-23.

ZHOU, G., SOUFAN, O., EWALD, J., HANCOCK, R. E. W., BASU, N. & XIA, J. 2019a. NetworkAnalyst 3.0: a visual analytics platform for comprehensive gene expression profiling and meta-analysis. *Nucleic Acids Research,* 47**,** W234-W241.

ZHOU, G., SOUFAN, O., EWALD, J., HANCOCK, R. E. W., BASU, N. & XIA, J. 2019b. NetworkAnalyst 3.0: a visual analytics platform for comprehensive gene expression profiling and meta-analysis. *Nucleic Acids Res,* 47**,** W234-w241.

ZHOU, Y., ZHOU, B., PACHE, L., CHANG, M., KHODABAKHSHI, A. H., TANASEICHUK, O., BENNER, C. & CHANDA, S. K. 2019c. Metascape provides a biologist-oriented resource for the analysis of systems-level datasets. *Nat Commun,* 10**,** 1523.

ZIMMERMANN, M., BERNIER, C., KAISER, B., FOURNIER, S., LI, L., DESJARDINS, J., SKELDON, A., RIMKUNAS, V., VELOSO, A., YOUNG, J. T. F., ROULSTON, A. & ZINDA, M. 2022. Guiding ATR and PARP inhibitor combinationswith chemogenomic screens. *Cell Rep,* 40**,** 111081.